WRI-97-R032

WESTERN RESEARCH INSTITUTE

"Providing solutions to energy and environmental problems"

FINAL REPORT

PRELIMINARY EVALUATION OF A PROCESS USING PLASMA REACTIONS TO DESULFURIZE HEAVY OILS

Prepared for
U.S. Department of Energy
Morgantown, West Virginia

September 1997

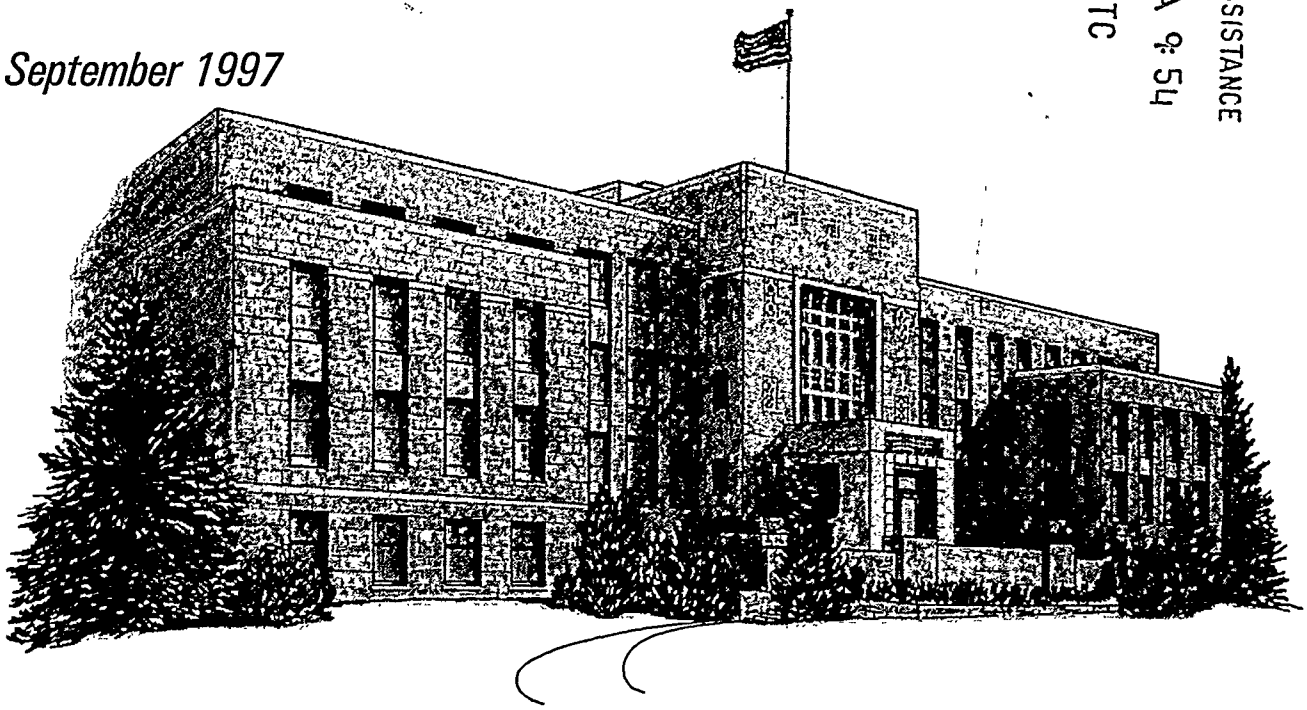

DISCLAIMER

DISCLAIMER

Portions of this document may be illegible in electronic image products. Images are produced from the best available original document.

WRI-97-R032

PRELIMINARY EVALUATION OF A PROCESS USING PLASMA REACTIONS TO DESULFURIZE HEAVY OILS

Final Report

By
R. Will Grimes
Francis P. Miknis

September 1997

Work Performed Under Cooperative Agreement
DE-FC21-93MC30126
Subtask 4.2

For
U.S. Department of Energy
Office of Fossil Energy
Federal Energy Technology Center
Morgantown, West Virginia

By
Western Research Institute
Laramie, Wyoming

DISCLAIMER

TABLE OF CONTENTS

LIST OF TABLES AND FIGURES

EXECUTIVE SUMMARY

Western Research Institute (WRI) has conducted exploratory experiments on the use of microwave-induced plasmas to desulfurize heavy oils. Batch mode experiments were conducted in a quartz reactor system using various reactive and nonreactive plasmas. In these experiments a high-sulfur asphalt was exposed to various plasmas, and the degree of conversion to distillate, gas, and solids was recorded. Products from selected experiments were analyzed to determine if the plasma exposure had resulted in a significant reduction in sulfur content.

Exploratory experiments were conducted using reactive plasmas generated from hydrogen and methane and nonreactive plasmas generated from nitrogen. The effects of varying exposure duration, sample temperature, and location of the sample with respect to the plasma discharge were investigated. For comparative purposes two experiments were conducted in which the sample was heated under nitrogen with no plasma exposure.

The experiments using reactive (hydrogen and methane) plasmas consistently produced more distillate than similar experiments using nonreactive nitrogen plasmas. Sample temperature had a minimal effect on conversion to distillate in these exploratory experiments. The location of the sample with respect to the discharge strongly affected conversion and product distribution. Typically conversions increased as the distance between the sample and the discharge was decreased. This held true for both the reactive and the nonreactive plasmas. Total (100%) conversion of the sample to gas and solids resulted when the sample was placed within the discharge. Under these conditions no distillate was produced.

Distillate containing approximately 28% less sulfur than the feedstock represented the maximum desulfurization attained in the plasma experiments. This same level of desulfurization was also attained by heating the sample under nitrogen with no plasma exposure. For similar conversions, heating the sample under nitrogen with no plasma exposure generated more distillate and less gas than either the reactive or nonreactive plasmas. From these exploratory experiments it does not appear that plasma reactions using the simple configurations employed in this study represent a viable method for the desulfurization of heavy oils.

INTRODUCTION

Objective

The objective of this task was to provide data needed to assess the potential viability of a process to desulfurize heavy oils through the use of plasma reactions.

Background

Due to a continuing decline in supplies of sweet light crude, heavy oils are becoming increasingly important as refinery feedstock. Unfortunately, heavy oils tend to be considerably more difficult to process than the lighter crudes. The physical and chemical properties of heavy oils differ significantly from those of lighter crudes, and therefore, their use presents some special challenges for refiners. Heavy oils are typically characterized as containing less hydrogen and considerably more sulfur, nitrogen, oxygen, and metals than the lighter crudes. The high levels of sulfur typically found in heavy oils is of particular significance in the refining process.

Sulfur is undesirable in liquid fuel products for a number of reasons and is also frequently responsible for corrosion problems in refinery equipment. To meet the demand for low-sulfur distillate products and reduce corrosion problems, many petroleum refineries have incorporated a feedstock desulfurization process. A number of processes can decrease sulfur levels in refinery feedstock (Speight 1981), however, hydrodesulfurization processes are most commonly employed for this purpose.

Hydrodesulfurization processes remove sulfur through the catalytic reaction of hydrogen with sulfur-containing constituents of the petroleum. The gaseous hydrogen sulfide produced by this reaction is separated from the liquid products to yield hydrocarbons with greatly reduced sulfur content. The relative ease of the gas/liquid separation and the high level of sulfur removal typically achieved by the process have led to a nearly universal acceptance of hydrodesulfurization as the best method for desulfurizing petroleum.

Application of hydrodesulfurization processes to heavy oils is compromised by the deposition of coke and metals on the catalyst. These deposits tend to deactivate the catalyst, necessitating frequent regeneration and/or replacement, which adds considerably to the cost of desulfurization. Thus, for the heavy oils for which desulfurization is most necessary, the best available process has significant shortcomings. A desulfurization process that removes sulfur as hydrogen sulfide without the use of catalysts could represent an important step forward in the use of heavy oils as refinery feedstock.

Studies conducted by Amano and co-workers (Amano et al. 1984 and 1985) have shown that hydrogen atoms generated in a microwave discharge can react directly with coal to produce

liquids that are practically free of heteroatoms. These experiments suggest that H atoms generated in a microwave discharge might also react with other hydrocarbon-containing materials, such as heavy oils and petroleum resids, to produce low-sulfur liquid products.

Exploratory experiments were conducted to determine whether low-sulfur liquid products can be obtained by reacting a heavy oil feedstock material in hydrogen-rich microwave plasmas. In the various experiments, a high-sulfur asphalt feedstock was exposed to microwave plasmas generated using hydrogen (H_2), methane (CH_4), and nitrogen (N_2). Reaction products were analyzed to determine if the plasma exposure resulted in significant desulfurization. The results of these experiments are the subject of this topical report.

EXPERIMENTAL

Feedstock Material

A high-sulfur asphalt obtained from the Strategic Highway Research Program (SHRP) Materials Reference Library (Cominsky et al. 1989) was used as feedstock in all the experiments.

Simulated Distillation

This procedure is a gas chromatographic technique for determining distillation profiles of materials that are not 100% distillable below 544K. The chromatographic data are divided into desired distillate fractions from correlations between gas chromatography (GC) retention times and normal alkane boiling points. The concentration (weight percent) of each distillate fraction is determined using response factors obtained from standard samples. The results are reported as concentration (weight percent) of distillable materials versus temperature. The boiling ranges are chosen to correspond to those of the true boiling point distillation (Gary and Handwerk 1975).

Gas Analyses

Gas samples were analyzed using a Hewlett-Packard 5840-A gas chromatograph equipped with a flame photometric detector. Sulfur gases were analyzed on a 10 ft x 1/8 in. carbopak BHT column. Nitrogen carrier gas flow rate was 30 cc/min. The column oven was temperature programmed to hold at 20 °C for three minutes then heat at 25 °C/min to 120 °C.

Elemental Analyses

Carbon, hydrogen, and nitrogen were determined with a Perkin-Elmer 2400 automated CHN analyzer. Calibration was done with acetanilide, benzoic acid, carbazole, cholesteryl palmitate, and steric acid. Sulfur was determined with a Fisher 475 sulfur analyzer according to

American Society for Testing and Materials (ASTM) D4239. Oil standards from Alpha Chemical were used for calibration. Oxygen was determined by difference.

Experimental Procedures

The batch reactor shown schematically in Figure 1 was used for the majority of the experiments. The reactor consisted of two coaxial quartz tubes. The 19-mm o.d. (16.5-mm i.d.) outer tube was sealed at one end to form an elongated test tube that served as the sample holder. The 9-mm o.d. (6.5-mm i.d.) interior tube provided a flow path for the plasma so that its tail (the glow remaining outside the microwave field) could be made to impinge upon the surface of the heavy oil sample. The interior tube was attached to the outer tube by means of a stainless steel fitting with O-ring seals. The axial adjustment provided by this arrangement allowed the distance from the end of the interior tube to the sample to be varied.

Using various feed gases and feed gas combinations, microwave energy was used to generate plasmas. The system used to deliver microwave energy to the plasma consisted of a terminated waveguide applicator (Haugsjaa 1986) microwave generator, magnetic circulator, directional coupler, impedance matching device, and various waveguide sections. Figure 2 is a block diagram of the microwave system used in the testing.

Microwave energy was supplied by a Cober s6F industrial microwave generator. The generator power output was adjustable from 0 to 6 kW at a fixed frequency of 2.45 GHz. The generator was connected via a magnetic circulator and a Microwave Techniques twin stub tuner to a terminated waveguide applicator. The applicator was constructed by boring a 22-mm hole through the center of the broad faces of a standard WR284 waveguide termination. The distance from the center of the hole to the shorted end was equal to one half the width of the broad face.

The gas flow system is shown schematically in Figure 3. A Brooks 5850E mass flow controller was used to regulate and measure the inlet gas flow. A saturator and bypass completed the flow system upstream of the reactor. Downstream from the reactor condensable liquid products were collected in a 10-mL cold trap immersed in a slurry of dry ice and methanol. A rubber septum was provided through which grab samples of the product gas could be withdrawn by means of a gas-tight syringe. A throttle valve, vacuum trap, and rotary pump completed the downstream flow system. Reactor pressure was recorded using an Omega Q-15 pressure transducer connected to a strip chart recorder.

Three series of experiments were conducted using the batch reactor system and a high-sulfur asphalt feedstock. Series 1 experiments were conducted to determine if various hydrogen-rich microwave plasmas would selectively abstract sulfur from a high-sulfur asphalt material. Series 2 and 3 experiments were conducted to determine the effect of sample temperature and distance between discharge and sample on conversion to distillate and desulfurization.

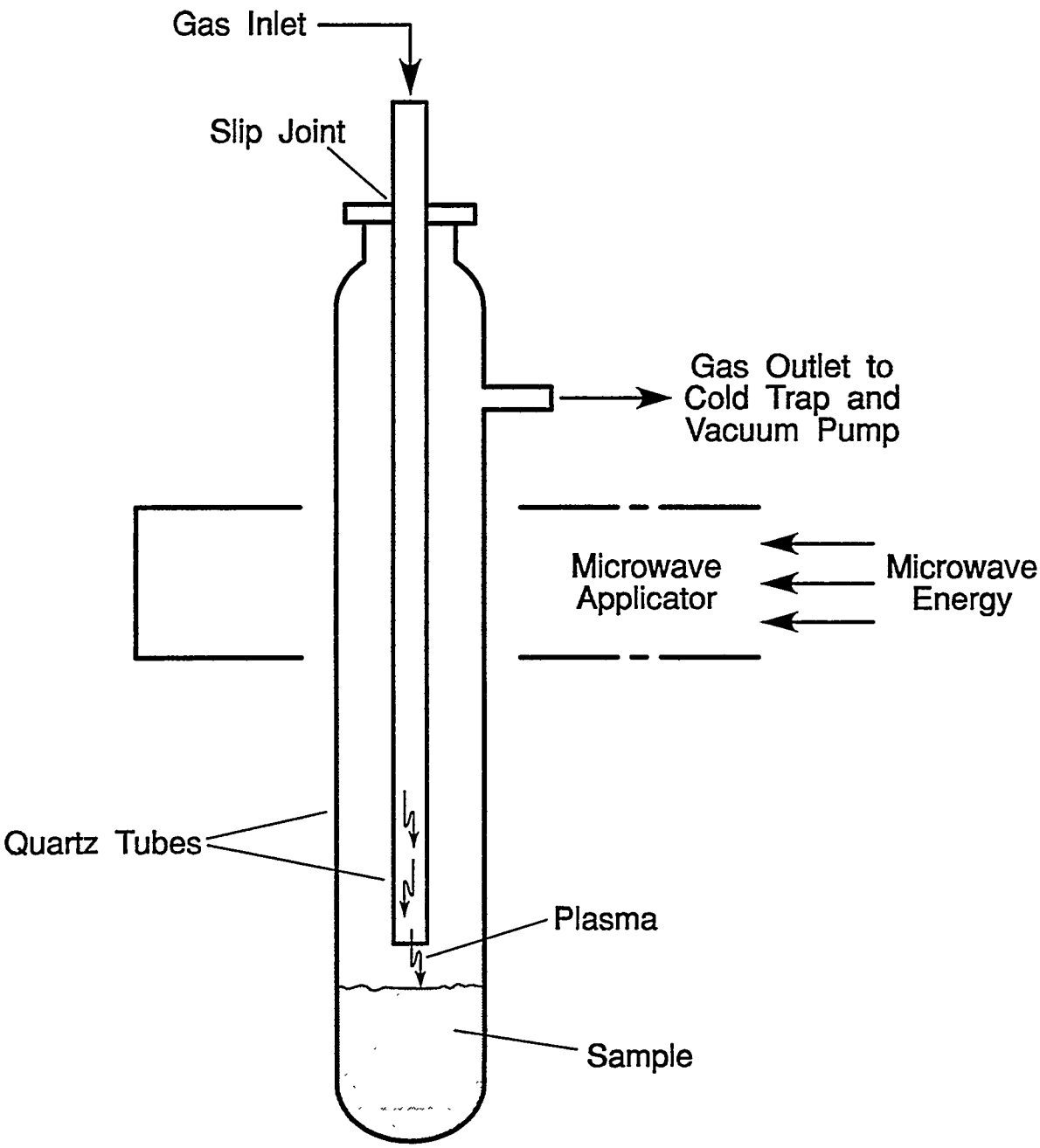

Figure 1. Batch Reactor System

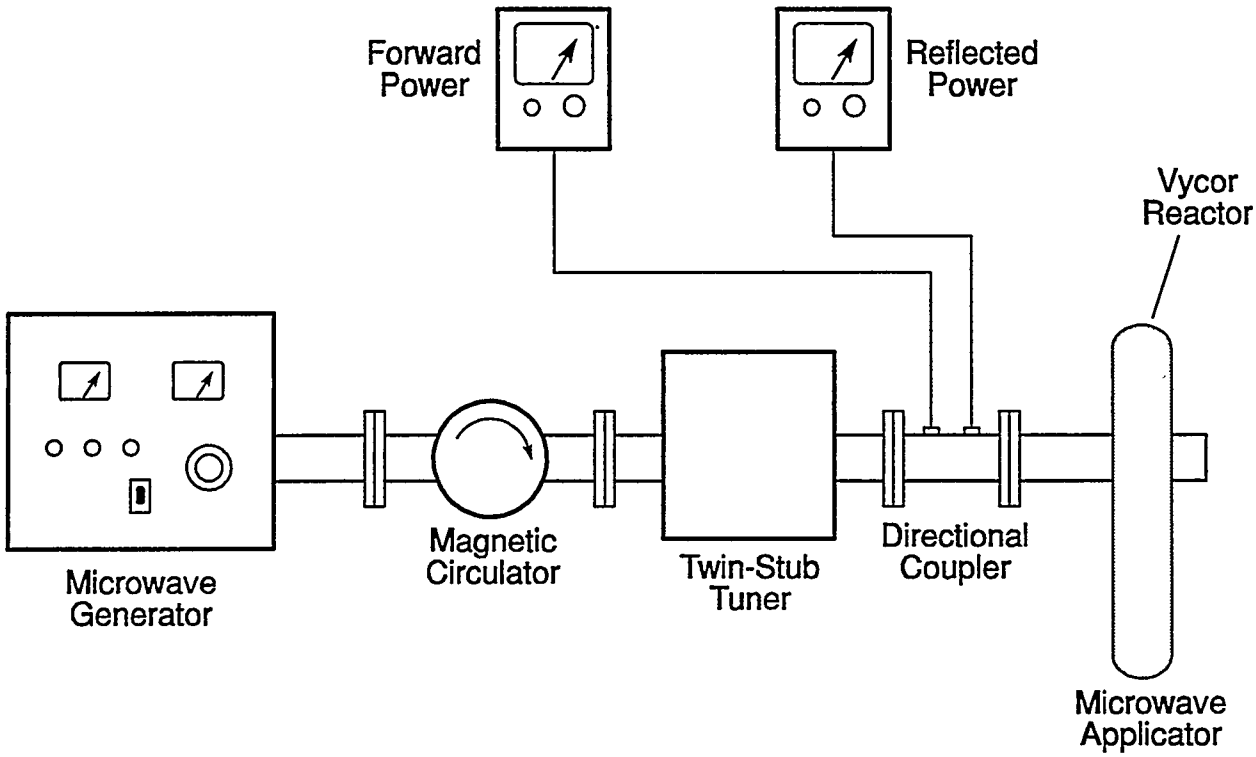

Figure 2. Block Diagram of Microwave Apparatus

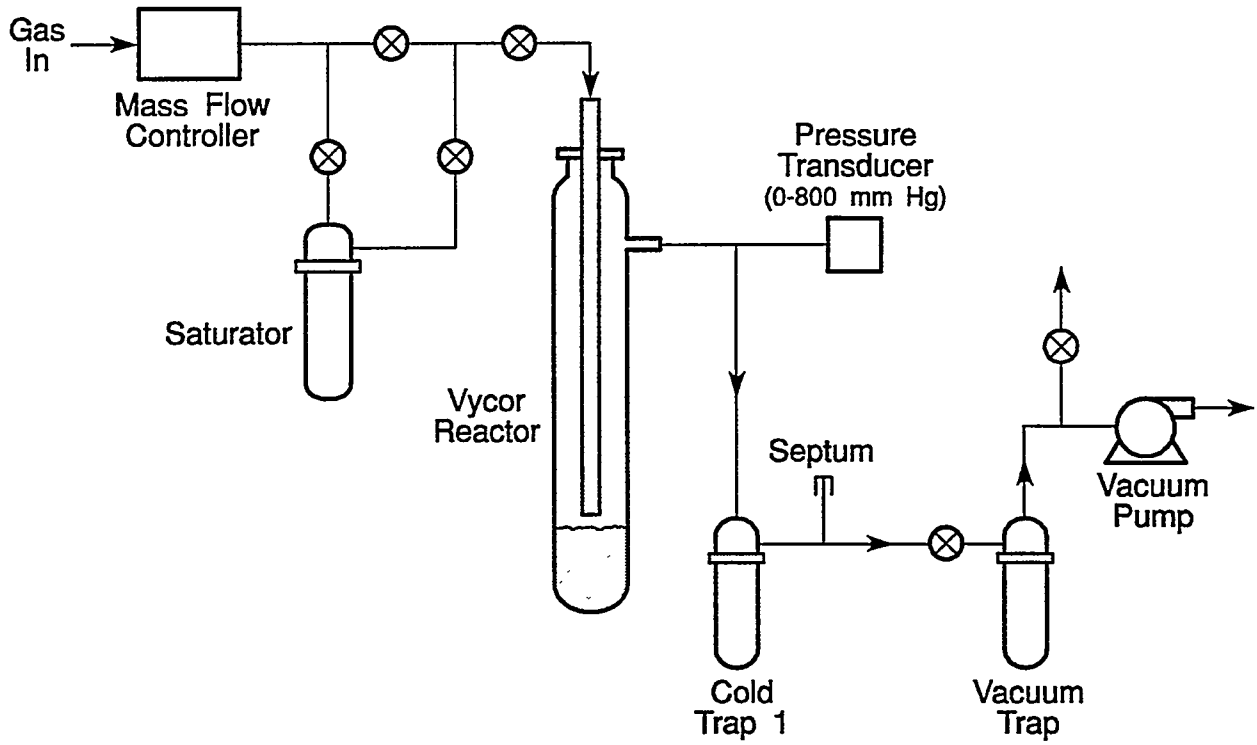

Figure 3. Schematic Diagram of Gas Flow System

RESULTS AND DISCUSSION

Series 1

In the Series 1 experiments high-sulfur asphalt samples were exposed to H_2, He, CH_4, or CH_4/H_2O plasmas. For these experiments, the asphalt sample was heated to 120 °C and gas flow was established at 36 scc/min (~100 mMol/hr). Microwave power was set at ~200 watts and remained constant throughout the test series. The interior reactor tube was adjusted so that its outlet end was fixed ~8 mm above the surface of the asphalt. Samples were exposed to the plasma for 165 minutes at a pressure of 6 torr (0.8 kPa), except for one test with hydrogen plasma in which the pressure was 15 torr (2.0 kPa). After each test, the cold trap and reactor were rinsed with methylene chloride and the rinsings were combined to form a composite sample.

Table 1 lists product distribution and conversion to distillable liquids and gas for these tests. Conversions are listed as percent of feed: (weight of distillate or weight of gas)/(weight of feed) x 100 and as percent of product: (weight of distillate or weight of gas)/(weight of distillate + weight of gas) x 100. Table 2 shows the results of C, H, N, S elemental analysis of the original asphalt and the combined reaction products. Test 1-1 served as a control with no plasma. Temperature, pressure, and flow were the same as used in the other tests.

Table 1. Conversion and Product Distribution for Series 1 Experiments

		distillate		gas		total
Test #	gas	% feed	% prod	% feed	% prod	% feed
1-1	H2	0.0	0.0	0.2	100.0	0.2
1-2	He	0.2	5.3	4.1	94.7	4.3
1-3	H2	2.4	14.3	14.5	85.7	17.0
1-4	CH4	5.1	43.4	6.7	56.6	11.8
1-5	CH4/H2O	4.4	37.8	7.2	62.2	11.6
1-6	H2	0.2	10.7	10.4	97.8	10.7

Table 2. C, H, N, S Analyses of Combined Liquid Products From Series 1 Experiments

Test #	C	H	N	S	H/C
feed	81.4	10.2	0.08	7.3	1.50
1-1	80.7	10.5	0.06	7.7	1.57
1-2	81.2	10.9	0.04	6.9	1.60
1-3	81.7	10.2	0.07	7.1	1.49
1-4	82.0	10.3	0.05	6.7	1.15
1-5	82.0	10.2	0.10	6.8	1.49
1-6	80.7	11.2	0.07	7.0	1.68

Elemental analyses of the original asphalt and the combined liquid reaction products for the Series 1 tests show no significant reduction in sulfur after exposure to the plasmas. From these data it does not appear that reactive species in the plasma selectively abstract sulfur from the hydrocarbon matrix. In view of the fact that the elemental composition of the product liquid was very similar to that of the feedstock, it appears that carbon, hydrogen, and sulfur were abstracted nearly stoichiometrically in the product gas. Conversion to distillable liquids was minimal in all the tests, and these liquids were not analyzed separately. Therefore, whether these liquids were low in sulfur was not determined.

In a study on the cracking of Athabasca bitumen residuum, Sanford (1994) noted that very little sulfur was removed from the hydrocarbon when conversions were low. Based on Sanford's work and the Series 1 test results, it was decided that higher conversions would be needed to evaluate the potential of plasma desulfurization.

Series 2

In the Series 2 experiments, four tests were conducted to explore the effect of sample temperature and location of the sample with respect to the discharge on conversion to distillable liquids. All four tests used hydrogen plasma with the inlet hydrogen flow maintained at 36 scc/min and a reactor pressure of 6 torr (0.8 kPa).

For Test 1, the asphalt sample was heated to 160 °C and exposed to hydrogen plasma for 270 minutes. At the start of this test, the outlet end of the interior tube was ~8 mm above the surface of the asphalt. This distance decreased due to slippage of the interior tube in the O-ring sealed fitting as the test progressed. At the end of the test, the interior tube had slipped to where its end was about even with the surface of the asphalt.

In Test 2, the sample was heated to 188 °C and exposed to hydrogen plasma for 166 minutes. The outlet end of the interior tube was fixed at ~8 mm above the surface of the asphalt.

For Test 3, the asphalt was moved closer to the microwave applicator so that the surface of the asphalt was just below the bottom of the waveguide. The asphalt was preheated to 180 °C and exposed to the hydrogen plasma for 25 minutes.

In Test 4, the asphalt was preheated to 180 °C and exposed to the plasma for 790 minutes. The cold trap was weighed at intervals as the test progressed. The end of the interior plasma tube was fixed at 8 mm above the asphalt surface for 700 minutes then lowered incrementally over the next 90 minutes so that its outlet end was about even with the surface of the asphalt at the end of the test.

Table 3 lists conversions and product distribution for the Series 2 experiments. Conversion was calculated as: [(weight of feed) - (weight of $MeCl_2$ soluble resid)]/(weight of feed) x 100. For the purpose of these tests, the methylene chloride soluble material remaining in the reactor after exposure to the plasma was considered to be unconverted. It is interesting to note that methylene chloride insoluble solids were formed in similar amounts in all the tests, and there was no apparent correlation between solids formation and degree of conversion. The first test seemed to form the most distillate, but this result is suspect because there was a leak in the reactor during the first half of the test.

Table 3. Conversion and Product Distribution for Series 2 Experiments

	total	distillate		solids		gas	
Test #	% feed	% feed	% prod.	% feed	% prod.	% feed	% prod.
2-1	31.3	8.2	26.2	3.6	11.3	19.5	62.4
2-2	32.8	6.1	18.5	4.5	13.7	22.2	67.8
2-3	29.7	5.9	20.0	4.6	15.6	19.2	64.4
2-4	45.4	7.0	15.3	3.6	7.9	34.8	76.7

Figure 4 shows distillate production for the length of time the asphalt sample was exposed to hydrogen plasma. The distance between the discharge and the asphalt surface was set at 8 mm for the first 700 minutes of the experiment, then gradually reduced for the remaining 90 minutes. Note that distillate production increased significantly as the distance between the discharge and the asphalt surface was decreased.

In this test, 0.11 grams of distillate was produced during the first 700 minutes of exposure to the hydrogen plasma with the outlet of the interior tube 8 mm above the asphalt. Nearly twice this amount (0.20 grams) was produced in the final 90 minutes with the end of the interior tube lowered to just above the surface of the asphalt.

Figure 5 shows the results of simulated distillation of the liquid collected in the cold trap for the Series 2 tests. For each test, about 50% of the distillate was light gas oil (195-340 °C). Test 3, in which the asphalt was placed near the discharge, produced more heavy distillate (>340 °C), while lower boiling liquids were favored in test 2 with the sample further from the discharge.

The results of the Series 2 experiments indicated that sample temperature had a negligible effect on distillate production. However, the distance between the discharge and the sample surface strongly influenced distillate production.

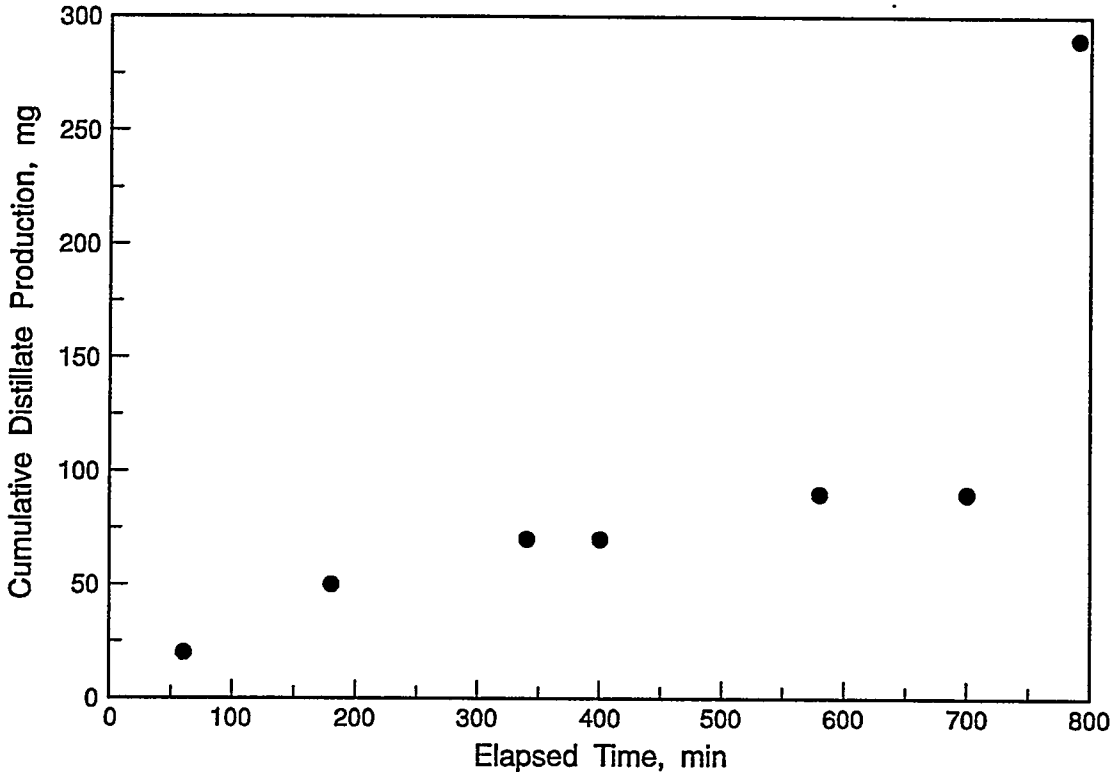

Figure 4. Distillate Production vs. Time, Experiment 2-4

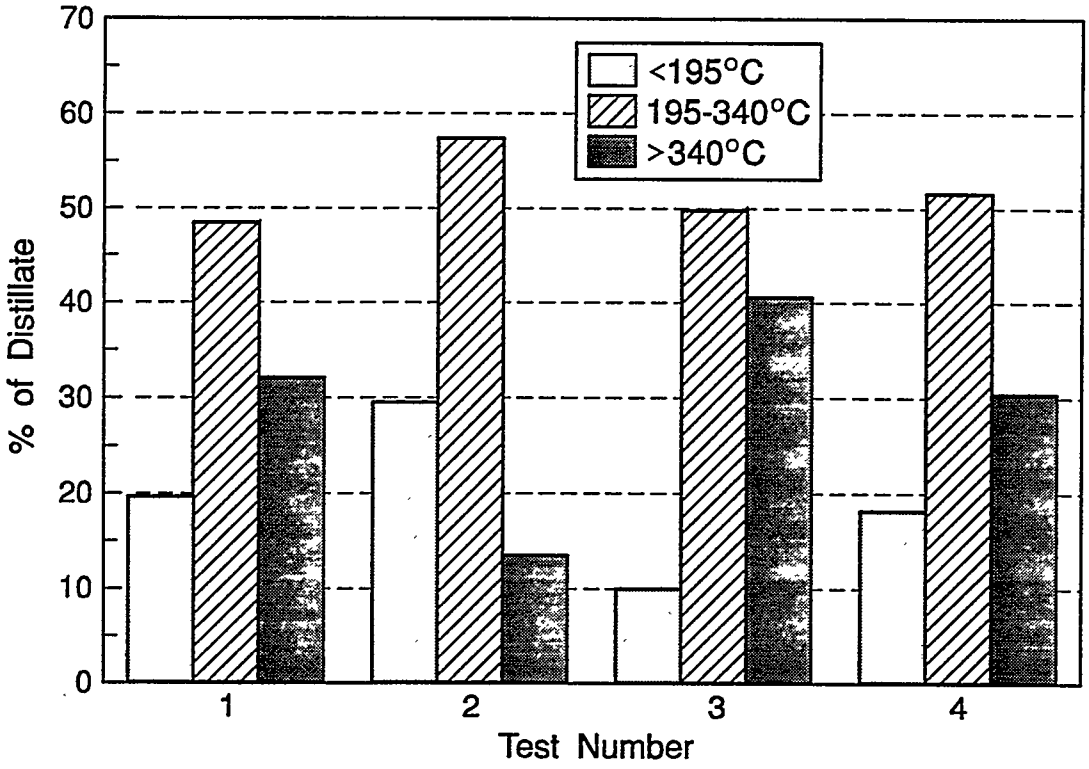

Figure 5. Results of Simulated Distillation of Distillate Product From Series 2 Tests

Series 3

In the Series 3 experiments, the distance between the plasma discharge and the sample was varied. For these experiments, gas flow was established at 36 scc/min (~100 mMol/hr) and microwave power was set as shown in Table 4. The asphalt sample was not heated for the Series 3 experiments. After each test, the reactor was rinsed with methylene chloride and the rinsings were filtered to provide separate samples of the methylene chloride soluble residual material and the insoluble solids.

Table 4 lists the experimental conditions, conversions, and product distribution for the Series 3 experiments. The distance column lists the initial distance in millimeters between the end of the interior plasma tube and the asphalt sample. Where this number is followed by a downward arrow, the interior plasma tube was moved incrementally toward the sample during the experiment so that its outlet was ~1 mm from the bottom of outer tube at the end of the test. Where the distance is followed by an upward arrow, the sample was moved closer to the microwave applicator as the test progressed.

Table 4. Experimental Conditions, Conversion, and Product Distribution for Series 3 Experiments

					conv	distillate		gas		solids	
test #	gas	press. (torr)	power (W)	distance (mm)	% feed	% feed	% prod	% feed	% prod	% feed	% prod
3-1	H_2	6	260	8	54.0	10.5	19.4	33.5	62.0	10.0	18.5
3-2	CH_4	6	260/300	8	60.0	10.5	17.5	32.5	54.2	17.0	28.3
3-3	N_2	6	260	8	37.6	5.0	13.2	23.8	63.2	8.9	23.7
3-4	H_2	6	260	8↓	93.5	26.0	27.8	50.5	54.0	17.0	18.2
3-5	CH_4	6	260	8↓	88.7	18.6	21.0	52.9	59.7	17.2	19.3
3-6	N_2	6	260	8↓	83.0	17.0	20.5	46.0	55.4	20.0	24.1
3-7	H_2	12	260	2↓	67.0	29.1	43.4	28.6	42.6	9.4	14.0
3-8	N_2	6	260	2↓	83.7	19.7	23.5	46.8	55.9	17.2	20.6
3-9	H_2	6	200	2↓	60.7	26.9	44.3	27.9	45.9	6.0	9.8
3-10	N_2	6	200	2↓	58.3	18.6	31.9	31.4	53.8	8.3	14.3
3-11	CH_4	6	260	25↑	54.5	19.0	34.9	21.5	39.4	14.0	25.7
3-12	H_2	6	260	40↑	89.1	14.4	15.9	59.7	67.0	14.9	16.8
3-13	H_2	6	250	40↑	39.5	5.5	13.9	25.0	63.3	9.0	22.8
3-14	H_2	6	700	0	100	0.0	0.0	68.7	68.7	31.3	31.3
3-15	N_2	6	0		48.8	29.4	60.2	5.5	11.2	13.9	28.6
3-16	N_2	40	0		84.7	39.3	46.4	30.6	36.1	14.8	17.5

In Tests 3-1, 3-2, and 3-3, the interior reactor tube was adjusted so that its outlet end was fixed ~8 mm above the surface of the asphalt. In these experiments, the samples were exposed to hydrogen, methane, or nitrogen plasmas for 60 minutes. In Test 3-2, the microwave power was increased to ~300 watts after about 20 minutes in order to provide a more stable plasma. The tests using hydrogen and methane plasmas showed higher conversion and produced more than twice as much distillate as the test using the nitrogen plasma. In all the tests, the majority of the product was gas, and all the tests produced significant amounts of methylene chloride insoluble solids.

Tests 3-4, 3-5, and 3-6 were essentially identical to Tests 3-1, 3-2, and 3-3 except that the outlet of the interior reactor tube was moved incrementally toward the asphalt sample as these tests progressed. Samples were exposed to hydrogen, methane, or nitrogen plasmas for 60 minutes with microwave power set at 260 watts. All of these tests showed a higher conversion, more distillate production, and more of the product as distillate than the corresponding tests in which the distance from the end of the interior plasma tube to the sample was fixed. As in the previous tests, the experiments that used hydrogen and methane plasmas showed higher conversion and produced more distillate than the test that used the nitrogen plasma.

Tests 3-7 and 3-8 duplicated Tests 3-4 and 3-6 except for the initial position of the outlet end of the interior reactor tube. In Tests 3-7 and 3-8, the outlet end of the interior reactor tube was moved incrementally toward the sample from an initial position 2 mm above the asphalt surface. The samples were exposed to hydrogen or nitrogen plasmas for 60 minutes with microwave power set at 260 watts. The experiment that used the hydrogen plasma showed a lower overall conversion but produced significantly more distillate than the test that used the nitrogen plasma. Compared to the corresponding tests that used an 8-mm initial distance between the interior plasma tube and the sample, both of these tests showed increased distillate production. Compared to the corresponding tests that used an 8-mm initial distance, overall conversion was lower for the test using hydrogen and slightly higher for the test using nitrogen.

Tests 3-9 and 3-10 duplicated Tests 3-7 and 3-8 except for the microwave power. In these tests, the samples were exposed to hydrogen or nitrogen plasmas for 60 minutes with microwave power set at 200 watts. The experiment that used the hydrogen plasma showed a slightly higher overall conversion and produced significantly more distillate than the test that used the nitrogen plasma. Compared to the corresponding tests that used higher power, these experiments resulted in lower overall conversion and less distillate production. Distillate represented a larger percentage of the total product for both tests than for the corresponding tests that used higher power.

In Tests 3-11, 3-12, and 3-13, the sample was moved closer to the microwave applicator as the tests progressed. In these tests, the position of the interior tube with respect to the sample surface remained constant while the entire reactor was raised so that the distance between the sample and the microwave applicator was decreased.

In Test 3-11, the sample was exposed to a methane plasma for 30 minutes. As the test progressed, the reactor was raised so that the distance between the sample and the microwave applicator was decreased to half the initial distance by the end of the test. This test resulted in a lower overall conversion than either of the previous tests that used methane plasmas. However, more feed was converted to distillate, and distillate represented a larger percentage of the total product in this test than in previous tests using methane plasmas.

In Test 3-12, the sample was exposed to a hydrogen plasma for 169 minutes. As the test progressed, the reactor was raised so that the sample was inside the microwave applicator at the end of the test. This test produced considerably less distillate than the tests using the hydrogen plasma in which the interior plasma tube was lowered toward the sample even though overall conversion was high. The major product from this test was gas. Solids and distillate were produced in nearly equal amounts.

In Test 3-13, the sample was exposed to a hydrogen plasma for 66 minutes. As the test progressed, the reactor was raised so that the sample was just below the microwave applicator at the end of the test. These conditions gave a low overall conversion with minimal distillate production. The conversion and product distribution for this test were very similar to those of Test 3-3.

In Test 3-14, the asphalt was placed within the plasma rather than downstream of the discharge. This experiment used a Kenmore kitchen-type microwave oven and a 250-ml round-bottom quartz flask configured to maintain a flow of hydrogen at a pressure of ~6 torr. The asphalt was coated around the circumference of the flask, and the flask was placed in the microwave oven fitted with a choke through which the gas flow connections were made. In this experiment, the sample was exposed directly to the hydrogen plasma for 15 minutes. This experiment resulted 100% conversion to gas and solids, with no distillate production.

In Tests 3-15 and 3-16, the sample was heated under nitrogen in the absence of a plasma using the same reactor and gas flow rate as in the tests with a plasma. In Test 3-15, the sample was heated for 30 minutes using a small flame from a laboratory burner. In Test 3-16, the sample was heated at 475 °C for 60 minutes in an electric tube furnace. In Test 3-15, about 50% of the sample was converted to products. The majority of the product was distillate, with very little gas production. Test 3-16 gave a greater overall conversion with increased distillate and gas production. Solids were produced in similar amounts in both of these thermal tests.

The production of distillate in the tests that used nitrogen plasmas shows that some distillate was produced by strictly thermal processes. A probable thermal influence is also indicated by the changes in distillate production associated with changes in position of the sample with respect to the discharge. However, more distillate was always produced in the tests that used plasmas containing potentially reactive hydrogen species than in similar tests that used nonreactive nitrogen plasmas. This result indicates that reactive hydrogen in the plasma may be responsible for some conversion of heavy oil to distillate.

For similar conversions, the strictly thermal tests (3-15 and 3-16) showed more distillate and less gas production than the tests that used plasmas. This result may be explained by conversion in the vapor phase of some of the distillate to gas as the products passed, albeit briefly, through the plasma zone.

Tables 5, 6, and 7 show the results of C, H, N, S elemental analyses of the feedstock, distillate product, methylene chloride soluble resid, and methylene chloride insoluble solids from selected Series 3 tests. Tests marked with an asterisk (*) in the sulfur column did not generate sufficient amounts of distillate or solids for sulfur analyses. Duplicate analyses of several samples did not exhibit good repeatability. Therefore, these results are presented only as a qualitative indicator of whether the plasma reactions were effective in removing sulfur from the hydrocarbon matrix.

The results of the elemental analyses of the various products of these exploratory experiments indicate that exposure to hydrogen-rich plasmas does not selectively abstract sulfur from the hydrocarbon matrix. While some tests show a modest reduction in sulfur in the distillate product, the greatest reduction shown (~28%) is too small to be significant in terms of a desulfurization process. Also note that the same reduction in sulfur was attained by simply heating the sample under nitrogen with no plasma exposure (Test 3-15).

Table 5. C, H, N, S Analyses of Distillate Product From Selected Series 3 Experiments

Test #	C	H	N	S	H/C
feed	80.7	10.4	0.7	6.1	1.55
3-12	82.2	8.2	0.7	*	1.20
3-13	75.8	8.4	0.8	4.4	1.33
3-2	87.8	7.5	0.8	*	1.03
3-5	84.5	8.2	0.9	7.5	1.16
3-6	80.7	9.5	1.0	6.2	1.41
3-8	81.9	9.8	0.8	4.4	1.67
3-15	81.9	11.4	0.5	4.4	1.67
3-16	79.8	11.2	0.5	*	1.68

Table 6. C, H, N, S Analyses of Methylene Chloride Soluble Resid From Selected Series 3 Experiments

Test #	C	H	N	S	H/C
feed	80.7	10.4	0.7	6.1	1.55
3-12	77.7	6.8	1.1	4.2	1.05
3-13	58.0	8.7	1.0	6.0	1.49
3-2	92.1	8.8	1.6	5.6	1.15
3-5	58.9	7.3	1.1	5.9	1.49
3-6	78.1	8.1	1.6	6.6	1.24
3-8	71.5	7.6	1.6	6.4	1.28
3-15	76.2	9.5	1.1	5.3	1.50
3-16	78.5	8.9	1.3	4.7	1.36

Table 7. C, H, N, S Analyses of Methylene Chloride Insoluble Solids From Selecte Series 3 Experiments

Test #	C	H	N	S	H/C
3-12	69.0	4.0	2.2	4.8	0.70
3-13	86.2	2.9	1.9	3.4	0.40
3-2	87.1	3.5	1.7	2.0	0.48
3-5	74.9	4.4	2.3	4.5	0.70
3-6	74.7	3.5	2.6	*	0.56
3-8	79.0	4.8	2.5	4.5	0.73
3-15	84.8	3.5	2.5	*	0.50
3-16	84.1	5.0	2.5	4.6	0.71

In general, the distillate product from the tests that used reactive plasmas (generated from either hydrogen or methane) appears to be more aromatic than the feedstock and the corresponding products from the tests that used nonreactive nitrogen plasma or simple heating without plasma. This result indicates that the reactive plasmas under the conditions used for these tests do not add hydrogen but rather tend to abstract hydrogen from the hydrocarbon matrix, forming aromatics that are more stable in the plasma environment (Boenig 1988). While this result appears to be at odds with those reported by Amano and co-workers, Amano used a much greater distance between the sample and discharge than was used in this study. The greater distance used by Amano would tend to limit thermal effects of the plasma and thus could lead to more saturated products.

SUMMARY AND CONCLUSIONS

Exploratory experiments have been conducted on the use of various plasmas as an alternative to catalytic desulfurization processes. In these exploratory experiments, samples of high-sulfur asphalt were exposed to microwave-induced plasmas, and conversion to distillate, gas, and solids was measured. The results of these experiments indicate that there was generally some reaction of the plasma species with the asphalt feedstock, but the results did not indicate that reactive plasma species selectively abstracted sulfur from the hydrocarbon matrix to any great extent.

One test using hydrogen plasma produced a distillate with 28% less sulfur than the feedstock; however, this level of desulfurization is minimal when compared to that obtained by catalytic hydrodesulfurization processes. This same level of sulfur removal was attained in a control experiment in which the asphalt was simply heated under nitrogen without the use of plasma. The results of these exploratory experiments do not indicate that heavy oils can be desulfurized using a simple plasma process.

REFERENCES

Amano, A., M. Yamada, T. Shindo, and T. Akakura, 1984, "Coal Liquefaction Induced by Hydrogen Atoms." *Fuel*, 63: 718-719.

Amano A., M. Yamada, T. Shindo, and T. Akakura, 1985, "Characterization of Liquid Product from the Reaction of Coal with Hydrogen Atoms." *Fuel*, 64: 123-124

Boenig, Herman V., *Fundamentals of Plasma Chemistry and Technology*, Technomic Publishing Company, Inc., Lancaster PA, 1988, 70 pp.

Cominsky, R.J., J.S. Moulthorp, W.E. Elmoreand, T.W. Kennedy, "SHRP Materials Reference Library Asphalt Selection Process: Rept. No. SHRP-IR-A-89-002," Strategic Highway Research Program, Washington, DC, 1989, 31 pp.

Gary and Handwerk, 1975, *Petroleum Refining Technology and Economics*, Marcel Dekker, Inc., 32 pp.

Haugsjaa, Paul O., 1986, "Microwave discharges in termination fixtures: An improved laboratory technique for exciting electrodeless discharges." *Rev. Sci. Instrum.* 57 (2): 167-169pp.

Sanford, Emerson C., "Influence of Hydrogen and Catalyst on Distillate Yields and the Removal of Heteroatoms, Aromatics, and CCR over a Wide Range of Conversions," *Energy and Fuels,* 1994, 8, 1276-1288.

Speight, James G., 1981, *The Desulfurization of Heavy Oils and Residua*, Marcel Dekker, Inc., pp 88-118

WRI-98-R028

WESTERN RESEARCH INSTITUTE
"Providing solutions to energy and environmental problems"

FINAL REPORT

PROCESS SUPPORT AND DEVELOPMENT FOR COMPCOAL™

Prepared for
U.S. Department of Energy
Morgantown, West Virginia

March 1998

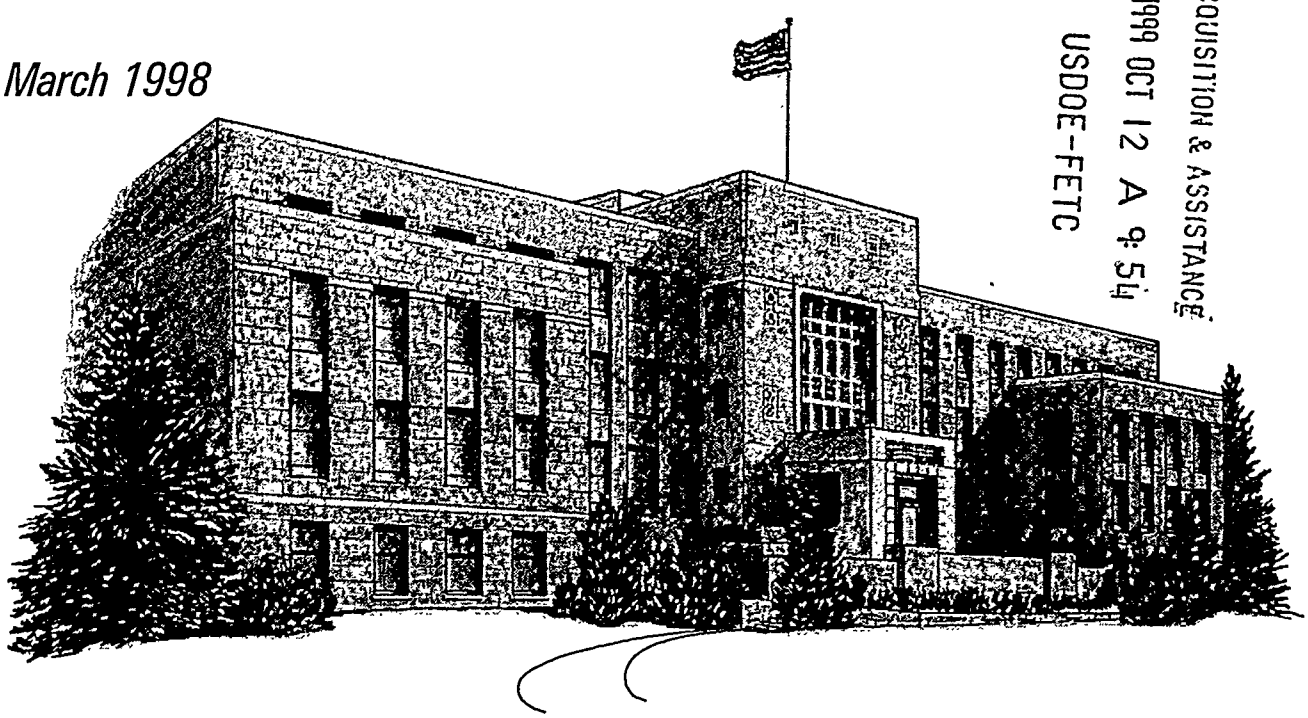

WRI-98-R028

PROCESS SUPPORT AND DEVELOPMENT FOR COMPCOAL™

Final Report

March 1998

By Norman Merriam

Work Performed Under Cooperative Agreement
DE-FC21-93MC30126 Subtask 2.4

For
U.S. Department of Energy
Office of Fossil Energy
Federal Energy Technology Center
Morgantown, West Virginia

By
Western Research Institute
Laramie, Wyoming

DISCLAIMER

TABLE OF CONTENTS

LIST OF FIGURES AND TABLES

EXECUTIVE SUMMARY

Powder River Basin (PRB) coal is relatively dusty and more subject to spontaneous combustion than bituminous coals. PRB coal and other low-rank coals tend to be highly reactive when freshly mined. They must be moved regularly (every week or two) to avoid ignition when fresh, but they become somewhat more stable after they have aged for several weeks. Coal has traditionally been dried to save on transportation costs, increase the heating value and selling price, prevent handling problems caused by freezing, improve the quality of coal used for coking and processing, improve efficiency and reduce maintenance of boilers, and increase the capacity of coking ovens. Drying western coal is likewise seen as an opportunity to increase the potential market for the product.

The principal deterrents to the use of thermal drying prior to shipment of western coals have been connected with problems of shipping and handling fine, dried products. Also, boilers designed for coal with a high heating value must be significantly derated if raw western coal, which has a lower heating value, is used as fuel. Nevertheless, a number of companies are developing drying processes for Powder River Coal. They have learned a great deal about processing PRB coal and continue to advance the technology. Other research, including that of Western Research Institute, is also adding to the store of know-how needed to successfully process PRB coal. It is expected that these continued efforts by many people will result in the profitable operation of at least one coal upgrading plant in the Powder River Basin within the next four to five years.

INTRODUCTION

Coal has traditionally been dried to save on transportation costs, increase the heating value and selling price, prevent handling problems caused by freezing, improve the quality of coal used for coking and processing, improve efficiency and reduce maintenance of boilers, and increase the capacity of coking ovens.

Coal drying was used in Europe before World War II, and the practice became widely used in the United States during the 1950s and 1960s. Early coal drying in the United States was largely confined to bituminous coals having low inherent moisture and was often done to remove moisture accumulated on the coal by wet processing used for coal cleaning. The need to dry coal was intensified by increased mechanization and increased beneficiation of coal, both resulting in increased production of fines. The development of the western coal mining industry presented new problems for those drying western coal.

Fluidized bed drying became widely used in the United States during the 1960s. In fluidized bed drying, a hot flue gas is generated by burning coal fines. The hot flue gas, having a low oxygen content, contacts a bed of coal in a dryer at a high velocity, causing the coal to flow like a fluid. The heat in the gas dries water from the coal and blows the dust from the dryer. Evaporation of the water from the surface of the coal prevents the temperature of the coal from rising. If all of the water is removed from the surface of the coal, the temperature of the coal increases rapidly. These processes work well as long as all operations continue without disturbance. However, upsets in the system, such as a temporary interruption in the flow of wet coal into the dryer, can result in hot gas with a higher than normal oxygen content contacting the coal while the temperature of the coal is abnormally high. This can result in fires and explosions in the drying systems. Consequently, it is common practice to leave some water on the coal to limit the temperature of the coal to well below that needed for ignition. Also, dryers often have special control systems, built in sprinkler systems, and blowout doors to limit or control damage resulting from fires and explosions.

EARLY ATTEMPTS TO DRY WESTERN COALS

Characteristics of Western Coals

Powder River Basin (PRB) coal is relatively dusty and more subject to spontaneous combustion than bituminous coals. PRB coal and other low-rank coals tend to be highly reactive when freshly mined. These reactive coals must be moved regularly (every week or two) to avoid ignition when fresh, but they become somewhat more stable after they have aged for several weeks.

The different character of low-rank western coals was recognized early (Luckie and Draeger 1976) in the development of mining in the Powder River Basin, Wyoming. These authors, who were adapting the McNally Flowdryer to western coals, used the generic term "western coals" to mean coals characterized by their high moisture content and weathering behavior, and they reported the moisture content and drying characteristics of western coals to be "quite different from bituminous coals." They also reported that "an examination of western coals would not be complete without a discussion of moisture readsorption and autogenous heating...and western coals exhibit a much greater tendency toward autogenous heating..." They cited references postulating that the autogenous (spontaneous) heating is caused by low-temperature oxidation and the heat released by wetting the dried coal when moisture is readsorbed. They suggested these problems could be overcome by: cooling the dried coal to ambient temperature; controlled pretreatment (oxidation and addition of moisture) of dried coal; addition of oxidation inhibitors to dried coal; and coating of dried coal. The tests resulted in a dried subbituminous coal containing 12 wt % moisture. (Residual moisture is commonly left on dried coal to counteract the tendency for dried coal to be dusty and to exhibit spontaneous heating.)

Hand (1976) reported that tests with the Parry dryer, which was developed by the Colorado School of Mines Research Institute for western subbituminous coal and lignite drying, used a residual moisture content of 1.5 to 3.0 wt % as an objective when drying subbituminous coal from the Powder River Basin of Wyoming and lignite from the Denver Basin in Colorado. Considerable reduction in particle size was noted with the dried coals. Number 6 fuel oil and asphalt emulsions were used to coat dried lignite to decrease the tendency of the product to spontaneously combust. Hand reported that the principal deterrents to the use of thermal drying prior to shipment of western coals were connected with problems of shipping and handling fine, dried products.

Reason for Drying

A study published in 1980 (Anonymous 1980) based on work by James Kindig of Hazen Research and Patrick Phillips of Rocky Mountain Energy Co. and using capital cost estimates for thermal drying from McNally Pittsburgh Manufacturing Corporation compared the results of the use of wet and dry Decker coal with Illinois Monterey coal. The tests were conducted at the Commonwealth Edison Powerton generating station near Pekin, Illinois. The tests indicated that the dried Decker coal was comparable or equal to Monterey coal on normal and maximum steam flow, feeder speed, and oxygen. The study also indicated that a boiler designed for coal with a high heating value must be significantly derated if raw western coal, which has a lower heating value, is used as fuel. Thus, drying western coal was seen as an opportunity to increase the potential market for the product.

Arco Process

Anaconda Minerals Co., which was later joined by Atlantic Richfield Company (Arco), developed a drying process for PRB coal during the early 1980s by using a 4 ton/hour pilot plant in

Tucson, Arizona. The fluidized bed drying process used conventional equipment with a proprietary product treatment step (Skinner et al. 1984). The developers conducted laboratory research to determine methods to avoid low-temperature oxidation of the product. They developed methods using cooling, controlled preoxidation, treatment with carbon dioxide, and spray application of oil or chemical solution. The process was licensed to Kaiser Engineers.

In describing the process, Kaiser Engineers (1989) noted that the process was particularly suited to subbituminous coals, whose moisture could be reduced from 30 wt % to 10 wt %. The Kaiser report referred to proprietary technology developed during a 10-year research program by Arco Coal Company and stated that an important feature was the deactivation treatment of the dried and cooled coal. According to the report, deactivation prevented moisture readsorption and reduced dust problems associated with the fines by coating the dried coal with a material that was virtually solid at room temperature.

Low-Temperature and High-Temperature Drying

Many efforts have been made to overcome the problems of dust formation and spontaneous heating while keeping the cost of processing within the very competitive limits of the markets for coal. The University of North Dakota Energy Research Center explored the use of various drying techniques to upgrade low-rank coals (Willson et al. 1987). They found that coals dried at low temperature readsorb moisture after cooling and return to essentially the original equilibrium moisture level. In contrast, they found that the processes using temperatures high enough to alter the structure of the coal particles resulted in reduced readsorption of moisture. They also concluded that the lowered equilibrium moisture levels resulted from the removal of carbon dioxide from the coal during high-temperature drying.

In a typical low-temperature drying process, the coal bed is contacted by hot gas to evaporate moisture and carry it from the coal bed. The temperature of the coal bed remains low (150 to 200°F) until nearly all the surface water is removed from the coal because the evaporation of moisture cools the coal. Thus, drying processes that leave moisture on the coal are low-temperature processes. High-temperature processes must remove all of the moisture from the coal to raise the temperature of the coal to the 500°F and higher temperatures at which significant structural changes occur in the coal. The readsorption of moisture by coals dried at temperatures lower than a few hundred degrees F is consistent with experience at Western Research Institute (WRI) (Boysen et al. 1990). WRI also experienced substantial reduction of equilibrium moisture in coals dried to temperatures above 500°F (Merriam and Turner 1993).

Dried (or processed) PRB coal is even dustier and more susceptible to spontaneous combustion than the raw coal. Also, PRB coal dried at low temperature typically readsorbs about two-thirds of the moisture removed by drying (Boysen et al. 1990). This readsorption of moisture releases

the heat of adsorption of the water, which is a major cause of spontaneous heating of low-rank coals at low temperature. In some of the high-temperature coal drying processes, moisture is added to the coal as part of the cooling operation or after the coal has been cooled to reduce the tendency of the dried coal to readsorb moisture during storage.

ACTIVITIES RELATED TO PROCESSING PRB COAL

AMAX Dryer

AMAX Coal Company pioneered development of PRB coal by being one of the first companies to open a mine in the Powder River Basin. AMAX constructed a dryer at its Belle Ayr mine in 1988 and continued development with pilot-plant briquetting tests. In the process, coal was dried by contact with a hot stream of fluidizing gas (Figure 1). The gas comprised flue gas from the combustion of coal dust, air, and recycled gas. The hot drying gas contained less than 5% oxygen. The dried coal, which contained 12 to 13 wt % moisture, entered the cooler at 180 to 190°F where it was cooled to about 100°F by contact with air. The cooled product was mixed with 2 to 4 gallons of number 6 fuel oil per ton to control product dustiness and help inhibit readsorption of moisture. The Lien article (1990) discussed problems caused by loss of feed and degradation of particles in the dryer. It also stated that a major concern has been the stability of the product.

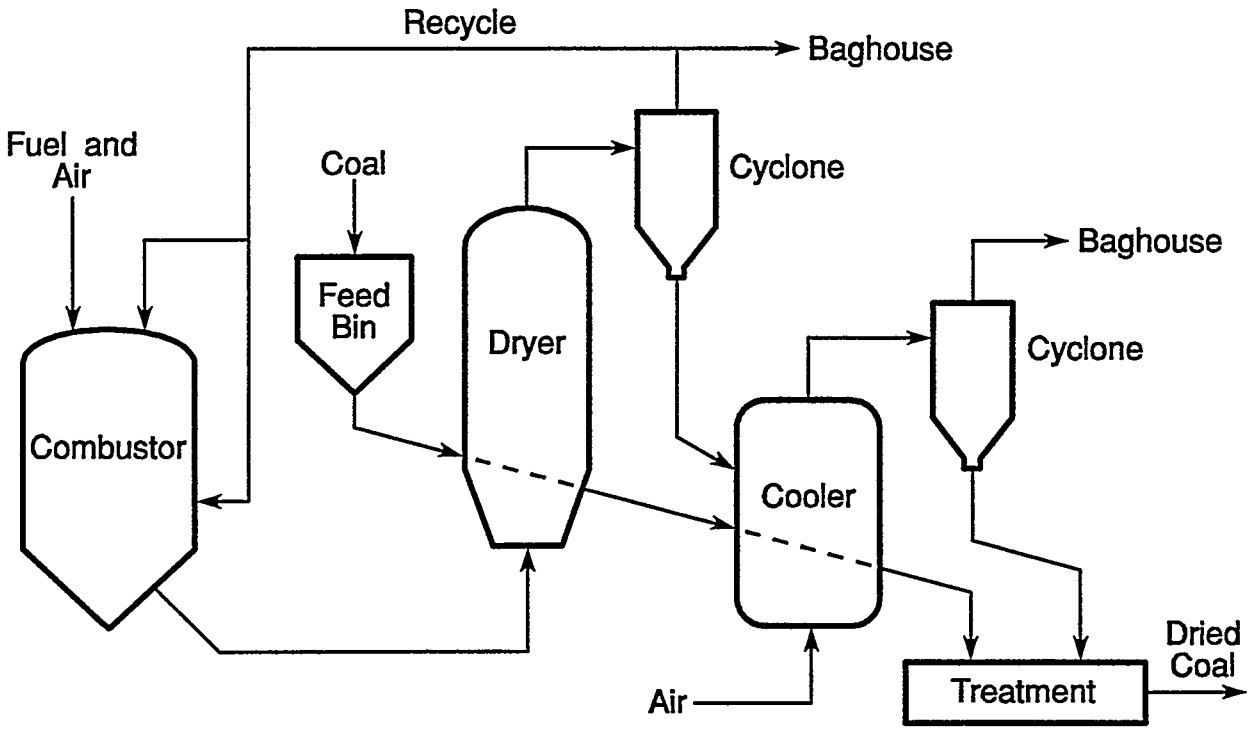

Figure 1. Coal Drying System Used at the AMAX Belle Ayre Mine

AMAX Coal Company conducted pilot plant briquetting tests (Woessner et al. 1993) to develop methods for improving the handling and storage characteristics of fines from the drying operation and to reduce the dust problem with dried coal. This program includes an intensive testing and evaluation effort to control the quality of the briquettes produced. The developers have determined conditions that permit formation of acceptable physical strength in briquettes but report that they have not yet overcome spontaneous heating problems in stockpiles of briquettes.

K-Fuel® Process

Koppelman was awarded patents (U.S. Patents 4,728,339 and 5,071,477) for use of temperatures of 200 to about 1200°F, pressures of 300 to about 3000 psig, and residence times of 1 minute to 1 hour to process organic carbonaceous materials (coal) to effect a desired physical and chemical modification...whereby a substantial reduction in the residual moisture content...[is realized] to improve physical properties, including increased heating value. The second patent describes the use of steam at high pressure to effect a controlled thermal restructuring, with the upgraded product possessing increased heating values. These patents are the basis for the K-Fuel® Process.

The rights to the K-Fuel® Series B technology were purchased by Heartland Fuels Corporation (HFC), a holding of Wisconsin Power and Light (WP&L). In the Series B Process, coal is fed into a reactor at atmospheric pressure (See Figure 2). The coal is then contacted by high-pressure steam, removing the moisture from the coal and altering the structure of the coal to form a fuel with high heating value and low moisture. Some of the sulfur in the low-sulfur coal is removed during the processing. The typical product has a heating value of about 12,000 Btu/lb and contains about 1% moisture. Following intensive pilot plant testing and completion of a preliminary design, HFC is seeking financing to construct a commercial-scale plant at a mine in the Powder River Basin.

Syncoal Project

The Syncoal Process is used at a Clean Coal I demonstration plant located at Western Energy Company's Rosebud mine near Colstrip, Montana. The Rosebud Syncoal Partnership is a partnership between Western Energy Company, a subsidiary of Montana Power Company's nonutility group, and a subsidiary of Northern States Power. In the Syncoal Process, coal is passed through two vibrating fluidized bed reactors (Figure 3) where it is contacted by hot gas at low pressure to dry the coal and remove carboxyl groups and volatile sulfur compounds. The process is designed to heat the coal sufficiently that a small amount of tar is released to seal the dried product from reaction with oxygen. The hot, dried coal is cooled to below 150°F by direct contact with a spray of water and a vibratory fluidized cooling stage. The dried coal is further desulfurized by pneumatically separating pyrite-rich ash (Western Energy Company 1992).

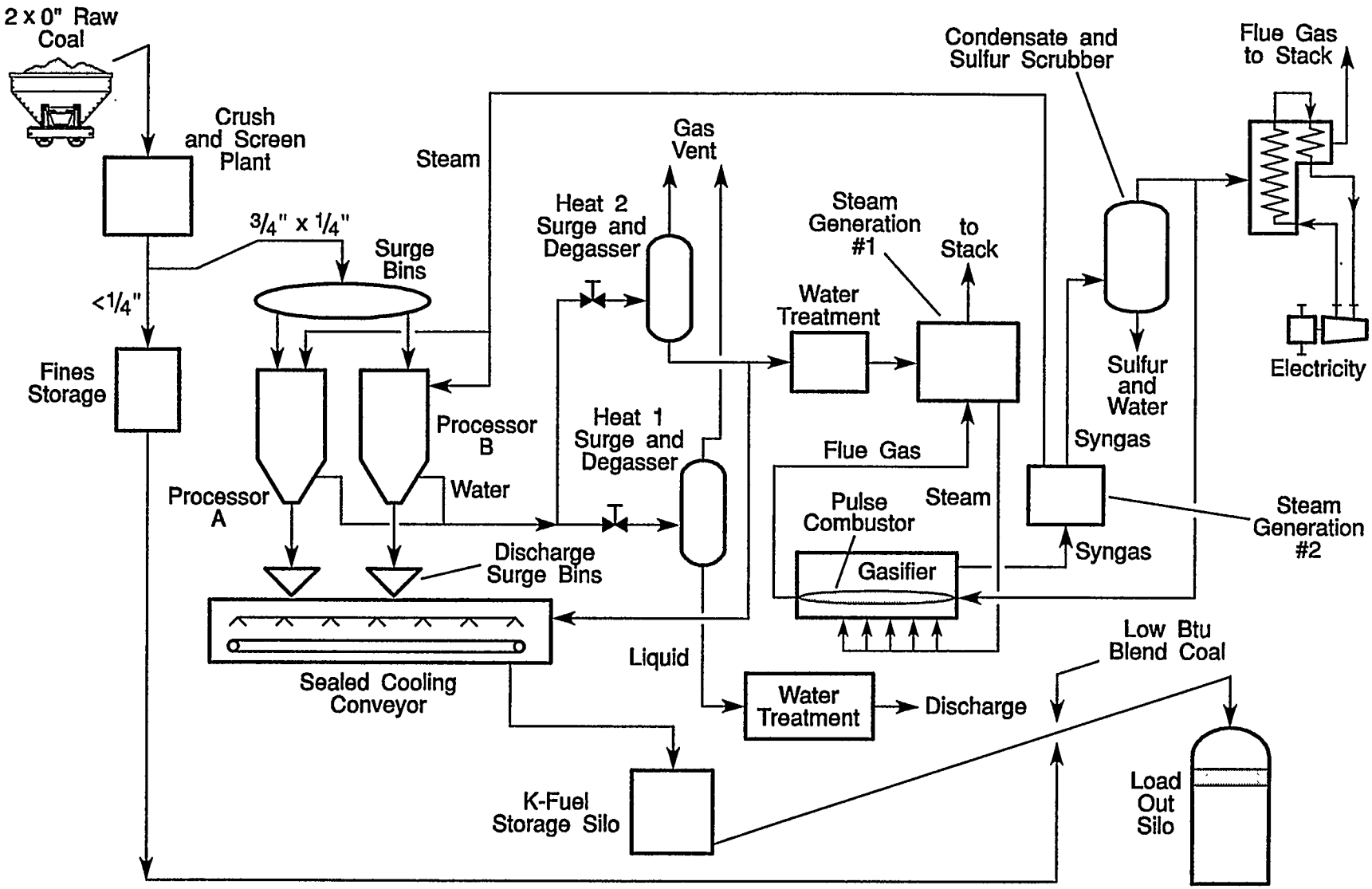

Figure 2. Process Schematic of K-Fuel® Series B Process for Planned Commercial Plant

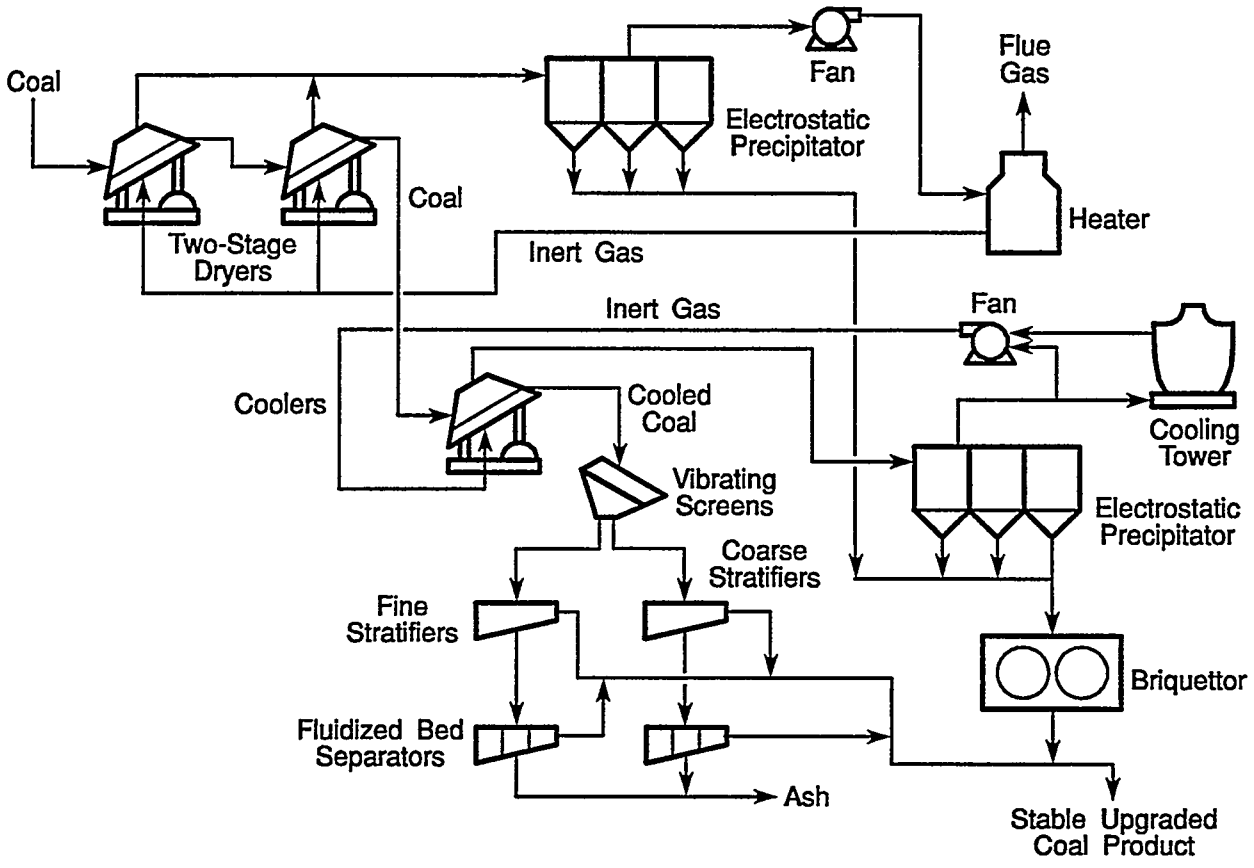

Figure 3. Syncoal Process Used at Western Energy Company's Rosebud Mine

The 1,000 tons per day demonstration plant began operating in April 1992. The nominal production of the plant is 988 tons per day of coarse coal and 240 tons per day of briquetted fines. As operational testing has proceeded, dustiness and stability have emerged as product quality issues (Sheldon and Heintz 1993). Problems developed when it was discovered that the product began to spontaneously heat after sitting in a silo for two days (Pittsburgh Energy Technology Center Review 1993). When it became obvious that the spontaneous combustion problem had not been solved, research personnel from Pittsburgh Energy Technology Center began work to help Rosebud Syncoal solve the problem. The Syncoal engineering team is developing a product stabilization unit process step, which is currently being tested in a 500 lb/hr unit and which will be incorporated into the demonstration plant next year if it is successful. The dust handling equipment was modified to upgrade that system in August 1993.

Carbondry™ Process

The Carbondry™ Process (Simmons and Simmons 1992) has been tested at the pilot-plant scale at Carbontec's facility at Bismarck, North Dakota. The process involves a hot oil first stage drying unit to drive moisture from the coal and a hot flue gas second stage drying unit to complete drying of the moisture coated coal. The dryers operate at atmospheric pressure in the 260 to 420°F temperature range. Coal flows through both stages of drying on a wire mesh conveyor belt. The process uses a coating of oil on the surface of particles to protect against readsorption of moisture and spontaneous heating. Published data indicate that the product made from PRB coal using the process contains about 6 to 10 wt % moisture and has a heating value ranging from 11,200 to about 11,700 Btu/lb.

The Carbondry™ Process was selected by the U.S. Department of Energy for a Clean Coal IV project in the fall of 1991 (*Clean Coal Today* 1991). The $34 million project provided for a 250,000-ton-per-year plant to be built and operated at the Cordero Mining Company mine near Gillette, Wyoming. The project failed to come to fruition after the mine was sold in early 1992.

ENCOAL Project

The ENCOAL LFC mild gasification process is used at a commercial demonstration facility located at Triton Coal Company's Buckskin mine north of Gillette, Wyoming (McPherson 1992). In the ENCOAL process (Figure 4), coal is fed into a rotary grate dryer where it is heated by a hot gas stream to reduce the moisture content. The temperature of the coal is controlled to avoid emission of significant amounts of methane, carbon dioxide, or carbon monoxide in the dryer. The dried coal is conveyed to the pyrolyzer where it is carefully heated to control the properties of the fuel products. The partially devolatilized solids are quenched and cooled to produce process-derived fuel. Liquid is condensed from the pyrolyzer off gas after removal of particulates to produce coal-derived liquids (ENCOAL Corporation 1990).

The plant, which was built in 1991 and 1992 as part of a Clean Coal III project estimated to cost $73 million, is designed to process 1,000 tons per day of PRB coal. Following the completion of construction in April 1992, the ENCOAL plant entered the start-up phase of the project. The plant was successfully operated for 16 days late in April of 1993 (U.S. Department of Energy 1993) after several mechanical problems were overcome. Following the extended run, the plant was shut down for modifications. The process-derived fuel, which has been tested in a bench-scale combustion unit using samples of several hundred pounds, has not yet attained the same resistance to spontaneous combustion as the SGI pilot-plant samples (McCord et al. 1993). No test burns have been conducted in commercial-size power plants. The economics of the process are not expected to be known until the economic study is completed near the end of the project in 1994.

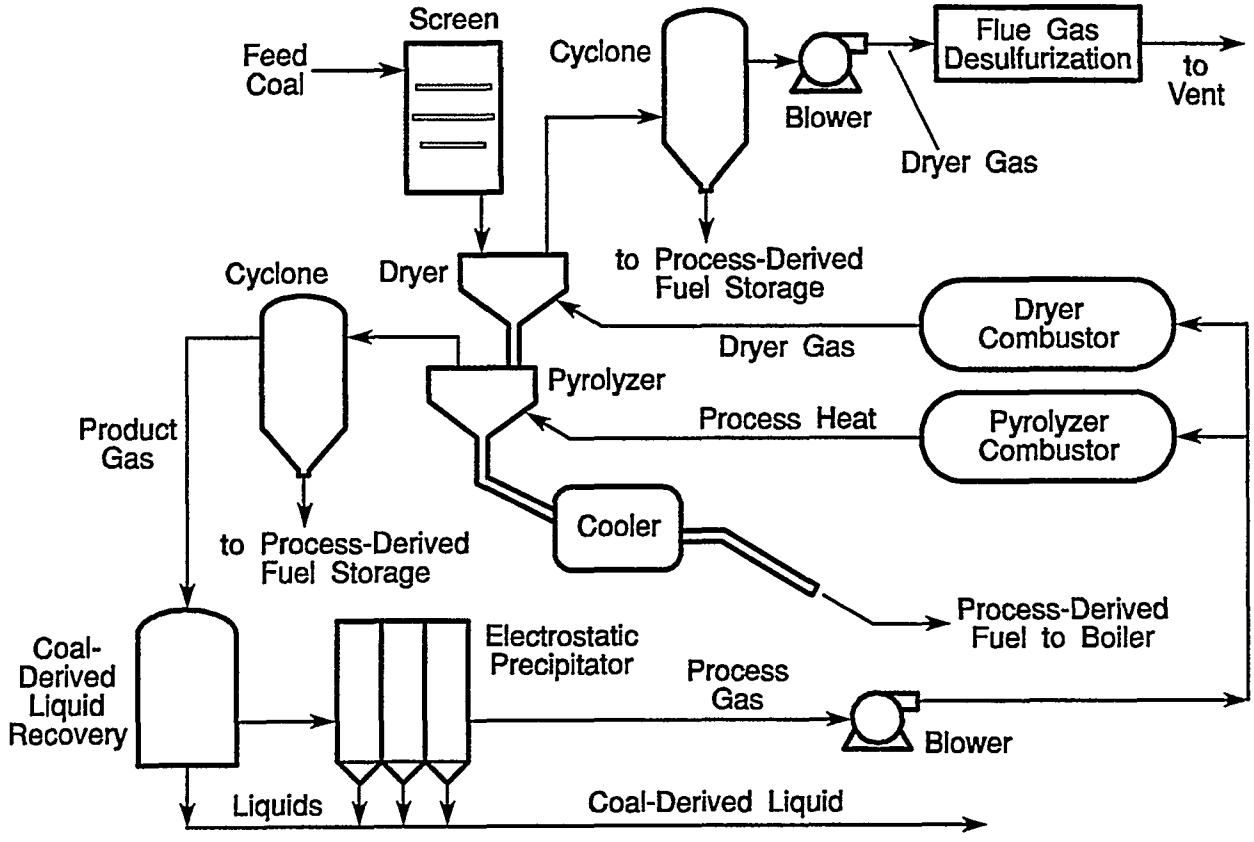

Figure 4. ENCOAL LFC Process Used at Triton Coal Company's Buckskin Mine

BASIS FOR FUTURE DEVELOPMENTS

CANMET Research

Research conducted at CANMET (Ogunsola and Mikula 1992) has shown that liability of dried subbituminous coal and lignite to demonstrate spontaneous combustion can be reduced by treating the dried coals with steam (Figure 4). The effectiveness of the treatment does not increase above temperatures of about 300°C (572°F). This work also shows that liability to spontaneous combustion correlates with the equilibrium moisture content (tendency of the dried coal to readsorb moisture) and the oxygen-containing chemical groups in the coal. Thus, a process that can remove the oxygen-containing chemical groups from the coal and reduce the equilibrium moisture of the dried product should produce a product that is resistant to spontaneous combustion.

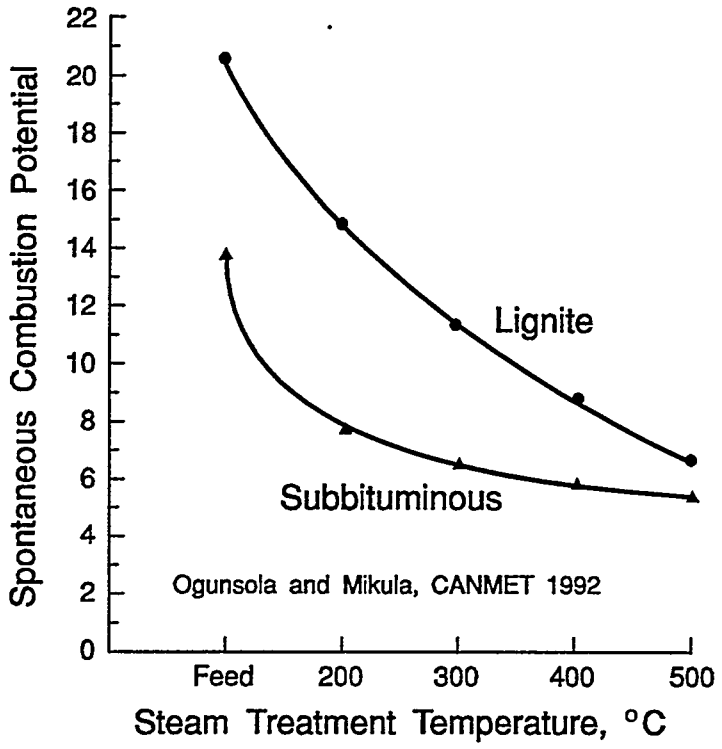

Figure 5. Reduction of Liability to Spontaneous Combustion by Treating With Steam

Exxon Research

Researchers at Exxon (Isaacs and Liotta 1987) showed that weathering of dried PRB coal occurs over a period of about 15 days (Figure 6) in which the freshly dried coal reacts with oxygen from the air to increase the oxygen content of the coal. This oxidation of the coal represents a small change in the composition of the coal (the oxygen-to-carbon ratio increases from 0.19 to 0.21), but we have observed at WRI that this aging substantially reduces the tendency of the dried coal to exhibit spontaneous combustion.

BASIS FOR FUTURE DEVELOPMENTS

Western Research Institute

WRI experience with dried PRB coal is that the dried coal is highly reactive and is frequently observed to ignite spontaneously. The coal is most susceptible to spontaneous combustion when is has been freshly processed. Dried coal that has been aged for several weeks and contacted air is less likely to spontaneously combust than freshly dried coal. This "aging" characteristic has been used by processors in an effort to prevent spontaneous combustion by incorporating a low-temperature oxidation step at the end of some drying processes.

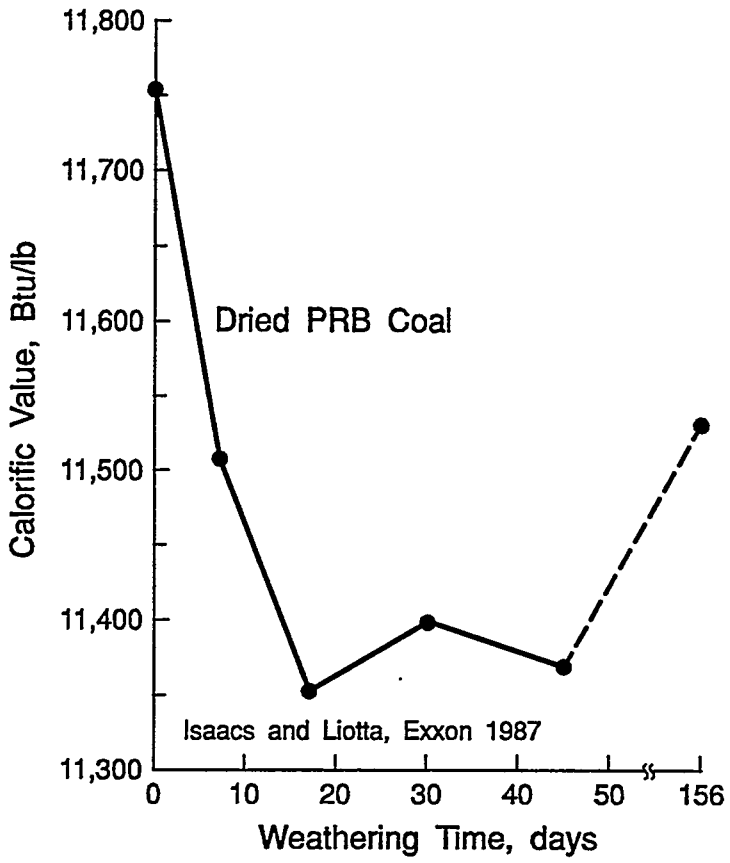

Figure 6. Weathering of Powder River Basin Coal

Low-temperature oxidation reduces the heating value of the coal, reduces its ability to repel moisture, and is known to increase the unburned carbon remaining in the ash following combustion. Ingram and Rimstidt (1984) attributed the increased moisture in naturally oxidized coals to the increase in surface area caused by the physical effects of weathering and an increase in organic acids, which are known to attract water to coal particles. Water molecules are generally thought to attach to polar oxygen sites in coal, although this varies greatly with the different types of coal.

WRI conducted tests intended to compress the "aging" demonstrated at Exxon Research into a period of a few minutes (Merriam and Turner 1993) by reacting the dried coal with very small amounts of air at temperatures of about 650 to 750°F. We were able to control the liability to spontaneous combustion (Figure 7) by controlling the amount of air we permitted to react with the coal (a fraction of 1% of the air required for combustion of the dried coal was used in the aging treatment) and the temperature at which we conducted the "instant aging." Significantly, we found that this reaction of the coal with air in this temperature range caused 12 to 15 times as much oxygen to be removed from the coal as was present in the air reacted with the dried coal (Figure 8).

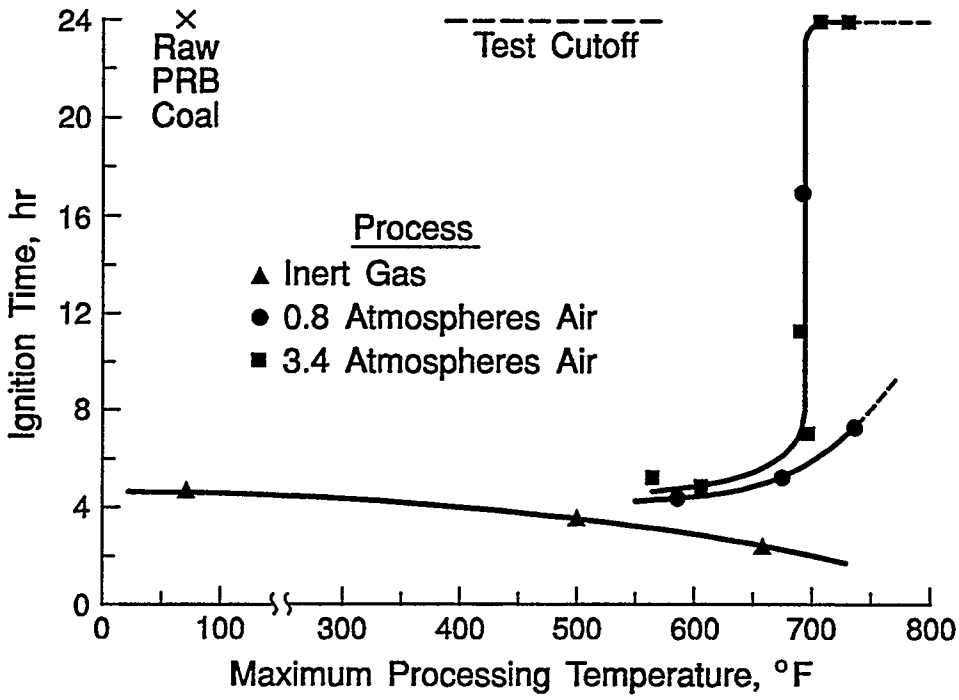

Figure 7. Control of Spontaneous Combustion in Dried Powder River Basin Coal With Air Treatment

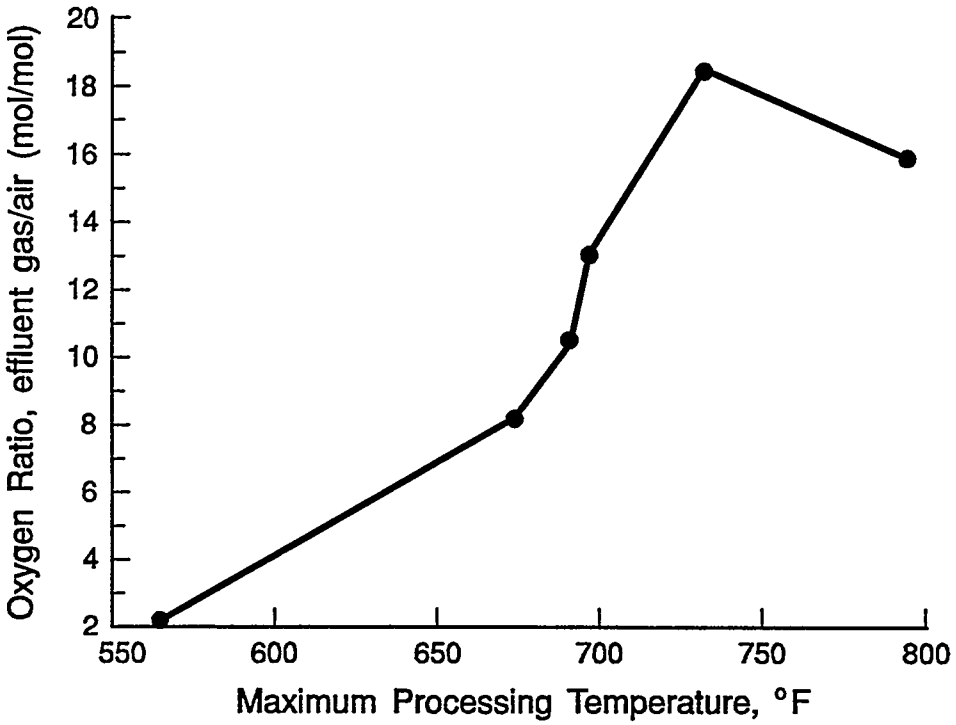

Figure 8. Removal of Oxygen From Dried Powder River Basin Coal Through Air Treatment

We also found that this reaction of the dried coal with air reduced the equilibrium moisture content of the treated dried coal (Table 1). The product from this treatment retains nearly all of the volatiles in place to seal off pores and restrict adsorption of oxygen and has a heating value of 12,000 to 12,700 Btu/lb (Table 2).

Table 1. Equilibrium Moisture Content of Eagle Butte Coal, Dried Coal, Briquettes, and Treated Coal, wt %

	Duplicate Tests	
Eagle Butte Feed Coal	25	26
Dried in Air, 6 hr, 220°F	22	22
Fluid Bed Dried in CO_2 to 550°F	17	17
Briquettes-Dried Coal-10% Fines	14	14
Dried Coal Heated in 3.4 Atm Air and 793°F	10	11
One Millimeter Glass Beads	1	1
Ottawa Sand	0	0

Table 2. Characteristics of the COMPCOAL Product

Test	11	10	12	6
Temperature, °F	565	691	697	708
Volatiles, wt %	40.2	36.7	35.4	34.5
Heating Value, Btu/lb	12,009	12,439	12,600	12,725

Merriam (1993) also found that 70 to 80 wt % of the mercury is removed from the PRB coal when the coal is heated between 300 and 550°F (Figure 9). The mercury is emitted from the coal along with the gases produced during the decarboxylation, which occurs after the water is removed by drying.

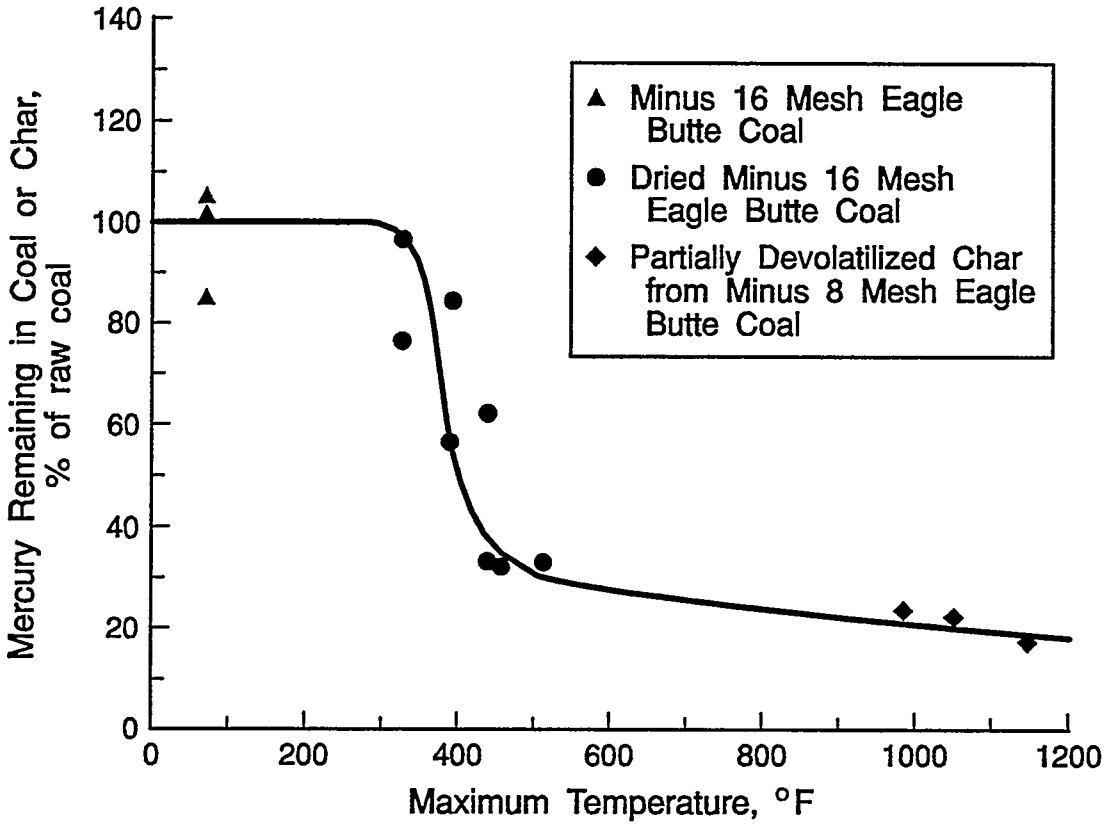

Figure 9. Removal of Mercury from Powder River Basin Coal by Heating

CONCLUSIONS

AMAX, Carbontec, ENCOAL, K-Fuel®, and Syncoal continue to develop their respective processes. They have learned a great deal about processing PRB coal, and continue to advance the technology. Others are also adding to the store of know-how needed to successfully process PRB coal. It is expected that these continued efforts by many people will result in the profitable operation of at least one coal upgrading plant in the Powder River Basin within the next four to five years.

REFERENCES

Boysen, J. E., C. Y. Cha, F. A. Barbour, T. F. Turner, T. W. Kang, M. H. Breggren, R. F. Hogsett, and M. C. Jha, 1990, Development of an Advanced Process for Drying Fine Coal in an Inclined Fluidized Bed, Final Report. Laramie, WY, WRI Report to DOE, DOE/PC/88886-T5.

Clean Coal Today, 1991, Cordero Coal Upgrading Demonstration Project, Fall, 3.

Coal Age, 1980, "Dried Coal is a Better Buy," May, 149-158.

ENCOAL Corporation, 1990, Program Update.

Hand, J. W., 1976, Drying of Western Coal, *Mining Congress Journal*, May, 30-32.

Ingram, G. R., and J. D. Rimstidt, 1984, Natural Weathering of Coal. *Fuel*; 63 (3): 292-296.

Isaacs, J. J., and R. Liotta, 1987, Oxidative Weathering of Powder River Basin Coal, *Energy and Fuels*, 1, 349-351.

Lien, T. J., 1991, AMAX Advances Low-Rank Coal Drying. *Coal*, December, 49-51.

Luckie, P. T., and E. A. Draeger, 1976, The Very Special Considerations Involved in Thermal Drying of Western Region Coals, *Coal Age*; January, 106-109.

Kaiser Engineers, 1989, Proposal for Design, Construction, and Operation of 15-ton/hr Subbituminous Coal Drying Demonstration Plant. Proposal to U.S. DOE, Jan 1989.

McCord, T. G., J. P. Frederick, and W. F. Farmayan, May 1993, The ENCOAL Project: Status of the Plant and Product Testing. 17th Low Rank Fuels Symposium, Energy and Environmental Research Center, Grand Forks, ND.

McPherson, R., 1992, The Next Generation of Power Generation. Coal Market Strategies Tenth Annual Conference, Western Coal Council, Wheat Ridge, CO.

Merriam, N. W., and T. F. Turner, 1993, COMPCOAL™: A Profitable Process for Production of A Stable High-Btu Fuel from Powder Basin Coal. Laramie, WY, WRI Report to DOE, WRI-93-R008.

Merriam, N. W., 1993, Removal of Mercury from Powder River Basin Coal by Low-Temperature Thermal Treatment. Laramie, WY, WRI Report to DOE, WRI-93-R021.

Ogunsola, O. I., and R. J. Mikula, 1992, Effect of Thermal Upgrading on Spontaneous Combustion Characteristics of Western Canadian Low Rank Coals. *Fuel*, vol. 71, January 3-8.

Pittsburgh Energy Technology Center Review, 1993, Problem-Solving Partnerships. Spring 1993, 32-34.

Sheldon, R. W., and S. J. Heintz, August 1993, Rosebud Syncoal Partnership Advanced Coal Conversion Process Demonstration Project. Draft of Report to Second Annual Clean Coal Technology Conference, U. S. DOE, Atlanta, September 1993.

Simmons, J., and J. J. Simmons, 1992, The Carbondry™ Process, An Innovative Approach to Drying Low Rank Coals. Proceedings of Coal Prep '92, McLean Hunter Presentations, Aurora, CO.

Skinner, J. L., L. B. Rothfield, B. F. Bonnecaze, S. W. Johnson, and Y. H. Li, 1984, Drying of Powder River Subbituminous Coal-Overview of a New Process. Coal Technology '84, 7th International Coal and Lignite Exhibition and Conference, Houston, TX.

Tomuro, J., S. Nogita, and Y. NaKamur, 1985, Reduction of Oxidation Rate of Coal by Coal-Derived Tar Coating. Proceedings 1985 International Conference on Coal Science, Pergamon Press, New York.

U.S. Department of Energy, 1993, Wyoming Clean Coal Fuel Plant Sets New Record for Operations. Techline # 2140, May 26,1993.

Western Energy Company, February 1992 Technical Progress Report. Submitted to U.S. DOE Pittsburgh Energy Technology Center.

Willson, W. G., S. A. Farnum, G. G. Baker, and G. H. Quentin, 1987, Low-Rank Coal Slurries for Gasification. *Fuel Processing Technology*, 15: 157-172.

Woessner, P. W., R. F. Hogsett, and K. Avery, 1993, AMAX Coal Briquetting Program, Presentation at the Western Coal Workshop, Gillette, WY, May 1993.

WRI-98-R004

WESTERN RESEARCH INSTITUTE
"Providing solutions to energy and environmental problems"

FINAL REPORT

MISCIBLE/IMMISCIBLE GAS INJECTION PROCESSES

Prepared for
U.S. Department of Energy
Morgantown, West Virginia

March 1998

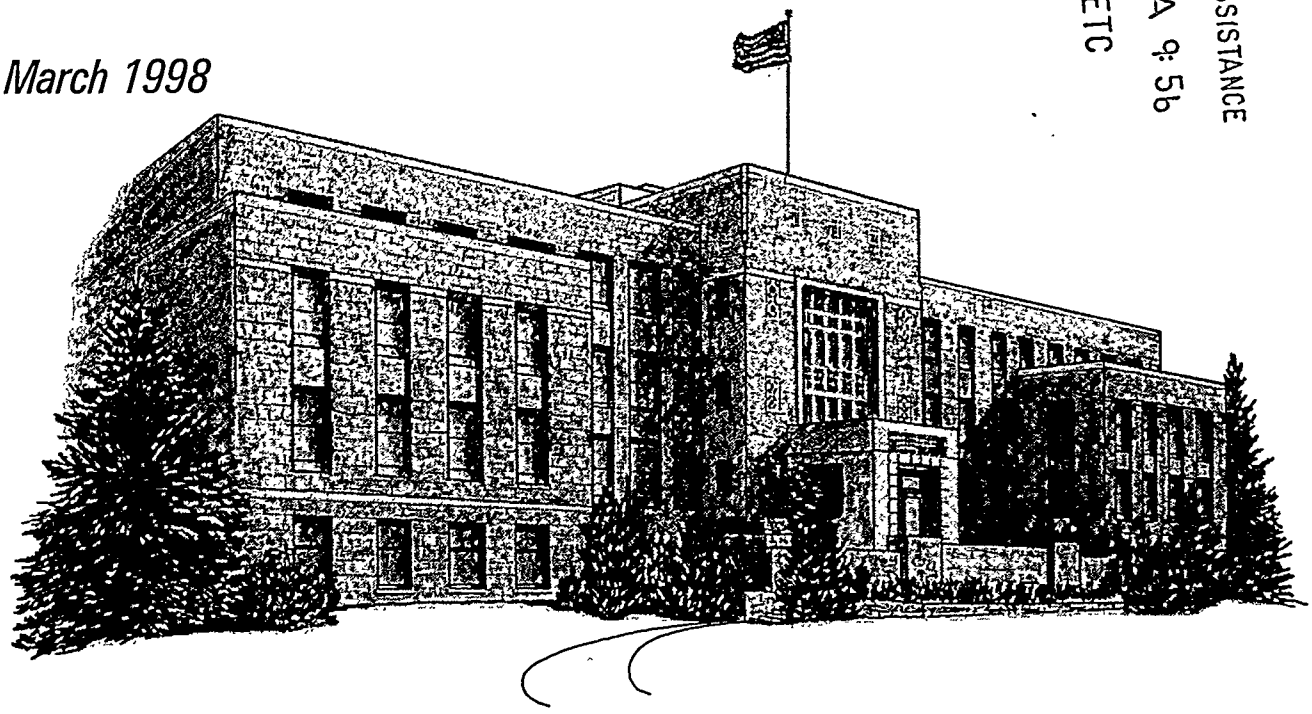

WRI-98-R004

MISCIBLE/IMMISCIBLE GAS INJECTION PROCESSES

Final Report

Reporting Period: February 1996–February 1998

By
L. J. Fahy
C. G. Mones
L. A. Johnson Jr.
F. M. Carlson

March 1998

Work Performed Under Cooperative Agreement
DE-FC21-93MC30126
Subtask 1.2

For
U.S. Department of Energy
Office of Fossil Energy
Federal Energy Technology Center
Morgantown, West Virginia

By
Western Research Institute
Laramie, Wyoming

DISCLAIMER

TABLE OF CONTENTS

LIST OF TABLES AND FIGURES

Table **Page**

Figure **Page**

EXECUTIVE SUMMARY

Gas injection processes are among the oldest fluid injection processes used in petroleum production. The early processes were primarily for pressure maintenance. In its annual production report, *Oil and Gas Journal* (1994) showed that over the past decade, gas injection processes have been the fastest growing form of enhanced production, even though the total number of projects has decreased.

If gas is injected into a rock that is at pseudo-residual oil saturation by waterflooding, it will invade the largest pores first (now filled with water), and water will become the intermediate phase. Water will be nonwetting with respect to the oil and wetting with respect to the gas. If gas is injected into such a system and then followed by water, the water will trap off a portion of the gas, leaving the gas as noncontinuous isolated globules in the large pore space. This trapped gas saturation interferes with the flow of water through the system so that the water, which was easily injected before gas trapping, now must be injected at a higher pressure to maintain the same water injection rate. This higher pressure allows the water to be diverted into the smaller pores still containing oil. Stated another way, the relative permeability to water is reduced by the trapping of gas, and barring solution in the liquid or compression of the gas, this gas will remain trapped and allow for a more favorable mobility ratio of the water to the oil.

The objective of these tests was to demonstrate the effect of gas trapping to enhance oil recovery from an oil-wet reservoir. Rather than treating the sand pack to make it oil-wet, WRI chose to simulate the water flooding of an oil-wet reservoir by using oil to displace water in a water-wet sand pack.

Four tests were conducted during 1996 to evaluate if gas trapping would improve oil recovery after waterflooding in an oil-wet reservoir. One test was planned to evaluate gas trapping when gas was injected alone, followed by renewed water injection. Two tests were planned to evaluate gas trapping when gas and water were co-injected. Two tests were needed to estimate which water:gas ratio would give the better incremental oil recovery.

The fourth test was planned as a base case with only gas injection after waterflooding. Gas trapping would not occur in this test, and any incremental oil recovery after waterflooding could not be attributed to gas trapping and would more closely represent gas interference.

During 1997, five additional tests were conducted to further evaluate the effects of gas trapping. Two tests were repeat runs of tests conducted in 1996 and one test was a base case. The base-case test was an oil injection only test to determine how much additional recovery was occurring

as a result of the gas trapping effect. The last two tests, Tests 8 and 9, were best-case scenarios and were conducted to simulate how gas trapping might be performed in the field.

For all tests, breakthrough occurred after .56 to .77 pore volumes of hexane had been injected, and water recovery at breakthrough varied between 56 and 69.4% of initial water in place.

Incremental water production was noted in seven of eight tests in which additional nitrogen or hexane injection occurred. The third test, a nitrogen:hexane injection test, did not experience the incremental water production response until almost the fifth pore volume, suggesting the nitrogen:hexane ratio was too high. If co-injection had been used, the nitrogen:oil ratio probably should have been approximately one. One of two gas interference tests did not experience incremental water recovery after gas injection.

While incremental water production attributed to gas trapping did occur, it did not occur until at least a pore volume had been injected, but all eight tests did recover more water than the base-case test in which only hexane was injected.

One-dimensional modeling predictions generally agree with the observed tube test incremental recoveries after gas breakthrough, suggesting an additional 5 to 8% incremental oil recovery may be possible if gas trapping is applied to an oil-wet reservoir.

INTRODUCTION

Gas injection processes are among the oldest fluid injection processes used in petroleum production. The early processes were primarily for pressure maintenance. In its annual production report, *Oil and Gas Journal* (1994) showed that over the past decade, gas injection processes have been the fastest growing form of enhanced production, even though the total number of projects has decreased.

Several authors have investigated the effects of gas saturation on oil recovery (Kyte et al. 1956, Land 1968, and Killough 1976). For an oil-wet system, Kyte concluded that an increased gas saturation reduces the injected water volume required to attain oil recovery. This work studies the effect of injecting additional gas after waterflooding has occurred to produce incremental oil in oil-wet systems. The enhancement of oil recovery in oil-wet systems by gas/water co-injection or gas injection followed by water injection results in part from the interference or "trapping" of the nonwetting phase (gas) by the intermediate phase (water).

Marathon (T.G. Monger-McClure, personal correspondence, 1994) and Amoco (M.H. Stein, personal correspondence, 1994) have indicated that there is much interest in carbon dioxide injection to recover oil from water–oil transition zones. It was suggested that these processes are poorly understood, and the effect of wettability may be a key, particularly in the Permian Basin, which is believed to be oil-wet. It is hoped that the results from this gas trapping study will lead to more efficient recovery strategies for the production of oil by gas in such oil-wet reservoirs.

EFFECT OF GAS TRAPPING IN OIL-WET SYSTEMS

It is hypothesized that oil-wet reservoirs can produce additional oil over that obtained by waterflooding alone if gas is also injected so that it can interfere with the flow of water through the rock. When water displaces oil in a two-phase, water–oil system that is oil-wet, it does so first from the largest pores, which predominate. As water saturation increases with continued displacement, smaller and smaller pores are invaded. Such a process is called a drainage process because the wetting phase is being "drained" from the system. As smaller and smaller pores are invaded, higher and higher capillary pressures are required to invade the pores. At some point it is easier for the water to flow through existing pathways than to invade smaller pores, so a pseudo-residual oil saturation is reached. If an agent such as gas, which is more nonwetting than the water, is introduced into the pore space so that it interferes with the water flowing through it, then this pseudo-residual oil can be further reduced. This, in turn, leads to increased oil recovery.

If gas is injected into a rock that is at pseudo-residual oil saturation by waterflooding, it will invade the largest pores first (now filled with water), and water will become the intermediate phase. Water will be nonwetting with respect to the oil and wetting with respect to the gas. If gas is injected into such a system and then followed by water, the water will trap off a portion of the gas, leaving the gas as noncontinuous isolated globules in the large pore space. This trapped gas saturation interferes with the flow of water through the system so water that was easily injected before gas trapping now must be injected at a higher pressure to maintain the same water injection rate. This higher pressure allows the water to be diverted into the smaller pores still containing oil. Stated another way, the relative permeability to water is reduced by the trapping of gas, and barring solution in the liquid or compression of the gas, this gas will remain trapped and allow for a more favorable mobility ratio of the water to the oil.

If gas and water are simultaneously injected into such a system so that both are at equal superficial velocities, again higher pressures in the water phase are attainable as the water is confined to the intermediate and smaller pore space, while the gas occupies the larger pore space. Again, this leads to further reduction in the pseudo-residual oil saturation and increased oil recovery. Here, the mechanism is not gas trapping, but strictly interference of the gas with the water and reduction of relative permeability to water. The gas in this case remains mobile rather than being trapped by water. Simultaneous injection of water and gas has a higher potential to recover oil from the smaller pore space than does the trapping mechanism discussed previously because higher gas saturations (lower relative permeabilities to water) are achievable. This higher potential to recover oil, however, is offset by the fact that the gas is free and highly mobile in the system, leading to less efficient displacement and increased gas requirements.

Finally, if water and gas are simultaneously injected, but at unequal superficial velocities, the displacement mechanism will be somewhere between the trapped gas case and the free gas saturation case.

TEST OBJECTIVE

The objective of these tests was to demonstrate the effect of gas trapping to enhance oil recovery from an oil-wet reservoir.

OPERATING PROCEDURES

Test Apparatus

Gas trapping experiments were conducted in a long tube apparatus, shown in Figure 1. The tube was made from 4.8-cm-dia. schedule 80 pipe, 304.8 cm long. High-pressure flanged connections were installed at each end.

Oil and water were injected by two independent Ruska pumps, while nitrogen was injected from high-pressure gas cylinders. Oil and water injection was metered by calibration of the Ruska pumps. Gas injection was metered by a mass flowmeter. Liquid production was collected and measured manually with a graduated cylinder. Cumulative gas production was measured with a wet-test meter.

Static pressure transducers and gauges were used to measure the tube inlet pressure, the system backpressure, the Ruska pump pressures, and the gas source pressure. The differential pressure (DP) across the tube was also measured when less than 45 kPa (180 inches of water). The injection fluid temperature was also measured at the top of the tube.

All pressures, the gas flow rate, and the injection fluid temperature were monitored with a data acquisition system and the data were stored at five-minute intervals. The oil and water injection rates were read and recorded manually from the Ruska pumps' vernier scales.

Experimental Plan

Four tests were conducted during 1996 to evaluate if gas trapping would improve oil recovery after waterflooding in an oil-wet reservoir. One test was planned to evaluate gas trapping when gas was injected alone, followed by renewed water injection. Two tests were planned to evaluate gas trapping when gas and water were co-injected. Two tests were needed to estimate which water:gas ratio would give the better incremental oil recovery.

The fourth test was planned as a base case with only gas injection after waterflooding. Gas trapping would not occur in this test, and any incremental oil recovery after waterflooding could not be attributed to gas trapping. As described above, this case would more closely represent gas interference.

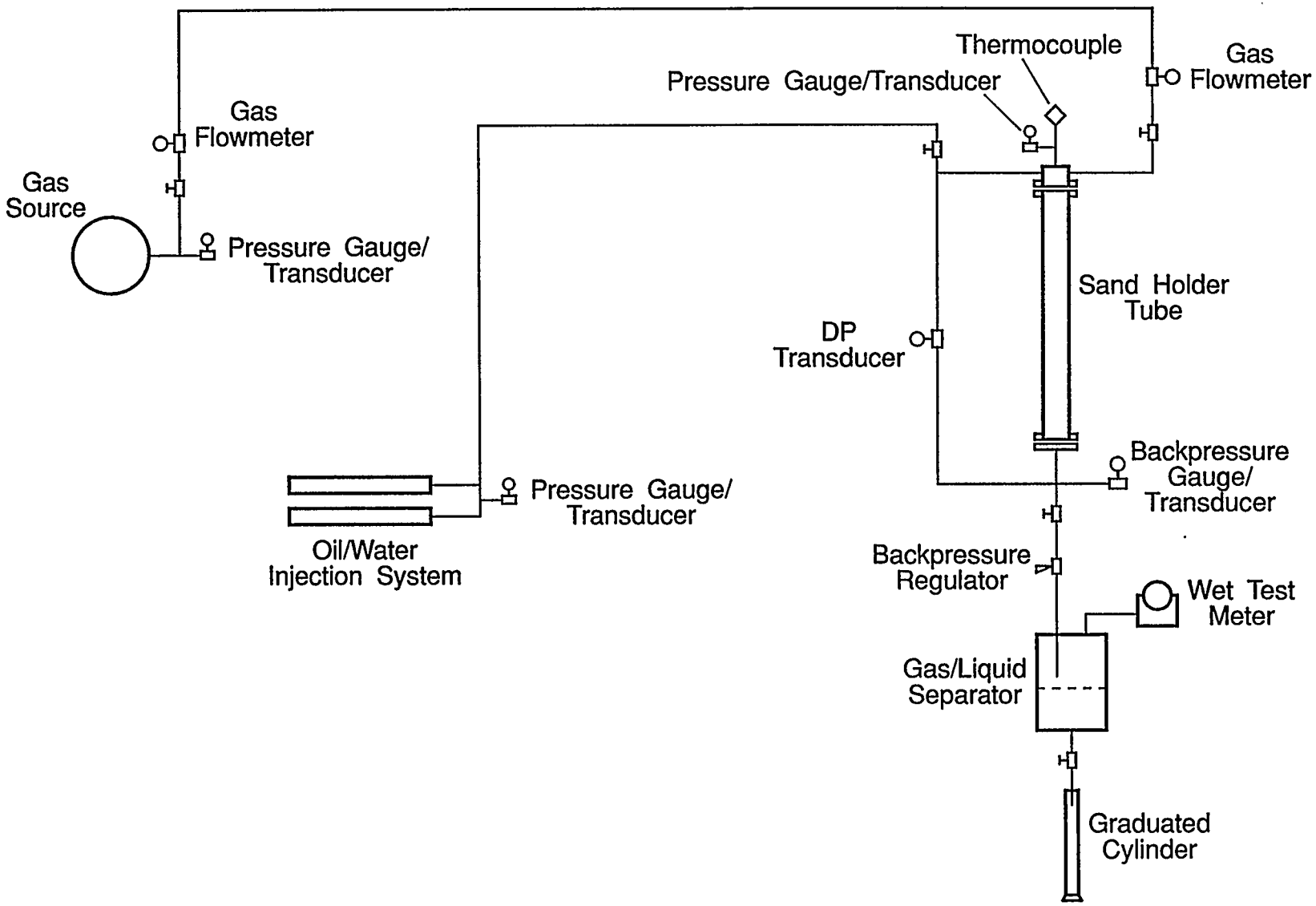

Figure 1. Gas Trapping Test Configuration

During 1997, five additional tests were conducted to further evaluate the effects of gas trapping. The fifth test was conducted to simulate only waterflooding where no gas injection occurred. This test was conducted to provide a baseline to determine how much additional recovery was occurring as a result of the gas trapping or gas interference effects. The sixth test was a repeat of the first test, which was conducted to evaluate gas trapping when gas was injected alone, followed by renewed water injection. The seventh test was a repeat of the fourth test with only gas injection after waterflooding. As in the fourth test, any incremental oil recovery after waterflooding could not be attributed to gas trapping and is probably due to gas interference.

The eighth and ninth tests were best-case scenarios and were conducted to simulate how gas trapping might be applied in the field. It appears that gas injection alone after waterflooding may yield better results than those achieved with gas co-injection. Also, gas trapping in the field is expected to be initiated early in the life of the waterflood. The simulation of the initial waterflooding was done for about 0.3 pore volumes and terminated just prior to breakthrough, leaving more recoverable product than in earlier tests. After the initial simulated waterflooding was done, gas was then injected for 0.6 to 0.7 pore volumes, which was past gas breakthrough. The tube was then subjected to simulated waterflooding to determine the improved recovery due to gas trapping.

Tube Packing

To prepare for packing, the tube bulk volume was determined by water displacement. The initial attempts at packing the tube were patterned after earlier work done by Terwilliger (1951). Small amounts of sand and water (approximately 3 cm) were added to the tube. The tube was then vibrated for about 1 minute before more sand and water were added. The process was repeated to completely fill the tube. After the tube was packed to the top with sand, water was added until a thin film of water was maintained above the sand pack. The volume of water added during packing was the tube pore volume. By knowing the tube pore volume and bulk volume, the sand pack porosity could be determined.

For each test, clean silica sand was packed into the tube. Preliminary tube packs used sieved 45-80 mesh sand. However, very high permeabilities were obtained with this procedure, suggesting possible flow of fluids between the outside sand grains and the wall of the tubing.

Similar packing procedures were used at Louisiana State University. Discussions with J. Walcott of Louisiana State University (personal communication, August 1996) prompted two major changes. First, unsieved 40–140 mesh silica sand was used for subsequent tube packing attempts. Second, in addition to vibrating the tube, the sand pack was further compressed by dropping a tamping bar approximately one meter about five times between each addition of sand and water.

These modified tube packing procedures allowed the tube to be packed to an acceptable permeability. However, it was found that the achievable tube permeability varied with each sack of sand, and as sand was removed from a sack, the sand size distribution changed. Consequently, the amount of tamping required had to be increased or decreased to obtain the desired permeability range. Several attempts were often required to achieve an acceptable tube permeability. As a result, a fairly high range of permeabilities were used in these nine tests.

Test Description

To eliminate the need for altering the natural wettability of the sand from water-wet to oil-wet (see Discussion below), hexane was used as the intermediate phase. This is a direct analogy to water being the intermediate phase in an oil-wet system.

The packed tube was mounted vertically in the tube holder, and all instrumentation and flow lines were attached. Deionized water was then injected at the top of the tube and produced from the bottom of the tube at a rate of 130 cc/hr, until a uniform tube differential pressure was obtained. The backpressure regulator at the bottom of the tube was typically maintained at 6895 to 7584 kPa (1000 to 1100 psig).

Static pressure transducers and gauges were used to measure the system backpressure and the pressure of the tube inlet, the Ruska pumps, and the gas source. The differential pressure across the tube was also measured when it was less than 45 kPa (180 inches of water). The injection fluid temperature was also measured at the top of the tube.

After stable water injection and production rates were achieved, water injection was terminated and hexane injection was started. Hexane injection continued until production approached a hexane:water ratio (OWR) of 50.

After reaching residual water saturation conditions, different scenarios were conducted for the four 1996 tests. These were:

1. Nitrogen injection at 108 cc/hr at sand pack pressure conditions, followed by hexane injection at 120 cc/hr

2. Nitrogen injection at 57 cc/hr at sand pack pressure conditions concurrently with hexane injection at 60 cc/hr

3. Nitrogen injection at 38 cc/hr at sand pack pressure conditions concurrently with hexane injection at 100 cc/hr

4. Nitrogen injection at 108 cc/hr at sand pack pressure conditions for 4 pore volumes without additional hexane injection.

During 1997, the hexane injection phase for the five tests was conducted with the same rate, 120 cc/hr, as in the first four tests conducted during 1996, except for Tests 5 and 7 in which the initial hexane injection phase was conducted at 100 and 25 cc/hr, respectively. After the initial hexane injection, the following 1997 scenarios were conducted:

5. Hexane injection continued at 100 cc/hr for 8.66 pore volumes to simulate waterflooding of an oil-wet reservoir without gas interference or gas trapping

6. Nitrogen injection at 111 cc/hr at sand pack pressure conditions for 1.24 pore volumes, followed by hexane injection at 120 cc/hr

7. Nitrogen injection at 25 cc/hr at sand pack pressure conditions for 5.11 pore volumes without additional hexane injection

8. After only 0.30 pore volumes of hexane injection, nitrogen injection at 117 cc/hr at sand pack pressure conditions for 0.63 pore volumes, followed by hexane injection at 120 cc/hr

9. After only 0.31 pore volumes of hexane injection, nitrogen injection at 113 cc/hr at sand pack pressure conditions for 0.73 pore volumes, followed by hexane injection at 120 cc/hr.

DISCUSSION

As discussed, it is hypothesized that oil-wet reservoirs could be made to produce additional incremental oil by employing gas trapping techniques. To test the gas trapping mechanism in a laboratory setting, the sand pack would first have to be rendered oil-wet. It is a rather involved process to render a core or sand pack oil-wet (Tiffin 1983). Tiffin made Berea cores oil-wet by treating the cores with Quilon-C™. Rather than treating the sand pack to make it oil-wet, WRI chose to simulate a drainage process by using oil to displace water.

Hexane was chosen as the water-displacing fluid (i.e. the intermediate phase). To simplify modeling of the process, it was desirable to have a single component oil that was immiscible with the

water and sparingly miscible with the injected gas. Also, the viscosity of the hexane was less than that of the water it was displacing, presenting an adverse viscosity ratio, similar to many field conditions.

To further simplify these initial experiments and eliminate any possible miscible displacement effects, nitrogen was used as the injection gas rather than carbon dioxide.

Typical water injection projects at field scale operate with a velocity of approximately 0.3 meter/day. Terwilliger (1951) presented an equation to determine the gravity drainage rate. In his thesis, Lepski (1995) chose a gas injection rate less than Terwilliger's gravity drainage rate. However, to minimize capillary end effects, injection rates an order of magnitude greater than field conditions were used except for Tests 5 and 7, in which only the gravity drainage rate was exceeded.

As discussed above, four tests were completed during 1996. The first test involved injecting nitrogen after the sand pack was hexane flooded to the target OWR, followed by renewed hexane injection to displace incremental water. The next two tests involved co-injection of nitrogen and hexane after the sand pack was hexane flooded to the target OWR. The fourth test used only nitrogen injection after the sand pack had been hexane flooded to residual water saturation.

During 1997, five additional tests were completed. Test 5 was a base-case simulation of waterflooding of an oil-wet reservoir without gas trapping. For this test, hexane injection without gas injection was conducted for 8.7 pore volumes. These results provide a comparison of anticipated results without gas injection. Test 6 was a repeat of the first test, which involved injecting nitrogen after the sand pack was hexane flooded to the target OWR, followed by renewed hexane injection to displace incremental water. Tests 7 and 4 were gas interference tests in which only nitrogen injection was used after the gas pack had been hexane flooded to residual water saturation. Test 4 and Test 7 were conducted to determine if the incremental water recovery experienced in the first three tests was due to gas trapping or if a similar recovery could be achieved by gas interference.

Tests 8 and 9 were similar except that different sand pack permeabilities were used. Again, these two tests were best-case scenarios and were conducted to simulate how gas trapping might be applied in the field. Initial hexane injection was terminated after only 0.3 pore volumes, so gas injection was initiated early in the life of the flood, similar to what might happen in the field. Gas injection was conducted alone without hexane co-injection and was limited to only 0.6 to 0.7 pore volumes, which was enough for gas breakthrough. Based on the results from the previous tests, this scenario was expected to provide the best gas trapping conditions and would yield the most realistic incremental recovery.

RESULTS

Tube packing resulted in a reasonable range of porosities and permeabilities for the nine tests (see Table 1). These values were similar to values obtained by Terwilliger (1951) and Lepski (1995). Consequently, it was believed that results were not affected by variations caused by the packing of the tubes.

The differential pressure response with time was similar for all the tests. The DP increased as hexane displaced water until the point of hexane breakthrough, after which the DP stabilized or decreased. The increase in tube DP results from a decrease in overall mobility caused by hexane displacing water. After breakthrough of hexane, the system DP tends to decrease because of the reduced viscosity of hexane, 0.0006 Pa·s (0.6cp), in comparison to water, 0.001 Pa·s (1.0cp). In general, the effect of mobility was not apparent after nitrogen injection started. The pressure profiles for the nine tests are summarized in Figures 2 through 10.

Cumulative water recoveries as a function of total pore volumes of hexane and nitrogen injected are presented in Table 2 and Figures 11 through 19. The first four tests experienced hexane breakthrough at 0.6 to 0.65 pore volumes injected. The 1997 tests experienced hexane breakthrough between 0.56 and 0.77 pore volumes injected.

Incremental water recovery coincided with nitrogen breakthrough for Tests 1, 2 and 4. The greatest amount of incremental water production occurred in Test 2, which had a hexane:nitrogen ratio approaching one for the co-injection phase after reaching the target OWR for the hexane injection phase.

Test 3 did not experience any incremental water production until almost 3 additional pore volumes had been injected beyond nitrogen breakthrough. This suggests that the hexane:nitrogen co-injection ratio was too high, thus the gas trapping mechanism was ineffective.

Test 1 exhibited the lowest residual water saturation, but it is hypothesized that the method of operating this test was responsible for the increased recovery. Unlike later tests, Test 1 was shut in after initial water breakthrough and the target OWRs were achieved (see Figure 6). The shut-in period allowed time for the hexane and water phases to gravity segregate. The segregation resulted in a higher water saturation in the bottom portion of the tube than if injection had been continuous. This increased water saturation occurred in the largest pore volumes. On subsequent injection, the displacing fluids reentered the largest pore space and resulted in a more efficient sweep of the remaining water and a higher recovery than in subsequent tests, which employed continuous injection. Test 6 was a repeat of Test 1 except that the system was not shut in after hexane injection. As

expected, this test had a higher final water saturation because gravity segregation was not allowed to occur. However, more incremental water recovery attributed to gas trapping occurred than in Test 1.

Test 4 was conducted to compare the recoveries attained by the gas trapping mechanism with displacement or interference by gas only. Therefore, no additional hexane was injected after reaching the target OWR. Instead, gas injection was established and continued for the duration of the test. Under these conditions, incremental water was produced after nitrogen breakthrough in quantities similar to those from the gas trapping tests. This response may suggest that gas displacement or interference is as effective in recovering incremental oil as gas trapping. It should be noted however, that Test 4 experienced difficulties with the backpressure regulator. Therefore, it is conceivable that significant differential pressures developed in the tube, which may have resulted in higher-than-anticipated water recoveries. Test 4 was repeated in Test 7. Similar ultimate water recoveries were achieved for these two tests; however, unlike in Test 4, there was no indication of incremental recovery as a result of gas injection in Test 7 .

Test 5 was conducted with hexane injection only. This test provided a comparison for all other tests involving gas injection or potential gas trapping. This oil-only test had the lowest water recovery of all nine tests, suggesting that gas injection was enhancing the ultimate water recovery, either by gas interference or gas trapping.

Test 6 and the two best-case scenario tests, Tests 8 and 9, had ultimate water recoveries of 70 to 72%. Incremental recoveries attributed to gas trapping were also similar, at 7.7 to 8.1%. However, in Tests 8 and 9, 0.6 to 0.7 pore volumes of gas were injected compared to 1.2 pore volumes injected in Test 7. Gas breakthrough occurred after about 0.6 to 0.69 pore volumes for all three tests, suggesting that this was all the gas that was needed to cause the gas trapping effect to occur.

MODELING

Preliminary simulations were performed during 1996 to establish a first approximation for incremental recoveries from gas trapping and to aid in the experimental design. When specific data were not available, Corey-type (1954) relationships were used to provide estimates for the relative permeabilities of the gas and water phases.

The modeling investigated recoveries in both horizontal and vertical flood orientations. Predictions of recovery from horizontal flood orientations used the oil (dead oil) and rock properties

reported by Tiffin (1983) in his horizontal water-alternating-gas (WAG) tube-flood studies. Tiffin did not report relative permeability or capillary pressure data for the Torpedo core used in the studies. Therefore, Corey relative permeability and straight-line capillary pressure relationships were used when simulating the horizontal flooding. To conduct the simulated displacements, water was assigned the oil properties and oil (a displacing phase) the water properties. Gas was assumed to be immiscible.

Modeling of recovery in a vertical tube orientation assumed injection of the displacing fluid in the gravity direction. Since the predictions for the vertical floods were intended as design studies for the laboratory experiments, these simulations employed rock properties that were typical of a sand pack. The modeling used relative permeability and capillary pressure data for an unconsolidated sandstone (Guarnaccia et al. 1992). The simulations used the liquid properties of hexane and decane to represent the intermediate phase and the water wetting phase. Gas was assumed to be immiscible.

These preliminary simulations investigated the effects of WAG cycle duration, injected gas:oil ratio, initial pressure, injection pressure, and injection rate (i.e. differential pressure). The results from all of the simulations predicted an incremental water recovery from gas trapping of approximately 2 to 5% on a volume basis. This range of predictions is generally consistent with the observed incremental recoveries from the tube experiments following the gas breakthrough.

One-dimensional matching simulations generally predicted higher recoveries with and without gas trapping than were actually achieved in the tube tests. However, the gas trapping tests indicated higher water recoveries than the tests conducted without gas trapping. Predicted incremental water recoveries due to gas trapping were similar to the incremental water recoveries achieved in the tube tests.

During 1997, oil–water relative permeabilities curves were developed from the production results of Test 5, the oil-only run (Welge 1952). By using these relative permeabilities, matches between the predicted and actual one-dimensional water recoveries were achieved. Unfortunately, there were not enough data from the tube tests to determine gas–liquid relative permeabilities. To date, the gas–liquid permeabilities used to model these tests have been based on a Corey-type relationship for an unconsolidated sand, and attempts have not been made to adjust the gas–liquid permeabilities to match the tube tests.

A hypothetical three-dimensional case was developed to evaluate the potential for applying gas trapping on a field scale. In this case, a quarter of a five spot, simulating 160-acre injection-production well spacing, was used. Three layers were chosen such that a thin, high-permeability or fast layer was included to affect the other two thicker, low-permeability layers. The thin layer had

a permeability thickness value 20 times greater than those of the thicker layers. Consequently, the thin layer took 20 times more fluid than the thick layers initially.

As in the tube tests, the simulations were designed to inject oil to displace water. Oil was injected initially and terminated just before the thin fast layer experienced breakthrough. Nitrogen was then injected at a volume that at reservoir conditions is similar to the oil injection rate. Nitrogen injection was also terminated before gas breakthrough in the fast layer. After terminating nitrogen injection, oil was again injected for several pore volumes.

In no case was gas trapping successful in minimizing the 20 times greater injection into the fast layer. However, depending on the gas trapping coefficient chosen, water production from the two thicker layers was improved after gas injection.

CONCLUSIONS

For all tests, breakthrough occurred after .56 to .77 pore volumes of hexane had been injected, and water recovery at breakthrough varied between 56 and 69.4% of initial water in place.

Incremental water production was noted in seven of eight tests in which additional nitrogen or hexane injection occurred. The third test, a nitrogen:hexane injection test, did not experience the incremental water production response until almost the fifth pore volume, suggesting the nitrogen: hexane ratio was too high. If co-injection had been used, the nitrogen:oil ratio probably should have been approximately one. One of two gas interference tests did not experience incremental water recovery after gas injection.

While incremental water production attributed to gas trapping did occur, it did not occur until at least a pore volume had been injected, but all eight tests did recover more water than the base-case test in which only hexane was injected.

One-dimensional modeling predictions generally agree with the observed tube test incremental recoveries after gas breakthrough, suggesting an additional 5 to 8% incremental oil recovery may be possible if gas trapping is applied to an oil-wet reservoir.

Table 1. Gas Trapping Test Results Summary

Test #	1	2	3	4	5	6	7	8	9
Porosity, %	34.7	37.2	40.4	33.4	37.6	34.5	32.5	33.7	35.8
Kw at 100% Water Saturation, darcy	8.856	1.925	5.482	8.262	3.69	1.22	0.36	0.61	2.76
Ko at Residual Water Saturation, darcy	0.753	0.523	0.279	0.211	0.56	0.26	0.09	0.13	0.41
Average Injection Pressure, kPa/psig	6984/1013	7053/1023	7143/1036	7136/1035	6984/1013	7053/1023	7143/1036	7136/1035	—
Average Tube Backpressure, kPa/psig	6964/1010	6950/1008	7067/1025	7060/1024	6964/1010	6950/1008	7067/1025	7060/1024	—
Average Hexane Injection Rate, cc/hr	120	120 then 60	120 then 100	120	100	120	25	120	120
Average Nitrogen Injection Rate, cc/hr at sand pack pressure	108	57	38	108	—	111	71	117	113
Average Hexane/Nitrogen Injection Ratio	—	1.1	2.6	0.0	—	—	—	—	—
Water Saturation after Hexane Injection, %	22.4	39.2	40.2	40.2	—	40.8	29.4	70.0	69.5
Water Saturation after Nitrogen Breakthrough	18.9	37.2	38.4	32.9	—	38.6	27.7	36.2	38.0
Final Water Saturation, %	15.9	23.5	30.5	25.2	32.9	27.8	26.1	28.1	27.8

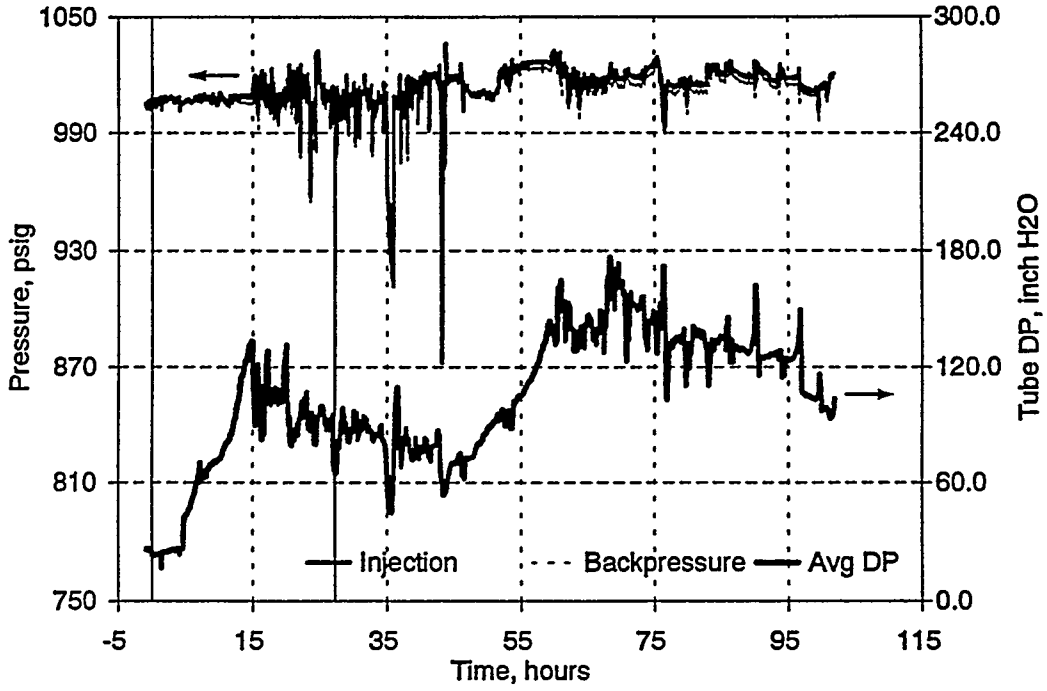

Figure 2. Test 1 Pressure Profile

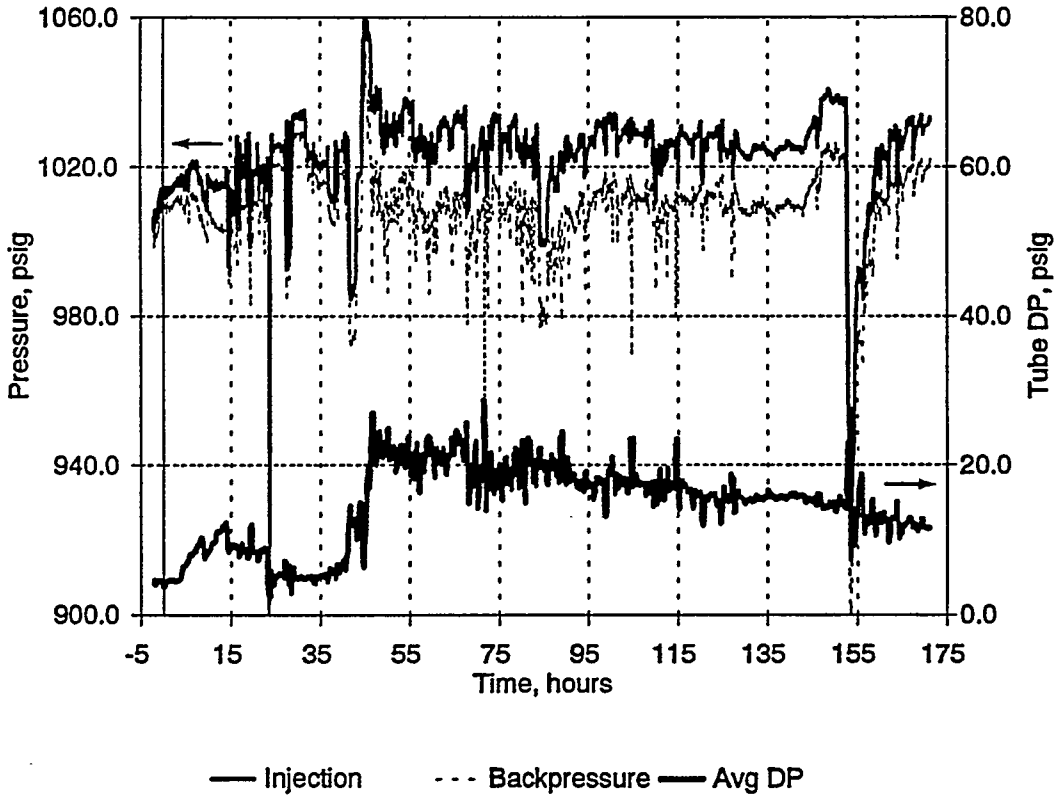

Figure 3. Test 2 Pressure Profile

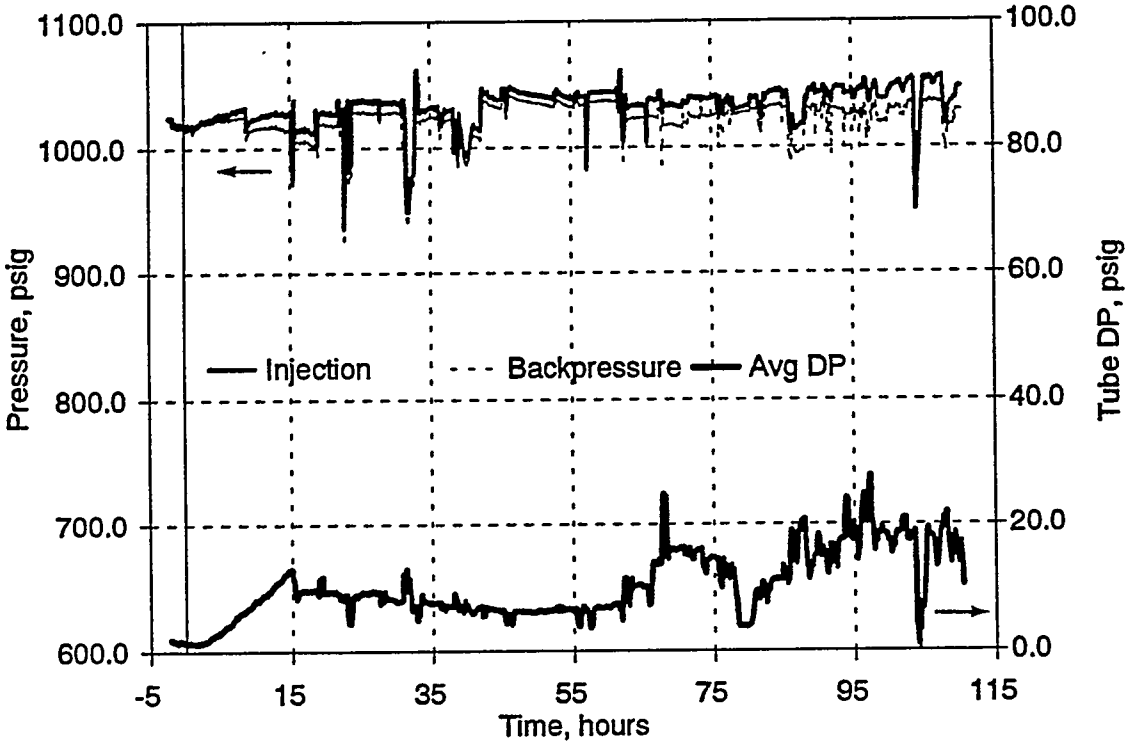

Figure 4. Test 3 Pressure Profile

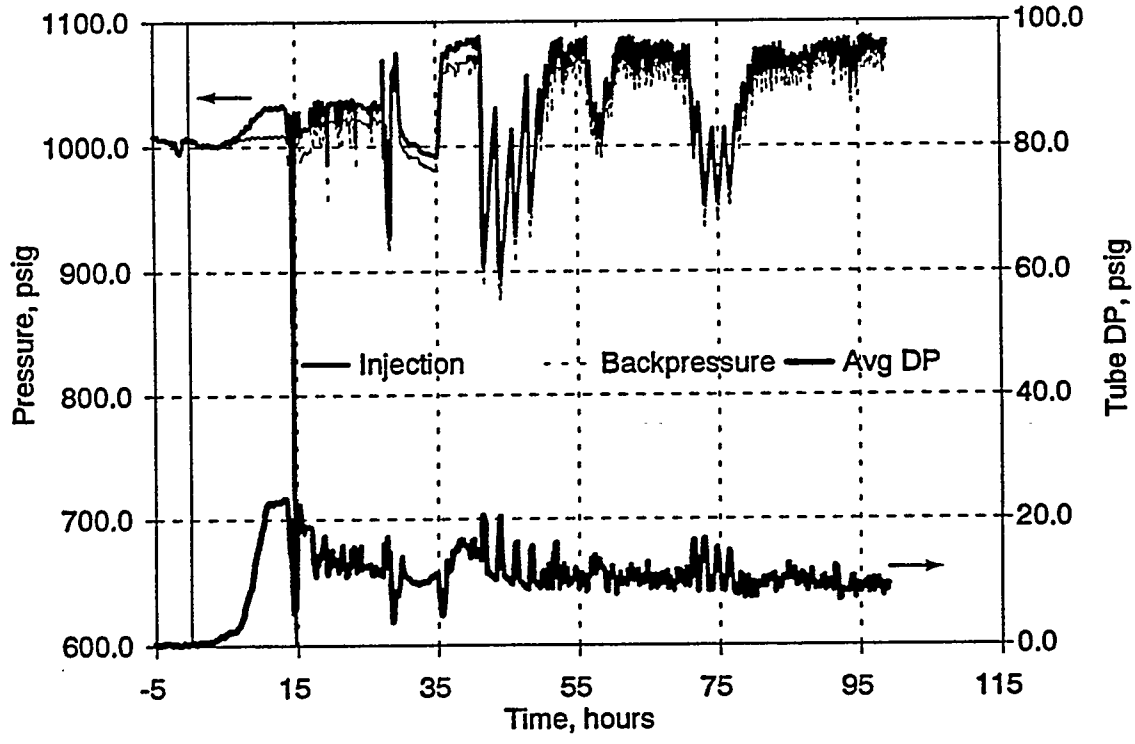

Figure 5. Test 4 Pressure Profile

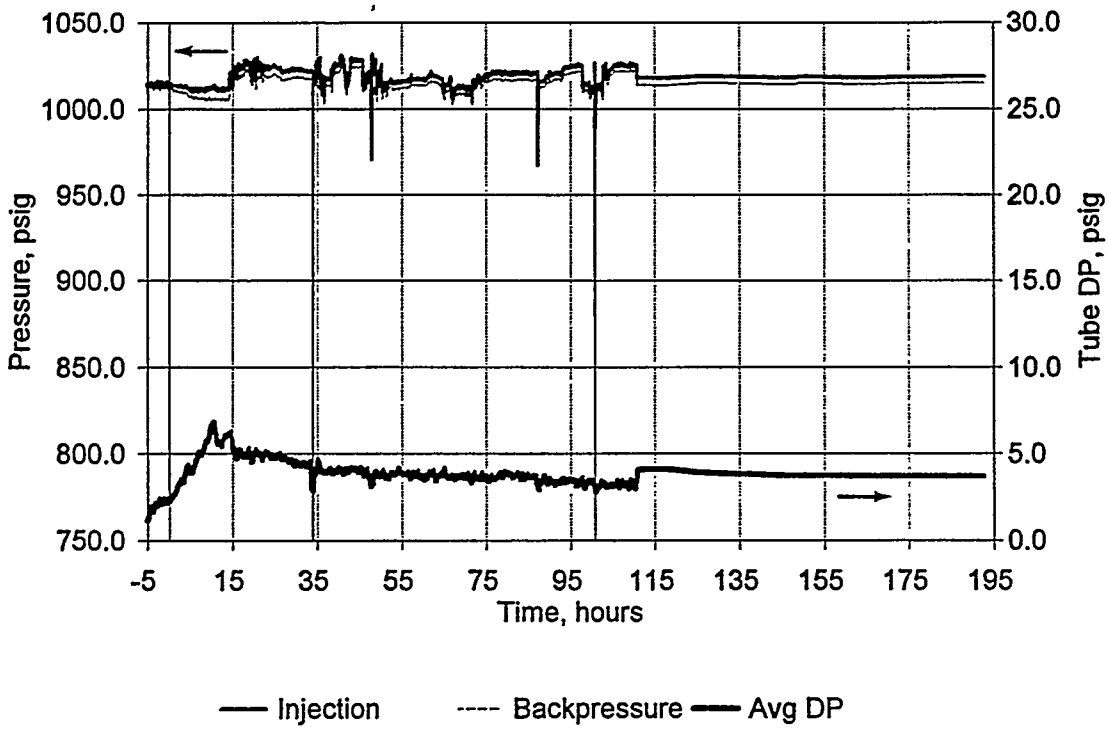

Figure 6. Test 5 Pressure Profile

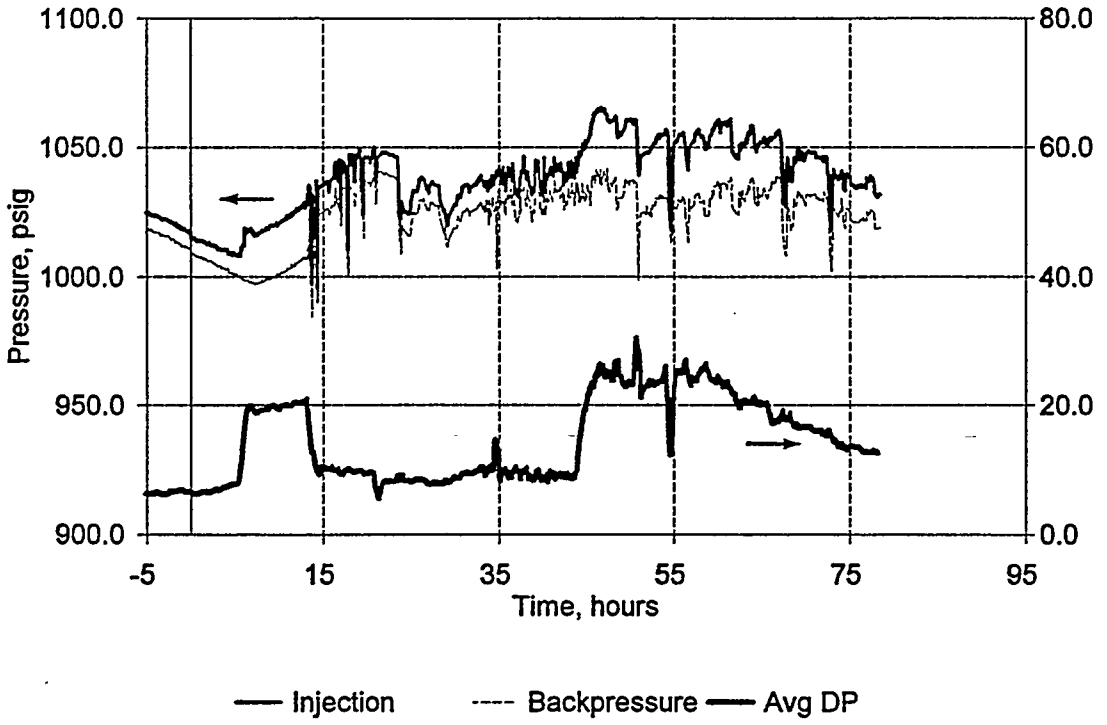

Figure 7. Test 6 Pressure Profile

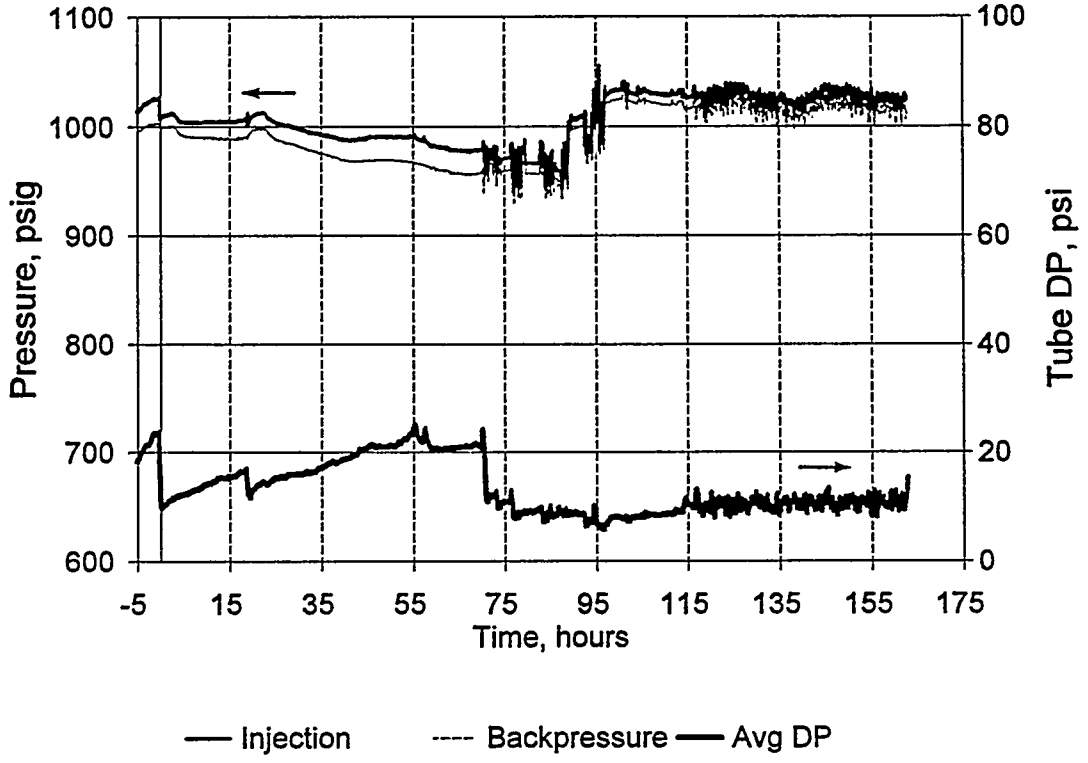

Figure 8. Test 7 Pressure Profile

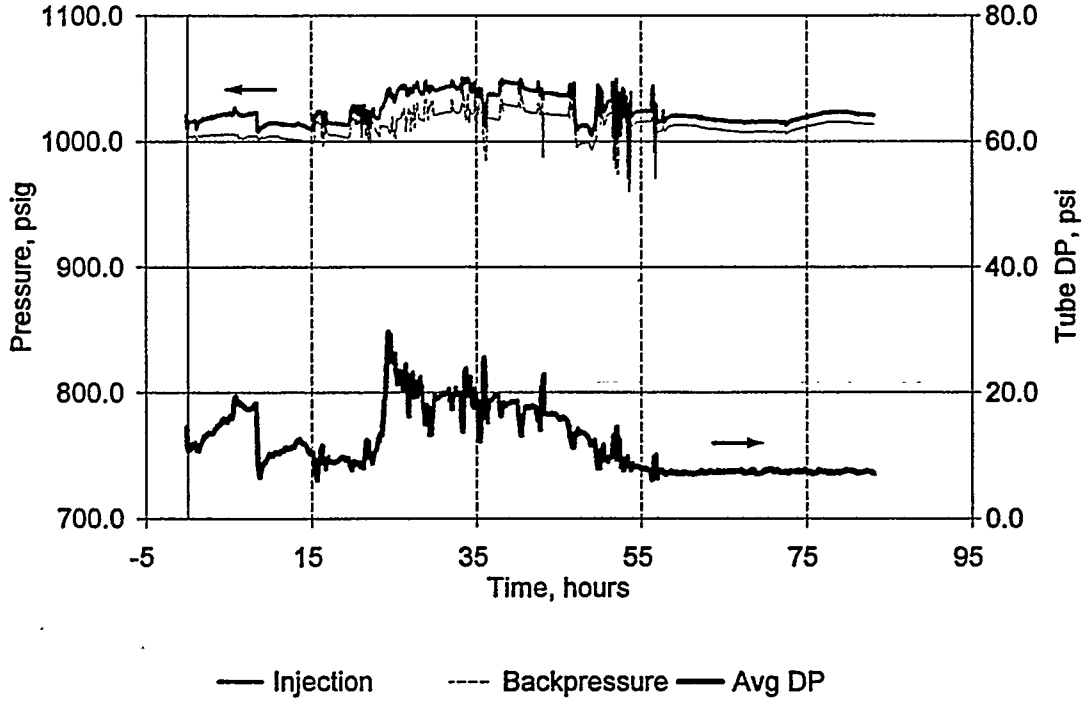

Figure 9. Test 8 Pressure Profile

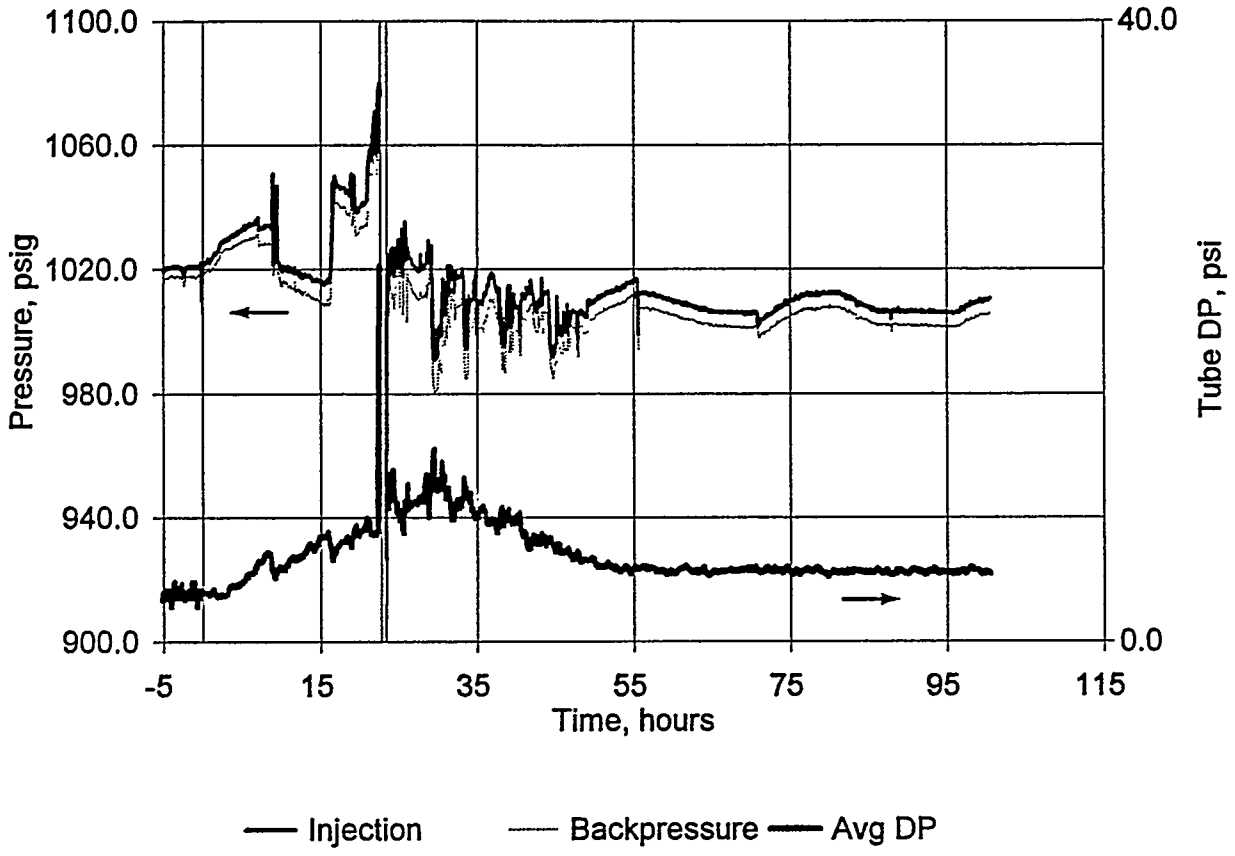

Figure 10. Test 9 Pressure Profile

Table 2. Gas Trapping Test Results Summary

Test #	1	2	3	4	5	6	7	8	9
Hexane Breakthrough, Total Pore Volumes Injected/% Water-in-Place Recovery	0.65/62.1	0.61/60.0	0.61/59.8	0.64/59.8	0.56/56.1	0.59/58.3	0.77/69.4	0.75/62.8	0.73/62.0
Hexane Injection off, Total Pore Volumes Injected/% Water-in-Place Recovery	2.30/77.6	—	—	1.45/64.5	—	1.03/59.2	1.06/70.6	0.30/30.0	0.31/30.6
Nitrogen Injection on, Total Pore Volumes Injected/% Water-in-Place Recovery	2.30/77.6	1.10/60.7	0.99/60.2	1.45/64.5	—	1.03/59.2	1.06/70.6	0.48/44.4	0.31/30.6
Nitrogen Breakthrough, Total Pore Volumes Injected/% Water-in-Place Recovery	3.10/80.9	2.10/62.8	1.94/61.4	2.17/67.1	—	1.71/61.4	??	1.08/63.8	1.00/63.3
Nitrogen Injection off, Total Pore Volumes Injected/% Water-in-Place Recovery	3.25/80.9	—	—	—	—	2.24/64.5	—	1.11/63.8	1.04/64.5
Hexane Injection Restart, Total Pore Volumes Injected/% Water-in-Place Recovery	3.25/80.9	—	—	—	—	2.24/64.5	—	1.11/63.8	1.04/64.5
Total Injection/Recovery, Total Pore Volumes Injected/% Water-in-Place Recovery	5.50/84.1	9.10/76.5	6.50/69.5	5.50/74.8	8.66/67.1	4.36/72.2	6.17/73.9	4.88/72.0	5.53/72.2
Incremental Water Production Response, Total Pore Volumes Injected	3.1	2.4	4.7	2.1	—	2.2	—	1.2	1.5
Incremental Water Recovery After Nitrogen Breakthrough, %	3.2	13.7	8.1	7.7	—	7.7	—	8.1	7.7

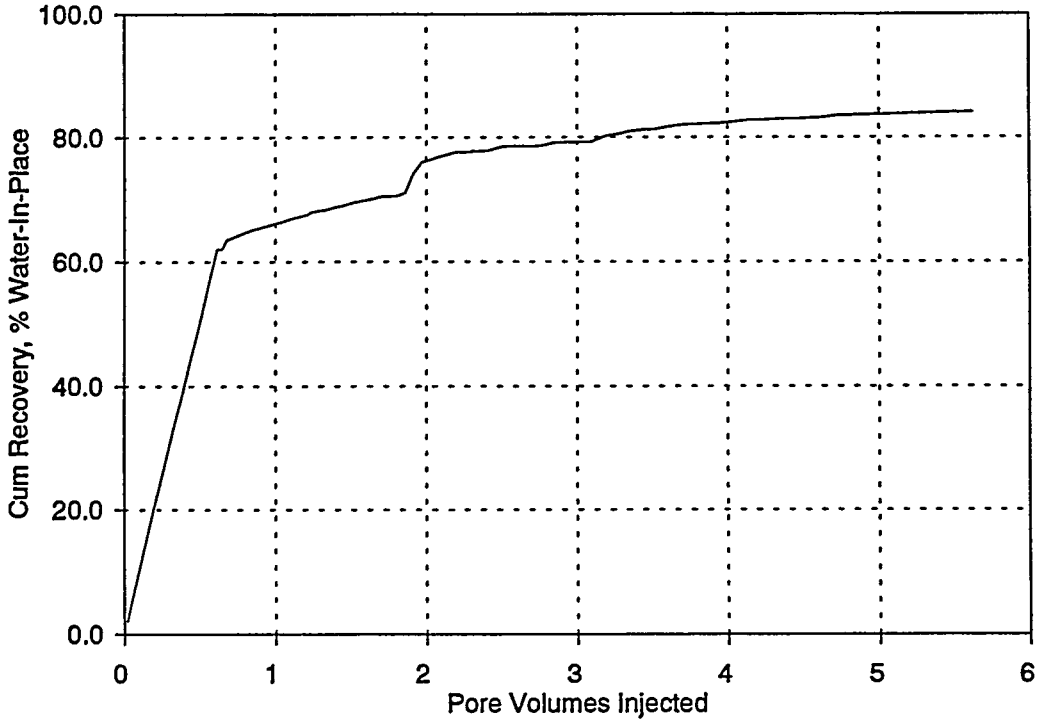

Figure 11. Test 1 Cumulative Water Recovery

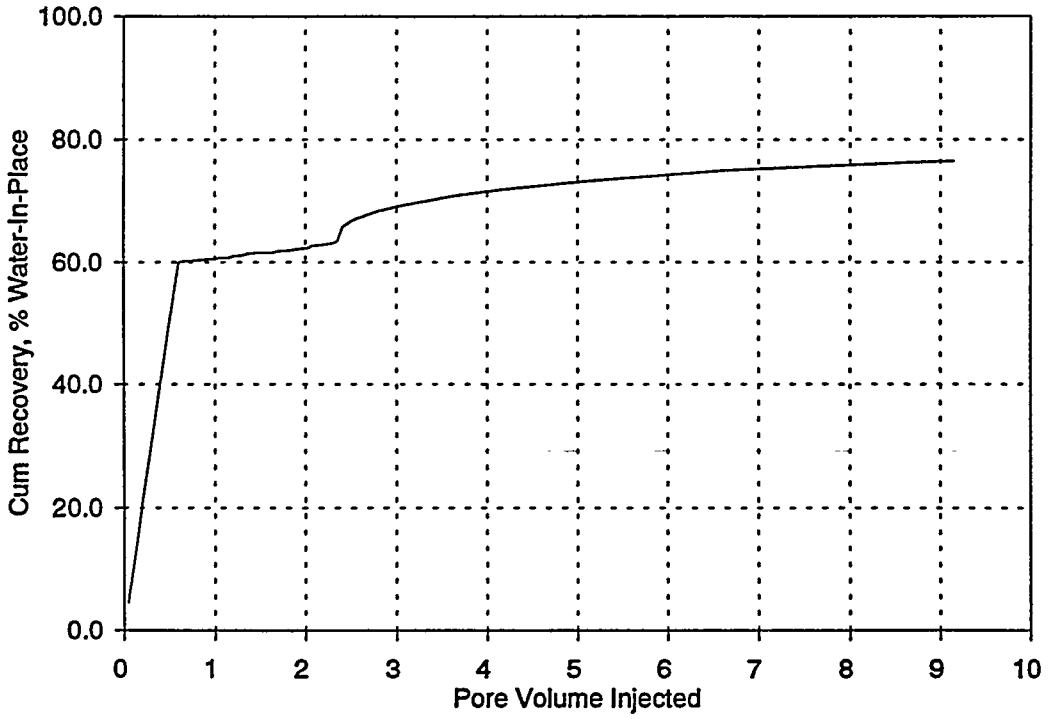

Figure 12. Test 2 Cumulative Water Recovery

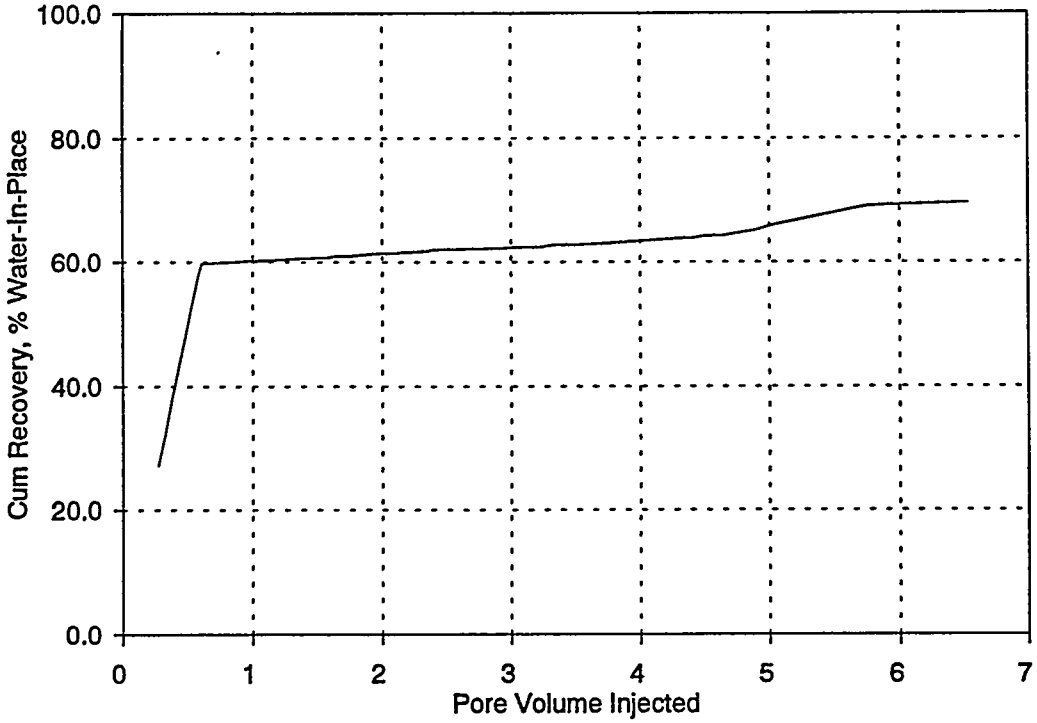

Figure 13. Test 3 Cumulative Water Recovery

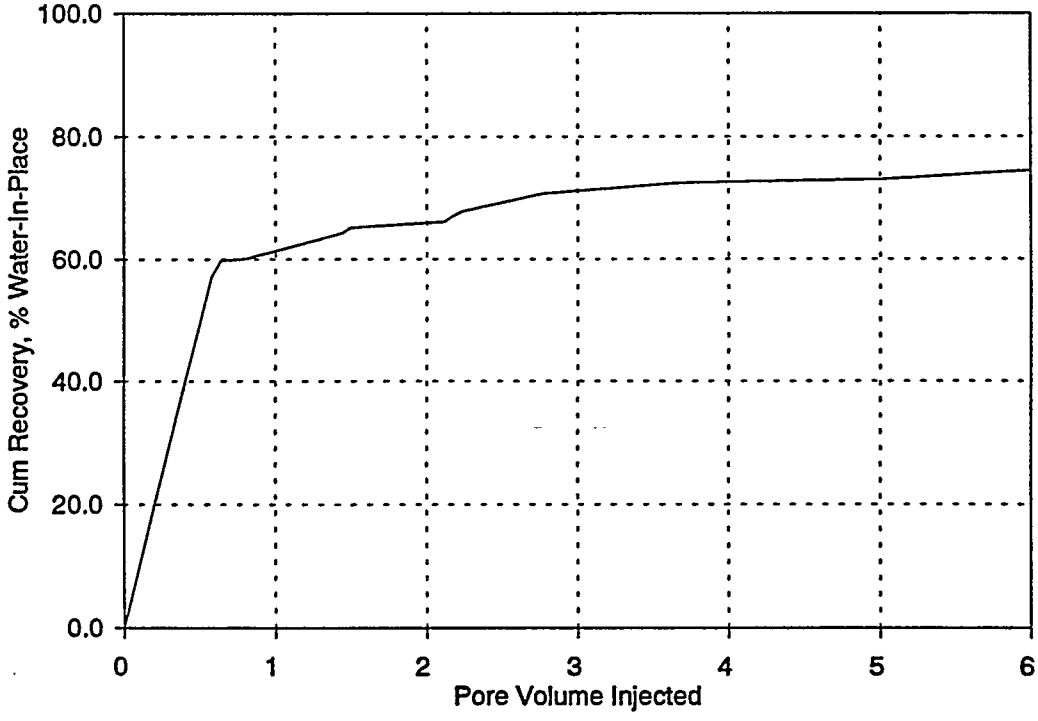

Figure 14. Test 4 Cumulative Water Recovery

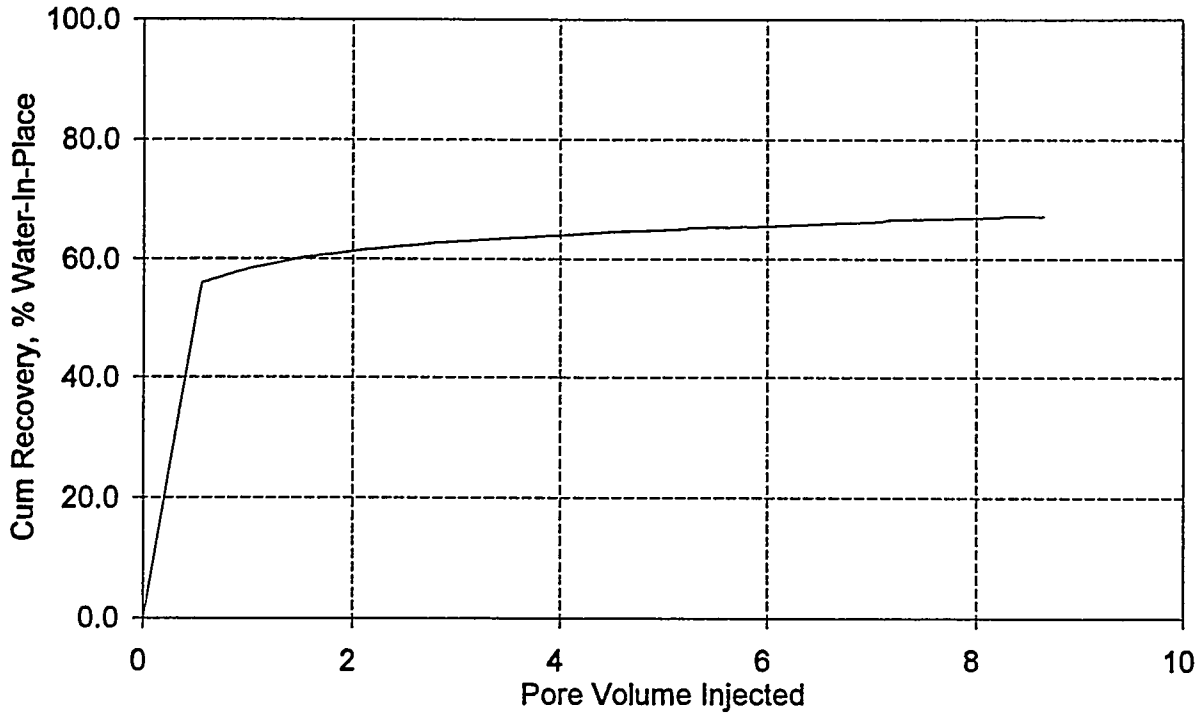

Figure 15. Test 5 Cumulative Water Recovery

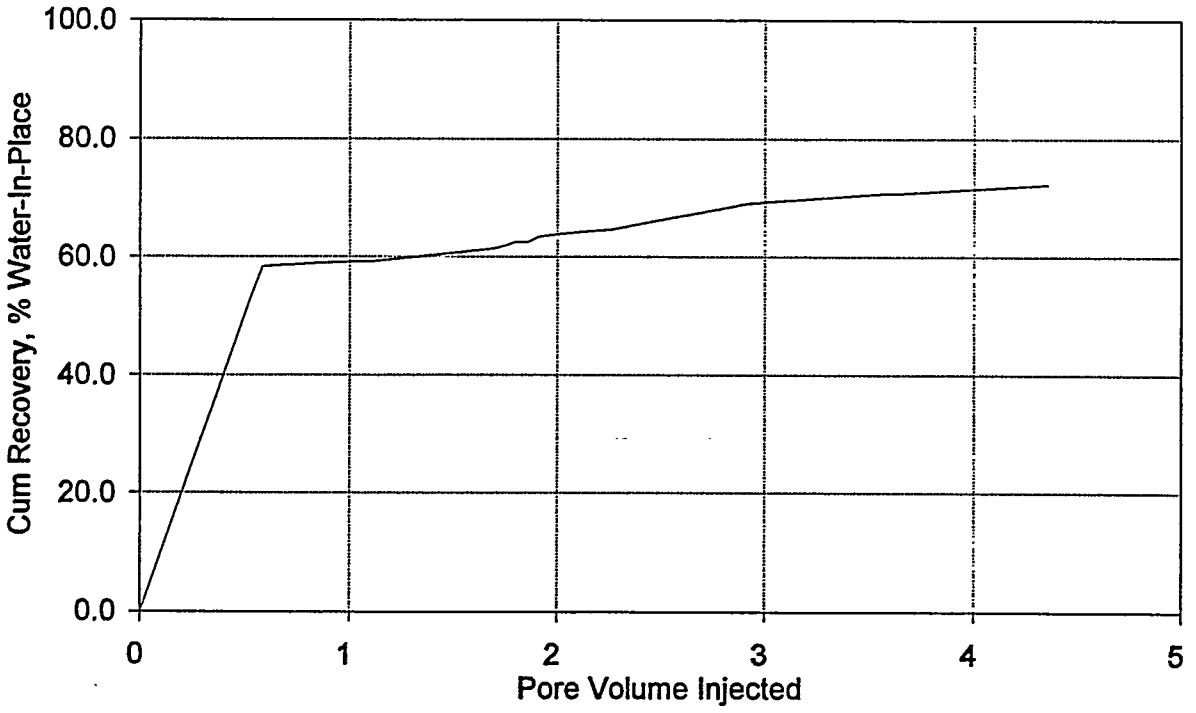

Figure 16. Test 6 Cumulative Water Recovery

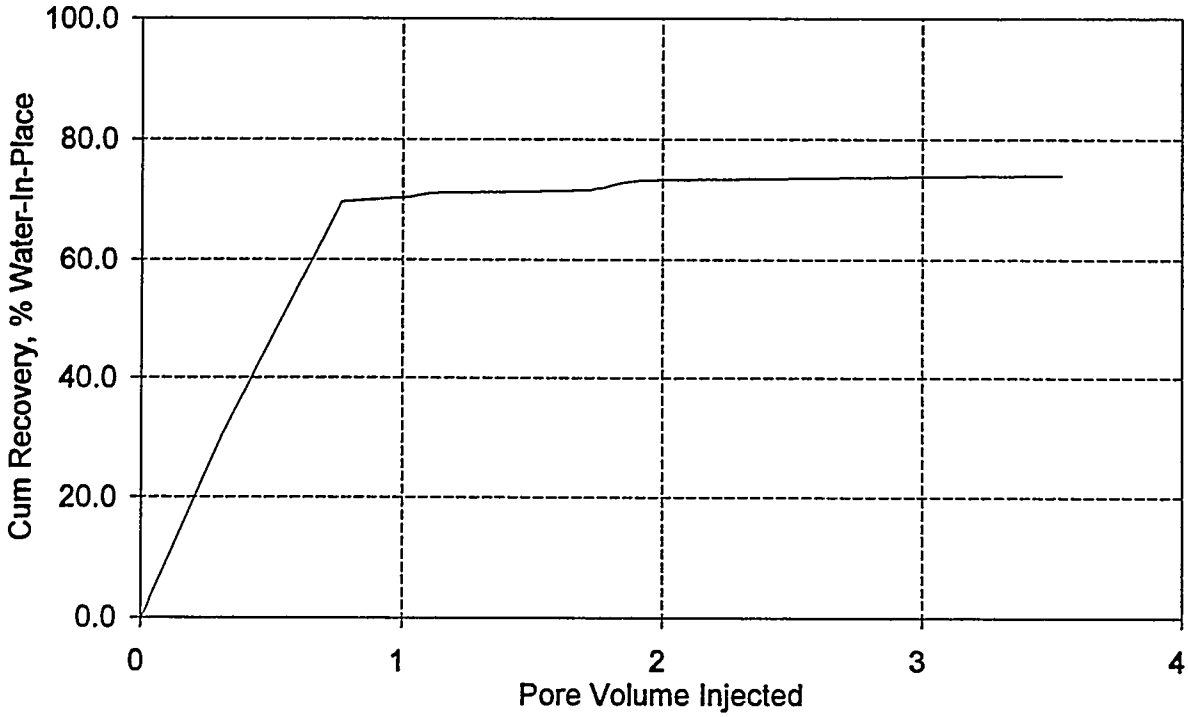

Figure 17. Test 7 Cumulative Water Recovery

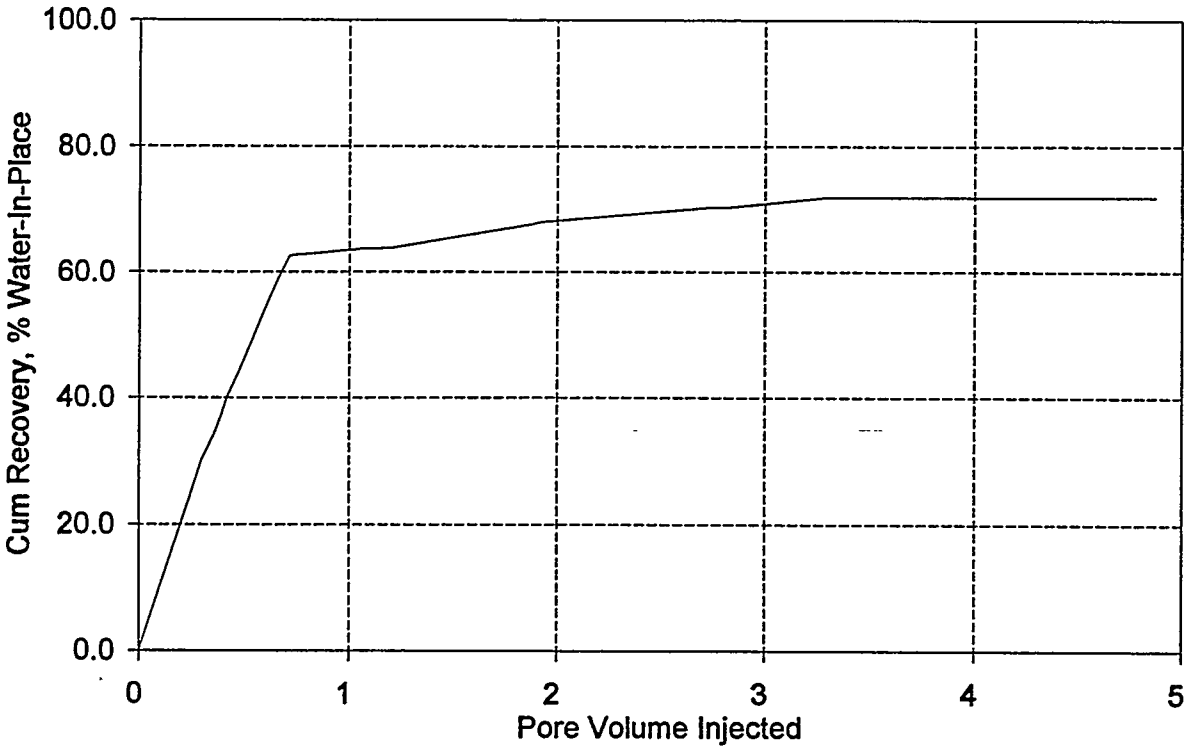

Figure 18. Test 8 Cumulative Water Recovery

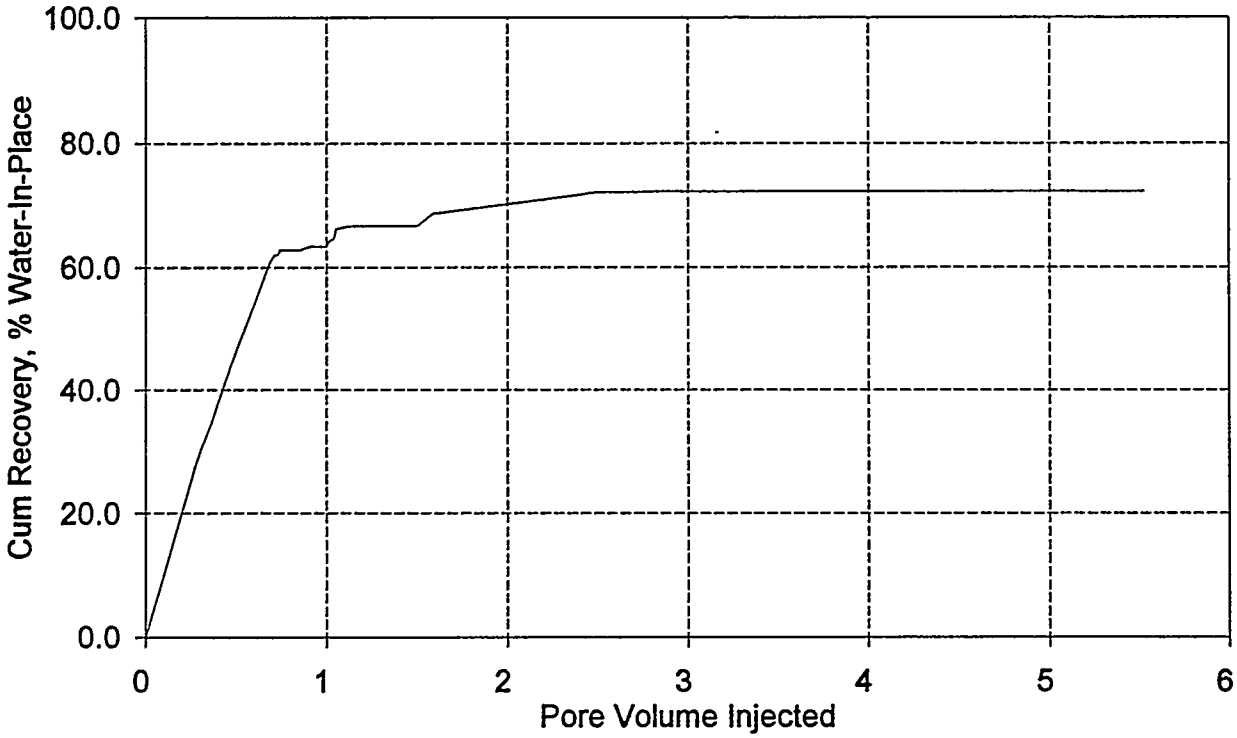

Figure 19. Test 9 Cumulative Water Recovery

REFERENCES

Corey, A.T., 1954, *Producer's Monthly*, 38, November 1954.

Guarnaccia, J.F., P.T. Imhoff, B.C. Missildine, M. Dostrom, M.A. Celia, J.H. Dane, P.R. Jaffe, and G.F. Pinder, 1992, "Multiphase Chemical Transport in Porous Media," EPA Environmental Research Brief, EPA/600/5-92/002.

Killough, J.E., 1976, "Reservoir Simulation With History-Dependent Saturation Functions," *Transactions SPE of AIME*, Volume 261, pp. 37-48.

Kyte, J.R., R.J. Stanclift Jr., S.C. Stephan Jr., and L.A. Rapoport, 1956, "Mechanism of Water Flooding in the Presence of Free Gas," *Transactions of AIME*, Volume 207, pp. 215-221.

Land, C.S., 1968, "The Optimum Gas Saturation for Maximum Oil Recovery From Displacement by Water," SPE 2216, 43rd Annual Fall Meeting, Houston, TX.

Lepski, B., *Physical Modelling of Oil Displacement By Gas In Water Flooded Zones*, Master of Science Thesis in Petroleum Engineering, Louisiana State University, Baton Rouge, LA, May 1995.

Oil and Gas Journal, 1994, Annual Production Report, September 26, 1994, pp. 51-79.

Tiffin, D.L., and W.F. Yellig, 1983, "Effects of Mobile Water on Multiple-Contact Miscible Gas Displacements", *Society of Petroleum Engineers Journal*, June 1983, pp. 447-455.

Terwilliger, P.L., L.E. Wilsey, H.N. Hall, P.M. Bridges, and R.A. Morse, 1951, "An Experimental and Theoretical Investigation of Gravity Drainage Performance," *Petroleum Transactions*, AIME, Vol. 192.

Welge, H. J., 1952, "A Simplified Method for Computing Oil Recovery by Gas or Water Drive," *Petroleum Transactions, AIME,* Vol. 195, pp. 91-98.

WRI-98-R025

WESTERN RESEARCH INSTITUTE
"Providing solutions to energy and environmental problems"

FINAL REPORT

COMPCOAL™: A PROFITABLE PROCESS FOR PRODUCTION OF A STABLE HIGH-BTU FUEL FROM POWDER RIVER BASIN COAL

Prepared for
U.S. Department of Energy
Morgantown, West Virginia

April 1998

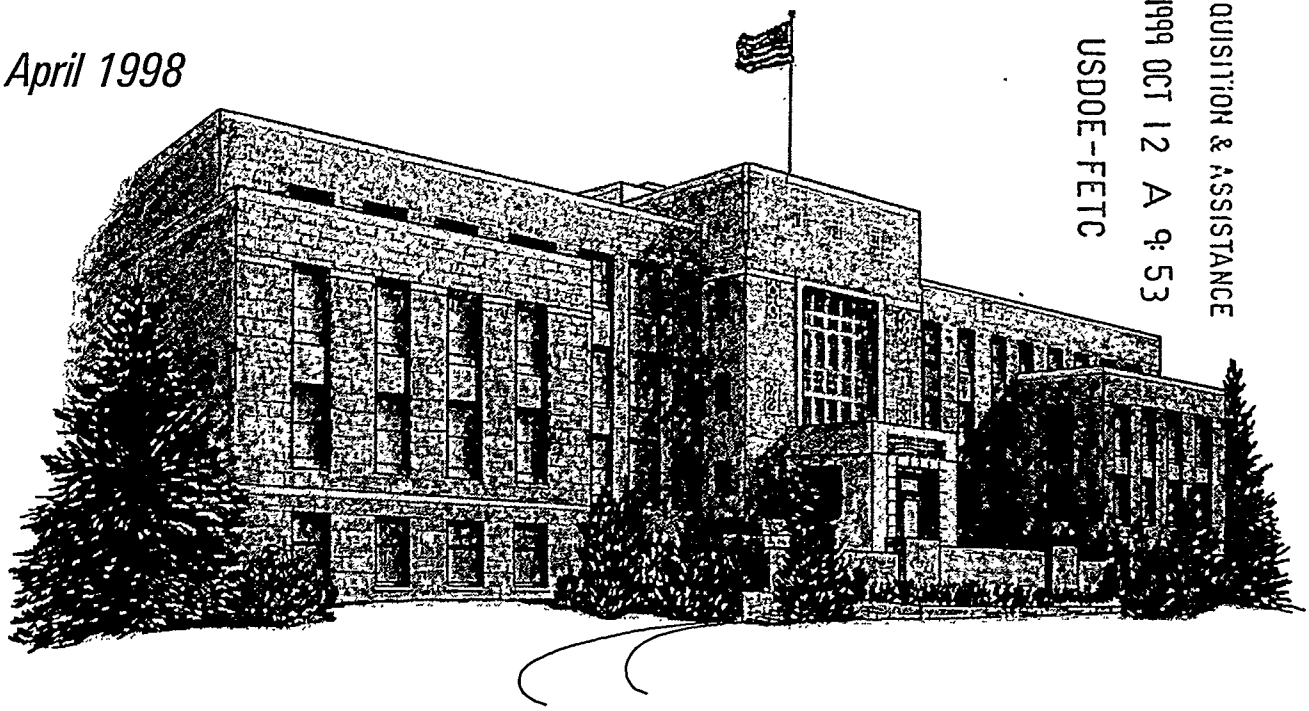

WRI-98-R025

COMPCOAL™: A PROFITABLE PROCESS FOR PRODUCTION OF A STABLE HIGH-BTU FUEL FROM POWDER RIVER BASIN COAL

Final Report

By
N.W. Merriam
T.F. Turner

April 1998

Work Performed Under Cooperative Agreement
DE-FC21-93MC30126 Subtask 2.1

For
U.S. Department of Energy
Office of Fossil Energy
Federal Energy Technology Center
Morgantown, West Virginia

By
Western Research Institute
Laramie, Wyoming

DISCLAIMER

TABLE OF CONTENTS

LIST OF TABLES

LIST OF FIGURES

EXECUTIVE SUMMARY

The COMPCOAL™ process was developed by Western Research Institute (WRI) to produce a stable, high-Btu fuel from Powder River Basin (PRB) and other low-rank coals. The process is designed to overcome the problems of oxidation and spontaneous combustion, readsorption of moisture, and dust formation from the friable coal.

PRB coal is susceptible to low-temperature oxidation and self-heating, particularly after it has been dried. Using "accelerated aging" to prevent self-heating of dried PRB coal not only stabilizes the dried coal but also increases the heating value of the COMPCOAL product.

The stabilized COMPCOAL product has a heating value of 12,000 to 12,700 Btu/lb, contains 35 to 40 wt % volatiles, and is comparable to unprocessed PRB coal in self-heating and low-temperature oxidation characteristics. The self-heating tendency can be controlled by slightly adjusting the "aging" step in the process.

In the process, crushed coal is dried by direct contact with hot gas in a fluidized bed dryer. The coal is heated to a temperature of 500 to 600°F (260 to 316°C), which is sufficient to dry the coal to zero moisture (by proximate analysis) and to remove about 3-4 wt % of the volatiles from the coal by partial decarboxylation. The hot, dried coal is transferred to a second reactor where it is heated to about 700°F (371°C) by contact with a small flow of air. The air contact heats the coal and converts coal tars to liquids while oxidizing the active sites on the coal particles. This "instant aging" causes the coal to be resistant to oxidation at low temperature. The flow of air through the pyrolysis reactor is too small to carry significant quantities of coal liquids away from the hot particles. The stabilized coal particles are mixed with fines from the dryer and the mixture is briquetted at a temperature of about 600°F (316°C). The briquettes are cooled to about 250°F (121°C) by contact with a mist of water sprayed onto the briquettes in a gas-tight cooling conveyor.

Our economic evaluation of the process indicates that the process can be profitable if the high-Btu, low-sulfur product is sold for a price of about $15 per ton or higher. We estimate the discounted cash flow rate of return from a 1,000 tons per day COMPCOAL plant to be from 51 to 79% when using 50% debt financing and from 29 to 42% when using all equity financing.

INTRODUCTION

Western Research Institute (WRI) is developing a process to produce a stable, clean-burning, premium fuel from Powder River Basin (PRB) coal and other low-rank coals. This process is designed to overcome the problems of spontaneous combustion, dust formation, and readsorption of moisture that are experienced with PRB coal and with processed PRB coal. This process, called COMPCOAL™, results in a high-Btu product that is intended for burning in boilers designed for midwestern coals or for blending with other coals.

PRB coal is relatively dusty and subject to self-ignition compared to bituminous coals. Dried (or processed) PRB coal is even more susceptible to spontaneous combustion than the raw coal. Also, PRB coal dried at low temperature typically readsorbs about two-thirds of the moisture removed by drying. This readsorption of moisture releases the heat of adsorption of the water which is a major cause of self-heating of low-rank coals at low temperature. PRB coal and other low-rank coals tend to be highly reactive. These reactive coals must be mixed regularly (every week or two) when fresh. However, they become somewhat more stable after they have aged for several weeks.

Low-temperature oxidation reduces the heating value of the coal, makes the coal less able to repel moisture (hydrophobicity), and is known to increase the unburned carbon remaining in the ash. Ingram and Rimstidt (1984) attribute increased moisture in naturally oxidized coals to increase in surface area caused by the physical effects of weathering and an increase in hydrophilic functional groups able to chemisorb water (organic acids are known to attract water to coal particles). Water molecules are generally thought to attach to polar oxygen sites in coal (this varies greatly with the different types of coal).

Many efforts have been made to overcome the problems of dust formation and self-heating while keeping the cost of processing within the very competitive limits of the markets for coal. The University of North Dakota Energy Research Center has explored the use of various drying techniques to upgrade low-rank coals (Willson et al. 1987). They found that coals dried at low temperature readsorb moisture after cooling and return to essentially the original equilibrium moisture level. In contrast, they found that the processes using temperatures high enough to alter the structure of the coal particles resulted in reduced readsorption of moisture. They also concluded that the lowered equilibrium moisture levels resulted from the rejection of carbon dioxide by the decarboxylation reactions which occur during high-temperature drying. The readsorption of moisture by coals dried at temperatures lower than a few hundred degrees Fahrenheit and reduction of equilibrium moisture in coals dried to about 500 to 700°F (260 to 316°C) is consistent with WRI experience, (Boysen et al. 1990).

A drying process was developed for PRB coal during the early 1980s. Initial work was done by Anaconda Minerals Co., later joined by Atlantic Richfield Co., using a 4 ton/hr pilot plant in Tucson, Arizona. The process has been licensed to Kaiser Engineers. The process uses fluidized bed drying in conventional equipment with a proprietary product treatment step (Skinner et al. 1984). The developers conducted laboratory research to determine methods to avoid low-temperature oxidation of the product. They developed methods using cooling, controlled preoxidation, treatment with carbon dioxide, and spray application of oil or chemical solution.

Koppelman was awarded patents (U.S. Patents 4,728,339 and 5,071,477) for use of "temperatures from 200 to about 1200°F, pressures from 300 up about 3000 psig, and residence times of 1 minute to 1 hour to process organic carbonaceous materials to effect a desired physical and chemical modification...[and]...a substantial reduction in the residual moisture content...to improve physical properties, including an increased heating value." The second patent describes the use of steam at high pressure to effect a controlled thermal restructuring, with the upgraded product possessing increased heating values. These patents are the basis for the K-Fuel® process.

Lien (1991) discusses the problems and progress AMAX has experienced with a McNally Pittsburgh dryer at the AMAX Belle Ayr mine. In this process, coal is dried by contact with a hot stream of fluidizing gas. The gas is composed partly of flue gas from combustion of coal dust with air and partly of recycled gas. The hot drying gas contains less than 5% oxygen. The dried coal, which contains 12 to 13 wt % moisture, enters the cooler at a temperature of 180 to 190°F (82 to 88°C) and is cooled to about 100°F (38°C) by contact with air. The cooled product is mixed with 2 to 4 gallons of number 6 fuel oil per ton to control product dustiness and help inhibit readsorption of moisture. Lien (1991) discusses the problems of upsets in the process caused by loss of feed and the experience with degradation of particles in the dryer. He also states that a major concern has been the stability of the product.

The Syncoal process is used at a Clean Coal I demonstration plant located at Western Energy Company's Rosebud mine near Colstrip, Montana. In the process, coal is passed through two vibrating fluidized bed reactors where it is contacted by hot gas to dry the coal and remove carboxyl groups and volatile sulfur compounds. The dried coal is further desulfurized by pneumatically stratifying the product to separate pyrite-rich ash (Western Energy Company 1992).

The Carbondry process (Simmons and Simmons 1992) has been tested at the pilot-plant scale at Carbontec's facility at Bismarck, North Dakota. The process involves a hot oil first stage drying unit and a flue gas drying unit. The process uses a coating of oil on the surface of particles to protect against readsorption of moisture and spontaneous heating. Published data indicate that the product made from PRB coal using the process contains about 6 to 10 wt % moisture and has a heating value ranging from 11,200 to about 11,700 Btu/lb.

The ENCOAL LFC process is used at a commercial demonstration facility at Triton Coal Company's Buckskin mine north of Gillette, Wyoming (McPherson 1992). In the process, coal is roasted to drive off moisture, coal liquids, and sulfur compounds. The plant, which was built using an award from Clean Coal III, produces a crude coal liquid and solid process derived fuel.

Numerous mechanical treatments are available for stabilizing coal products by reducing the surface contact with air. These include briquetting, pelletizing, and extruding with or without an added binder. An excellent list of references describing the use of a binder in pelletizing is given in U.S. Patent 4,615,712 (Wen), which describes the production of humic acid from oxidation of coals or leonardite and the use of the humic acid as a binder.

BACKGROUND

It is relatively easy to develop a process to drive the moisture from PRB coal. It is considerably more challenging to develop a process that can remove the moisture from the coal, alter the coal structure to minimize readsorption of moisture, and prevent oxidation and spontaneous combustion of the finished product. We have dried coal and done partial decarboxylation in our past work (Merriam et al. 1990). Drying minus 8 mesh PRB coal in a fluidized-bed reactor at atmospheric pressure results in all of the moisture being removed when the temperature of the coal in the bed reaches 350°F (177°C) (Figure 1). Continued heating of the coal as it moves along the cross-flow bed

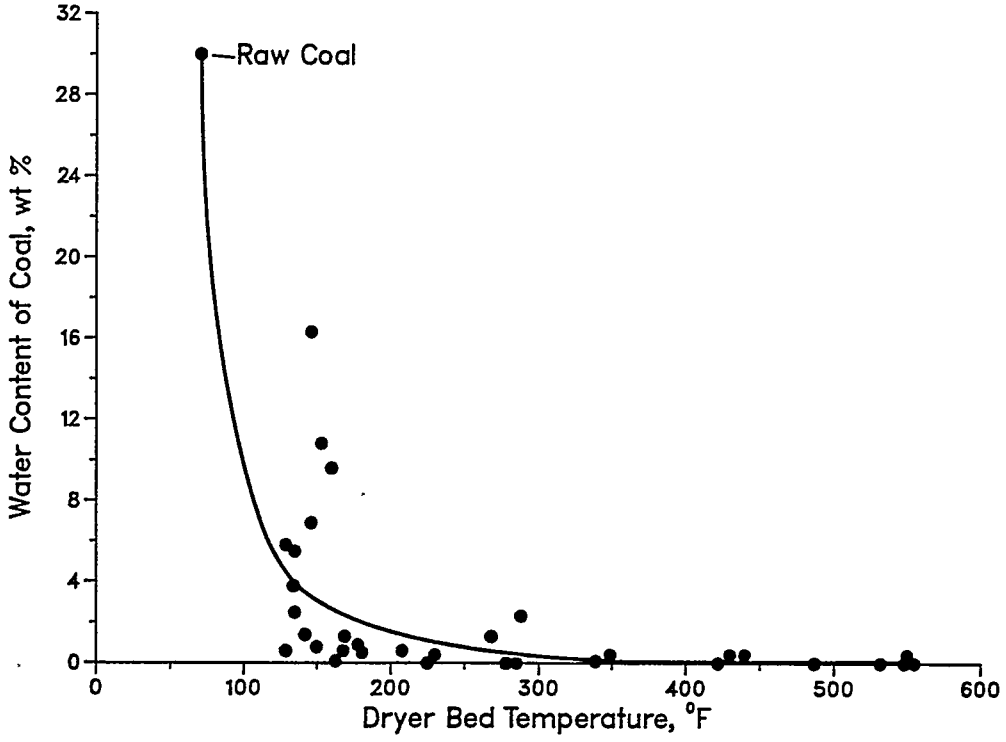

Figure 1. Drying Curve for Minus 8 Mesh PRB Coal Using Various Flow Rates of Fluidizing Gas

results in the partial decarboxylation, which removes oxygen from the coal in the form of carbon dioxide and carbon monoxide along with some methane (Figure 2). This removal of oxygen increases the heating value of the product, and it has been reported to reduce the susceptibility of the coal to spontaneous heating (Tomuro et al. 1985). However, our experience with PRB coal treated in this manner is that the coal is highly reactive and ignites spontaneously. The coal is most susceptible to self-ignition when it has been freshly processed. Dried coal that has been aged for several weeks (and has contacted air) is less likely to self-ignite.

Early attempts at WRI to stabilize dried coal (Boysen et al. 1990) focused on heating the coal to a slightly higher temperature to reduce the tendency to readsorb moisture (Figure 3). This work, which was done using minus 28 mesh PRB and Usibelli coals in a fluidized-bed reactor, indicates that the equilibrium moisture can be reduced to about 13 wt % by heating the coal to about 700°F (371°C) (Thomas, K.P., personal communication, memorandum dated December 16, 1991). However, it is necessary to heat the coal to about 1100°F (593°C) to reduce the equilibrium moisture to about 10 wt %. The coal tars become mobile in PRB coal at temperatures just above 600°F (316°C). Much loss of liquids would occur if the coal was heated to 1100°F (543°C) in the presence of fluidizing gas.

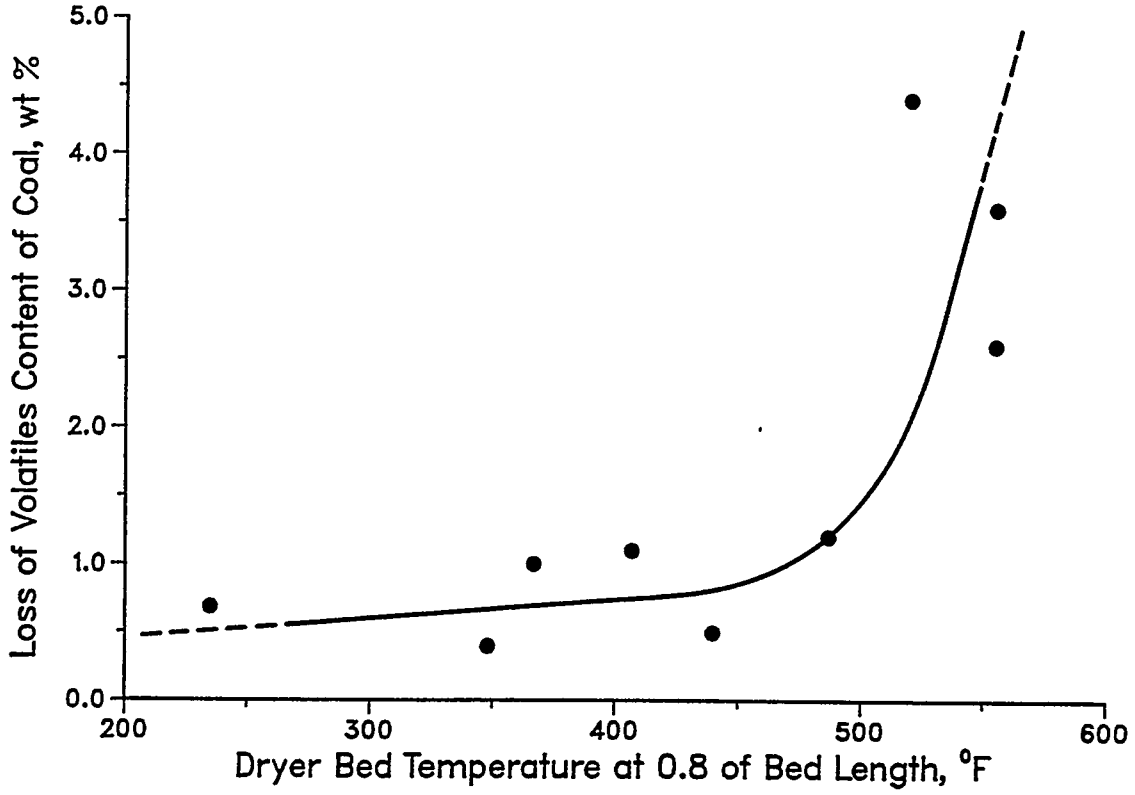

Figure 2. Partial Decarboxylation of Minus 8 Mesh PRB Coal in a Fluidized Bed Dryer

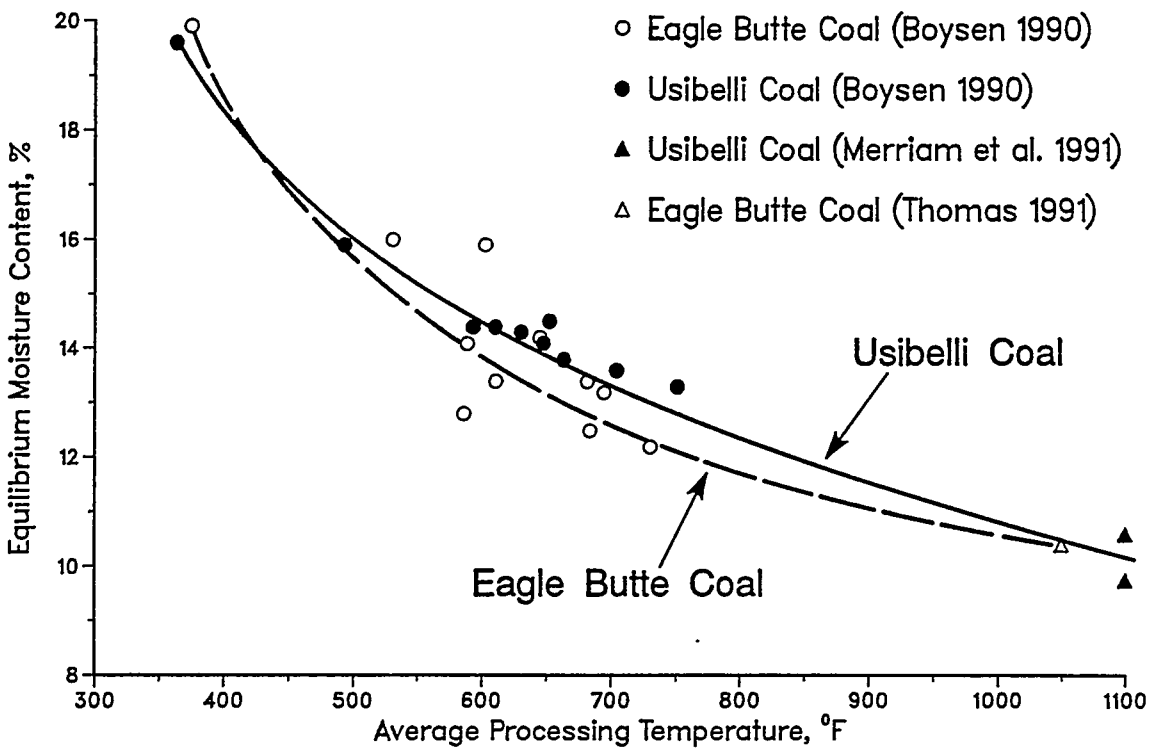

Figure 3. Equilibrium Moisture Content of Coals Subjected to Mild Pyrolysis

We later added a stabilization reactor to the pyrolysis reactor to coat char with the high-boiling fraction of the coal liquids driven from the coal in the pyrolysis reactor (Merriam and Sethi 1992). This work showed that we could further depress the equilibrium moisture to about 8 wt %. (Most of the increase in temperature that starts low-temperature oxidation is caused by the heat of adsorption of water upon the coal particles.)

STABILIZATION OF PROCESSED COAL

Self-Heating and Oxidation

We conducted numerous tests to determine how much various treatments affect the self-heating and low-temperature oxidation tendencies of raw and processed PRB coal. Samples were evaluated by contacting the coal or processed coal with oxygen saturated with water vapor at a temperature of 122°F (50°C) in an adiabatic chamber (Figure 4). The test results are evaluated graphically by plotting the temperatures in the samples versus time. The intersection of the slope of the initial heating curve and the slope of the curve after the temperature has started to rise is used as the time to

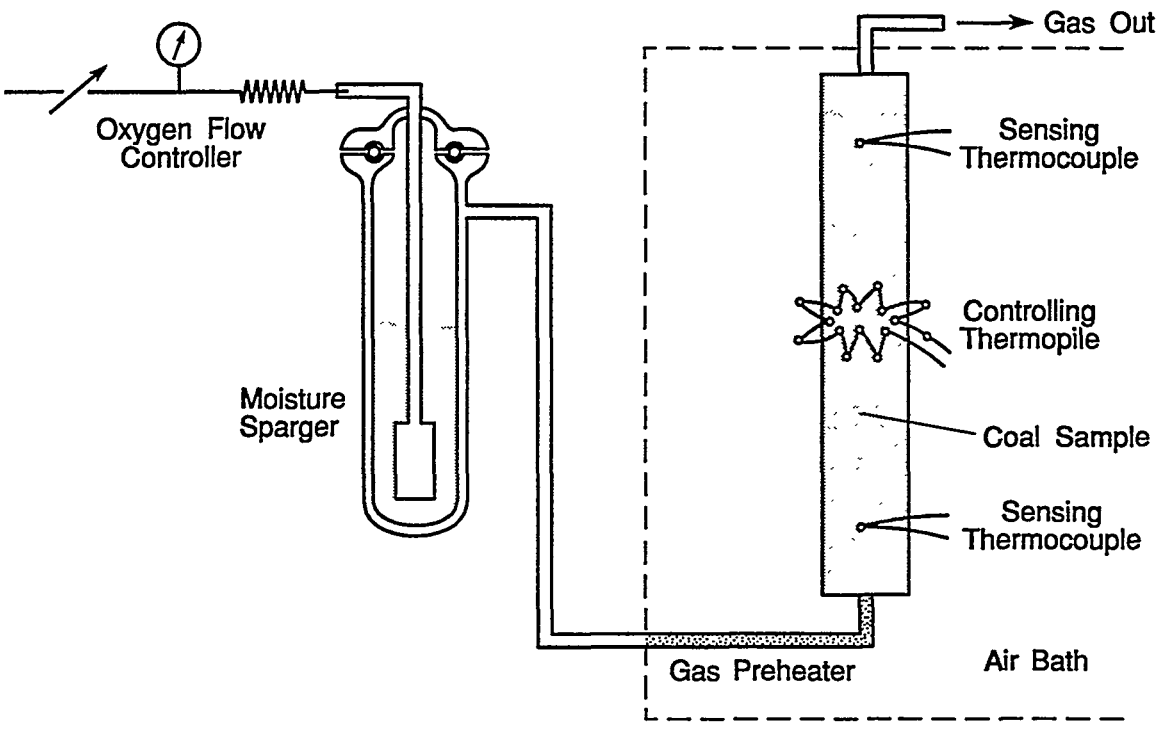

Figure 4. Apparatus Used to Determine the Susceptibility of Coal to Self-Heating and Oxidation

ignition. Tests are continued until the inflection point in the heating curve is defined or until the test has continued for 24 hours. Our experience has shown that an inflection point in the heating curve rarely develops after 24 hours of heating using this method. The results of the self-heating tests (Table 1) are used to compare the effectiveness of different processing conditions.

The tests to study the effects of temperature and oxygen on the self-heating of dried PRB coal were conducted using a small stirred autoclave heated by immersion in a heated bed of fluidized sand (Figure 5). Samples of coal that had been dried in a fluidized bed to 550°F (288°C) were split into 50-gram aliquots inside a nitrogen filled glove box to avoid contact with air. The aliquots were transferred into the reactor inside the glove box. The autoclave was then assembled and the gas pressure was cycled from 0 to 60 psig three times to flush unwanted gas from the reactor. The autoclave was then lowered into the heated sand for 35 minutes, including about 10 minutes at the desired maximum temperature. Upon completion of the test the autoclave was removed from the sand bath and immersed in water to rapidly cool the treated coal. Gas samples were obtained for analysis by transfer into evacuated containers. The treated coal was removed from the autoclave in the nitrogen filled glove box, and samples were placed in containers under a nitrogen blanket for further analysis.

Table 1. Time to Ignition for Minus 16 Mesh Raw, Dried, and Processed Coal, hr

	Temp °F	Duplicate Tests	
Raw Eagle Butte Coal		>24	>24
Coal Dried at Various Conditions			
N_2, 5 times @ 1 hr each	220	17	>24
N_2, 1 time for 5 hr	220	6	8
Air, 1 time for 6 hr	220	24	24
Fluid Bed, CO_2, 5 min (A)	550	4	5
Dried Coal from (A) Heated in N_2			
Batch in Stirred Reactor	565	4	4
Batch in Stirred Reactor	658	2	3
Dried Coal from (A) Heated in 0.8 Atm Air			
Batch in Stirred Reactor	586	4	5
Batch in Stirred Reactor	675	6	5
Batch in Stirred Reactor	692	10	>24
Batch in Stirred Reactor	723	7	8
Dried Coal from (A) Heated in 3.4 Atm Air			
Batch in Stirred Reactor	565	4	6
Batch in Stirred Reactor	675	4	5
Batch in Stirred Reactor	691	14	9
Batch in Stirred Reactor	697	7	8
Batch in Stirred Reactor	708	>24	>24
Batch in Stirred Reactor	732	>24	>24

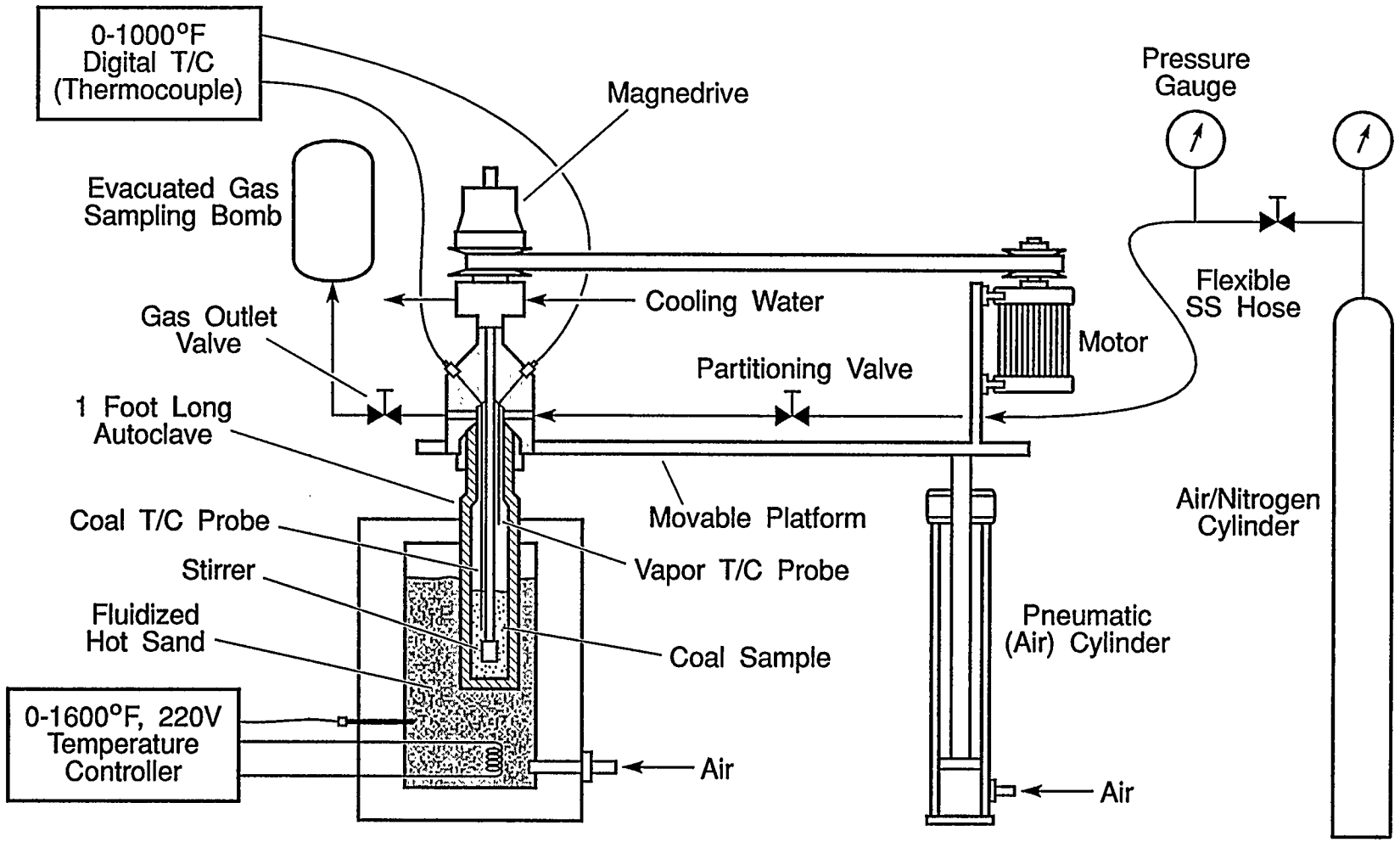

Figure 5. Stirred-Batch Reactor Used to Perform the "Accelerated Aging" Stabilization of Dried PRB Coal

The data in Table 1 show characteristics and trends that were used to guide the development of the COMPCOAL process. The section of Table 1 showing "coal dried at various conditions" indicates that coal moved into and out of the drying oven five times (which was incidentally exposed to air) and the sample dried in air both show relatively long ignition times. This pattern of data is an indication that exposure of dried coal to air at 220°F (104°C) results in some resistance to self-heating relative to the coal samples dried in nitrogen.

The samples dried in nitrogen and carbon dioxide show reduced ignition times, with increasing temperature over the range of temperatures from 220, 550, 565, and 658°F (104, 288, 296, and 348°C). We therefore conclude that heating the dried coal in inert gas increases the susceptibility to self-heating as the temperature is increased in the range studied. The dried coal heated in a small amount of air (at a starting pressure of 0.8 atmospheres at our laboratory) indicates a trend opposite to that shown by dried coal heated in nitrogen. The dried coal heated in air shows increased resistance to self-heating (longer ignition times) as the temperature is increased from 585 to 703°F (307 to 373°C). The trend when heating in air using a starting pressure of 0.8 atmospheres is not strong, but appears to be real.

The dried coal heated using more air available to react with the coal (a starting air pressure of 3.4 atmospheres) shows a strong and definite trend of increasing resistance to self-heating and oxidation. This last trend is also very sensitive to the temperature of the coal in the stirred bed when the oxygen is reacting with the dried coal (Figure 6). The pattern between the groups (heating in inert gas, heating in 0.8

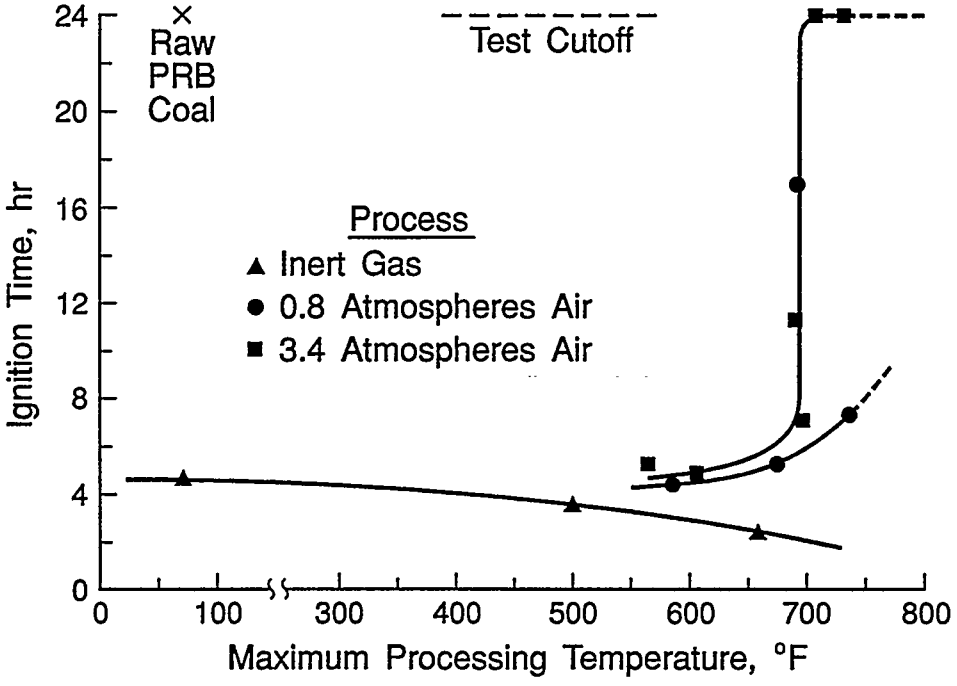

Figure 6. The Effects of Temperature and Oxidation on the Self-Heating Characteristics of Dried PRB Coal

atmospheres of air, and heating in 3.4 atmospheres of air) also shows a consistent trend of increasing resistance to self-heating and oxidation as the quantity of oxygen available to react with the dried coal is increased.

Tests with air in the stirred, batch reactor with an initial pressure of 3.4 atmospheres show a change in the quantity and composition of gas produced (Figure 7) in the temperature range of the tests. At the lower temperatures a small amount of gas composed of predominantly carbon dioxide, with lesser amounts of carbon monoxide and traces of methane is produced. The volatiles removed at the higher temperatures are mostly noncondensible gases. In the upper part of the temperature range the volume of gas produced is increased greatly and the concentration of the methane and the ethane in the gas increases. Significantly, no oxygen is detected in the effluent gas, indicating that the oxygen in the air at the start of the tests is completely reacted with the coal. However, the consumption of the oxygen from the air by the coal is more than offset by the oxygen that is removed from the coal by the processing (Figure 8). The carbon dioxide and carbon monoxide emitted from the coal contain many times as much oxygen as is consumed from the air in the reactor.

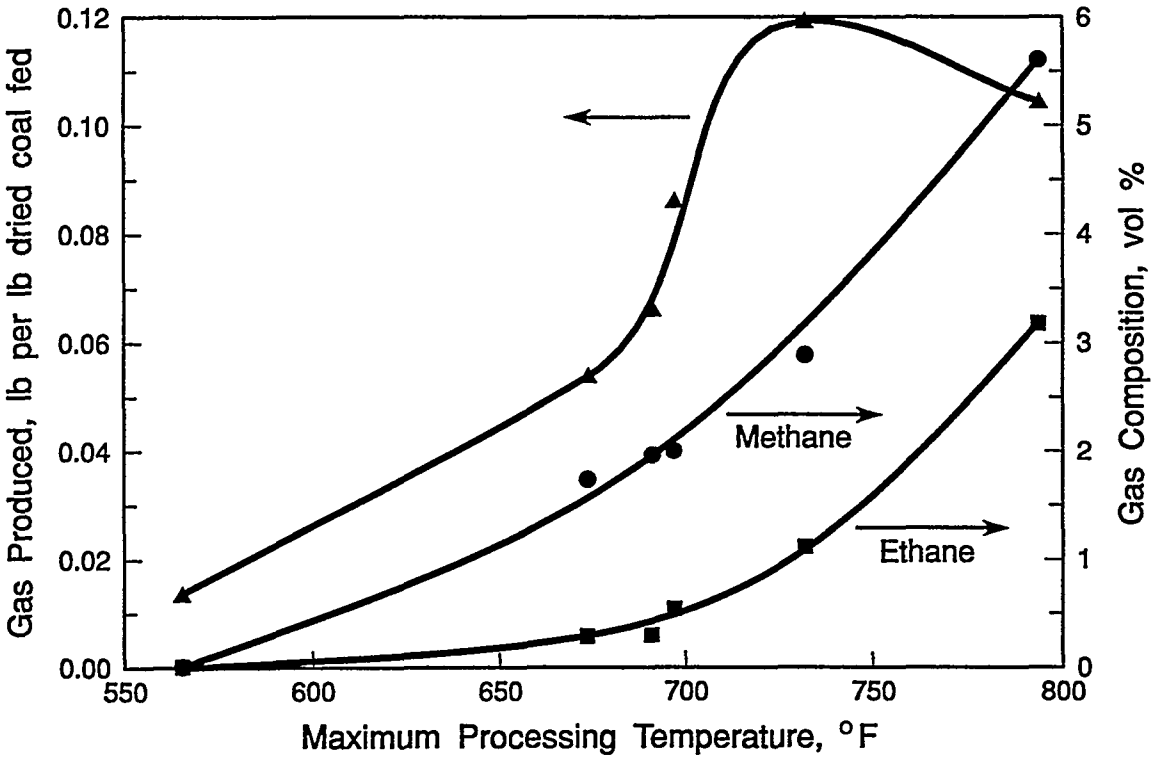

Figure 7. The Change in Composition of Gas Produced at Temperatures Below and Above the Onset of Stabilization

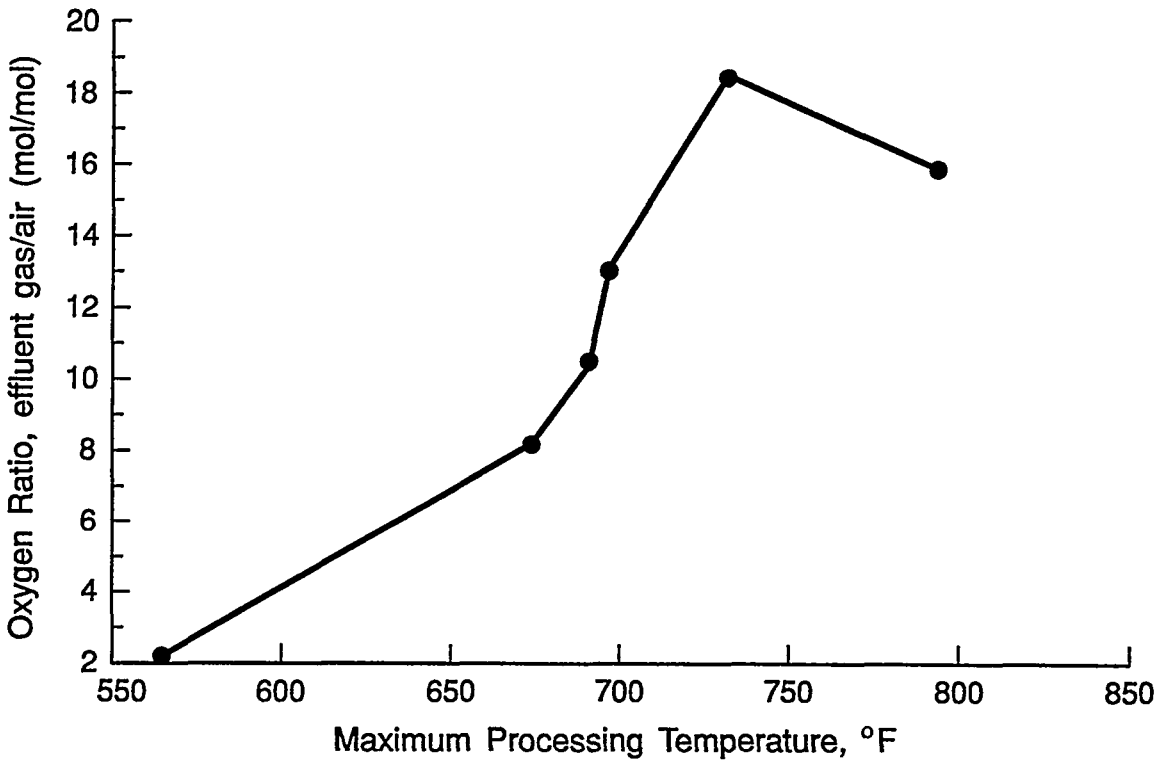

Figure 8. The Oxygen Released from the Coal is Many Times the Oxygen Taken Up by the Accelerated Aging

Readsorption of Moisture

The tendency of processed coal to readsorb moisture is a characteristic that must be considered as a determinant of the quality of any dried or pyrolyzed coal. We have used the test for equilibrium moisture (ASTM D1412) as a measure of the maximum quantity of water that coal and processed coal can adsorb. The test is actually intended to measure the water content that a coal seam can contain. In the test, coal is crushed to minus 28 mesh and soaked in deionized water for 3 hours. The excess water is then removed from the coal by filtration and the coal is held in a sealed container at 98% relative humidity for 48 hours. The water content of the coal is then determined. We think this test may represent conditions that are somewhat more severe than processed coal may typically be exposed to, but we use it because it is an accepted ASTM procedure, and the test does not appear to overstate the readsorption characteristics of the coal by much.

We use equilibrium moisture as an indication of the stability of the products from the various processing conditions we have tested. Low equilibrium moisture is indicative of a stable processed coal.

The results of our tests (Table 2) show that coal dried to 550°F (288°C) is less susceptible to readsorption of moisture than the raw coal. (However, dried coal, when untreated, is more susceptible to oxidation than raw coal.) Forming the dried coal into briquettes reduces the tendency to readsorb moisture even further, while the accelerated aging at 793°F (423°C) reduces the equilibrium moisture still more.

Table 2. Equilibrium Moisture Content of Eagle Butte Coal, Dried Coal, Briquettes, and Treated Coal, wt %

	Duplicate Tests	
Eagle Butte Feed Coal	25	26
Dried in Air, 6 hr, 220°F	22	22
Fluid Bed Dried in CO_2 to 550°F	17	17
Briquettes Made from Dried Coal	13	9
Briquettes-Dried Coal-10% Fines	14	14
Dried Coal Heated in 3.4 Atm Air and 793°F	10	11
One Millimeter Glass Beads	1	1
Ottawa Sand	0	0

We have not yet tested the obvious combination of briquettes made from coal treated in the "accelerated aging" process. The beads and sand are included to show that materials having no porosity and nonpolar surfaces have an equilibrium moisture content of about zero.

Characteristics of Stabilized Coal

The stabilized coal produced by reacting dried PRB coal with air using the stirred batch reactor contains 35 to 40 wt % volatiles and has heating values of 12,000 to 12,700 Btu/lb (Table 3 and Figure 9).

Table 3. Characteristics of the COMPCOAL Product

Test	11	10	12	6
Temperature, °F	565	691	697	708
Volatiles, wt %	40.2	36.7	35.4	34.5
Heating Value, Btu/lb	12,009	12,439	12,600	12,725

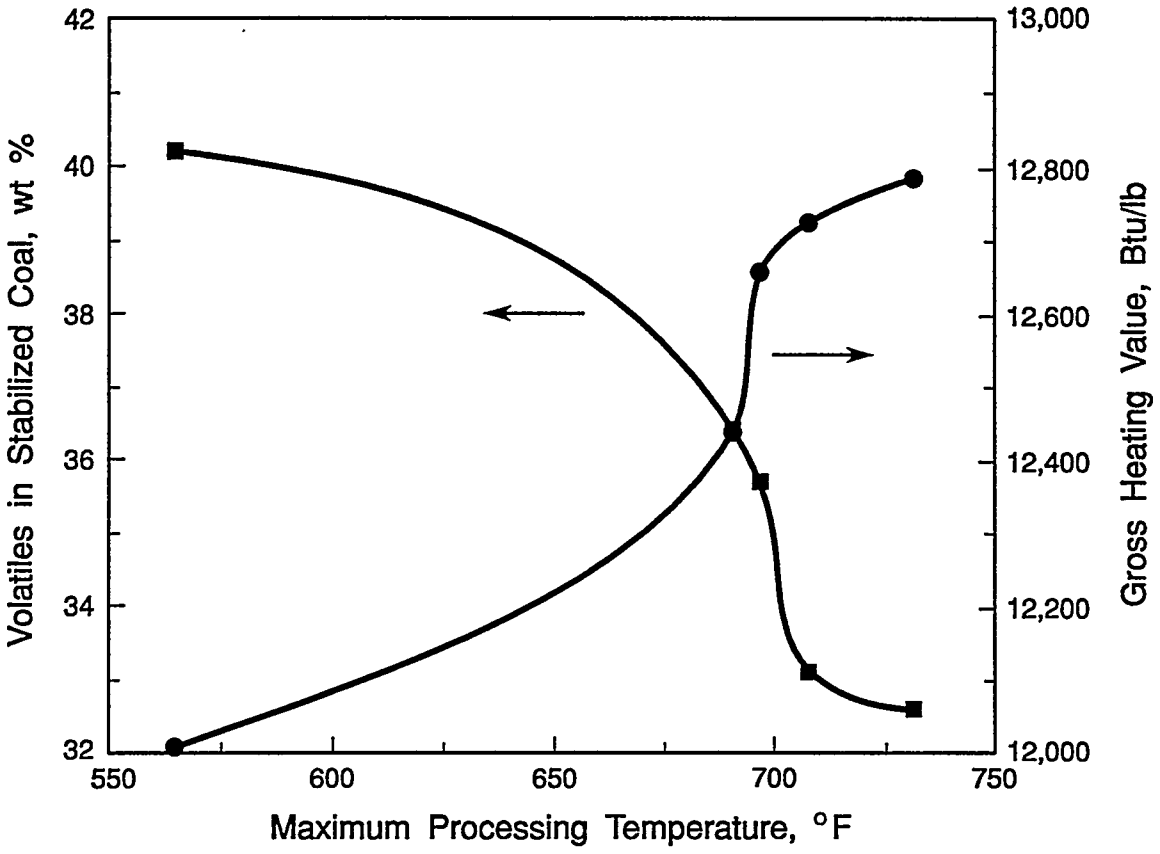

Figure 9. Volatile Content and Heating Value of the COMPCOAL Product

DESCRIPTION OF THE COMPCOAL PROCESS

In the COMPCOAL process, sized coal is dried to zero moisture content and additional oxygen is removed from the coal by partial decarboxylation as the coal is contacted by a stream of hot fluidizing gas in the dryer (Figure 10). The hot, dried coal particles flow into the pyrolyzer where they are contacted by a very small flow of air. The oxygen in the air reacts with active sites on the surface of the coal particles, causing the temperature of the coal to be raised to about 700°F (371°C) and oxidizing the most reactive sites on the particles. This "instant aging" contributes to the stability of the product while only reducing the heating value of the product by about 50 Btu/lb. Less than 1 scf of air per pound of dried coal is used to avoid removing any of the condensible liquid or vapors from the coal particles. The pyrolyzed coal particles are mixed with fines from the dryer cyclone and dust filter and the resulting mixture is fed into a briquettor at about 600°F (316°C). Briquettes are cooled to about 250°F (121°C) by contact with a mist of water in a gas-tight mixing conveyor. The cooled briquettes are transferred to a storage bin where they are accumulated for shipment.

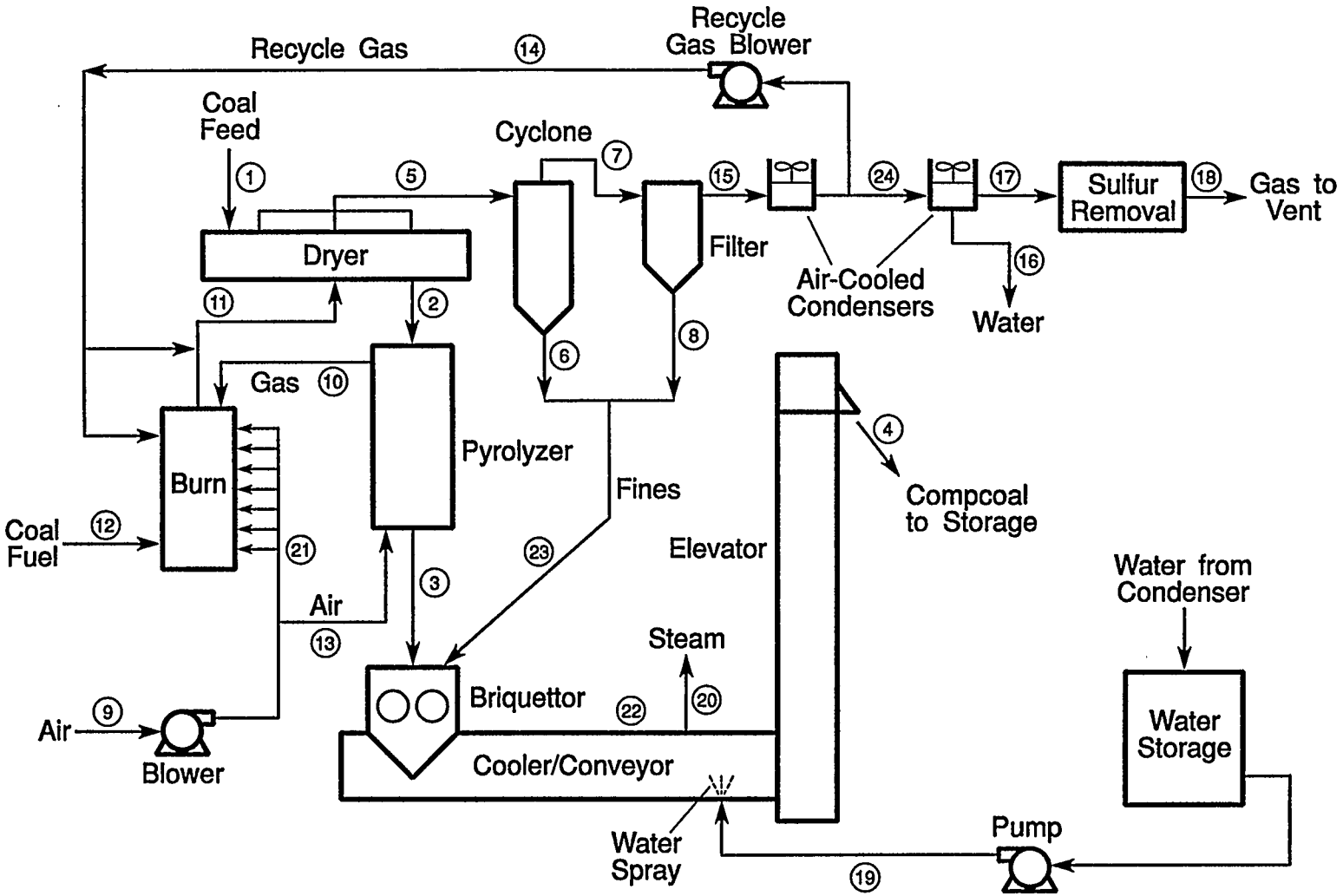

Figure 10. Identification of Stream Flows and Conditions Used to Size Equipment for the COMPCOAL Process

An important feature of the process is the avoidance of pyrolysis in the dryer and use of the onset of pyrolysis in the pyrolyzer to stabilize the particles. In the dryer, where the gas flow rate is high, the coal remains below the temperature at which liquids and vapors are formed. In the pyrolyzer, the temperature is raised to form liquids in the coal particles, but the gas flow is kept low to avoid stripping liquids out of the coal. In this manner, a high flow rate of gas can be used to carry heat into the dryer and subsequently, in the pyrolyzer, the tars in the coal may be melted and refrozen without producing a substantial loss of liquid or vapors from the coal.

A recycle gas stream is used to carry heat into the dryer while limiting the temperature at which fluidizing gas enters the dryer. Heat for drying is produced by burning coal using a low NO_x burner. Vapors from the pyrolyzer are incinerated in the burner. The flue gas is mixed with recycled gas to lower the temperature at which the fluidizing gas enters the dryer. The water is removed from the dryer effluent gas by condensation in air-cooled condensers supplying a nearly dry stream for sulfur removal. The water from the condensers is sprayed onto the hot COMPCOAL briquettes in the cooling conveyor where the water is converted into steam.

The process we describe herein is not yet optimized. For example, if we can tolerate a wet gas stream in the sulfur removal unit, then one of the air-cooled condensers is not needed, and only the recycle portion of the dryer effluent gas needs to be cooled.

WRI has experience with the drying portion of the process using minus 8 mesh PRB coal at feed rates of 90 to 150 lb/hr in tests lasting from 24 to 120 hours (Merriam et al. 1990). The pyrolysis (stabilization) portion of the process is presently being developed using a batch, laboratory-scale reactor. We plan to conduct tests using a continuous-flow, bench-scale reactor for the next phase of development.

ECONOMIC EVALUATION OF THE PROCESS

The process flow diagram (Figure 10) and the stream flows and conditions (Table 4) were used to size equipment for a 1,000 ton per day (TPD) COMPCOAL plant (Table 5). We estimated the cost of capital equipment items (Table 6) by proportioning the published costs of similar equipment (Hogsett et al. 1991) designed for a 1,000 TPD mild-gasification plant using PRB coal. We have assumed that the plant would be located at a PRB mine and would use existing crushing and screening equipment. The plant would operate for 24 hours per day 330 days per year and would produce 615 tons of COMPCOAL product per day.

The largest single cost of operation of the plant is the purchase of the feed coal (Table 7), which we have priced at $4.50 per ton. We have estimated the cost of operation based on two operators per shift and three supervisory or professional employees.

Table 4. Stream Flows and Conditions for a 1,000 TPD COMPCOAL Plant

Stream	Material	Flow, MPPH	Temp, °F	Press, psia	Enthalpy, MMBtu/Hr
1	Feed Coal	83.3	60	12.5	0.0
2	Dry Coal	48.8	575	15.5	8.80
3	Pyrolyzed Coal	45.5	650	15.0	9.40
4	COMPCOAL Product	51.3	250	12.5	3.41
5	Gas from Dryer	136.5	400	14.5	18.57
6	Fines	5.9	300	12.5	0.51
7	Gas from Cyclone	130.6	400	13.5	18.06
8	Dust from Filter	0.2	300	12.5	0.02
9	Air to Blower	37.8	60	12.5	0.0
10	Gas from Pyrolyzer	2.1	650	16.5	0.39
11	Fluidizing Gas	107.9	1200	16.0	59.04
12	Coal Fuel	5.4	60	12.5	0.0
13	Air to Pyrolyzer	1.1	100	17.0	0.01
14	Dryer Recycle Gas	65.0	250	17.0	6.50
15	Gas to Condensers	130.4	400	13.0	18.04
16	Water from Cond.	28.0	150	12.5	1.21
17	Gas to Desulf	37.5	150	12.5	1.08
18	Gas to Vent	37.5	150	12.5	1.08
19	Water to Cooler	5.6	60	40.0	0.0
20	Steam from Cooler	5.6	300	12.5	6.29
21	Air to Burner	36.7	100	17.0	-0.47
22	Briquetted COMPCOAL	51.6	650	12.5	10.66
23	Fines	6.1	300	12.5	0.51
24	Gas to Sec Cond	65.5	250	12.5	4.97

Table 5. Description of Equipment Needed for a 1,000 TPD COMPCOAL Plant

---

Coal Feed System
Assume crusher, screens, belts already in place
Add feed conveyor, feed bin, feed screws, rotary valves
Feed conveyor - 41.7 TPH, 24-in. wide, 120 ft long, 25 hp
Feed bin - 25 ton capacity
Feed screws (3) - carbon steel (CS), 6 in., 20 ft long, 2 hp
Rotary valves (3) - CS, 8 x 10 in., 2 hp

Reactors
Dryer - (2) IFB, 3 min coal residence time, 10 by 30 ft
Pyrolyzer - 200 cu ft, 10 ft tall, 13 ft dia, CS
Cooling conveyor - Gas-tight, 30 ft long, 18-in. wide, 650°F inlet temperature, 25 TPH, 10 hp, 6 in. water

Blowers
Air blower - 38 MPPH, 9700 acfm, 12.5 psia suct, 5 psi Dp, 120 hp
Dryer gas blower - 65 MPPH, 17,600 acfm, 12.5 psia and 250°F inlet, 5 psi Dp, 900 hp

Cyclones, Bag Filters, and Dust Collector
Dry effl. cycl. - (5) 140 MPPH, 400°F, 14.5 psia, 50 M acfm, CS
Bag filters - (4) 140 MPPH, inlet 14 psia and 400°F, (1-5 psig), 50 M acfm, CS
Dust collector - CS, 20 M acfm, 25 hp

Burner
Heat release 50 MM Btu/hr, refractory lined, no heat transfer surface, 22 psia and 1500°F, fuel - 5.4 MPPH coal and 2.1 MPPH gas

Vent Gas Scrubber
Limestone slurry for SO_2 removal. Gas 38 MPPH, 10,300 acfm, inlet 150°F, 12.5 psia, 500 ppm SO_2

Air-Cooled Condensers
Primary - 6.5 MM Btu/hr, 130 MPPH, inlet 400°F and 13.0 psia outlet 250°F,
CS tubes, 10 hp
Secondary - 34 MM Btu/hr, 65 MPPH, inlet 250°F and 12.5 psia, outlet 150°F,
SS tubes, 20 hp

Briquetting System
System includes conveyor, feed screws, screens, recycle crusher and elevator.
52 MPPH of dried coal at 650°F

Table 6. Cost of Capital Equipment for a 1,000 TPD COMPCOAL Plant, $1,000

Number	Equipment	Cost	Installed
1	Feed Conveyor - 24 in. 120 ft. 25 hp	195	389
1	Feed Bin - 25 ton capacity	60	113
3	Feed Screws - CS 6 in. 2 hp each	233	464
4	Rotary Valves - CS 8 by 10 in. 2 hp	22	42
2	Dryers - IFB 30 ft by 10 ft	1200	1,800
1	Pyrolyzer - 13 ft dia by 10 ft tall	129	297
1	Cooling Conveyor - 30 ft gas tight	80	160
1	Air Blower - 9700 acfm, 120 hp	109	217
2	Dryer Recycle Blowers - 17,600 acfm	423	800
5	Dryer Cyclones - CS 50 M acfm	138	248
5	Cyc Rotary Valves - CS 6 by 8 in. 1 hp	45	85
4	Bag Filters - CS 20 M cam, 25 hp	60	240
1	Burner - 48 MM Btu/hr	405	648
2	Water Pumps - 20 gpm, 2 hp each	12	37
1	Bucket Elevator - 30 ft, 52 MPPH	65	130
1	Water Tank - CS 10 M gal	25	50
1	Primary Condenser - 6.5 MM Btu/hr	37	77
1	Secondary Condenser - 34 MM Btu/hr	145	307
1	COMPCOAL Storage Bin - 430 ton	240	454
1	Briquetting System - 60 MPPH 650°F	910	1,365
1	Loading Conveyor - 24 in. 120 ft	195	389
1	Flue Gas Scrubber - 10,300 acfm	184	341
2	Product Storage Silos - 6500 ton each		2,000
	Cost of Equipment		10,653
	Sales Tax-5%, Const Mgmt-5%, Engr-10%		2,138
	Contingency - 20%		2,138
	Total Capital Cost		14,929
	Annual Deprecation - 10 year straight line		1,497

Table 7. Operating Costs for a 1,000 TPD COMPCOAL Plant, $1,000

Coal - 351,400 tons @ $4.50	$1,581
Labor - 3 Supervisors, 53,000 per year	159
Labor - 8 Operators, 45,000 per year	360
Maintenance - 4% of capital cost	599
Depreciation - 10 year straight line	1,497
Limestone - 5 TPD @ $18/ton	30
Propane (startup) - 10,000 gal @ $.60	6
Sludge Disposal (Desulfurization)	30
Electrical Power - 1130 hp @ $0.055/kWh	304
Interest Expense @ 10% (50% debt, 50% equity)	748
Annual Operating Cost	$5,314

The plant has three sources of revenue: revenue from the sale of the product, the special fuel production credit, and savings in freight costs. The high-Btu, low-sulfur product is expected to sell for a premium price because it can be used in boilers designed for high-Btu coal. It can also be blended with other coals to lower the sulfur content and to raise the heating value. We have treated the sales price of the COMPCOAL product as a variable in our economic evaluation to determine the sensitivity of the return on investment to different price levels.

The special fuel production credit (Internal Revenue Code article 29 section (c)(2)(b)) authorizes the credit for liquid, gaseous, or solid synthetic fuels produced from coal including such fuels when used as feedstocks. The credit is equivalent to $3 for the production and sale of qualified fuels for each quantity of fuel that would yield energy equal to that of a barrel of oil (5.8 million Btu). The $3 per 5.8 million Btu is equivalent to a credit of $13 per ton of COMPCOAL product. The IRS has required that fuel from coal be upgraded by one rank (from subbituminous to bituminous) to qualify for the credit. The initial credit applied to production from facilities placed in service after 1979 and before 1993 but was later extended by Congress and is currently in effect.

We have assumed that the reduction in shipping costs will flow to the investor and become a part of the return on the investment. The high-Btu value of the COMPCOAL product will result in a one-third reduction in the tons shipped. The savings are based upon a freight rate of $20 per ton.

The use of 50% debt financing (Table 8), as would be expected if the plant is owned by a utility company, results in higher return on investment than does use of equity financing only (Table 9). The debt financed plant has a net income at a price of over $15 per ton while the equity financed plant has a net income at a sales price of less than $15 per ton.

Table 8. Return on Investment from a 1,000 TPD COMPCOAL Plant Using 50% Debt Financing, $ million per year

Sales Price $/ton	15	20	25	30
Income from Sales	3.04	4.06	5.08	6.09
Freight Savings	1.90	1.90	1.90	1.90
Operating Income	4.94	5.96	6.98	7.99
Operating Cost	5.31	5.31	5.31	5.31
Net Income	(0.37)	0.65	1.67	2.68
Fed Inc Tax (36%)	0	0.23	0.60	0.96
Income After Tax	(0.37)	0.42	1.07	1.72
Depreciation	1.50	1.50	1.50	1.50
Spec Fuel Prod Credit	2.64	2.64	2.64	2.64
Cash Flow	3.77	4.56	5.21	5.86
Discounted Cash Flow Rate of Return, %	51	62	70	79
				Basis = 351,400

TPY coal, 330 days per year, 203,148 TPY of COMPCOAL, Freight -$20/ton, Investment - $7,483,500

Table 9. Return on Investment from a 1,000 TPD COMPCOAL Plant Using Equity Financing, $ million per year

Sales Price $/ton	15	20	25	30
Income from Sales	3.04	4.06	5.08	6.09
Freight Savings	1.90	1.90	1.90	1.90
Operating Income	4.94	5.96	6.98	7.99
Operating Cost	4.57	4.57	4.57	4.57
Net Income	0.37	1.39	2.41	3.42
Federal Income Tax (36%)	0.13	0.50	0.87	0.96
Income After Tax	0.24	0.89	1.54	2.19
Depreciation	1.50	1.50	1.50	1.50
Special Fuel Production Credit	2.64	2.64	2.64	2.64
Cash Flow	4.38	5.03	5.68	6.33
Discounted Cash Flow Rate of Return, %	29	34	39	42

Investment - $14.929 million

REFERENCES

Boysen, J.E., C.Y. Cha, F.A. Barbour, T.F. Turner, T.W. Kang, M.H. Breggren, R.F. Hogsett, and M.C. Jha, 1990, Development of an Advanced Process for Drying Fine Coal in an Inclined Fluidized Bed, Final Report. Laramie, WY, WRI Report to DOE, DOE/PC/88886-T5.

Hogsett, R.F., M.C. Jha, and The Ralph M. Parsons Co., 1991, Development of an Advanced Continuous Mild Gasification Process for the Production of Coproducts, Topical Report for Task 4.6, Technical and Economic Evaluation. AMAX R & D Center, Golden, CO.

Ingram, G.R., and J.D. Rimstidt, 1984, Natural Weathering of Coal. *Fuel*; 63 (3): 292-296 (Mar 1984).

Lien, T.J., 1991, AMAX Advances Low-Rank Coal Drying. *Coal*, December, pp. 49-51.

McPherson, R., 1992, The Next Generation of Power Generation. Coal Market Strategies Tenth Annual Conference, Western Coal Council, Wheat Ridge, CO.

Merriam, N.W., C.Y. Cha, T.W. Kang, and M.B. Vaillancourt, 1990, Development of an Advanced, Continuous Mild-Gasification Process for the Production of Coproducts, Topical Report for Task 4, Mild Gasification Tests-System Integration Studies. Laramie, WY, WRI Report to DOE, DOE/MC/24268-3075.

Merriam, N.W., K.P. Thomas, and C.Y. Cha, 1991, Mild Gasification of Usibelli Coal in an Inclined Fluidized-Bed Reactor. Laramie, WY, Western Research Institute Report, WRI-91-RO21.

Merriam, N.W., and V.K. Sethi, 1992, Status of Development of a Process to Produce a Premium Solid Fuel From Powder River Basin Coal. Laramie, WY, WRI Report to DOE, WRI-92-RO56.

Simmons, J., and J.J. Simmons, 1992, The Carbondry™ Process, An Innovative Approach to Drying Low Rank Coals. Proceedings of Coal Prep '92, McLean Hunter Presentations, Aurora, CO.

Skinner, J.L., L.B. Rothfield, B.F. Bonnecaze, S.W. Johnson, and Y.H. Li, 1984, Drying of Powder River Subbituminous Coal-Overview of a New Process. Coal Technology '84, 7th International Coal and Lignite Exhibition and Conference, Houston, TX.

Tomuro, J., S. Nogita, and Y. NaKamur, 1985, Reduction of Oxidation Rate of Coal by Coal-Derived Tar Coating. Proceedings 1985 International Conference on Coal Science, Pergamon Press, New York.

Western Energy Company, February 1992 Technical Progress Report. Submitted to U. S. DOE Pittsburgh Energy Technology Center.

Willson, W.G., S.A. Farnum, G.G. Baker, and G.H. Quentin, 1987, Low-Rank Coal Slurries for Gasification. *Fuel Processing Technology*, 15: 157-172.

APPENDIX

Production of Premium Solid Fuel from Powder River Basin Coal

PRODUCTION OF PREMIUM SOLID FUEL FROM POWDER RIVER BASIN COAL

Coal and products made by the treatment of coal have the potential to undergo spontaneous combustion. Spontaneous combustion is a problem for two reasons: the safety considerations associated with a fire in a large coal pile and the economic loss caused by combustion of a large mass of coal. To address this problem, research has been conducted to understand spontaneous combustion of coal (Smith and Lazzara 1987, Smith et al. 1991. and Unal et al. 1993) and to predict a coal's tendency to spontaneously combust (Miron et. al, 1990, Page et al. 1993 and Litton and Page 1994).

There have been two general approaches to evaluating the tendency for a coal to undergo spontaneous combustion: calorimetric measurements and oxygen absorption. Methods based on calorimetric measurements have been developed by the Bureau of Mines (Smith and Lazzara, 1987) and Western Research Institute (WRI) (Barbour, unpublished results). The Bureau of Mines has also developed a method based on oxygen absorption (Miron et al. 1990). Since the oxygen absorption method is simpler to perform than calorimetric measurements and the calorimetric method developed by WRI differs from that developed by the Bureau of Mines, it was decided to develop the capabilities of the oxygen absorption method at WRI.

The oxygen absorption method measures the pressure drop in a sealed flask containing a known mass of coal over a 7-day period. Research has shown that the pressure drop is caused by the absorption of oxygen by the coal. In addition, the amount of oxygen absorbed correlates with the minimum self-heating temperature (SHT) of many coals (Miron et al. 1990). The minimum self-heating temperature is a measure of the tendency of a coal to spontaneously combust (Smith and Lazzara 1987). The scale by which the potential for spontaneous combustion is assigned is as follows:

- SHT less than 70 °C—the coal has a high potential for spontaneous combustion.
- SHT between 70 and 100 °C—the coal has a medium risk for spontaneous combustion.
- SHT greater than 100 °C—the coal has a low potential for spontaneous combustion.

Instrumentation

An instrument was constructed to measure the pressure drops in six sealed flasks. The heart of the instrument is six miniature pressure transducers. These transducers are Omega model PX 1326-015AV micro transducers with a range of 0-15 PSIA. The pressure of each transducer is obtained from an Omega model DP 2000-S2 digital transducer indicator. The indicator is switched between the transducers with a rotary switch.

All the components are mounted on a metal rack. The rack is also fitted with a flex frame stand to support the transducers and the reaction flasks. The reaction flasks consist of glass flasks fitted with 24/40 ground glass joints that match the joints attached to the transducers. Three sizes of reaction flasks are available for use with this unit: 500, 250, and 125 ml.

Method Development

The method described by Miron et al. (1990) is straightforward. A 50-g sample of coal is dried, placed in a 500-ml reaction flask, and sealed. The pressure in the flask is measured at the start of the experiment and again after 7 days. The pressure drop is used in a linear relationship that estimates the effective minimum self-heating temperature that relates to the sample's tendency to undergo spontaneous combustion. However, evaluation of the method and a series of preliminary experiments show that 50 g of sample of a highly reactive coal will absorb all of the oxygen available in the atmosphere of a 500-ml flask at the barometric pressure of Pittsburgh, Pennsylvania, where the method was developed. When the experiments are performed at the higher elevation of Laramie, Wyoming, the 50-g sample of a reactive coal will also absorb all of the available oxygen in the reaction flask. Since less oxygen is available at the higher elevation, absorption of all of the oxygen will not produce as high a pressure drop as observed at Pittsburgh, and the method will predict a higher than actual SHT.

This concern was overcome by using the ratio of the average barometric pressures at Laramie and Pittsburgh to adjust the mass of coal used in the analysis. The mass of coal used in a 500-ml reaction flask at Laramie is 40 g. Results with this sample size are consistent with results reported by Miron et al. (1990).

A problem with the size of available samples was encountered. It appears that the amount of sample available for analysis is often less than the 40 g required for the 500-ml reaction flask. For samples having less than 40 g of material, the mass of sample used for analysis is reduced by factors of 2 or 4 so that reaction flasks of volumes 250 and 125 ml respectively can be used. Table A-1 provides a summary of the results from a series of experiments using 40, 20, and 10 g of dried Fort Union coal in duplicate analyses. The estimated values for SHT range from 58 to 60 °C. This variation is well within experimental error for the method and shows that smaller sample sizes can be used.

Table A-1. Comparison of Estimated SHT Values for Samples of 40, 20, and 10 g of Laboratory Dried Powder River Basin Coal

Samp. Size, g	40	40	20	20	10	10
SHT, °C	60	60	58	58	58	58

Two other modifications were made to the method reported by Miron et al. (1990). The pressures at the beginning and end of the analysis are corrected for temperature. This was done because of the large variation in room temperature observed in our laboratory. The second modification was to account for the pressure drop caused by the adsorption of water vapor in the air. This correction is performed by using the relative humidity in the air at the start of the experiment. These corrections were made to minimize the effects of random errors caused by temperature fluctuations and changes in the relative humidity.

The result of the modification was the development of the following linear relationship to estimate SHT:

$$SHT=120.0-(0545X[pi-pf-pw])$$

where Pi = temperature-corrected initial pressure in the reaction chamber.

Pf = temperature-corrected final pressure in the reaction chamber.

Pw = partial pressure of the water vapor represented by the relative humidity.

Application to Treated Coal Samples

One of the reasons for developing the oxygen absorption method was to be able to evaluate coals that are treated to remove water and stabilized to reduce the tendency for spontaneous combustion. A sample of treated coal product (dried PRB coal) was analyzed by the oxygen absorption method and by calorimetry. The results from the calorimetry studied show the product has a very low tendency for spontaneous combustion.

Since there is not a data base using this method for treated coal products, four different sample preparation procedures were evaluated. These procedures include: (1) the sample as received, (2) the sample as received but ground, (3) the sample as received but dried at 70 °C, and (4) the sample ground and dried at 70 °C. This suite of procedures was selected because the particle size of the product was larger than the range of particle sizes studied by Miron et al. (1990), and the method calls for drying the sample at 70 °C before analysis. The purpose of the drying step is to displace hydrocarbon gases in the coal so that during the analysis they are not released and mask the pressure drop caused by oxygen absorption.

The results of these experiments are listed in Table 2. Examination of the results shows that the SHT values determined for samples that were analyzed without any preparation and those that were analyzed with only grinding are the same. Therefore, breaking the particles and exposing the interior surfaces does not affect the tendency of the product to undergo spontaneous combustion. However, the two samples that were dried at 70 °C have SHT values that are significantly lower. The values for the two dried samples indicate the treated product presents a medium risk for spontaneous combustion, while those that were not dried show a low potential for spontaneous combustion. These differences in the SHT values are significant and are the basis for assigning different levels of risk to the same material.

Table A-2. Comparison of Estimated SHT Values for Samples of Treated Coal Products Using Different Preparation Procedures

Sample Preparation	SHT
As Received	108
As Received	108
As Received and Ground	108
As Received and Ground	108
As Received and Dried	85
As Received and Dried	89

The method proposed by Miron et al. (1990) requires the samples to be dried at 70 °C prior to analysis. The purpose of drying is to remove hydrocarbon gases. During analysis it has been found that these gases will be evolved and mask the pressure drop caused by absorption of oxygen. This reduces the measured pressure drop and leads to estimates the of SHT that are higher than actual value. In the case of the treated coal product, the material evolved during drying is not known, but it does represent about 1.5% of the mass of the coal.

Since we do not know the composition of the material evolved from the treated coal product, it is not possible to evaluate the results from the oxygen absorption tests listed in Table 2. If the material evolved during drying is a hydrocarbon gas, then the SHT values for the dried samples are correct. However, if the material is a species, such as carbon dioxide adsorbed to the product during treatment, then drying destroys the product and the values for the as received samples are correct.

In terms of the treatment process and the goals of the project, it is tempting to operate the method without drying the samples. However, if the results of this analysis are to be reported to potential investors and referenced to the method of Miron et al. (1990), the composition of the material evolved from the product must be determined and this data used to justify why the drying step should be ignored.

Status of the Method

The method for evaluating the potential of coals to undergo spontaneous combustion has been completed with the necessary documentation and development of a standard operating procedure. A copy of the standard operating procedure follows. The method has not yet been sufficiently adapted to a level to be used for evaluation of products from coal treatment as discussed above. It will require further calibration to be reliable as an indicator of processed coal.

Recommendations

We are addressing two items to complete development of this method. First, the nature of the material evolved from the drying of treated coal samples needs to be addressed. These data are needed to establish a justification for not drying the treated coal product if the results indicate drying destroys the integrity of the sample. This effort should complete the method for these types of samples.

Second, a data base needs to be developed for the method. This is being done by obtaining samples from a variety of coals and analyzing them by this method. In addition to analysis by the oxygen absorption method, they should also be analyzed by WRI's calorimetry method. This will provide a basis for comparison and allow data previously obtained by calorimetry to be used with the same rating system reported by Miron et al. (1990).

REFERENCES

Litton, C.D., S.J. Page, 1994, Coal Proximate Analyses Correlations with Airborne Respirable Dust and Spontaneous Combustion Temperature, *Fuel*, 73(8), pp 1369-1370.

Miron, Y., A.C. Smith, and C.P. Lazzara, 1990, Sealed Flask Test for Evaluating the Self-Heating Tendencies of Coals, Bureau of Mines Report of Investigations, RI 9330, 18 pages.

Page, S.J., J.A. Orangiscak, and J. Quatto, 1993, Coal proximate Analysis Correlation with Airborne Respirable Dust, *Fuel*, 72(7), pp 965-970.

Smith, A.C., and C.P. Lazzara, 1987, Spontaneous Combustion Studies of U.S. Coals, Bureau of Mines Report of Investigations, RI 9079, 28 pages.

Smith, A.C., Y. Miron, and C.P. Lazzara, 1991, Large-Scale Studies of Spontaneous Combustion of Coal, Bureau of Mines Report of Investigations, RI 9346, 30 pages.

Unal, S., S. Piskin, and S. Dincer, 1993, Autoignition Tendencies of Some Tulkish Lignites, *Fuel*, 72(9), pp 1357-1359.

STANDARD OPERATING PROCEDURE

Procedure Title: Self-Heating Temperature Using Oxygen Absorption for Measurement of Spontaneous Combustion of Coal

I. Summary of Method

Spontaneous combustion of coal is both an economic concern and a safety hazard experienced for certain coals during storage and transportation. Predictive capabilities are needed to identify coals that have the potential to undergo spontaneous combustion. The method described in this Standard Operating Procedure is used to estimate the tendency for different coals to undergo spontaneous combustion and is based on a method reported by Miron et al. (1990).

The method uses the measurement of the pressure drop caused by the absorption of oxygen by a coal sample in a closed system. The amount of oxygen absorbed by a coal sample has been shown to be directly proportional to its tendency to self-heat and lead to spontaneous combustion (Miron et al. 1990). The method uses a known mass of coal in a sealed reaction chamber attached to a microtransducer. The pressure drop measured by the transducer is read after 7 days. The pressure drop is then used to calculate the self-heating temperature. There are six transducer/reaction chamber units available in the pressure measurement device, so a total of six samples can be analyzed at a time.

II. Apparatus and Materials

a. Coal drying tubes fitted with a nitrogen purge.

b. Drying oven capable of maintaining 70 °C.

c. Analytical balance.

d. Pressure drop measurement device based on microtransducers.

e. Glass reaction chambers (flasks) fitted with 24/40 ground glass joints, six each of the following sizes: 500 ml, 250 ml, and 125 ml.

III. Analytical Procedure

a. Up to six samples can be analyzed at a time using the current pressure drop measurement device available at WRI. Duplicate and blank analyses can be performed as frequently as determined to be necessary based on the availability of sample.

b. Care must be taken to exclude air from the coal sample as much as possible. When possible, the operations should be performed in a glove bag/box.

c. Determine the mass of coal required for a 500 ml reaction chamber by using the following formula:

$$\text{Mass of coal} = 50\text{g} \times (P/736\ \text{mm~lg})$$

where P = average barometric pressure at the test site.

For experiments performed at the barometric pressure of Laramie, Wyoming (580 mm Hg), the mass of coal is calculated to be 40 g.

d. If sufficient sample is not available to perform the experiment in a 500 ml reaction chamber using the mass of coal calculated in step III.b., scale the experiment by dividing the mass of coal calculated in step III.b. by 2 or 4 so that there is more coal available than is needed for the test.

e. Dry the coal sample at 70 °C under a nitrogen sweep for a minimum of 24 hours or until a constant weight is obtained.

f. Select the correct reaction chamber size by dividing 500 ml by the scaling factor identified in step III.c. (500/1, 500/2, or 500/4).

g. Weigh the mass of dried coal sample, as calculated in step III.b., into the appropriate size reaction chamber, as determined in step III.d.

h. Clean the coal dust from the ground glass joint, coat joint with stopcock grease, and attach the reaction chamber to the pressure drop measurement device. Be sure a tight seal is made in the ground glass joint, because a leak will destroy the pressure drop measurement.

i. Immediately record the date, time, and pressure in the reaction chamber as read from the pressure meter. This measurement is the initial pressure of the reaction chamber.

j. Measure and record the relative humidity and temperature at which the relative humidity is recorded.

k. After 7 days record the date, time, and pressure in the reaction chamber. This is the final pressure of the reaction chamber.

l. Calculate the minimum self-heating temperature (SHT) using the spread sheet as described in the next section. Report the results.

m. Remove and discard coal sample from the reaction chambers. Clean reaction chambers, being certain to clean all grease and coal dust from the ground glass joint and the matching joint on the transducer. A solvent such as toluene may have to be used to ensure all grease is removed. Coal dust may scratch the ground glass joint and prevent an airtight seal.

IV. Calculation

a. The minimum self-heating temperature (SHT) is calculated with a spread sheet routine. The SHT is calculated using the following equation:

$$SHT = 120.0 - (0.545 \times [Pi - Pf - PW])$$

where Pi = temperature-corrected initial pressure in the reaction chamber.

Pf = temperature-corrected final pressure in the reaction chamber.

Pw = partial pressure of the water vapor represented by the relative humidity.

b. The water saturation value must be determined for the temperature at which the relative humidity is determined. This value is obtained from the attached table.

c. Data is input into the routine as shown by the underlined entries on the example sheet attached to this standard operating procedure. Data entry includes:

1. Test identification number and the analysis date.

2. The sample identification for each coal sample analyzed and the mass of each sample.

3. The room temperatures at the start of the test (initial temperature) and at the end of the end of the test (final temperature).

4. The relative humidity and the room temperature where the humidity was measured at the start of the test.

5. The water saturation value for the provided room temperature.

6. The initial and final pressures in each flask.

d. The spreadsheet routine will correct the pressure reading for temperature and calculate the vapor pressure of the water represented by the relative humidity.

e. Initiate the calculation of the results in the spread sheet, verify that the results are reasonable (greater than 35 and less than 120), print the data, file one copy, and submit the second copy to the sample submitter.

V. Interpretation of Results

a. The method of estimating the self-heating temperature of coals with the pressure drop caused by oxygen absorption is based on earlier studies relating the minimum self-heating temperatures of selected coals with their tendency to spontaneously combust as determined by calorimetry (Smith and Lazzara 1987).

b. Based on this study, the following scale was developed to identify the tendency of coals to self heat.

- SHT less than 70 °C—the coal has a high potential for spontaneous combustion.
- SHT between 70 and 100 °C—the coal has a medium risk for spontaneous combustion.
- SHT greater than 100 °C—the coal has a low potential for spontaneous combustion.

VI. References

Miron, Y., A.C. Smith, and C.P. Lazzara, 1990, Sealed Flask Test for Evaluating the Self-Heating Tendencies of Coals, Bureau of Mines Report of Investigations, RI 9330, 18 pages.

Smith, A.C., and C.P. Lazzara, 1987, Spontaneous Combustion Studies of U.S. Coals, Bureau of Mines Report of Investigations, RI 9079, 28 pages.

WRI-98-R011

WESTERN RESEARCH INSTITUTE

"Providing solutions to energy and environmental problems"

FINAL REPORT

EVALUATION OF ALTERNATE FREE RADICAL INITIATORS FOR HEAVY OIL/PLASTICS CO-PROCESSING

Prepared for
U.S. Department of Energy
Morgantown, West Virginia

April 1998

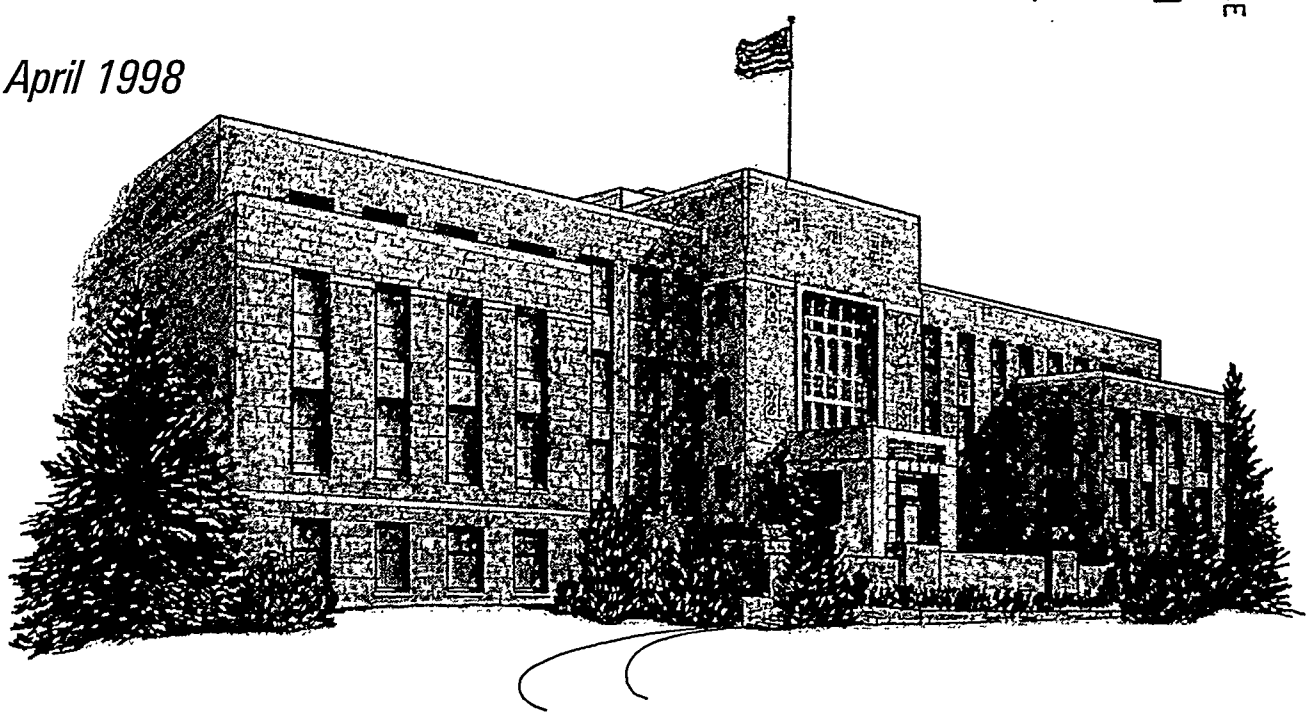

WRI-98-R011

EVALUATION OF ALTERNATE FREE RADICAL INITIATORS FOR HEAVY OIL/PLASTICS CO-PROCESSING

Final Report

By
F.D. Guffey
F.A. Barbour

April 1998

Work Performed Under Cooperative Agreement
DE-FC21-93MC30126 Subtask 4.1

For
U.S. Department of Energy
Office of Fossil Energy
Federal Energy Technology Center
Morgantown, West Virginia

By
Western Research Institute
Laramie, Wyoming

DISCLAIMER

ABSTRACT

Western Research Institute (WRI) is developing a low-temperature thermal decomposition process to alleviate the problems associated with disposal of waste plastics and at the same time generate a product stream in the gasoline boiling range for use in the refining and petrochemical industries. The technology being developed by WRI is significantly different from conventional thermal decomposition processes used to recover distillates from waste plastics. The key to this difference is the application of a free radical initiator that allows operation of the process at temperatures below those used in other thermal decomposition processes. The WRI technology utilizes a free radical initiator to enhance thermal decomposition of waste plastics in the presence of a low-value heavy oil at temperatures below those normally used for thermal decomposition. Operation of the process at lower temperatures produces higher yields of distillate product and lower yields of gaseous and char products than conventional processes.

The activity of the initiator was identified in earlier research and the active species was found to be polyvinyl chloride (PVC). However, PVC is not the free radical initiator of choice because it can add chlorine to the distillate product. Chlorine can not be tolerated by refineries because of its adverse effect on processing equipment. This study was undertaken to identify an alternate free radical initiator and to characterize its activity so the heavy oil/plastics conversion process can be optimized.

TABLE OF CONTENTS

LIST OF TABLES AND FIGURES

EXECUTIVE SUMMARY

The United States generates in excess of 180 million tons of municipal solid waste, or garbage, each year. Of this mass, plastics represent about 8.3% or 15 million tons (Kuznesof and VanDerveer 1995). Disposal of these wastes is becoming a serious problem because landfill site capacity is decreasing. In the last ten years, the number of landfill sites has dropped from 18,500 to 6,000. This decrease has placed an additional burden on municipalities in dealing with the disposal of solid wastes. The problem will become more serious in the future as states begin to pass more stringent legislation regulating landfill disposal. The only practical solution to this problem is to decrease the volume of material being disposed of in landfill sites through rigorous conservation and recycling efforts.

Plastics represent one segment of solid wastes that can be recycled to decrease the mass of solids and yield value-added products. Conventional approaches to address recycling of municipal waste plastics rely on secondary or tertiary recycling processes (Ehrig 1992). Secondary recycling processes recycle the bulk plastics back to the plastics industry for the manufacture of new products. Tertiary recycling processes utilize plastic wastes as a carbon-containing resource and thermally process the plastics to produce a low-molecular-weight distillate (Mackey 1995).

Secondary recycling of waste plastic involves collection, sorting, reclamation, and reuse of the plastic material. There are several problems associated with large-scale secondary recycling anticipated in the future, and secondary recycling is expected to be able to recycle only 7 to 15% of the waste plastics in the municipal solid waste stream (Mackey 1995). Therefore, secondary recycling alone will not eliminate the burden of waste plastics on landfill site capacity. An alternate philosophy is to convert the polymeric structure to smaller chemical molecules such as the monomeric units and related chemical structures (tertiary recycling). This improves the market for the products because the market is not a "to-be-developed" manufacturing process but existing plants in the refining and petrochemical industries.

Western Research Institute (WRI) is developing a low-temperature thermal decomposition process to alleviate the problems associated with disposal of waste plastics and at the same time generate a product stream in the gasoline boiling range for use in the refining and petrochemical industries. The technology is significantly different from conventional thermal decomposition processes used to recover distillates from waste plastics. The key to this difference is the application of a free radical initiator. The WRI technology utilizes the initiator to enhance thermal decomposition of waste plastics in the presence of a low-value heavy oil at temperatures below those normally used for thermal decomposition. Operation of the process at lower temperatures produces higher yields of distillate product and lower yields of gaseous and char products than conventional thermal decomposition processes.

The activity of the initiator was identified in earlier research studying the thermal decomposition of polymers. The activity was first observed as a decrease in the temperature required to thermally decompose plastics in the presence of a heavy oil (Guffey et al. 1991). These experiments identified the initiator as polyvinyl chloride (PVC) (Guffey and Barbour 1996). However, PVC is not the free radical initiator of choice for a commercial process because it can incorporate chlorine into the distillate product (Conrad Industries 1995). Chlorine cannot be tolerated in the distillate product because it is deleterious to refinery equipment and will cause downstream processing problems. For this reason, this study was undertaken to identify and characterize the activity of an alternate free radical initiator that does not contain chlorine. The important findings from this research can be summarized as follows:

1. I1 and I2 have been identified as alternate free radical initiators for use in the heavy oil/plastics conversion process. These two polymers have activity comparable to that of polyvinyl chloride.

2. Reasonable changes in the concentration of I1 or I2, in the range of 5 to 15%, do not have a significant effect on plastics conversion.

3. Increases in reaction time cause the expected increase in both plastics conversion and distillate yield.

4. Within the limits of the initiator addition frequencies studied, increase in the mass of initiator added each time has a more significant effect on the increase in plastics conversion than increases in the addition frequency.

5. The results also suggest there is an optimum free radical initiator frequency.

INTRODUCTION

Western Research Institute (WRI) is developing a low-temperature thermal decomposition process to alleviate the problems associated with disposal of waste plastics and at the same time generate a product stream in the gasoline and diesel fuel boiling range for use in the refining and petrochemical industries. This process is an alternative to landfill disposal and provides the opportunity for a profitable business venture.

The United States generates in excess of 180 million tons of municipal solid waste, or garbage, each year. Of this mass, plastics represent about 8.3%, or 15 million tons (Kuznesof and VanDerveer 1995). Disposal of these wastes is becoming a serious problem because landfill site capacity is decreasing. In the last ten years, the number of landfill sites has dropped from 18,500 to 6,000. This decrease has placed a burden on municipalities for the disposal of solid wastes. The problem will become more serious in the future as states begin to pass more stringent legislation regulating landfill disposal. The only practical solution to this problem is to decrease the volume of material being disposed of in landfill sites through rigorous conservation and recycling efforts.

Plastics represent one segment of solid wastes that can be recycled to decrease the mass of solids and yield value-added products. Conventional approaches to the recycling of municipal waste plastics rely on secondary or tertiary recycling processes (Ehrig 1992 and Mackey 1995). Secondary recycling processes recycle the bulk plastics back to the plastics industry for the manufacture of new products. Tertiary recycling processes utilize plastic wastes as a carbon-containing resource and thermally process the plastics to produce a low-molecular-weight distillate (Mackey 1995).

Secondary recycling of waste plastic involves collection, sorting, reclamation, and reuse of the plastic material. Several recycling efforts have been instituted across the country and are receiving a great deal of community support. However, there are several problems associated with the large-scale secondary recycling anticipated in the future. The first problem is the separation of bulk waste plastic into individual polymer types, which is necessary to ensure the quality of the products manufactured from the recycled plastic (Stein 1995). This separation is normally done manually and is costly. This will affect the price of products manufactured from recycled plastic and decrease the economic advantage of using recycled plastic.

The second problem is critical to the health and safety of our society. This is the possible contamination of the plastic with organic material associated with the plastic. Waste plastic has material associated with it that is difficult and costly to remove in the reclamation step. This is particularly true for plastic wastes from the food service industry, chemical laboratories, and hospitals where, in some cases, the contaminates associated with the plastic may be classed as

hazardous wastes. This hazardous waste can be introduced into society through products made from recycled plastic (Sadler 1995 and Kuznesof and VanDerveer 1995).

A third problem is developing markets for recycled plastics. Current efforts have been directed toward replacing virgin plastics with recycled plastics in the manufacture of durable goods, such as park benches, curb stops, and building materials (Saba and Pearson 1995 and Stein 1995). As yet, recycled plastics have not been widely introduced into the consumer packaging industry. Currently, there are no restrictions on the use of recycled plastics for use in packaging food-related items, but its acceptance by consumers is questionable (Sadler 1995). For these reasons, the market for recycled plastics may be limited and easily saturated if large-scale recycling becomes a reality. This will decrease the economic benefit of recycling and discourage this conservation effort. In addition, secondary recycling is estimated to be capable of reclaiming only 7 to 15% of the waste plastics in the municipal solid waste stream (Mackey 1995). This does not have a significant impact on the effect of waste plastics on landfill site capacity.

An alternative philosophy that we have chosen for the recycling of waste plastics is to convert the polymeric structure into smaller chemical molecules such as the monomeric units and related chemical structures (tertiary recycling) (Mackey 1995). This improves the market for the products because the market is not a "to-be-developed" manufacturing process but existing plants in the refining and petrochemical industries, which experience limited supplies of low molecular-weight, heteroatomic free feedstocks from petroleum crude oils.

The process being developed by Western Research Institute (WRI) is based on co-processing waste plastics with a low value oil such as used motor oil. In addition, the thermal decomposition of the polymeric structure of waste plastics is assisted with the addition of a free radical initiator. The use of the free radical initiator allows operation of the process at lower temperatures, decreases coke and gas production, and improves plastics conversion. The initial experiments conducted by WRI identified and used polyvinyl chloride (PVC) as the free radical initiator. However, PVC is not the free radical initiator of choice because chlorine can be incorporated into the products (Conrad Industries 1995). Chlorine in the distillate product can cause processing problems in refinery equipment and destroys the economic value of the distillate product. The study reported here was undertaken to identify an alternate free radical initiator that does not contain chlorine, and define selected operating parameters of the alternate initiator.

BACKGROUND

The disposal of waste plastics presents a potentially serious strain on landfill site capacity. To address this, WRI has been evaluating recycling options to recover marketable products from the waste plastic stream (Guffey et al. 1991 and Guffey and Barbour 1996). Conventional

recycling approaches are limited by the need to separate the waste into individual plastic types and to develop a market for the products manufactured from recycled plastics. Yet, it is anticipated that these approaches will recycle only 7 to 10% of the plastics in the municipal solid waste stream (Ehrig 1992 and Mackey 1995). Western Research Institute initiated development of its own process to avoid these limitations. Currently, WRI holds a patent position for a low-temperature, thermal decomposition process for recycling waste plastics, and more filings are planned. The developmental efforts are addressing the processing of municipal waste plastics to produce a hydrocarbon stream in the gasoline and diesel fuel boiling ranges for use in the refining and petrochemical industries.

The technology being developed by WRI is significantly different from conventional thermal decomposition processes used to recover distillates from waste plastics. The key to this difference is the application of a free radical initiator that allows operation of the process at temperatures below those used in other thermal decomposition processes. The WRI technology utilizes the initiator to enhance thermal decomposition of waste plastics in the presence of a low-value heavy oil at temperatures below those normally used for thermal decomposition. Operation of the process at lower temperatures produces higher yields of distillate product and lower yields of gaseous and char products than conventional processes.

The activity of the initiator was identified in earlier research studying the thermal decomposition of polymers. The activity of the initiator was first observed as a decrease in the temperature required to thermally decompose plastics in the presence of a heavy oil. These early experiments indicated that the initiator was native to the plastics matrix, but the identity and possible mode of action were not determined (Guffey et al. 1991).

A later study was undertaken to identify the component in the plastics mixture responsible for the observed activity, to define this activity, and demonstrate the plastics/heavy oil co-processing concept in a semi-batch, recycle mode of operation (Guffey and Barbour 1996). The results identified polyvinyl chloride as the active initiator and suggested that PVC may act as a free radical initiator. In addition, the concept was demonstrated in the semi-batch, recycle mode of operation with respectable recoveries of distillate. However, use of PVC as a free radical initiator has significant disadvantages. Polyvinyl chloride can incorporate chlorine into the products (Conrad Industries 1995). Even small quantities of chlorine in the distillate product is not acceptable to the refining industry because of the possibility of converting it to hydrochloric acid, which has deleterious effects on processing equipment.

PURPOSE

The research discussed in this report was undertaken to (1) identify an alternate free radical initiator that does not contain chlorine, and (2) screen the activity of the new initiator to identify its effect on selected processing parameters that will control optimization of a process.

METHODOLOGY

Batch Reactor Design

The design of the batch reactor is provided in Figure 1. The reactor was constructed from a 24.1-cm (9.5-in) length of 10.2-cm (4-in) diameter, schedule 40 pipe. The bottom of the reactor was sealed with a 0.6-cm (0.25-in) thick steel plate that fit inside the pipe and was welded in place to make a seal. The top of the reactor was threaded to receive a mating pipe cap. The cap was fitted with four ports to receive a thermocouple, the initiator feed hopper, the vapor recovery line, and a line to admit nitrogen gas into the reactor. In addition, a packing gland was located in the center of the cap to accommodate the stirring shaft.

The reactor was heated with two Chromalox type HBT heaters rated at 650 J/sec (watts) each. The heaters were wired in series and controlled by Orion model E5CSX temperature controllers. Two controllers were employed in series to control the heaters. One controller was used to control the temperature of the heaters and was set to control at 468°C (875°F) because the heaters were not rated for exposure to temperatures above 482°C (900°F). The second controlled the temperature of the reaction medium and was set at the temperature designated for that experiment. Using the controllers in series protected the heaters from exposure to excessive temperatures and still controlled the temperature of the reaction medium. The reactor was insulated to reduce heat losses. The temperature rise time from ambient temperature to 375°C (707°F) was 20 minutes. The temperature control at 375°C (707°F) was +/- 3°C (5°F).

The distillate was collected as a vapor from the reactor through the vapor port in the cap of the reactor. The vapor was condensed in a water-cooled condenser and collected in a distillate receiver.

The initiator feed hopper consisted of a 1.3-cm (0.5-in.) stainless steel ball valve fitted with 15.2-cm x 0.95-cm (6-in x 0.375-in.) stainless steel tubing fitted with a packing gland. The initiator was introduced into the reactor by placing the desired mass of initiator in the stainless steel tube. A push rod was inserted into the tube through the packing gland and a seal made around the rod. The valve was opened and the rod pushed into the reactor. The initiator was discharged from the tube with the rod, similar to the action of a syringe. The rod was then pulled back past the valve, the valve closed, and the rod removed.

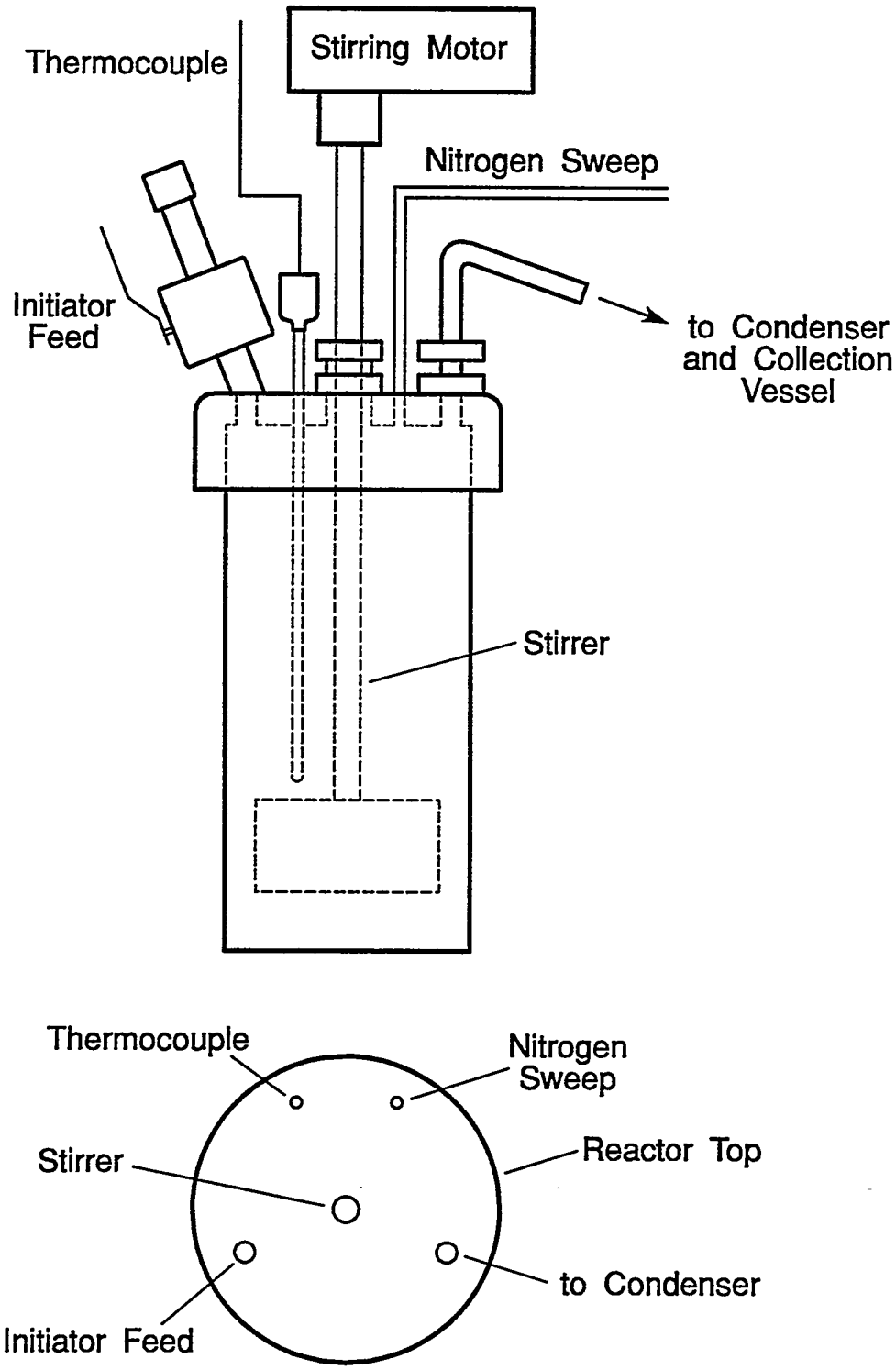

Figure 1. Schematic Diagram of the Batch Reactor Used to Study the Activity of Different Initiators

Experimental Procedure

The reactor was operated by first loading it with the desired masses of waste plastic and heavy oil. The reactor was then assembled, leak checked with nitrogen gas, and insulated. The reactor was heated to the desired set-point temperature (between 360 and 390°C [680 and 734°F]) and held at that temperature for the duration of the experiment. When the reactor reached the desired set-point temperature, the initiator was added if designated for the particular experiment. Additional initiator was added at the frequency designated for each particular experiment. Each experiment was conducted for the length of time designated, after which the insulation was removed, and the reactor quenched with air

The products from the experiment were collected and the mass of each measured. The residual or unreacted plastics were separated from the heavy oil by filtration except for unreacted polystyrene, which was collected from the oil by insolubility in heptane. The residual plastics, free from the heavy oil and solvent, were dried in a vacuum oven at 80°C (176°F). A material balance was performed around each experiment.

Reactor Feeds

Two heavy oils were used for these experiments. The first heavy oil was used motor oil obtained from a local service center. The second oil was Kendall SAE 30 weight, nondetergent motor oil. This oil was chosen for selected experiments performed in this study because it resembles used motor oil without introducing the interferences into the experiments that can be caused by light ends in used motor oil produced from use in an engine

The mixture of waste plastics feed was modeled after the composition of waste plastics found in the municipal solid waste stream (Thayer 1989). The basic composition of the waste plastics mixture used for this study is listed in Table 1. The waste plastics were collected by WRI employees and manually separated by plastic type. The plastics were then reduced to 0.3-cm (0.125-in) average particle size using a laboratory blender and dried at 100°C (212°F). The desired mass of each type of plastic was weighed for each experiment and combined in the reactor with the oil.

Table 1. Composition of Plastics Feed Used to Model Municipal Waste Plastics

Plastics Type	Abbreviation	Weight Percentage Used
High-Density Polyethylene	HDPE	36.8
Low-Density Polyethylene	LDPE	38.2
Polystyrene	PS	13.1
Polypropylene	PP	11.9

Four potential initiators were selected for this study. They are identified as I1, I2, I3, and I4. The initiators were obtained from Aldrich Chemical Company and used as received.

RESULTS AND DISCUSSION

The research effort reported here was directed at identifying an alternate free radical initiator that does not contain chlorine, and screening the activity of a new initiator to identify its effect on different processing parameters and on optimization of the process. This section is divided into three parts: (1) evaluation of the identified candidates, (2) evaluation of the concentration effects of selected initiators, and (3) evaluation of the effects of addition frequency and reaction time.

Evaluation of Potential Free Radical Initiators

A screening program was developed to evaluate the potential free radical initiators and compare them to the activity observed for polyvinyl chloride. The screening experiments were conducted in the batch reactor (Figure 1), and the experimental conditions are listed in Table 2. The initiator was added to the reaction at a level of 5% of the mass of waste plastics used in the experiment. The mass of initiator was divided into three equal mass fractions and introduced at 15 minute intervals during the course of the experiment. The first addition was made at experimental time 0 minutes. These conditions do not represent the optimum reaction conditions determined for use of PVC as a free radical initiator. However, the conditions selected for the screening experiments represent more difficult processing conditions and were selected because it was felt they would more accurately define the activity of the potential free radical initiators.

Table 2. Experimental Conditions Used for the Initiator Screening Experiments

Experimental Parameter	Value
Reaction Temperature, °C	390
Heavy Oil	Used Motor Oil
Oil/Plastics Mass Ratio	10:1
Experiment Duration, min.	45
Initiator Level, %	5
Initiator Addition Frequency, min.	15

The material balance results, distillate yields, and plastics conversions for the screening experiments are listed in Table 3. The table includes results for experiments using the four potential free radical initiators and PVC, and experiments in which no initiator was added to the reaction. Experiments using PVC and the four potential initiators were performed in duplicate. Examination of the results show mass balance closures range from 96 to 101% and are considered acceptable for this reactor system.

Table 3. Mass Balance Data for the Experiments Conducted to Evaluate the Effects of Different Free Radical Initiators on Plastics Conversion

Initiator	None	None	None	PVC	PVC	I1	I1	I2	I2	I3	I3	I4	I4
Reactants													
Heavy Oil, g	320.5	321.7	319.7	319.9	319.8	320.3	323.7	318.2	320.2	316.7	319.0	320.5	319.0
Waste Plastics, g	31.9	31.8	31.9	31.8	31.8	31.8	31.8	31.8	31.8	31.9	31.8	31.8	31.8
Initiator, g	0.0	0.0	0.0	1.8	1.8	1.8	1.8	1.8	1.8	1.8	1.8	1.8	1.8
Total, g	352.4	353.5	351.6	353.5	353.4	353.9	357.3	351.8	353.8	350.4	352.6	354.1	352.6
Products													
Distillate, g	65.2	158.9	115.5	132.6	149.1	160.2	155.5	75.9	149.5	137.1	152.0	169.4	159.6
Processed Oil, g	245.9	159.2	198.0	187.9	181.2	151.4	165.7	242.7	165.7	175.6	164.7	161.2	160.1
Processed Solids, g	30.8	30.9	30.9	29.7	29.5	28.7	29.1	29.4	29.5	30.3	30.1	30.0	30.5
Total, g	341.9	349.0	344.4	350.2	359.8	340.3	350.3	348.0	344.7	343.0	346.8	360.6	350.5
Closure, %	97.0	98.7	98.0	99.1	101.8	96.2	98.0	98.9	97.4	97.9	98.4	101.8	99.3
Distillate Yield, %	18.5	45.0	32.9	37.5	42.2	45.3	43.5	21.6	42.3	39.1	43.1	47.8	45.3
Plastics Conversion, %	3.5	2.8	3.1	9.0	9.6	9.8	8.5	7.6	7.2	5.0	5.4	5.7	4.1

Further examination of the results shows that the distillate yields vary widely. The variation in distillate yields is observed when used motor oil is used as the co-processing oil. Used motor oil contains low molecular weight species caused by pyrolysis of the oil from use in an engine, and contamination from gasoline. The low molecular weight species contribute to a significant portion of the produced distillate. In addition, water is present in used motor oil and contributes to difficulties in evaluation of distillate yield. Because of the water, we have found it difficult to obtain a suitable procedure to mix oils and maintain a uniform sample for study. However, the variation in distillate yields does not cause any problems in evaluation of the free radical initiator activity of the compounds being studied because the important indicator is the plastics conversion.

Table 4 lists the average distillate yields and plastics conversions for the experiments listed in Table 3. Examination of the results in Table 4 shows that all of the initiators used in these experiments produced higher plastics conversions than resulted from the experiments not using an initiator. These results indicate all of the candidates selected have some free radical initiator activity. Polyvinyl chloride provided the highest plastics conversion with 9.3% conversion. The conversion observed for PVC is followed closely by I1 (9.2%) and I2 (8.1%). The other two potential free radical initiators show some activity, but the activity is significantly lower than observed for the other two potential initiators.

Table 4. Comparison of Distillate Yields and Plastics Conversions for the Different Free Radical Initiators

	Average Yield or Conversion					
Initiator	None	PVC	I1	I2	I3	I4
Distillate Yield, %	32.1	39.9	44.4	32.0	41.1	46.6
Plastics Conversion, %	3.1	9.3	9.2	8.1	5.2	4.9

Based on the results listed in Table 4, I1 and I2 were selected as reasonable candidates to replace PVC in the heavy oil/plastics conversion process. Therefore, the remaining experiments discussed here were conducted using I1 or I2 as the free radical initiator.

Concentration Effects of I1 and I2

The screening experiments discussed above were conducted to identify the activity of the potential free radical initiators. Of the four potential initiators, I1 and I2 were selected for further study to gain insight into their activity as it relates to optimization of the heavy oil/plastics conversion concept. The first parameter investigated was the concentration of each of the two prospective initiators. Three concentrations (5, 10, and 15%) of each of the initiators, relative to the waste plastics charge, were used in these experiments.

The heavy oil used for these experiments was Kendall SAE 30, nondetergent motor oil. A new motor oil was selected for these experiments so the distillate yield could be monitored without interference from the low molecular weight components and water present in used motor oil. Each experiment was conducted for 30 minutes at 390°C (734°F). The mass of initiator added in each of the experiments was divided into six equal mass fractions and added to the reaction at a frequency of every five minutes.

The mass balance results, distillate yields, and plastics conversions for the experiments conducted with different initiator concentrations and an experiment conducted without addition of an initiator are listed in Table 5. The mass balance closures for these experiments range from 99 to 101% and are considered acceptable for this reaction system. The distillate yields for the experiments conducted with the addition of an initiator range from about 3 to 4%, and no significant trend is observed in the distillate yields as a function of the initiator concentration. Examination of the results does show an increase in plastics conversion with increased concentration of the free radical initiator added to the reaction. Also, the lowest level of plastics conversion (7.7%) is greater than the plastics conversion (4.0%) observed without the addition of an initiator.

Table 5. Mass Balance Data for the Experiments Conducted to Evaluate the Concentration Effects of I1 and I2 on Plastics Conversion in New Motor Oil

Initiator	None	I1	I1	I1	I2	I2	I2
Initiator Concentration, %	-	5	10	15	5	10	15
Addition Frequency, min.	-	5	5	5	5	5	5
Experiment Duration, min.	30	30	30	30	30	30	30
Reactants							
Heavy Oil, g	277.3	277.3	278.1	276.5	278.8	277.8	276.2
Waste Plastics, g	27.3	27.3	27.3	27.3	27.3	27.3	27.3
Initiator, g	0.0	1.4	2.7	4.1	1.4	2.7	4.1
Total, g	304.6	306.0	308.1	307.9	307.5	307.8	307.6
Products							
Distillate, g	7.2	8.0	12.7	13.1	10.7	10.9	10.2
Processed Oil, g	273.4	272.2	269.4	268.0	273.2	269.0	267.9
Processed Solids, g	26.2	25.2	24.9	26.0	24.7	24.5	24.1
Total, g	306.8	305.4	307.0	307.1	308.6	304.4	302.2
Closure, %	100.7	99.8	99.6	99.7	100.4	98.9	98.2
Distillate Yield, %	2.4	2.6	4.2	4.3	3.5	3.6	3.4
Plastics Conversion, %	4.0	7.7	8.8	11.1	9.5	10.3	11.7

Figure 2 shows the plastics conversion trends for each of the initiators as a function of the initiator concentrations. Initiator I2 promotes a higher plastics conversion at all concentrations than I1. However, the conversion from the two initiators appears to be converging at 15% initiator added to the reaction. Also the increase in plastics conversion between 5 and 10% initiator added is relatively small for both of the initiators. The increase in plastics conversion between 10 and 15% initiator is greater than observed between 5 and 10% but it is not as great as observed between 5% initiator and not using an initiator.

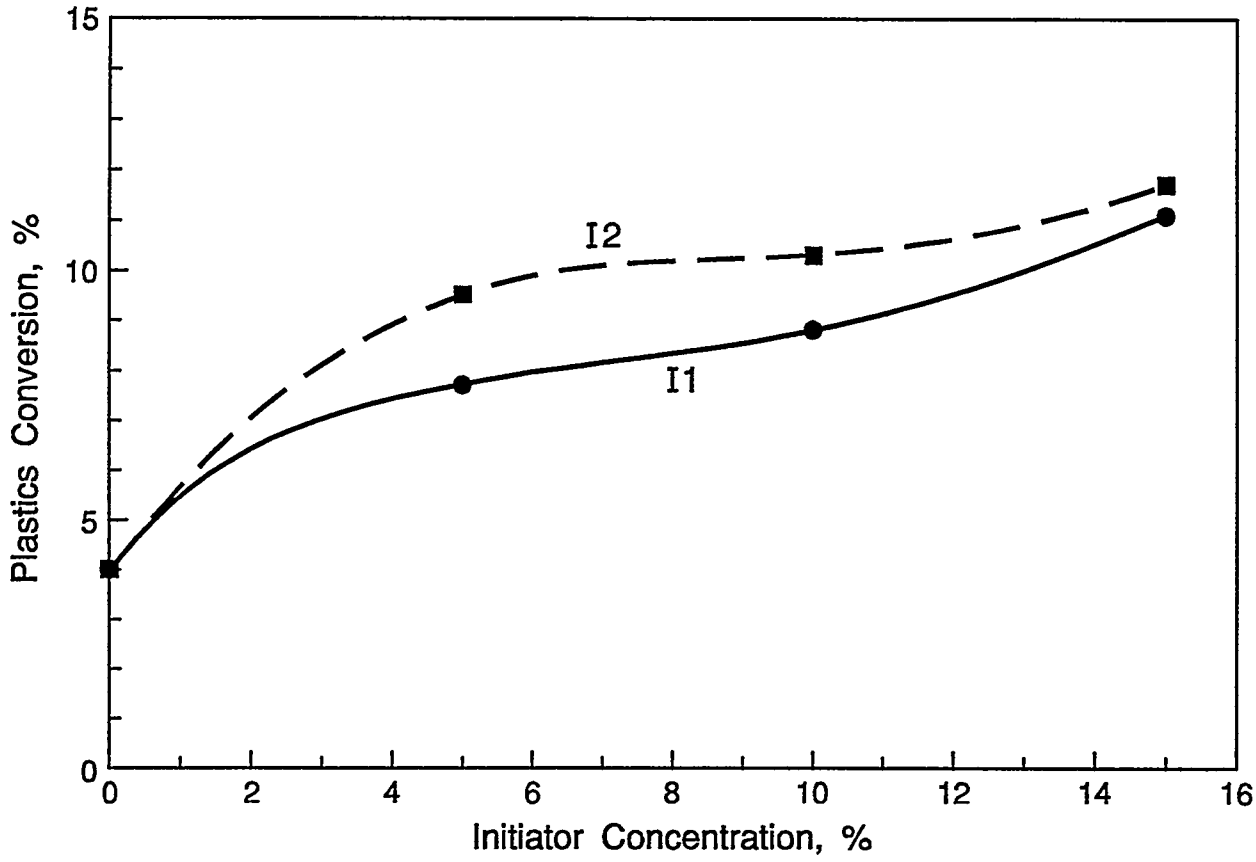

Figure 2. Plastics Conversion as a Function of Initiator Concentration for Experiments Conducted with Addition of I1 and I2

These results indicate two points for consideration in optimization of the heavy oil/plastics conversion concept. First, I2 appears to be slightly more active in promoting plastics conversion than I1. This is particularly true at the 5 and 10% concentration level. Second, there are no significant improvements in the plastics conversion at the higher concentrations of added initiator.

Effects of Experiment Duration and Addition Frequency

The final parameters investigated were the reaction time and frequency of initiator addition to the reaction. These were investigated together because of the ease in blocking the experimental plan to accommodate both of the parameters and minimize the number of experiments that need to be conducted. These experiments were conducted using I2 as the initiator at a level of 10% of the waste plastics charge. I2 was selected as the initiator for these experiments because the experiments discussed in the previous section indicate I2 is slightly more active than I1. The reaction times investigated, in addition to 30 minutes already used, were 45 and 60 minutes.

The frequency of addition of the initiator was approached from two perspectives. The first pair of experiments added the initiator six times during each experiment using the same mass of initiator at each addition as was used in the corresponding 30-minute experiment discussed in the preceding section. The time interval for each experiment was defined by dividing the reaction time by six initiator additions. Therefore, the frequency for the 45-minute experiment was 7.5 minutes, and 10 minutes for the 60-minute experiment. These experiments are referred to as equal initiator mass experiments. The second pair of experiments added the initiator at 5-minute intervals. The total mass of the initiator (2.7g) added to each experiment was the same, but the mass of initiator added at the 5-minute intervals was different for each experiment and was defined by dividing the total mass of initiator by the number of additions. Initiator was added nine times during the 45-minute experiment and 12 times during the 60-minute experiment. These experiments are referred to as equal frequency experiments. An additional experiment was conducted at 60 minutes using a 20-minute interval between initiator additions.

The mass balance data for these experiments are listed in Table 6. The table includes the initiator addition frequency in minutes and the total number of initiator additions for each of the experiments. The distillate yields and plastics conversions are also listed for each experiment. The mass balance closures range from 98 to 100% and are considered acceptable for this reactor system.

Figure 3 presents the trends observed in the distillate yield for increases in reaction time. There are two curves on the figure that represent the differences in the effects of adding the initiator on equal mass or equal frequency basis, as defined above. As expected, the distillate yield increases with increased reaction time for both cases of initiator addition frequency. The results show a higher distillate yield at 60 minutes of reaction time for the experiment conducted at equal mass additions of the initiator as compared to the experiment conducted with equal frequency addition of the initiator. The distillate yields for the experiments conducted with a reaction time of 45 minutes are comparable regardless of the frequency approach for initiator addition.

Table 6. Mass Balance Data for the Experiments Conducted to Evaluate the Effects of Initiator Addition Frequency and Experiment Duration on Plastics Conversion in New Motor Oil Using I2 as the Initiator

Initiator	I2	I2	I2	I2	I2
Initiator Concentration, %	10	10	10	10	10
Addition Frequency, min.	7.5	10	5	5	20
Number of Additions	6	6	9	12	3
Experiment Duration, min.	45	60	45	60	60
Reactants					
Heavy Oil, g	277.9	277.0	276.3	278.3	277.3
Waste Plastics, g	27.3	27.3	27.5	27.3	27.3
Initiator, g	2.7	2.7	2.7	2.8	2.7
Total, g	307.9	307.0	306.5	308.4	307.3
Products					
Distillate, g	18.1	28.1	17.5	22.0	22.3
Processed Oil, g	261.8	255.7	260.6	258.0	255.2
Processed Solids, g	23.9	22.6	23.7	23	22.8
Total, g	303.8	306.6	301.8	303.0	300.3
Closure, %	98.7	99.9	98.5	98.3	97.7
Distillate Yield, %	5.9	9.2	5.8	7.2	7.3
Plastics Conversion, %	12.5	17.2	13.8	15.8	16.5

Figure 4 shows the plastics conversion as a function of reaction time for each of the approaches to initiator addition frequency. As expected, the plastics conversion increases with increased reaction time for both cases of initiator addition frequency. At 45 minutes of reaction time, addition of the initiator on the equal frequency basis shows a higher plastics conversion (13.8%) than the experiment using equal mass addition of the initiator (12.5%). However, at 60 minutes of reaction time, the reverse is observed. The experiment conducted with equal mass addition of the initiator had 17.2% plastics conversion, while the experiment conducted with equal frequency addition of the initiator had 15.8% plastics conversion.

The experiments conducted using 60-minute reaction times with equal mass additions of the initiator produced the highest plastics conversion and distillate yield. This observation was extended with a third experiment conducted for 60 minutes with three equal mass additions of the initiator. Figure 5 presents the trend in plastics conversion as a function of initiator addition frequency (based on equal mass addition of the initiator). The curve in Figure 5 shows that an optimum frequency of addition exists between 10- and 20-minute addition intervals because the curve reaches its maximum in this region. The exact addition frequency can not be identified from these experiments because there is insufficient data available. However, the optimum frequency is between 10- and 20-minute addition intervals.

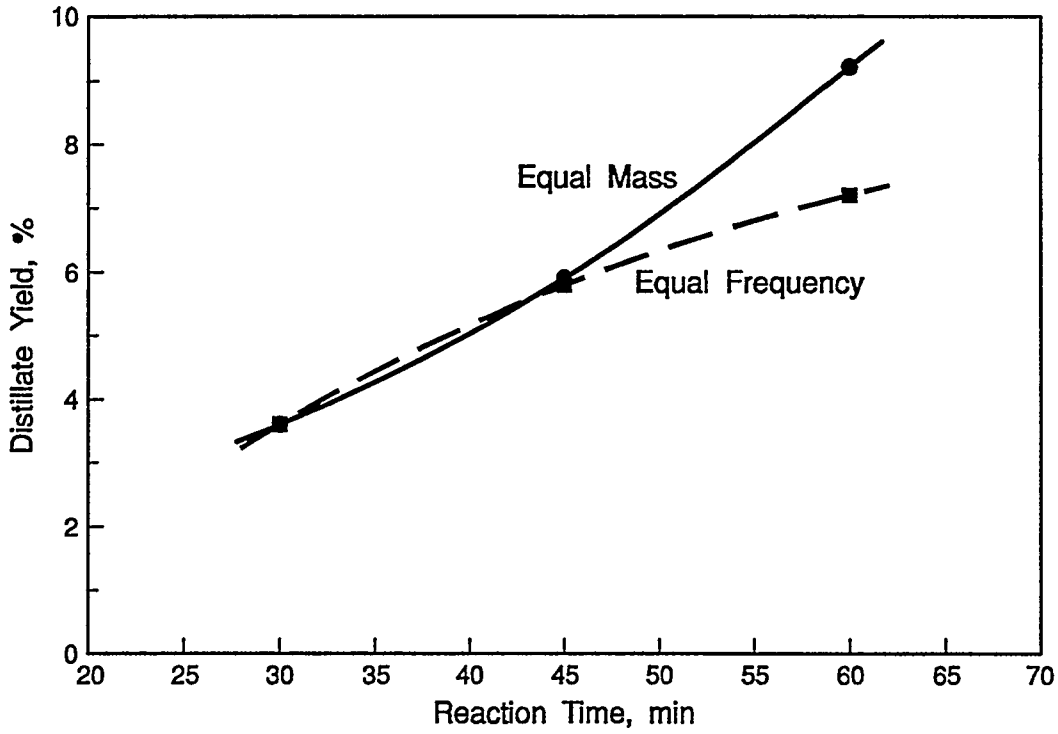

Figure 3. Trends Observed in Distillate Yield as a Function of Reaction Time for Experiments Conducted Using Equal Mass and Equal Frequency Approaches to Initiator Addition Frequency

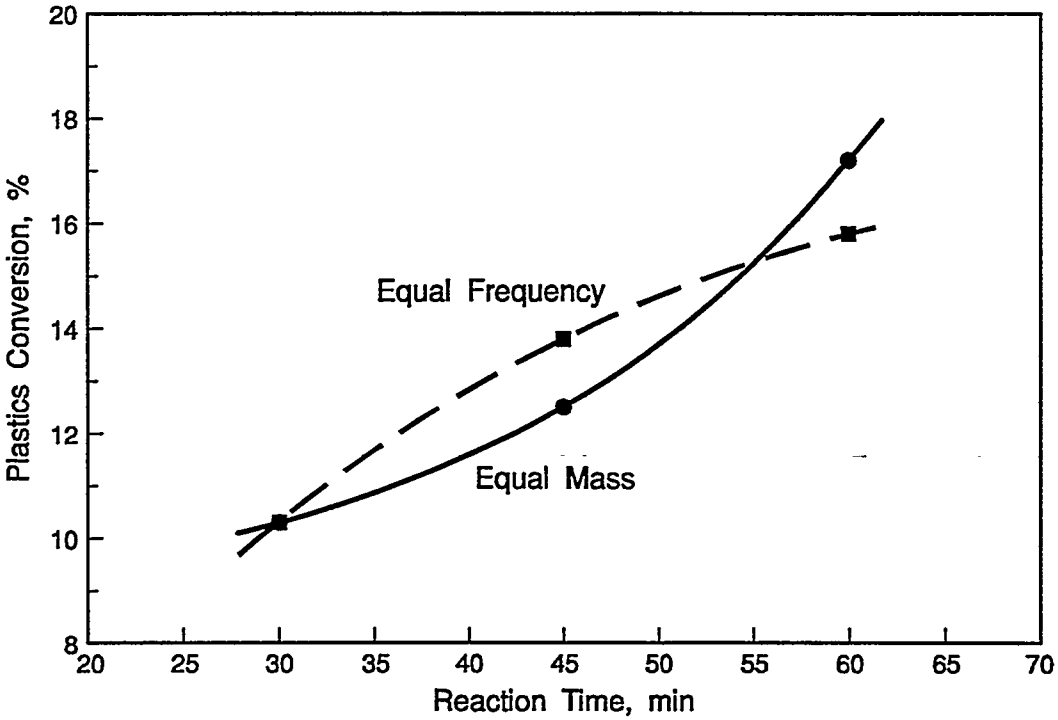

Figure 4. Trends Observed in Plastics Conversion as a Function of Reaction Time for Experiments Conducted Using Equal Mass and Equal Frequency Approaches to Initiator Addition Frequency

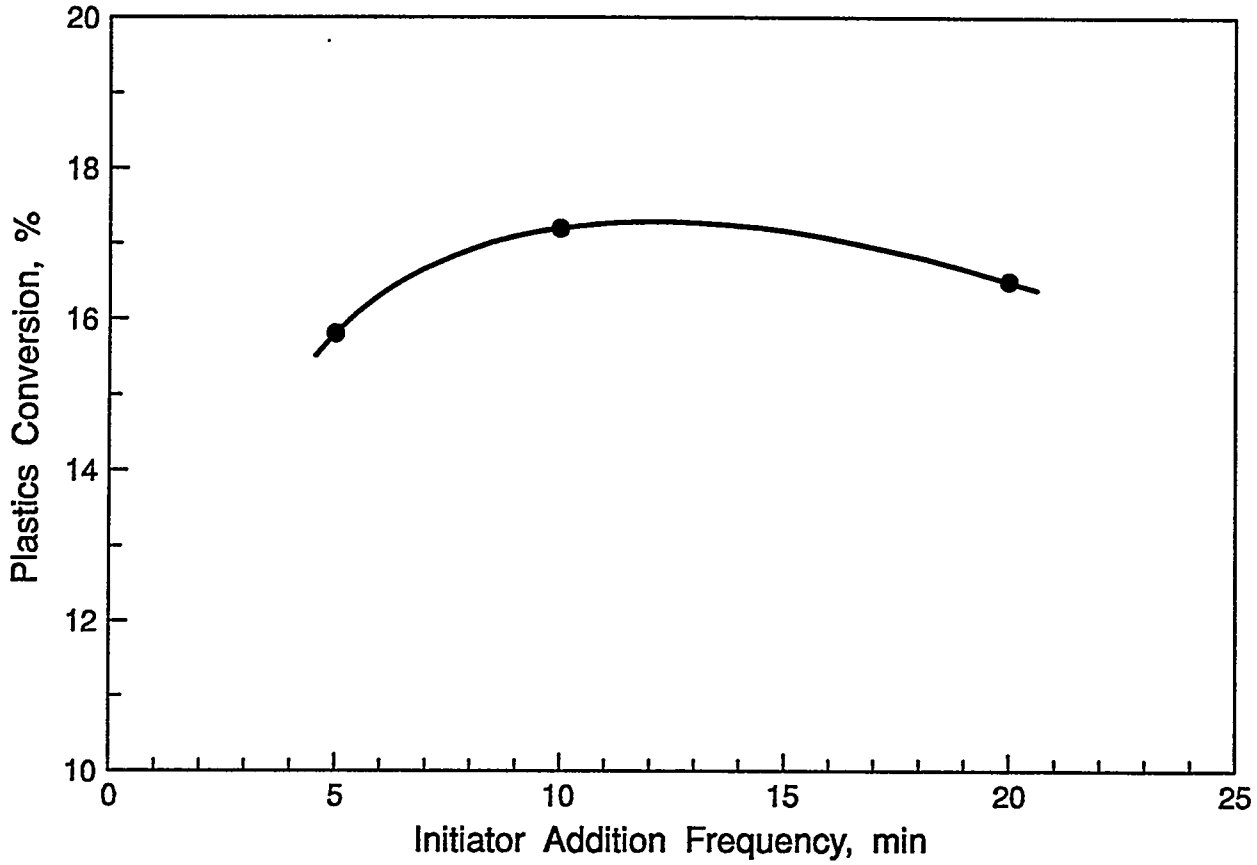

Figure 5. Observed Trend in Plastics Conversion as a Function of Initiator Addition Frequency

The results from this series of experiments show interesting trends that can be applied to optimization of the heavy oil/plastics conversion process. The first observation, as expected, is that increased reaction time (residence time) increases both distillate yield and plastics conversion. Second, at a constant percentage of initiator added to the reaction, the mass of initiator added at each addition is more important, within reasonable limits, than the frequency of addition. Third, for experiments using a 60-minute reaction time and a wide range of initiator addition frequencies, there appears to be an optimum frequency for maximum plastics conversion.

CONCLUSIONS

This investigation was undertaken to (1) identify an alternate free radical initiator that does not contain chlorine or other heteroatoms that can be deleterious to downstream processing in a refinery, and (2) evaluate selected operating parameters of the new initiator to determine their effects on optimization of the heavy oil/plastics conversion process. Based on the results of this investigation, the following conclusions can be made.

1. Four initiators were selected as potential free radical initiators. They were screened under rigorous reaction conditions, and all of the candidates were found to have free radical initiator activity. However, initiators I1 and I2 were found to be the most active.

2. In the initiator concentration range of 5 to 15% and using I1 or I2 as the free radical initiator added to the reaction, a proportional increase in plastics conversion was not observed with increased concentration of the initiator. These results indicate that reasonable changes in free radical initiator concentration will not have a significant effect on optimization of the heavy oil/plastics conversion process.

3. Evaluation of changes in the reaction time showed the expected increase in both plastics conversion and distillate yield.

4. Results from experiments using 10% I2 as the free radical initiator indicate an increase in the mass of initiator added to the reaction at each addition is more important to optimization than a higher frequency of addition with a lower mass of initiator, within the limits of the addition frequencies studies.

5. At a reaction time of 60 minutes and using I2 as the free radical initiator, the experimental results suggest there is an optimum frequency of addition between 10- and 20-minute addition intervals.

REFERENCES

Ahlstrom, B.H., 1985, Microstructures of Synthetic Polymers, in Liebman, S.A. and E.J. Levy, eds., *Pyrolysis and GC in Polymer Analysis*. Marcel Dekker, Inc. New York, NY, 262-266.

Conrad Industries, 1995, Advanced Recycling of Plastics, Final Report With the American Plastics Council, June 1995.

Ehrig, R.J., ed., 1992, *Plastics Recycling*. Hanser Publishers, Munich, 289 p.

Guffey, F.D., P.A. Holper, and D.E. Hunter, 1991, Summary of Laboratory Simulation Studies of the ROPE Process, Laramie, Wyoming, DOE Report in Press.

Guffey, F.D. and F.A. Barbour, 1996, Heavy Oil/Plastics Co-Processing, Laramie, Wyoming, DOE Report in Press.

Holman, J.L, J.B. Stephenson, and J.W Jensen, 1972, Processing the Plastics from Urban Refuse, U.S Bureau of Mines technical Progress Report, BuMines TPR-50, 20 p.

Kuznesof, P.M., and M.C. VanDerveer, 1995, Recycled Plastics for Food-Contact Applications *in* Rader, C.P. et al., ed., *Plastics, Rubber, and Paper Recycling A Pragmatic Approach.* American Chemical Society, Washington, DC, 389-403.

Mackey, George, 1995, A Review of Advanced Recycling Technology, *in* Rader, C.P. et al., ed., *Plastics, Rubber, and Paper Recycling A Pragmatic Approach.* American Chemical Society, Washington, DC, 161-169.

Rice, F.O, and K.F. Herzfeld, 1934, The Thermal Decomposition of Organic Compounds from the Standpoint of Radicals. IV. The Mechanism of Some Chain Reactions, *J. Amer. Chem. Soc.,* vol. 56, 284-289.

Saba, Raymond G., and Wayne E. Pearson, 1995, Curbside Recycling Infrastructure: A Pragmatic Approach, *in* Rader, C.P. et al., ed., *Plastics, Rubber, and Paper Recycling A pragmatic Approach.* American Chemical Society, Washington, DC, 11-26.

Sadler, George D., 1995, Recycling Polymers for Food Use: A Current Perspective, *in* Rader, C.P. et al., ed., *Plastics, Rubber, and Paper Recycling A Pragmatic Approach.* American Chemical Society, Washington, DC, 380-388.

Stein, Richard S., 1995, Polymer Recycling: Thermodynamics and Economics, *in* Rader, C.P. et al., ed., *Plastics, Rubber, and Paper Recycling A Pragmatic Approach.* American Chemical Society, Washington, DC, 27-46.

Thayer, A.M., 1989, Solid Waste Concerns Spur Plastic Recycling Efforts. *Chemical and Engineering News*, January 30, 7-15.

WRI-98-R027

WESTERN RESEARCH INSTITUTE
"Providing solutions to energy and environmental problems"

FINAL REPORT

DEVELOPMENT OF AN ON-LINE ALKALI MONITORING PROBE

Prepared for
U.S. Department of Energy
Morgantown, West Virginia

April 1998

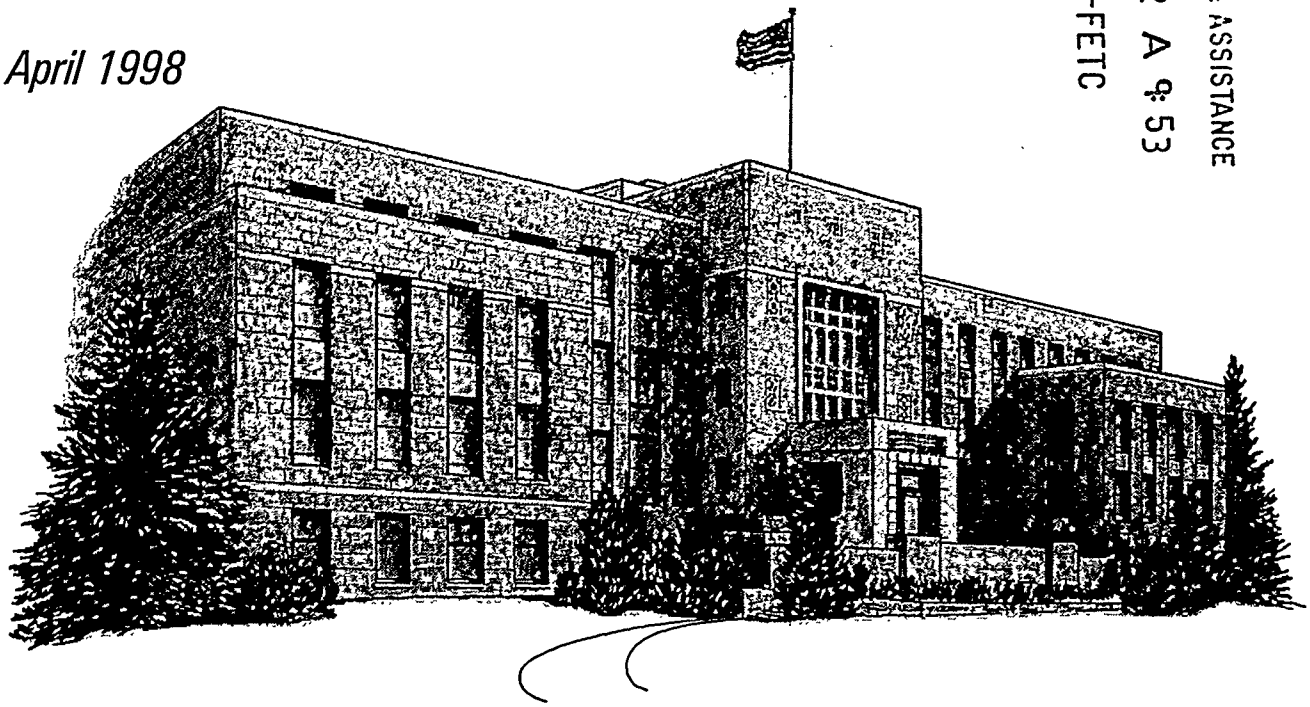

WRI-98-R027

DEVELOPMENT OF AN ON-LINE ALKALI MONITORING PROBE

Final Report

By
Vijay Sethi

April 1998

Work Performed Under Cooperative Agreement
DE-FC21-93MC30126 Subtask 2.2

For
U.S. Department of Energy
Office of Fossil Energy
Federal Energy Technology Center
Morgantown, West Virginia

By
Western Research Institute
Laramie, Wyoming

DISCLAIMER

DEVELOPMENT OF AN ON-LINE ALKALI MONITORING PROBE

PFBC (first and second generation), IGCC, and DCFT all require hot gas stream conditioning to not only protect the gas turbine against deposition, erosion, and corrosion, but in the case of IGCC and second generation PFBC, to also improve process efficiency and economics. Physical and chemical cleanup systems are being developed for handling high-pressure, high-temperature coal combustion and coal gasification streams. Physical cleanup devices being developed include ceramic candle filters, ceramic cross-flow filters, woven ceramic bag filters, advanced ceramic tube filters, nested fiber filters, and other concepts involving ash agglomeration technologies in conjunction with mechanical particulate removal devices.

Alkali compounds are considered to be the main chemical contaminant of concern. While physical cleanup devices can remove particulate, alkali in the combustion and gasification streams are likely to be in vapor form and if released during the combustion or gasification process, will arrive at the gas turbine in a form that can cause hot-corrosion and buildup.

Three notable efforts to measure the alkali vapor in these streams have included use of sorber beds (Argonne National Laboratory), extractive condensation (NCB, GE, ANL, Exxon etc.), and an on-line monitor "FOAMS" (Ames/METC).

Alkali measurements made using these techniques and probes have shown a great deal of variability. It is suspected that losses in the sampling line are a major source of error. As a result attempts are being made to develop alkali probes which minimize these losses by using inert materials of construction, and by ensuring that the gas sample extraction lines and other equipment are maintained at high enough temperatures to prevent condensation. Nevertheless, unless a truly on-line monitor is developed, the alkali content of the coal combustion and gasification streams measured by any of the available techniques will always be suspect.

As a part of this project, a new alkali monitoring concept was proposed for development and testing. The underlying principle for the proposed on-line probe was the determination of the dew point of the vapor phase compounds. Once the dew point has been established the concentration can be deduced from the available thermodynamic equilibrium data. The dew point of the vapor phase compounds can be established by force-condensing them onto sensors held at various temperatures. If the sensors can detect and discriminate the presence of liquid and solid phases, then the dew point can be readily measured. Two different detection methodologies proposed for testing and evaluation relied on the fact that (1) molten salts are better electrical conductors than their solid counterpart, and

(2) molten alkali compounds do cause very high corrosion rates in several different families of heat resistant metallic alloys.

The second method for sensing the presence of a molten layer of alkali compounds requires a complicated sensor/reference element arrangement, whereas the first method offers the possibility of a relatively compact sensor almost in the shape and form of a printed circuit on an insulator, such as an alumina wafer. Similarly, the probe design based on the second method inherently imposes a finite life for the sensing elements, and therefore will require periodic replacement. No such maintenance is envisioned for the first sensing method. On the other hand, a probe based on the second sensing method can not only be used as an on-line alkali monitor, but also as an on-line corrosion probe for monitoring the corrosion in an actual gas turbine. Turbine stage(s) for inspection can be identified from the corrosion information provided by such a probe. If sensing element material is selected to match the gas turbine materials then the actual corrosion rates can be deduced.

A series of crucible experiments were undertaken to verify that electrical conductance measurements can indeed be used to detect molten alkali compounds. A simple two-conductor probe was assembled from gold wires. The electrical resistance of the probe was measured by immersing the tips of the gold wires in alkali salts. By changing the furnace temperature the salts were taken through cycles of melting and freezing. Gap between the probe elements was about 2 mm, immersion depth used was about 1 mm. A dramatic change in the resistance was quite evident for temperatures greater than 801 C (1474 F), the melting temperature of NaCl.

A multi-element probe was also fabricated and underwent verification tests. The probe consisted of eight 1-mm wide gold stripes painted on a 35 mm x 13 mm x 2 mm alumina wafer. The gold stripes ran along the width of the wafer and the separation between the stripes was about 1 mm. Gold wires were attached to the gold stripes by mechanical means. The alumina wafer was assembled onto an air-cooled stainless steel block. Eight type K thermocouples were used to monitor the temperature of the wafer from the backside.

Verification tests conducted, used a deposited layer of an alkali compound or a mixture. The compound(s) was dissolved in water and then a thin layer of the solution was painted on the alumina wafer covering the gold stripes and the intervening gaps. The wafer was allowed to dry and then the entire probe assembly was installed in the furnace. Probe response as electrical resistance between neighboring stripes and the temperature profile of the wafer is recorded as the furnace temperature was increased to temperatures greater than the melting temperature of the alkali compound or

mixture. When a stable temperature profile was achieved the resistance map of the stripes was used to detect molten salt. The probe assembly could easily detect a change in the solid to liquid phase.

A test setup was constructed whereby alkali-laden gases could be contacted with candidate materials of construction. The setup consisted of gas metering and blending equipment, furnaces for heating and cooling the gases and test samples, and associated monitoring and control assemblies. Alkali vapor pressure was controlled by placing a known amount of the compound in the high-temperature zone of the furnace. A small sweep gas velocity was used to transfer the vapors to the lower temperature end of the furnace. All test fixtures and probe assemblies were to be exposed in the lower temperature zone. This arrangement was needed to ensures an equilibrium vapor pressure of the alkali compound commensurate with the operating temperature of the lower temperature zone of the furnace.

Further testing and development on the project was halted because of lack of funding for the second year of work. Nevertheless, the work completed led to a patent on the sensing scheme.

WESTERN RESEARCH INSTITUTE
"Providing solutions to energy and environmental problems"

FINAL REPORT

DEVELOPMENT OF A PORTABLE DATA ACQUISITION SYSTEM AND COALBED SIMULATOR

PART I: DEVELOPMENT OF A PORTABLE DATA ACQUISITION SYSTEM

Prepared for
U.S. Department of Energy
Morgantown, West Virginia

April 1998

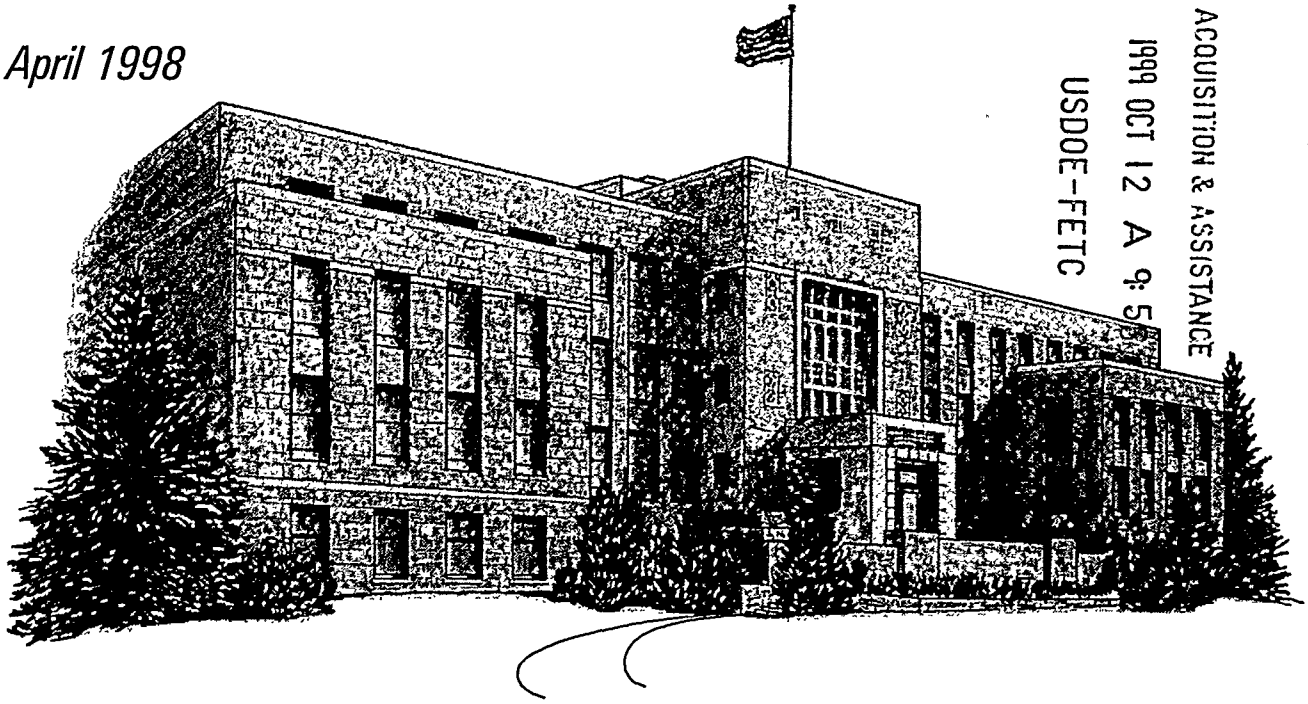

WRI-98-R010a

DEVELOPMENT OF A PORTABLE DATA ACQUISITION SYSTEM AND COALBED METHANE SIMULATOR

PART 1: DEVELOPMENT OF A PORTABLE DATA ACQUISITION SYSTEM

Final Report

By
F. A. Barbour
T. F. Turner
F. M. Carlson

April 1998

Work Performed Under Cooperative Agreement
DE-FC21-93MC30126 Subtask 1.3

For
U. S. Department of Energy
Office of Fossil Energy
Federal Energy Technology Center
Morgantown, West Virginia

By
Western Research Institute
Laramie, Wyoming

ACKNOWLEDGMENTS

The authors express thanks and appreciation to the United States Department of Energy for funding of the work under Contract Number DE-FC21-93MC30126. Appreciation is also extended to Amoco Southern Rockies Business Unit for providing the opportunity to WRI to attach the CBMDAS to its instrumentation. The authors would also like to thank the Amoco San Juan Operation Office for all its assistance in the field during the monitoring period.

DISCLAIMER

ABSTRACT

A portable coalbed methane data acquisition system (CBMDAS) has been assembled for acquiring production data in the field. This system can be quickly mobilized to enter the field and measure dynamic surface data associated with coalbed methane recovery. The CBMDAS can gather on-site helium tracer data to help determine whether communication exists between zones in an injection well and zones in producing wells. It is also capable of performing virtually continuous on-site gas analyses, including helium down to 10 ppm, carbon dioxide, nitrogen, methane, ethane, and propane. In addition, the CBMDAS can acquire and store flow, pressure, and temperature data related to coalbed methane recovery.

Western Research Institute (WRI) tested the CBMDAS at an Amoco field near Farmington, New Mexico, during April 1994. Amoco and WRI were conducting a coalbed methane pilot test in the area, and WRI was permitted to piggy-back its system with Amoco's data acquisition system. Comparisons of data obtained using the CBMDAS with analyses performed by WRI in Laramie, Wyoming, and with an outside laboratory showed good agreement. The Microsensor Technology Inc. (MTI) gas chromatograph (GC) provided an excellent check in the field for the CO_2 analyzer data. During a helium tracer test periodic grab samples were taken during the period of maximum helium response as shown by the CBMDAS. These grab samples were later analyzed by an independent laboratory using mass spectrometry. Comparison of the two methods of analysis produced favorable results.

TABLE OF CONTENTS

LIST OF FIGURES

EXECUTIVE SUMMARY

Western Research Institute has assembled a portable coalbed methane data acquisition system (CBMDAS) for acquiring production data in the field. This system can be mobilized quickly to go into the field to measure dynamic surface data associated with coalbed methane recovery. A four-wheel-drive van was modified to contain the portable data acquisition equipment. The van was equipped with a gas-powered electric generator and a heating and air conditioning system to maintain desired ambient temperatures.

Because power at field sites may be limited, the CBMDAS uses equipment with very low power consumption. Gas analyses are obtained with a low-powered (30 watts maximum) gas chromatograph, which is controlled by a dedicated low-powered personal notebook computer with a large data storage capacity. Carbon dioxide data are collected by continuous on-line analyzers powered by 12 volts DC. The analyzers consume approximately 3 watts each for operation. Battery-operated data loggers are used either in the van or at remote locations away from the van to obtain pressure and temperature signals and signals from the continuous CO_2 analyzers. Personal notebook computers periodically acquire the data from the data loggers.

The CBMDAS can gather on-site helium tracer data to help determine whether communication exists between zones in an injection well and in producing wells. It is also capable of performing virtually continuous on-site gas analyses, including helium down to 10 ppm, carbon dioxide, nitrogen, methane, ethane, and propane. For enhanced recovery projects, critical data such as CO_2 composition and helium composition can be processed on site so that the project can be effectively monitored. Data measuring frequencies can be adjusted as the data response dictates.

As a test of its capabilities, the CBMDAS was used to acquire process data from the Amoco-WRI Jointly Sponsored Research project titled, "Injection Into Coal Seams for Simultaneous CO_2 Mitigation and Enhanced Recovery of Coalbed Methane."

INTRODUCTION

Purpose

The objective of this work was to design, purchase, and install a coalbed methane data acquisition system (CBMDAS) in a mobile vehicle and to test the overall effectiveness of the instrumentation. Western Research Institute (WRI) undertook development of the system to advance its goal of developing and applying coalbed methane technologies with commercial clients.

To achieve this goal, a four-wheel-drive van was modified to house the necessary instrumentation and operating power. In a typical application of such instrumentation, monitoring requirements include the need for continuous gas analysis at both injection and monitor wells; round-the-clock helium tracer measurements at the monitor well; and acquisition and storage of flow, pressure, and temperature data at both injection and monitor wells. The equipment was tested at a remote field site near Farmington, New Mexico.

Background

Gas from coalbed methane represents a significant potential source of clean-burning fossil fuel. Typically, gas production from coalbeds is by pressure depletion. Although this technology is straight-forward and simple to apply in field-wide production schemes, there are several problems associated with pressure depletion of a reservoir. As reservoir pressure is reduced in the coalbed, matrix permeability to gas is reduced because of increased stress caused by increases in net overburden pressure. The reduction in permeability limits the reservoir's potential to produce gas. Since in a pressure depletion drive, the rate of gas production is proportional to well pressure, the economics of these reservoirs become less attractive as the reservoirs are produced. Finally, the rapid depressurization of the coalbed reservoir can result in significant dewatering of the coal and subsequent water production; this water production poses major environmental concerns.

The use of gas displacement technology for coalbed methane production involves the injection of a noncombustible gas into the coalbed. The introduction of a different gas into the coalbed can result in continually changing gas production characteristics. To follow these changes, the produced gas needs to be monitored more closely than gas produced by pressure depletion alone. The evaluation of both primary and enhanced coalbed methane production processes can be greatly facilitated by the ability to analyze produced gas at the wellhead. Coalbed production wells of interest are often in remote areas with limited or no power available for instrument operation. In analyzing gas at these wells, it an advantage to have both instrument power and the instrumentation together in one portable, compact package.

METHODOLOGY

Data Acquisition Van

Most of the equipment necessary to remotely monitor gas wells was housed in a four-wheel-drive van. The equipment in the van consisted of gas analyzers, a computer for analyzer control and data acquisition, and batteries with a generator to supply power for analyzer operation. The battery voltage was monitored continuously, and batteries were automatically charged when the voltage fell below 11.75 volts. An Onan generator housed in the analysis van provided the recharging capability. The Onan was fueled by gasoline and could supply power for approximately three weeks of unattended operation. Because of the potential for methane leaks, the van was equipped with an explosion monitoring device that would disable the generator if explosive conditions developed inside the van. The positions of these components in the van are shown in Figure 1. The relative positions of the status panel fixtures are detailed in Figure 2.

Gas Analyzers

Produced natural gas was analyzed using a Microsensor Technology Inc. (MTI) portable dual gas analyzer. This analyzer consisted of two separately controlled gas chromatograph (GC) modules, which were powered by 12-volt batteries consuming approximately 10 watts on a continuous basis. The first module contained a 10-m-long 5A molecular sieve PLOT column operated at 50°C. The second module contained an 8-m-long Poraplot Q column operated at 60°C. Sample detection for each module was by dual thermal conductivity detectors.

Helium analysis was performed on the 5A molecular sieve column. A detector sensitivity was used for this column resulting in a detection range from approximately 10 to 200 ppm for helium. Because the ability to analyze helium was desired, argon was used as a carrier gas for all gas analysis. Other gases detected using this column were oxygen, nitrogen, and methane. The methane concentration was too great for analysis at the high sensitivity setting, and methane concentration had to be determined on the other column. The time for a complete chromatographic determination was about three minutes, which allowed enough time for methane to elute so that it would not interfere with the next analysis.

The Poraplot Q column was used for the analysis of methane, carbon dioxide, ethane, and propane. The detector sensitivity for this column was adjusted so that the detection was in the percentage range (1 to 90 vol %). An air peak, which was the result of nitrogen in the gas, could also be detected using this column. Again, the time for analysis using this column was three minutes, which allowed for elution of the major gaseous components.

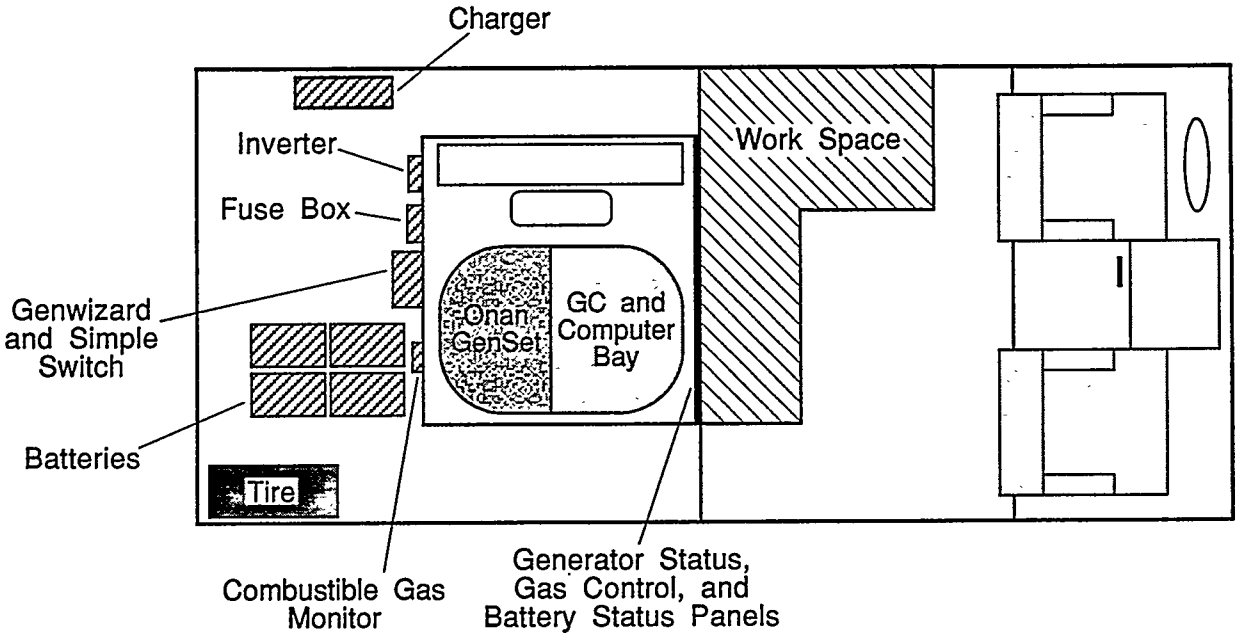

Figure 1. Equipment Positions in Data Acquisition Van

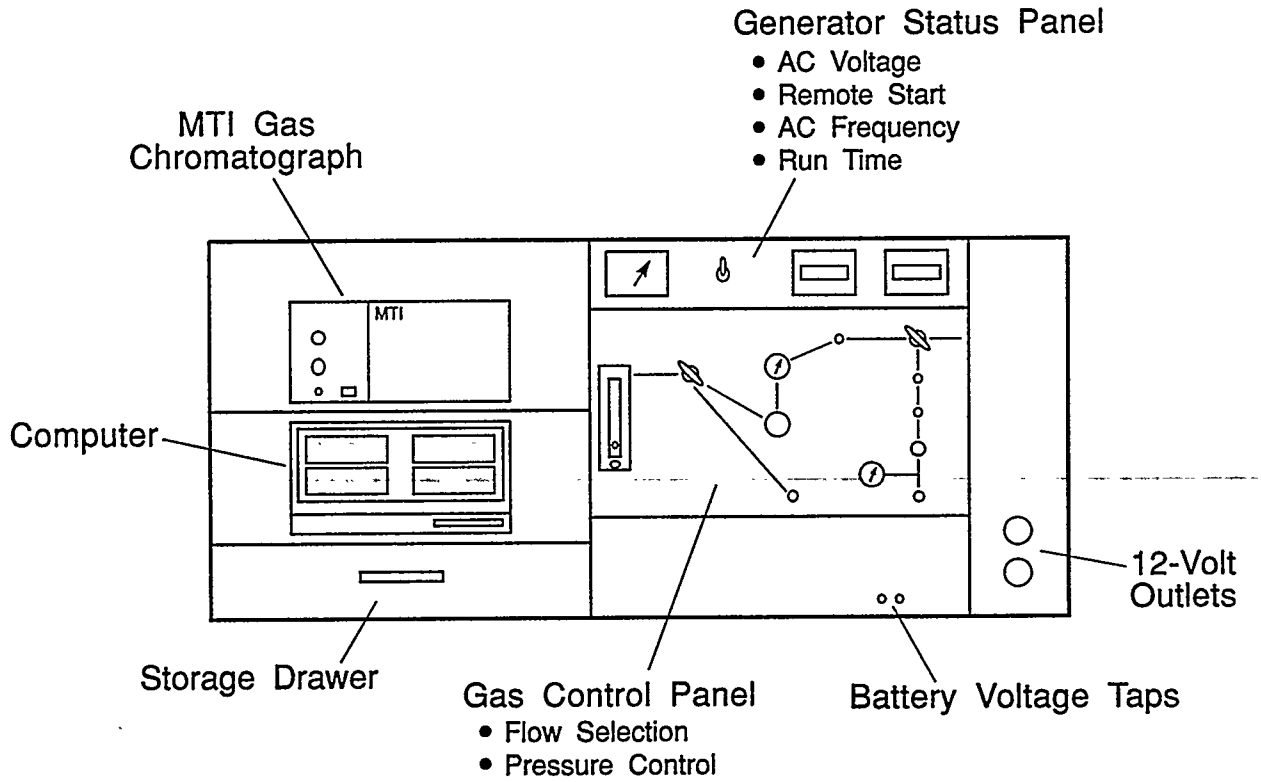

Figure 2. Generator Status Panel in Data Acquisition Van

Continuous analysis of the major components of the injected and produced gas streams is useful both for alerting the CBMDAS operator of changing conditions that may require immediate attention and for providing a backup for the MTI chromatograph. Therefore, continuous on-line CO_2 analysis was provided by two analyzers from NOVA Analytical Systems, Inc. Each unit was installed in a NEMA 4X enclosure, and operated on 12 volts DC. One of the units used an infrared sensor system to continuously monitor CO_2 from 0 to 25%. This analyzer was used on the monitoring well to detect CO_2 breakthrough. The second analyzer contained a thermal conductivity detector and could monitor CO_2 from 0 to 100%. This analyzer was used to monitor the CO_2 concentration of the displacement gas injected into the coalbed.

Data Acquisition

The MTI GC was operated from a notebook computer running EZChrom 200 software. The complete chromatographic signal was stored on the computer for each analysis, making it possible to reanalyze the data later. The EZChrom software not only collected chromatographic data but also controlled the GC parameters and initiated the analysis procedure. Remote control of the MTI GC was tested using the notebook computer modem coupled with a cellular phone using a Motorola cellular connection.

Battery-operated portable data logging systems from OMEGA Engineering, Inc. were used to store data from CO_2 analyzers. These loggers can operate on standard C-cell batteries for long periods of time while storing data internally. The data loggers contained modules for acquiring both thermocouple data and DC voltages. The loggers scanned input signal lines at predetermined intervals and stored the measured voltages. Pressure, temperature, and flow data were available from transducers at the individual meter runs. Signals passing from the transducers and CO_2 analyzers were 1 to 5 volts and required the installation of signal isolators to prevent the possibility of corrupting data. A GM model AUX4000-13 analog signal isolators were installed to provide the needed protection. These isolators also converted the signal from 1 to 5 volts to 0 to 2 volts, matching the input requirements of the OMEGA data loggers.

Sampling

Both dynamic and grab gas samples were taken during the testing of the CBMDAS. Gas at the injection and monitoring wells was sampled dynamically by reducing the pressure at the meter run using a two-stage regulator. A slipstream sample was reduced in pressure to approximately 3 psig ahead of the analyzers. The pressure required by the CO_2 analyzers was close to ambient. The sample pressure for the MTI GC needed to be below 30 psig to prevent damage to the instrument. Other wells associated with the formation were sampled by grab samples taken in 75-cc stainless steel

gas sampling containers. These samples were also analyzed by the MTI chromatograph at the monitoring well site.

RESULTS AND DISCUSSION

The CBMDAS was tested at a field site near Farmington, New Mexico, during April 1994. Amoco and WRI were conducting a Jointly Sponsored Research (JSR) coalbed methane pilot test in the Farmington, New Mexico, area (DE-FC21-93MC30127). Under the JSR agreement, Amoco was responsible for acquiring data for the JSR project, but WRI was permitted to piggy-back its system to Amoco's data acquisition system. This provided WRI with an opportunity to test and compare a portion of the CBMDAS with an existing permanently installed data acquisition system. Comparisons of the data obtained from the two data acquisition systems will be provided in reports covering the JSR project. Some general comments about the performance of the CBMDAS can be made.

Data Acquisition Van

The van functioned fairly well as a mobile office and laboratory during the initial field test. Generally, the CBMDAS van could be ready for operation within a couple of hours after arriving at a site. The four-wheel-drive capability was a great asset during CBMDAS setup and retrieval. While the roads at the field site were generally passable with two-wheel-drive vehicles, a small amount of rain made portions of the road passable only with four-wheel-drive.

All of the generator control and safety interlock equipment functioned properly during the onsite monitoring. Initially, there was a problem with the Onan engine, but after minor adjustment to the carburetor it started and ran properly. The Genwizard, which monitored the battery voltage and started the generator when needed, always performed correctly. While explosive conditions never developed during the monitoring, the combustible gas monitor did function properly when tested prior to the monitoring period.

The van suffered from one main fault, in that the heater drew too much current. This meant that the heater could only be operated while the Onan generator was running. The power requirement of the data acquisition equipment was low enough that the generator only came on about once a day. As a result, the heater would only run about four hours during a day. The temperature in the van would vary approximately 40°F during the course of a day.

Carbon Dioxide Analyzers

The CO_2 analyzers provided questionable accuracy. There appeared to be a fluctuation in the data from the CO_2 analyzers from night to day that was not evident in the MTI analysis. GC samples taken during the day were reasonably close to the results from the analyzer. After a short period of operation, the infrared detector CO_2 analyzer began to act erratically. The analyzer was shipped to the factory for repair, but on return still did not appear to function properly. The infrared CO_2 analyzer seemed to be highly sensitive to temperature and is not recommended for future projects of this sort.

To help eliminate the daily fluctuations, a heater was added to the small remote enclosure housing the thermal conductivity detector CO_2 analyzer and data logger at the production well. This appeared to help, but when the thermostat on the heater failed, the enclosure overheated, causing damage to the data signal wiring. No damage to the CO_2 analyzer was noted.

Data Acquisition

For the most part, the data acquisition system worked quite well. One of the data loggers had an intermittent power problem, which resulted in data loss. The logger was sent back to the factory and repaired. After this repair, no problem with the data logger was noted. The only other problem with the data loggers occurred when the remote enclosure overheated, as described. This did not damage the data logger electronically but did melt the data logger case. Once the data signal wiring was replaced, the data acquisition continued without any further problems.

The optical isolators, which electronically isolated Amoco's and WRI's data acquisition systems, proved to be valuable during the remote enclosure overheating. The Amoco system was not affected when the insulation on the data signal wires melted and the wires shorted to each other. Without the optical isolators, the Amoco system would have shorted out also, resulting in a complete loss of data for that time period.

Control of the GC by the computer using the EZChrom software worked with only minor problems. The computer used for this task was damaged in transit and had to be repaired. During the repair period a backup computer was used to control the GC. The GC ran for several weeks under the control of a computer with no problems. The unit was unattended at night as well as several days at a time during the tracer test period.

To provide additional flexibility and to reduce personnel costs, remote control of the MTI GC was attempted, but it did not work well. Carbon Copy software was used to provide the remote

capability, and the notebook computer modem was coupled with a cellular phone. The system appeared to work correctly when hard-wired phone connections were used. However, communication failed repeatedly when a cellular connection was used.

Gas Chromatograph

The MTI GC ran for several weeks with little trouble. Grab samples taken at several different wells presented a wide variety of gas compositions to be tested by the GC. Comparison of data obtained using the MTI GC and analyses performed by WRI at Laramie, Wyoming, and by an outside laboratory showed good agreement. The MTI GC provided an excellent check in the field for the CO_2 analyzer data.

The trace helium detection portion of the MTI GC was tested during a helium tracer test conducted in the field. Helium was introduced into the injection well and measured at a producer. The system was tested at a remote site, and the helium analyses were compared with those conducted by an independent laboratory using a mass spectrometer. Periodic grab samples were taken during the period of maximum helium response as shown by the CBMDAS. These grab samples were later analyzed by an independent laboratory. Comparison of the two methods of analysis produced favorable results. While the analyses were slightly offset, the same general trends could be noted. The difference between the two methods appeared to be in the background detected. When this difference was taken into account, the helium tracer data from the MTI GC system could be superimposed on the mass spectral data.

The temperature changes noted in the van during the tracer tests affected the operation of the MTI GC. As the temperature changed, the amount of sample injected on the column, as well as the column flow, changed slightly. The cooler the ambient temperature, the faster the components eluted from the GC column. Because the component identification is done by retention time, some changes could be great enough to move the peak out of the retention window. Since the entire chromatogram was stored, no data was lost. However, recovering the data required manually modifying the analytical method and analyzing the chromatogram. This could require a considerable amount of time if several days of data were to need reanalysis.

CONCLUSIONS

WRI has designed and implemented a mobile data acquisition system for the collection of process information from coalbed methane reservoirs. This data acquisition capability enhances WRI's marketability because many prospective coalbed methane developers lack the ability to acquire

process information. For enhanced coalbed methane projects, the capability of CBMDAS to analyze gas data gives WRI the ability to both evaluate process chemistry and perform reservoir analysis.

Generally, the testing and operation of the CBMDAS was quite successful. It was very advantageous to be able to test the system by piggy-backing it with an existing system for comparison. With the knowledge gained and some minor changes, the CBMDAS should function very well as a stand-alone data acquisition system.

Before the system is truly ready for operation, two issues need to be addressed. First and foremost is improving ambient temperature control of both the van and any remote equipment housings. This will eliminate most of the variation in data from day to night. Second, the ability to control the GC computer and data loggers from a remote site over a cellular link should be pursued, as the time-saving benefits will be significant.

THIS ONE REPORT RETURNED TO DOE PER K. DAS REQUEST NOV 15 99

WRI-98-RQ10b

#33

WESTERN RESEARCH INSTITUTE

"Providing solutions to energy and environmental problems"

FINAL REPORT

DEVELOPMENT OF A PORTABLE DATA ACQUISITION SYSTEM AND COALBED SIMULATOR

PART II: DEVELOPMENT OF A COALBED METHANE SIMULATOR

Prepared for
U.S. Department of Energy
Morgantown, West Virginia

April 1998

Full text not available

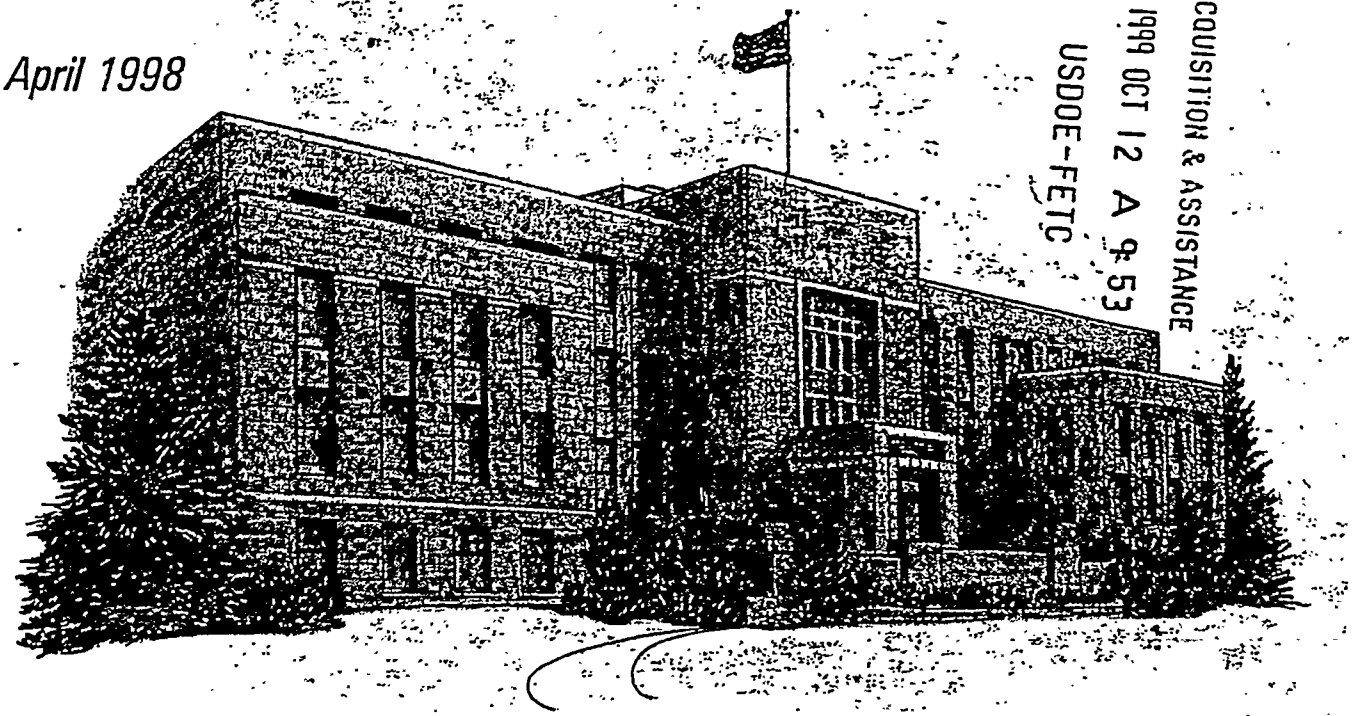

WRI-98-R015

WESTERN RESEARCH INSTITUTE
"Providing solutions to energy and environmental problems"

FINAL REPORT

BENCH-SCALE TESTING AND VERIFICATION OF PYROLYSIS CONCEPT FOR REMEDIATION OF TANK BOTTOMS

Prepared for
U.S. Department of Energy
Morgantown, West Virginia

April 1998

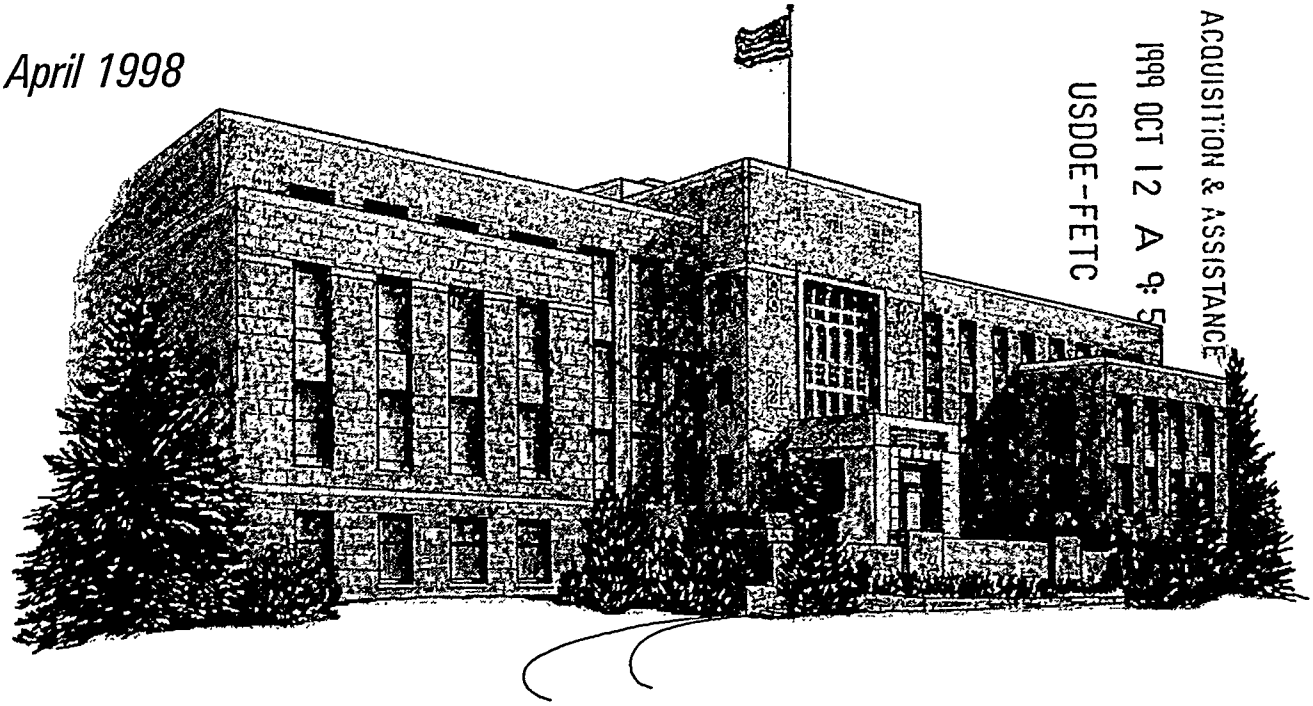

WRI-98-R015

BENCH-SCALE TESTING AND VERIFICATION OF PYROLYSIS CONCEPT FOR REMEDIATION OF TANK BOTTOMS

Final Report

By
Robert Satchwell

April 1998

Work Performed Under Cooperative Agreement
DE-FC21-93MC30126 Subtask 1.5

For
U.S. Department of Energy
Office of Fossil Energy
Federal Energy Technology Center
Morgantown, West Virginia

By
Western Research Institute
Laramie, Wyoming

DISCLAIMER

TABLE OF CONTENTS

LIST OF TABLES AND FIGURES

EXECUTIVE SUMMARY

Tank bottom wastes are being generated at a rate of about one million barrels a day. Cost-effective treatment methods are needed to dispose of these wastes in an environmentally acceptable manner. Western Research Institute (WRI) is in the process of developing, testing, and marketing its patented TaBoRR (Tank Bottoms Recovery and Remediation) technology to meet this need. However, WRI's preliminary survey of the tank bottom wastes being generated shows that some wastes contain large amounts of solids. These wastes cannot be handled by the TaBoRR process and hence require special treatment schemes. Some of the early work performed at WRI showed that through relatively mild thermal processing (pyrolysis) in a screw reactor, wastes with high solids content, including those generated by TaBoRR process as stripper bottoms, can be rendered into a safe, disposable, carbon-rich solid waste form.

A small project was undertaken for bench-scale verification of the pyrolysis concept for handling wastes with high solids content. An existing six-inch twin screw reactor was modified to perform these tests on various feedstocks.

Six different materials, ranging in water content from 0 to 40 percent, and solids content from 5 to 85 percent were pyrolyzed at temperatures between 1020 and 1050 −F. In all cases, a coked solid product was created. Oil recoveries were consistent with the hydrocarbon contents of the respective feeds.

Using the Toxicity Characteristics Leaching Procedure (TCLP), produced solids were analyzed for the eight Resource Conservation Recovery Act (RCRA) metals and were found to be well below the regulatory limits. Total petroleum hydrocarbon content of some of the produced solids was a little higher than the EPA limit; however this was primarily due to recondensation of some of the produced vapors. Recondensation can be readily prevented by redesigning the solids discharge system and providing an adequate sweep gas rate. All of the produced materials that were tested passed the paint filter test.

INTRODUCTION

Tank bottom wastes resulting from oil production, transportation, and refining are being generated at a rate of about one million barrels a day. Cost-effective treatment methods are needed to dispose of these wastes in an environmentally acceptable manner. To meet this need Western Research Institute (WRI) is developing, testing, and marketing the patented TaBoRR® (Tank Bottoms Recovery and Remediation) technology. However, WRI's preliminary survey of the tank bottoms wastes being generated shows that some wastes contain large amounts of solids. These wastes cannot be handled by the TaBoRR process and hence require special treatment schemes. Some early work performed at WRI showed that through relatively mild thermal processing (pyrolysis) in a screw reactor, wastes with high solids content, including those generated by TaBoRR process as stripper bottoms, can be rendered into a safe, disposable, carbon-rich solid form.

A small project was undertaken for bench-scale verification of the pyrolysis concept for handling wastes with high solids content. An existing six-inch twin screw reactor was modified to perform these tests on various feedstocks. The results are described in the following sections.

OBJECTIVES

The goal of the work was to establish the viability of the pyrolysis concept for the ultimate disposal of TaBoRR stripper wastes and some unique tank bottom wastes containing high concentrations of solids by defining the operating conditions (temperature and residence time) under which the wastes are rendered into a carbon-rich, landfillable form. Specific objectives of the work were:

1. modify an existing 6-inch twin-screw setup by installing a product collection train and upgrading the instrumentation,

2. determine the residence time and temperatures required to process the stripper bottoms created from the demonstration unit,

3. test and evaluate the pyrolysis concept using difficult and unique materials not suited for full TaBoRR processing,

4. characterize the gaseous and liquid products and establish disposal characteristics of produced solids.

EQUIPMENT DESCRIPTION

An existing 6-inch twin-screw reactor setup was modified for this work. The setup consists of an electrically heated twin screw that can process the tank bottoms and stripper bottoms at three progressively higher temperatures. The temperatures of the three heating zones are individually controlled along the length of the screw.

Electrical heaters were reconfigured to process feedstocks containing high levels of water. A liquid product recovery train consisting of coolers and condensers was installed. Provisions were made for gas sampling. Two different feed systems, a progressive cavity pump-based system and a screw-based lock hopper, were assembled for feeding different types of tank bottoms and stripper wastes. The processed solids collection system was modified such that on-the-fly sampling was possible. The data acquisition system was modified to control and record the temperatures in the three different zones of the twin-screw reactor.

A schematic of the reactor is displayed as Figure 1.

RESULTS

During the course of this project, six different materials were processed. In the following sections, the results for individual feedstocks are described. Each feedstock offered unique problems that often required the modification of the equipment configuration.

TaBoRR Stripper Bottoms

The shakedown tests were conducted using stripper bottoms from the Pease Oil Field Equipment Company material processed in the TaBoRR demonstration plant. The material had been stripped at temperatures ranging from 650 to 775 °F. Material was drawn from the stripper bottoms storage tank located at the 300 bbl/d TaBoRR plant into a 55-gallon drum. The material had an initial boiling temperature of about 570 °F.

The material was processed with the three zones of the twin-screw reactor operating in the following temperature ranges: Zone 1, 820-1010 °F, Zone 2, 970-1070 °F, and Zone 3, 970-1070 °F. The tests employed nitrogen as a sweep gas. Several problems were encountered during these tests. These included inability to pump the material, feed line plugging, uncontrolled dumping of feed into the reactor by the screw-type feeders, and the clogging of production lines and concomitant pressure buildup in the reactor.

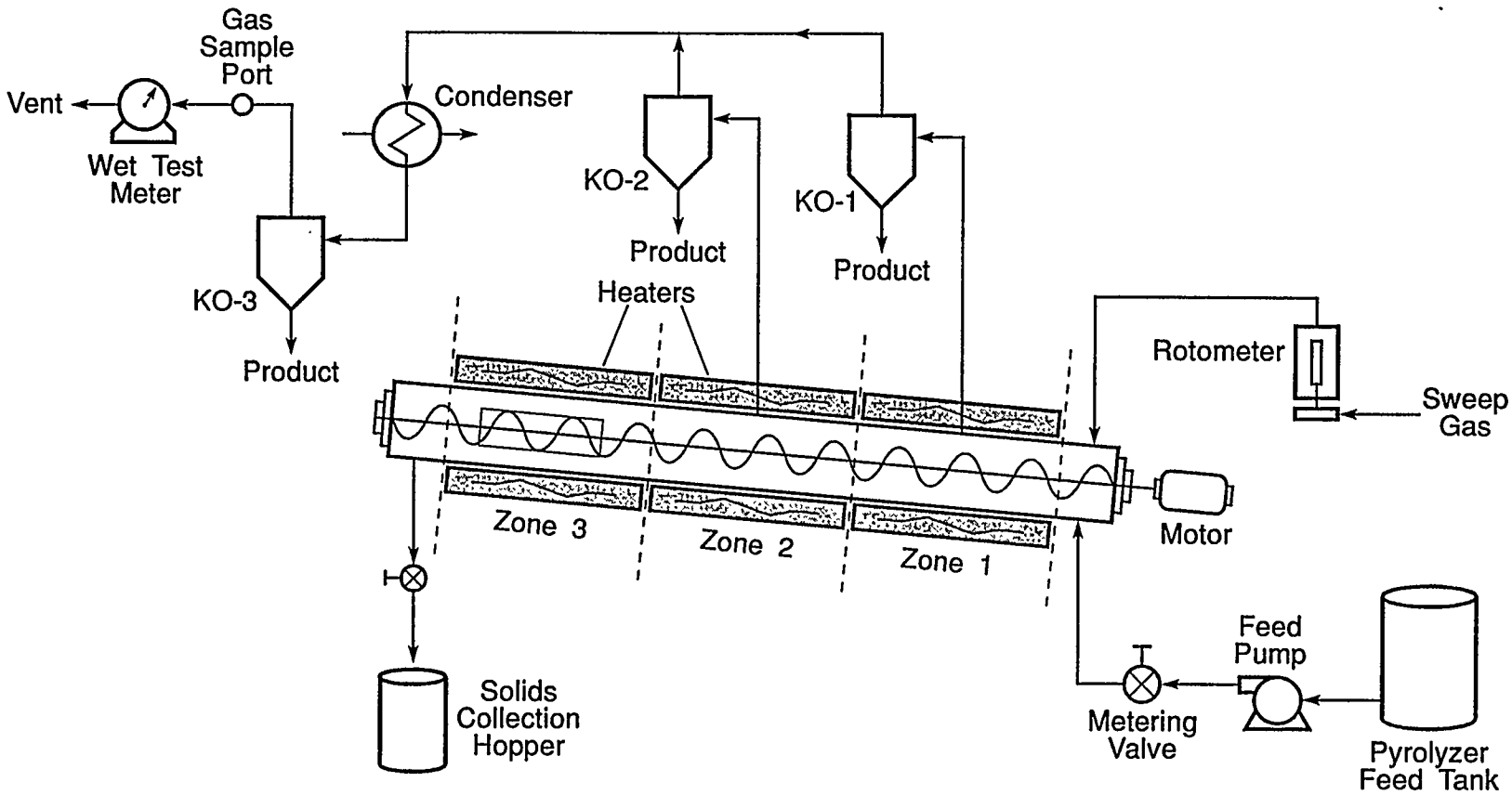

Figure 1. Schematic of the Six-Inch Twin Screw Setup Used for Pyrolysis Tests

Relatively small quantities of solids were produced during these tests, presumably because (1) the reactor interior was being coated with coke, (2) the material had a relatively low solids content, and (3) the processing temperatures used were very high. Nevertheless, a solid product ranging in size from 0.05 inch to 1 inch was produced. The solids produced were wetted with condensate as they cooled in the collection hopper. During some of the early tests, instruments for measuring gas production were not installed, and therefore an exact material balance could not be ascertained. However, by using gas analysis with nitrogen as a marker, gas production rates were determined. These gas production rates were also verified using a wet test meter. Mass closures greater than 90+ percent were obtained after gas production equipment was installed.

The amount of liquid produced during the shakedown tests was in the 60 to 70 weight percent range. The amount of solids recovered was less than 5 weight percent, and the balance was reported as gas. Gases produced during these tests were periodically sampled and analyzed using gas chromatography. Some representative pseudo-steady-state data are given in Table 1.

Table 1. Analyses of Gases from Pease Oil Stripper Bottoms (mole percent)

COMPONENT	664-95-1215	664-96-1315	664-100-1150	664-100-1306	664-100-1453
Hydrogen	8.54	8.91	10.07	10.06	10.42
Nitrogen	3.71	4.28	3.32	3.95	4.00
Oxygen	0.00	0.00	0.00	0.00	0.00
Argon	0.00	0.00	0.00	0.00	0.00
Carbon Monoxide	0.29	0.28	0.26	0.24	0.25
Methane	28.80	28.62	27.64	28.27	28.19
Carbon Dioxide	0.34	0.39	0.42	0.41	0.37
Ethylene	17.15	16.51	17.00	17.25	16.28
Ethane	12.02	12.06	12.17	11.98	12.06
Propanes	19.20	18.51	19.04	18.43	18.20
Butanes	9.95	10.43	10.08	9.42	10.23

Aleyaska Material

A 55-gallon drum of material was received from Aleyaska Pipeline operations through a contractor. The material was presumably generated from tank cleaning operations. Analyses performed at WRI showed that the material contained 50 weight percent solids, and about 30 weight percent water. Two test runs were conducted with this material. The material was processed at about 975 - 1020 °F. Material throughput for these tests was low because of the higher heat of vaporization required for water.

As expected, the liquid product consisted mostly of water, with a layer of oil. Solids produced during these tests were black and powdery. Overall material balance for the two tests was about 90 percent. The material partitioning of the three streams was 50 percent solids, 40 percent liquids, and 10 percent gas. Gases produced during these tests were periodically sampled and analyzed using gas chromatography. Some representative data are given in Table 2.

Table 2. Analyses of Gases Produced from Aleyaska Material (mole percent)

COMPONENT	12/5/96-12:56	12/5/96-13:57
Hydrogen	22.89	20.97
Nitrogen	39.30	36.70
Oxygen	0.00	0.00
Argon	0.01	0.09
Carbon Monoxide	3.91	2.65
Methane	3.91	2.27
Carbon Dioxide	25.13	32.05
Ethylene	1.15	0.78
Ethane	1.04	1.20
Propanes	1.73	2.31
Butanes	0.94	0.97

Peak Material

This material was obtained from Aleyaska Pipeline operations and was sent to WRI by Peak Oilfield Services, a contractor interested in operating a pyrolysis unit in Alaska. WRI's analysis showed the material to contain approximately 40 percent water and 40 percent solids.

The material was processed in the twin-screw setup with the three zone temperatures set at 1000, 1000, and 1050 °F. During the test, however, the temperatures in the first two zones dropped considerably. At steady state the temperature in Zone 1 ranged from 750 to 840 °F, and in Zone 2 the temperature ranged from 920 to 940 °F.

As in the case of the other Aleyaska material, the liquid product consisted mostly of water with a layer of oil. Solids produced during these tests were black and powdery. Overall material balance for the tests was nearly 100 percent. The material partitioning of the three streams was 25 percent solids, 50 percent liquids, and 25 percent gas.

Gases produced during these tests were periodically sampled and analyzed using gas chromatography. Some representative pseudo-steady-state data are given in Table 3.

Table 3. Analyses of Gases Produced from Peak Material (mole percent)

COMPONENT	664-102-1118	664-104-1235	664-104-1355
Hydrogen	13.58	10.07	10.06
Nitrogen	18.45	3.32	3.95
Oxygen	0.00	0.00	0.00
Argon	0.00	0.00	0.00
Carbon Monoxide	0.33	0.26	0.24
Methane	28.33	27.64	28.27
Carbon Dioxide	0.89	0.42	0.41
Ethylene	11.65	17.00	17.25
Ethane	9.12	12.17	11.98
Propanes	12.52	19.04	18.43
Butanes	5.12	10.08	9.42

Canadian Production Sand and Slop Oil

A 55-gallon drum of production sand was received from a major oil producer in Canada. The nominal composition of the feedstock provided by the producer to WRI was approximately 10 percent water and 5 percent oil. The producer also provided WRI with a 55-gallon drum of slop oil with a nominal composition of 10 percent water and 20 percent solids. The intent was to demonstrate the applicability of the pyrolysis concept for the disposal of the production sand, as well as the co-processing of slop oil and production sand. Through conversations with producers in Canada, we learned that these and similar oilfield streams are expensive disposal liabilities in the Lloydminster area.

Two tests were performed. One used sand only, and the other used a 50-50 volumetric mixture of production sand and slop oil.

For the production sand tests, the three zones were operated at 930, 1000, and 1050 °F. Solids produced during the test were black and the consistency of fine beach sand. Small quantities of liquid were produced that separated into oil and water in the collection pots. Overall closure for the test was greater than 110 percent. Excess material is believed to have been a result of increased coking caused by the high concentration of sand removed by the scraping action of the screw against the wall of the reactor. The material partitioning of the three streams was 79 percent solids, 6 percent liquids, and 15 percent gas.

Gases produced during these tests were also sampled and analyzed using gas chromatography. Some representative data are given in Table 4.

Table 4. Analyses of Gases from Canadian Production Sand (mole percent)

COMPONENT	664-106-2	664-106-3	664-106-4
Hydrogen	10.07	10.06	10.42
Nitrogen	3.32	3.95	4
Oxygen	0.00	0.00	0
Argon	0.00	0.00	0
Carbon Monoxide	0.26	0.24	0.25
Methane	27.64	28.27	28.19
Carbon Dioxide	0.42	0.41	0.37
Ethylene	17.00	17.25	16.28
Ethane	12.17	11.98	12.06
Propanes	19.04	18.43	18.2
Butanes	10.08	9.42	10.23

For the production sand and slop oil blend tests, the three zones operated at 1000, 1000, and 1050 °F. Solids produced during the test were similar to those produced from production sand alone. The produced liquid separated into oil and water in the collection pots. Overall closure for the test was 107 percent. As stated earlier, the excess material is believed to have been a result of increased

coking caused by the high concentration of sand removed by the scraping action of the screw against the wall of the reactor. The material partitioning in the three streams was 80 percent solids, 9 percent liquids, and 11 percent gas.

Amoco Tank Bottoms

The material was provided by the producer in three 5-gallon buckets. The material had the consistency of gelatin. WRI's analysis showed the material to contain 65 weight percent water and 15 weight percent solids. The material is a production waste being stored in tanks on an Indian Reservation in Wyoming.

The material was processed in the twin-screw reactor during two separate tests. During the first test, the temperatures for the three zones were set at 920, 1000, and 1000 °F. However, substantial cooling occurred when feed was introduced. The heaters were rewired for the second test, and the feed system was upgraded to feed at a slower rate. The processing temperatures for the second test were: Zone 1, 840 - 900 °F, Zone 2, 1010 - 1040 °F, and Zone 3, 1030 - 1050 °F.

As with the Aleyaska and Peak materials, the liquid product consisted mostly of water with a layer of oil. Solids produced during these tests were black and powdery. The overall material balance for the tests was nearly 100 percent. The material partitioning in the three streams was 21 percent solids, 73 percent liquids, and 6 percent gas.

Gases produced during these tests were periodically sampled and analyzed using gas chromatography. Some representative data are given in Table 5.

Table 5. Analyses of Gases Produced from Amoco Material (mole percent)

COMPONENT	664-111-1	664-111-2	664-111-4
Hydrogen	17.28	22.53	23.95
Nitrogen	45.26	37.71	38.98
Oxygen	0	0	0
Argon	0	0	0
Carbon Monoxide	1.85	2.48	2.42
Methane	9.53	12.91	10.7
Carbon Dioxide	8.96	7.67	7.9
Ethylene	3.65	2.62	2.75
Ethane	4.4	4.4	4.06
Propanes	6.39	6.37	6.53
Butanes	2.68	3.31	2.72

DISPOSAL CHARACTERISTICS OF SOLIDS

WRI conceived and developed the pyrolysis concept for oilfield wastes with the intent that the produced solids would be environmentally benign. Any inorganic components present in the feedstock were concentrated in the produced solids yet encapsulated as a low hydrogen:carbon carbonaceous matrix and were hence not mobile.

Some of the produced solids and solids extracted from the feed were subjected to the Toxicity Characteristics Leaching Procedure (TCLP) and analyzed for the eight Resource Conservation Recovery Act (RCRA) elements listed in 40 CFR 261.24. The data for the solids produced from the pyrolysis of the Aleyaska material, the Amoco material, and the Canadian production sand are presented in Table 6. The table also shows the regulatory limit for these elements. The data for the unprocessed Canadian production sand are also included for comparison. In all cases, the values for the produced solids are well below the regulatory limits, and in the case of Canadian production sand, the values for the produced solids are below those for the unprocessed material.

Table 6. Analytical Results for Eight TCLP-Extracted RCRA Metals

	Aleyaska	Amoco	Candian Production Sand		RCRA
Metal	Processed	Processed	As Received	Processed	Upper Limit
Silver, mg/L	< 0.01	< 0.01	< 0.01	< 0.01	5 mg/L
Arsenic, µg/L	1.14	0.56	5.43	5.37	5 mg/L
Barium, mg/L	1.28	0.57	0.33	0.23	100 mg/L
Cadmium, mg/L	0.01	< 0.01	0.01	0.02	1 mg/L
Chromium, mg/L	0.02	0.02	0.02	0.02	5 mg/L
Mercury, µg/L	< 1	0.76	< 0.05	0.13	5 mg/L
Lead, µg/L	<0.05	0.37	< 1	< 1	0.2 mg/L
Selenium, µg/L	<2	< 2	< 2	< 2	1 mg/L

In the Canadian oil fields of Alberta, the Alberta Environment Protection Tier 1 criteria establish a limit on the leachable chlorides, sodium, calcium, and magnesium. To demonstrate that the processed sand was less prone to leaching than the raw material, samples were analyzed for water-soluble sodium. The value for the unprocessed Canadian production sand was 1280 ppm, whereas the corresponding value for the processed sand was 276 ppm.

The produced solids were also analyzed for total petroleum hydrocarbons (TPH), according to Method 418.1 and subjected to the Paint Filter Test (PFT) according to modified Method EPA SW846 9095. The TPH value for produced solids from the Amoco material was 515 ppm, whereas for the Aleyaska material it was 738 ppm. The solids passed the PFT. Similarly, the petroleum hydrocarbons in the naptha range were determined for the as-received and processed production sand. The values determined were 300 and <2 ppm, respectively.

SUMMARY AND CONCLUSIONS

Tests were conducted to verify the pyrolysis concept for the ultimate disposal of oilfield wastes and TaBoRR stripper bottoms. An existing 6-inch screw setup was modified and instrumented. Six different materials, ranging in water content from 0 - 40 percent and solids content from 5 - 85 percent, were pyrolyzed at temperatures of 1020 -1050 °F. In all cases, a coked solid product was created. Oil recoveries were consistent with the hydrocarbon contents of the respective feed materials.

Produced solids were analyzed for the eight TCLP-extracted RCRA metals and were found to be well below the regulatory limits. The produced materials also passed the paint filter test. Total petroleum hydrocarbon content of some of the produced solids was a little higher than the Wyoming Department of Environmental Quality limit; however, this was in the most part due to recondensation of some of the produced vapors. This recondensation can be readily prevented by redesigning the solids discharge system and providing an adequate sweep gas rate.

WRI-98-R006

WESTERN RESEARCH INSTITUTE
"Providing solutions to energy and environmental problems"

FINAL REPORT

HAZ-FLOTE™: EX-SITU DECONTAMINATION OF MATERIALS

Prepared for
U.S. Department of Energy
Morgantown, West Virginia

April 1998

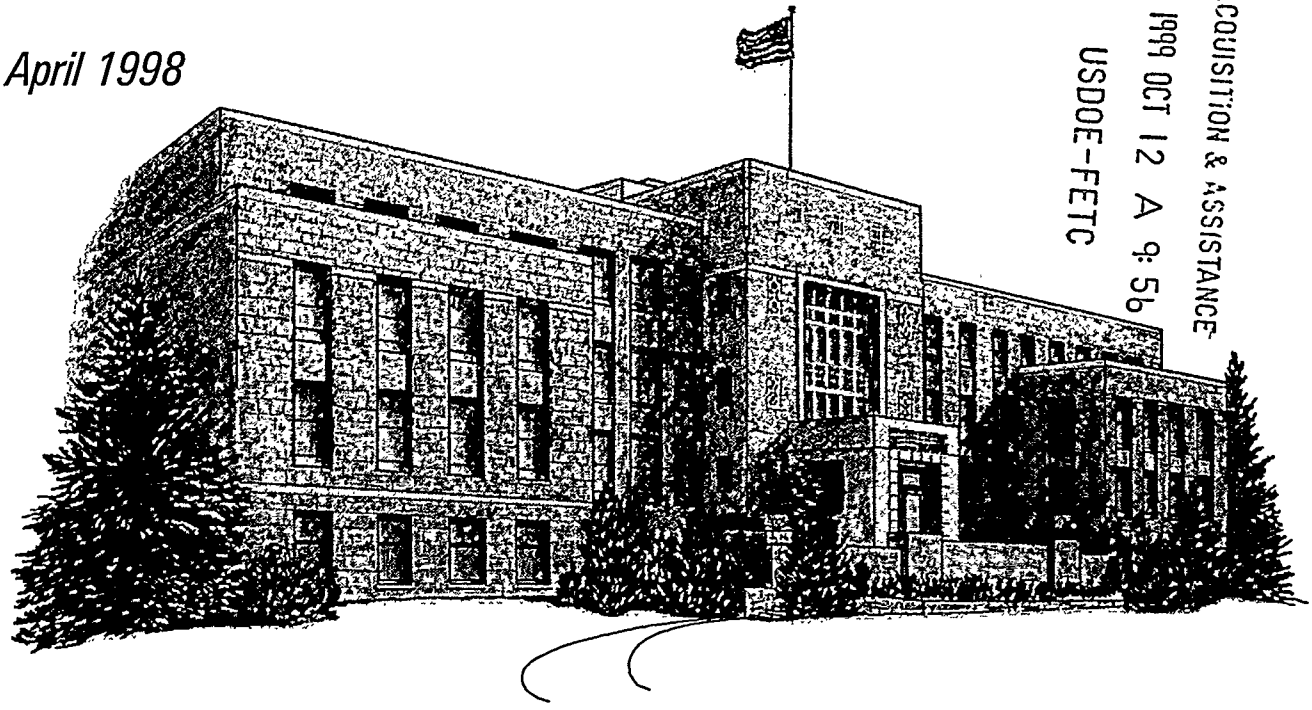

WRI-98-R006

HAZ-FLOTE™: EX-SITU DECONTAMINATION OF MATERIALS

Final Report

By
Terry H. Brown
Al Bland

April 1998

Work Performed Under Cooperative Agreement
DE-FC21-93MC30126 Subtask 3.2

For
U.S. Department of Energy
Office of Fossil Fuel
Federal Energy Technology Center
Morgantown, West Virginia

By
Western Research Institute
Laramie, Wyoming

DISCLAIMER

TABLE OF CONTENTS

LIST OF TABLES AND FIGURES

Tables **Page**

Figure **Page**

LIST OF TABLES AND FIGURES

Tables **Page**

Figure **Page**

EXECUTIVE SUMMARY

Western Research Institute (WRI), in conjunction with the U.S. Department of Energy (DOE), Federal Energy Technology Center, is developing a soil remediation technique called Haz-Flote™. The technique consists of two steps, chemical treatment and scrubbing and removal from aqueous solution. In the scrubbing step, contaminants are dissolved in an aqueous solution. Reagents are added to adjust the solution chemistry conditions. The aqueous solution containing the contaminants is then transferred to a separaton unit. Contaminants are separated from the aqueous solution, and the clean liquid is returned to the scrubber for reuse.

Initial tests were conducted for petroleum contaminated materials employing a number of chemical combinations. The most promising chemicals used in this study showed about a 75% reduction in organic carbon content in the coarse fraction. This reduction demonstrates that the treatment can remove some petroleum contaminants from the coarse fraction. Tests were also conducted using the fine fraction of the petroleum contaminated soil. The preliminary results show that the HazFlote process separates a portion of the hydrocarbons from the very fine soil fraction under less than optimum conditions. After treatment, the organic carbon content of the fine-size fraction was about 26% lower than that of the feed material. The treated material collected from the unit had 54% more organic carbon content than the column feed. Optimization of the equipment and the chemistry of the treatment system should enhance these results significantly.

The bulk of the work using the Haz-Flote process has been focused on removing mercury from contaminated soil fines. A sample of mercury contaminated soil was obtained, and the distribution of mercury within the various size fractions was determined. The -200 mesh (<75 um) material contains the majority of the mercury contaminant. For convienience, the sample was sieved through a 70 mesh screen. All of the testing was conducted on the -70 mesh (<212 um) fraction. This fraction contained on average 122 mg/kg mercury before processing. Mercury concentrations after processing were reduced to as low as 0.95 mg/kg of dry soil. This represents >99% mercury reduction for the fine fraction. Tests have removed >99.5% of the mercury from the scrubber solution.

INTRODUCTION

Background

There are thousands of known contaminated sites in the United States, including Superfund sites, Resource Conservation Recovery Act (RCRA) corrective action sites, underground storage tanks, U.S. Department of Defense sites, U. S. Department of Energy sites, mining refuse piles, and numerous other hazardous metals and organic contamination sites. Only a small percentage of these sites has been cleaned up. Several technologies are available to remediate soil at these sites. Unfortunately, many of these technologies are only effective for materials coarser than approximately 200 mesh (>75 um). The fine materials are disposed of or treated at considerable expense. As a result, the costs associated with the remediation of contaminated soils are often quite high.

Western Research Institute (WRI) is developing a soil cleaning technique based on release of the contaminant to an aqueous medium followed by column flotation, removing the contaminant from the solution. This technique may provide a method that can remove contaminants from fine-textured soils, sediments, and sludges. The Haz-Flote™ process will require low capital investment, low operating costs and will reduce costs of disposal of the fine fraction at waste disposal sites. This process will extend the use of soil washing techniques to contaminated sites that are currently remediated using more costly technologies.

Using froth flotation for the beneficiation of mineral ores was first practiced in the late 1800's, with the process flourishing during the early 1900's. The use of a column in the flotation process was patented in the early 1960's. However, it was not until about 1981 that a surge in commercial interest for using column flotation in the ore beneficiation processing was seen. Column flotation systems have been used in a number of applications, including copper, molybdenum, lead, zinc and tin cleaning in the minerals mining industry, bulk sulfide roughing of gold ores, coal cleaning, and phosphate flotation.

A number of investigators have used foam separation techniques to remove ions such as mercury, cadmium, and copper from aqueous systems. Okamoto and Chou (1975) showed that the removal of mercury ions from aqueous solutions was almost quantitative by chelating the ions with the surfactant 4-dodecyldiethylenetriamine. In another study, the cationic surfactant hexadecyltrimethylammonium bromide was used in a foam fractionation study to remove trace levels of mercury (II)-nitro complexes (Miller and Sullivan 1971). Another type of foam flotation process, colloid flotation, has been successfully used to remove mercury from seawater (Voyce and Zeitlin 1974), and molybdenum from seawater (Kim and Zeitlin 1971). In these applications, iron (III) hydroxide was used as a sorption surface for the target elements (elements targeted for removal). The resulting iron (III) hydroxide element complex was bound by sodium dodecylsulfate, making it hydrophobic. This final complex could easily attach to an air bubble and

could be removed from the solution via flotation. Huang and Wilson (1976) reported the use of adsorbing colloid flotation batch separations of mercury and cadmium from aqueous solutions down to concentrations of 20 ppb.

The literature shows that the use of foam separation techniques to clean mineral ores and to remove potentially toxic elements and complexes from aqueous solutions can be successful. Therefore, it is very probable that these techniques can be used to separate elements such as mercury from soils. In addition, petroleum products that have charge systems that can be complexed with a number of collectors, rendering them hydrophobic, should also have a high probability for removal from soil materials.

This final report describes the work done to date using Haz-Flote technology to remove petroleum products (crude oil) and mercury from contaminated soil materials.

Anticipated Benefits

The development of innovative technologies to handle the various cleanup problems on a national and international scale is commonplace. Many innovative soil washing technologies have been developed during the past few years that can effectively remediate contaminated materials. However, these technologies usually require considerable investment in equipment, and the cleanup costs of soil material are relatively high (in excess of $140 to $270 per m^3). These costs result from the elaborate nature of the processes, the costs for power, and the chemical costs.

The Haz-Flote technology has numerous advantages over other ex-situ soil washing techniques. Capital investment and operating costs are low, and the process results in high levels of re-emplacement of the cleaned material on site. Haz-Flote has the capability to clean the fine fraction (< 100 mesh) of the soil, resulting in the replacement of 95+% of the material back on site, reducing the costs of disposal. The Haz-Flote technology can expand the application of soil washing technology to heavy soils (clay type soils) to which current soil washing practices are not applied. WRI is not aware of any other soil washing technologies that demonstrate this ability at the expected cost on a per ton basis. This technology is considered excellent for Superfund and other organic and inorganic contaminated sites.

OBJECTIVE

The objective of this research is to develop a low-cost method for remediation of contaminated soil fines, sediments, and sludges. The process will be developed as an ex-situ treatment technology for the removal of organics and metals from contaminated soils and other materials. The emphasis will be on the cleanup of fine materials (i.e., < 100 mesh materials).

TECHNICAL APPROACH

Haz-Flote is an ex-situ treatment technology for materials contaminated with organics and metals. The process incorporates the use of specifically designed chemical reagents with a novel separation approach. The evaluations were conducted on mercury contaminated soils and on petroleum contaminated soil materials. The cleaned matrix will be dewatered and available for return to the site.

Characterization of contaminated material was conducted to determine the chemical and physical nature of the materials. The particle-size classification was determined for each material studied. In addition, the levels of contaminant were determined for each particle size class.

Scrubbing or mixing tests using a bench-scale unit were conducted to provide initial information or screening tests for the various combinations of chemicals that were planned for use in the study.

Haz-Flote testing required a significant effort to determine the parameters and the levels required to successfully remove the contaminants from the materials studied. Important parameters included slurry percent solids, pretreatment requirements, gas flow rates, and collector/frother combinations required to provide good removal and stable froth. Shakedown and modifications to the system are expected to take considerable time and effort.

RESULTS AND DISCUSSION

Activity I. Design and Construction of the Column Flotation Unit

The initial work associated with this project dealt with the development of facilities to accommodate the research effort. Appropriate equipment was purchased, the laboratory was modified for the placement of the equipment, and a column flotation unit was designed and constructed (Figure 1). The column flotation unit is 7.6 cm in diameter, 6.7+ m tall, and made of glass. The unit is supported by a thickener for mixing contaminated soil materials with appropriate conditioning chemicals and a sludge pump for feeding the column. The system was tested and found to be mechanically sound.

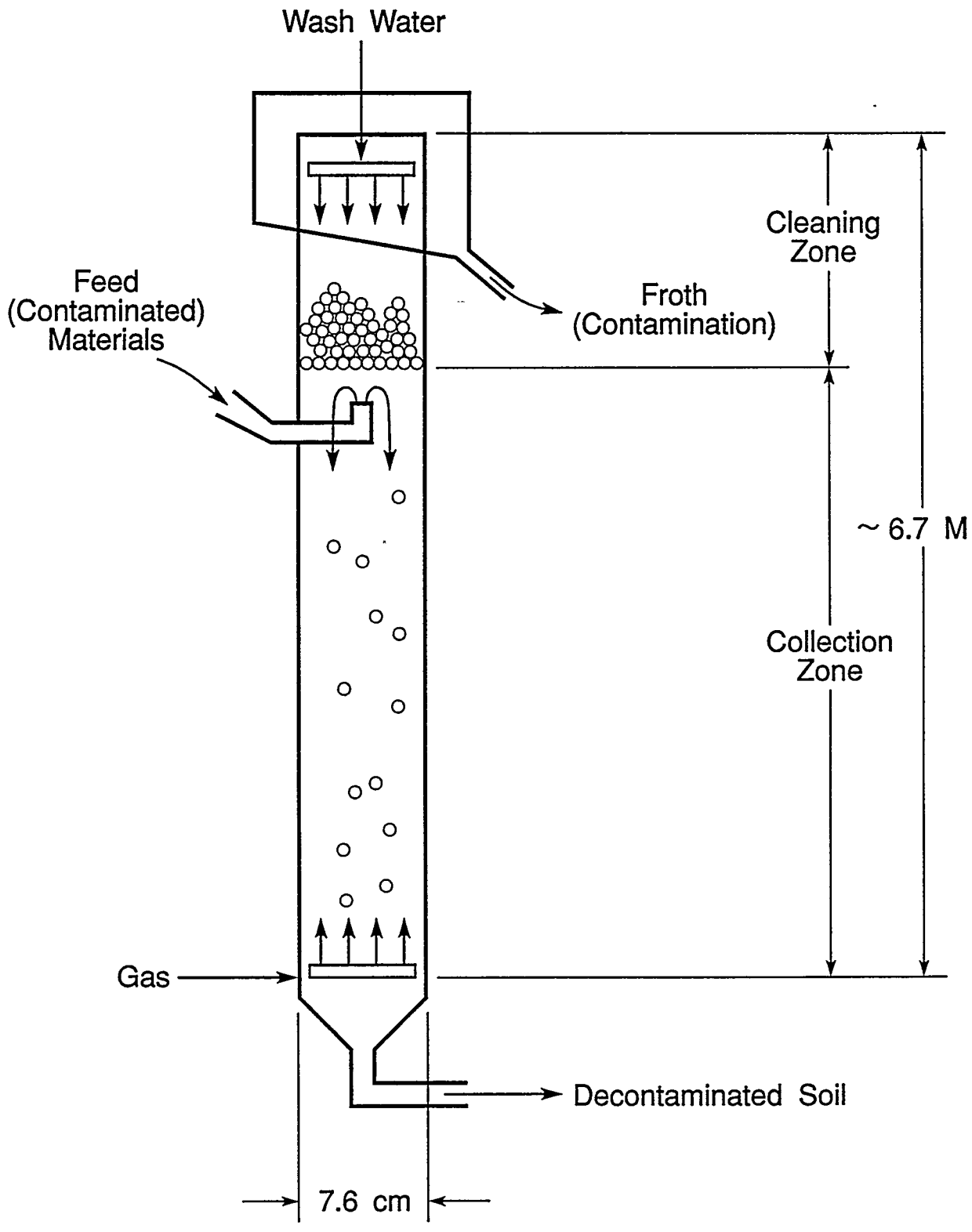

Figure 1. Column Flotation Unit Constructed

Activity II. Shakedown Tests for the 7.6-cm Diameter Column Flotation Unit

Two tests were conducted to determine whether the 7.6-cm dia. column could be effectively used to reconcile the chemicals required for the efficient removal of the petroleum and mercury contaminates.

Procedures

In the initial test, a soil contaminated with crude oil was mixed with water and Tide (surfactant) in a large stainless steel thickener tank. The column was initially filled with water, and air was sparged into the system as the contaminated material was pumped into the column. As the material settled in the column, the rising air bubbles rose to the top of the column and exited it as a froth.

This test revealed several problems with the equipment and showed that some sample preparation would be needed prior to injection into the system. As a result of these problems, the test did not provide an assessment of the process. During the pumping, segregation of particle sizes appeared to cause major problems, especially since the slurried material was initially being pumped about 5.2 m vertically to the injection port to the column. Subsequently, the feed system was elevated so that the feed pulp flowed at a slight downward angle into the column. In addition, a trap was added at the column bottom to collect settled solids, and the overflow tube was routed vertically over a weir to provide control of the liquid level in the column.

In the second test, a sample of soil was screened to -100 mesh and saturated with crude oil. During the actual operation of the process in a field situation, a hydrocyclone will be employed to separate the soil by size class. The contaminated soil was mixed with water, 4-methyl-2-pentanol (collector) at a concentration of 90 ppm, and a small amount of Tergitol (frother). The mixture was pumped into the column as the air was sparged into the system. Froth, settled solids, and liquid underflow from the bottom of the column were collected.

Results

The mechanics of the system worked well following modification. The modified mixer system suspended a uniform pulp that could be pumped into the column at a controlled rate. Three distinct effluent streams were generated, and representative samples were collected. The collapsed froth did not appear to differ appreciably from the underflow liquid. The settled solids looked cleaner than the feed but still had the smell of oil. This provided a qualitative indication that the flotation process was working, however, at a low efficiency.

Conclusions

The results of this experiment indicate that mechanically the system works well with the exception of considerable turbulence present in the column even at low air flow rates. However, the scrubber and flotation chemical tests were not resolved, and the removal of the crude oil contaminate was less than satisfactory. It is expected that considerable preliminary testing will be required to achieve efficient removal of contaminants. During the testing a large amount of waste was generated using the 7.6-cm diameter column. Therefore, subsequent testing was conducted using a smaller column, significantly reducing the amount of waste generated.

Activity III. Bubble Size and Turbulence Tests

Problems found in the initial testing included the coalescence of bubbles, forming larger bubbles, and the presence of turbulence in the column. Tests were conducted to evaluate the effects of various chemicals and combination of chemicals, types of gas spargers, and superficial air velocities on bubble size and froth stability.

Procedures

Testing was done to determine which chemical combinations would provide appropriate bubble size and froth stability. Various dosages of chemicals mixed in beakers and air-sparged with a Mott cylindrical gas sparger were used.

Subsequent tests were conducted in a glass column 7.6 cm i.d. and 61 cm long. The column was fitted with either one or two 1 cm by 7 cm cylindrical stainless steel Mott spargers, a 5.1-cm dia. stainless steel disc sparger, or a 2.2 cm by 6.4 cm fabric sparger. Gas flow to the sparger was measured with a calibrated rotameter, and the pressure drop across the system was measured with a 0-15 psig pressure gauge. Water containing various dosages of flotation chemicals was placed in the column, and nitrogen was bubbled through the solutions. Nitrogen flow rates ranging from 35 to 1333 std. cm^3 min^{-1} were used. These flow rates provided superficial gas velocities of 0.013 cm s^{-1} to 0.48 cm s^{-1}.

Three tests were conducted using a hydrocarbon contaminated soil prepared with Shannon crude oil and a soil containing large amounts of clay. The soil was ground in a pulverizer and screened to pass through a 100 mesh sieve. The -100 mesh fraction was saturated with Shannon crude oil (a light crude oil). The saturated soil contained about 17.73% by weight of crude oil. The hydrocarbon contaminated soil sample was scrubbed with water and various combinations of Dowfroth 250, surfonic N-95, and sodium hydroxide.

Tests were conducted by scrubbing the hydrocarbon contaminated soil with water and various reagents. The scrubbing was done in a 3 L beaker using a high-speed laboratory mixer.

After mixing, the coarser particles were allowed to settle, and the liquid was decanted into the column where it was bubbled for 10 minutes with nitrogen at a superficial velocity of 0.48 cm^3min^{-1}. Liquid samples taken before and after the bubbling were analyzed for carbon content using a Coulometrics total carbon analyzer. The systems were observed for visual indications that oil was separated from the soil sample.

Results

The results from these tests are summarized in Table 1. Of the collectors evaluated, sodium dodecylsulfate produced the most froth and the highest froth stability. Oleic acid and dodecylamine did not produce a froth when used without a frother. A thin froth layer of minimal stability was generated from solutions of oleic acid (collector) mixed with 4-methyl-2-pentanol (frother). Mixtures containing dodecylamine and 4-methyl-2-pentanol did not produce a froth. Sodium dodecylsulfate produced a stable froth without the addition of a frother. With the addition of a frother, sodium dodecylsulfate formed significant amounts of stable froth.

The effects of reagents, types of gas sparger, and superficial velocities on bubble size and turbulence are shown in Table 2. All chemicals evaluated reduced the bubble size and increased turbulence even at low dosages. The disc sparger generally provided smaller bubbles and higher turbulence than the Mott sparger. Pressure drops were higher with the disc sparger, indicating that it is made from a finer frit than the Mott sparger.

Increasing superficial velocity generally seemed to increase turbulence. However, even with very low superficial velocities, backmixing was evident in the column for all the tests in which chemicals were added. The carbon content of the liquid taken from the scrubber before and after bubbling in the column is presented in Table 3. The data provide an indication of the scrubbing efficiency of the flotation process.

The feed soil contained about 0.156 g of carbon contaminant per g of feed, assuming that the Shannon crude contains about 88% by weight carbon. The 45 g of contaminated soil used for each test contained 7.02 g of contaminant as carbon. The contaminated soil was placed in the scrubber with 1500 g of water. If the entire hydrocarbon contaminant was suspended in the liquid, the carbon content of the liquid pool would be about 4680 ppm. Carbon content of the scrubber liquid was well below this level for all the tests, indicating that only a small fraction of the hydrocarbon contaminant was suspended in the scrubbing operation. However, in every test the carbon content of the liquid increased after flotation. This result could be related to air bubbles stripping carbon from the surfaces of particles through hydrophobic bonding or to stratification of the oil as the liquid was allowed to settle. The flotation test was compared to a test in which the scrubber-treated material was allowed to quiescently settle. It was found that quiescent settling was more effective for separating suspended hydrocarbons from the wash water than bubbling in a turbulent flotation column.

Table 1. Froth Volume and Stability with Various Reagents and Reagent Dosages

Reagent 1 Chemical	Dosage ppm	Reagent 2 Chemical	Dosage ppm	Froth Volume[a]	Froth Stability[b]
4-Me-2-Pentanol	5			1	0
4-Me-2-Pentanol	10			1	1
4-Me-2-Pentanol	15			1	1
4-Me-2-Pentanol	20			2	1
Oleic Acid	5			0	0
Oleic Acid	10			0	0
Oleic Acid	20			0	0
Oleic Acid	40			0	0
Oleic Acid	60			0	0
Oleic Acid	100			0	0
Dodecylsulfate	10			2	1
Dodecylsulfate	20			2	2
Dodecylsulfate	40			3	3
Dodecyl Amine	10			0	0
Dodecyl Amine	20			0	0
4-Me-2-Pentanol	20	Oleic Acid	20	1	1
4-Me-2-Pentanol	20	Oleic Acid	50	1	1
4-Me-2-Pentanol	20	Dodecylsulfate	20	3	3
4-Me-2-Pentanol	20	Dodecylsulfate	50	3	3
4-Me-2-Pentanol	20	Dodecyl Amine	20	0	0
4-Me-2 Pentanol	20	Dodecyl Amine	50	0	0
4-Me-2-Pentanol	10	Dodecylsulfate	20	2	2
4-Me-2-Pentanol	20	Dodecylsulfate	20	2	2
4-Me-2-Pentanol	30	Dodecylsulfate	20	2	3
4-Me-2-Pentanol	40	Dodecylsulfate	20	2	3
4-Me-2-Pentanol	50	Dodecylsulfate	20	3	3

[a] Volume:
0 = none
2 = medium
3 = high

[b] Stability:
0 = unstable 1 = low 1 = slightly stable
2 = stable
3 = very stable

Table 2. Bubble Size and Turbulence at Various Chemical Dosages and Superficial Velocities

Sparger	Velocity cm/sec	Chemical	Dosage ppm	Bubble Size[a]	Turbulence[b]
Disc	0.31	none	0	0	1
Disc	0.31	4-Me-2-Pentanol	10	1	2
Disc	0.14	4-Me-2-Pentanol	10	1	2
Disc	0.48	4-Me-2-Pentanol	10	1	2+
Disc	0.31	4-Me-2-Pentanol	20	2	2
Disc	0.31	4-Me-2-Pentanol	50	3	2
Disc	0.31	4-Me-2-Pentanol	100	3	2
Disc	0.009	4-Me-2-Pentanol	66	3	2
Disc	0.31	4-Me-2-Pentanol	66	2	2
Disc	0.04	4-Me-2-Pentanol	66	3	2-
Mott	0.31	none		0	0
Mott	0.04	none		0	0
Mott	0.31	4-Me-2-Pentanol	20	1	1-
Mott	0.31	4-Me-2-Pentanol	50	1	1+
Mott	0.31	4-Me-2-Pentanol	1100	1	2
Mott	0.31	Dowfroth 250	50	2	2
Mott	0.31	Surfonic N-95	50	1	2
Mott	0.31	2-Propanol	50	1	2

[a] Bubble Size
0 ≥ 2 mm
1 = 1 mm
2 = 0.5 mm
3 < 0.5 mm

[b] Turbulence
0 = nonturbulent
1 = transitional
2 = turbulent

Table 3. Effect of Bubbling on Carbon Content of the Liquid Phase from Contaminated Soil Washing with Various Chemicals

Chemical	Dosage ppm	Superficial Velocity cm/sec	Carbon Before ppm	Carbon After ppm
None		0.48	38.8	82.7
Sodium Hydroxide	400	0.48	50.1	184.2
Hydrochloric Acid	5966	0.48	46.3	59.0
Dodecylsulfate	41	0.48	48.0	86.5
Igepal CA-720	50	0.48	34.0	74.2

Conclusions

1. Dodecylsulfate alone or in combination with 4-methyl-2-pentanol provides a good volume of stable froth.

2. Gas bubble size is affected by sparger porosity, reagent dosage, and gas flow rate.

3. Reagent additions that decrease bubble size also increase turbulence.

4. Turbulence in the liquid pool is evident even at very low superficial gas velocities.

5. The scrubber chemicals tested were not very efficient in suspending the hydrocarbon contaminant in the liquid phase.

6. A portion of the hydrocarbon contaminant floats to the surface when it is suspended in the liquid phase.

7. Quiescent settling was more effective for separating suspended hydrocarbons from the wash water than bubbling in a turbulent flotation column.

8. The efficiency of the scrubbing step must be increased dramatically before the flotation step can be meaningfully evaluated.

Activity IV. Scrubber and Flotation Tests for Soils Contaminated with Petroleum Hydrocarbons

Scrubber Tests

The objectives of these tests were to find a reagent or reagent combination capable of separating a hydrocarbon contaminant (crude oil) from a clay soil and to suspend the contaminant in the liquid phase where it would be amenable to flotation.

Procedures

For a typical scrubber chemical test, a sample of contaminated soil was mixed with water and the test reagent. After mixing, the pulp was allowed to settle and the liquid was decanted from the surface of the settled solids. The settled solids were then rinsed by mixing with clean water and allowed to settle. A particle-size cut was made based on relative settling velocities. Particles that settled from the mixture in 15 minutes were called coarse solids, and particles remaining suspended after 15 minutes were called fine solids.

Test variables included the mixer, pulp density (weight of the feed/weight of the pulp), reagents and reagent dosages, and rinse water volume. Three different contaminated soil samples were used in the testing. The first tests used either a contaminated soil sample prepared in the laboratory by mixing a -100 mesh soil sample with Shannon crude oil or the -100 mesh soil without added crude oil. The third soil was obtained from an oil well site in central Wyoming.

This petroleum contaminated material represents soils that are contaminated with crude oil and have been affected by environmental influences for a number of months.

Prior to the initiation of the tests, the Coulometrics total carbon analyzer was modified so that it would accept solid samples. Solid samples were slurried with water when collected. The samples were placed on watch glasses and air-dried overnight before being analyzed for total carbon content. Sample weight loss during combustion in the carbon analyzer was greater than the mass accounted for as carbon. Also, the ratio of weight loss to carbon mass varied from sample to sample, indicating that another variable besides carbon content was influencing the results. This variable was assumed to be differing moisture content among the air-dried samples, probably due to differences in textures. To eliminate this variable, sample mass was corrected using soil moisture content. Carbon content was then reported on a dry basis.

The total carbon analyzer with sample weight correction seemed to provide consistently comparable results. Carbon content for the feed soil agreed well with its calculated carbon content and was repeatable throughout the test program. The sample weight corrections may result in unrealistically high carbon values for the very fine soil particles from which water of hydration is removed in the combustion furnace. Nonetheless, carbon content among samples with similar particle-size distributions should be comparable.

Results

The results of the scrubber chemical tests in terms of carbon removal are summarized in Table 4. The reduction in carbon content is the percentage of the carbon in the feed that was removed in the scrubbing operation. The soil sample prepared in the laboratory contained some inorganic carbon. Therefore, accounting for the inorganic carbon will increase the apparent efficiency of the various chemicals but will not change their relative efficiencies.

Flotation Tests

The objective of these tests was to provide an effective and efficient method of removing contaminants from the scrubber solutions and the fine soil fraction.

Procedures

Tests were conducted for the petroleum contaminated materials using a number of collectors, frothers and other conditions. Combinations of various surfactants and pH modifiers were used at various dosages. Tests were conducted using the 7.6-cm diameter by 61-cm length column described previously in this report. The carbon content of the samples before and after treatment was used to approximate the efficiency of the process. Carbon analyses were done using the total carbon analyzer described in the previous section.

Table 4. Summary of Scrubber Chemical Tests*

Sample	Feed	Mixer	Reagent 1	Dose	Reagent 2	Dose	Note**	-C%
46-5	1	1	NaOH	2459			0	32
46-6	1	1	NaOH	647			0	52
46-7	2	1	NaOH	647			0	80
46-8	2	1	NaOH	2459			0	84
54-1	1	1					0	36
54-2	1	1	NaOH	647			0	37
54-3	1	1	NaOH	2589			0	36
54-4	1	1	NaOH	6470			0	33
54-5	1	1			DF 250	40	0	29
54-6	1	1	NaOH	647	DF 250	40	0	36
54-7	1	1	NaOH	2589	DF 250	40	0	37
54-8	1	1	NaOH	6470	DF 250	40	0	38
	2	Uncontaminated untreated soil blank						83
	2	Uncontaminated untreated soil blank						83
60-1	1	2					24	4
60-2	1	2	NaOH	1000			24	11
60-3	1	2	NaOH	12000			24	20
60-4	1	2	NaOH	100000			24	18
67-1	1	3					1	21
67-2	1	3	NaOH	582			1	20
67-3	1	3					25	24
67-4	1	3					2	12
67-5	1	3	NaOH	582			2	21
67-6	1	3					2	20
67-7	1	3					3	21
67-8	1	3	NaOH	582			3	17
67-9	1	3					3	38
67-10	1	Contaminated soil blank dried on watch glass						15
67-11	1	3					6	66
67-12	1	3					4	8
71-1	1	3	DDA	39	EtOH	1553	4	-70
71-2	1	3	Dawn	1941			4	4
71-3	1	3	Tide	9903			4	-45
71-4	1	3	DDA	39	EtOH	1553	0	25
71-5	1	3	Dawn	1941			0	44
71-6	1	3	Tide	9903			0	81
75-11	1	3	DDA	39	EtOH	1553	4	-70
75-12	1	3	Dawn	1941			5	-16
75-13	1	3	Tide	9903			5	54

Sample	Feed	Mixer	Reagent 1	Dose	Reagent 2	Dose	Note**	-C%
75-1	1	4	Tide	7767			6	48
75-2	1	4	Tide	7767			6	62
75-3	1	4	Dawn	194	MeOH	29126	6	33
75-4	1	4	Tide	7767			7	49
75-5	1	4	Tide	7767			8	55
75-6	1	4	Dawn	194	MeOH	29126	4	-25
	2		Uncontaminated untreated soil blank					81
	2		Uncontaminated untreated soil blank					82
	2		Uncontaminated untreated soil blank					92
81-1	1	4	Tide	7767			10	58
81-2	1	4	Tide	7767			9	-13
81-3	1	4	Tide	7767			2	79
81-4	1	4	Tide	1942			2	53
81-5	1	4	Tide	388			2	16
81-6	1	4	Tide	7767			3	79
81-7	1	4	Tide	1942			3	56
81-8	1	4	Tide	388			3	11
81-9	1	4	Tide	7767			11	82
81-10	1	4	Tide	1942			11	57
81-11	1	4	Tide	388			11	7
81-12	1	4	Tide	7767			12	19
81-13	1	4	Tide	1942			12	10
81-14	1	4	Tide	388			12	11
89-1	1	4	Tri X100	10			1	0
89-2	1	4	Tri X100	40			1	18
89-3	1	4	Tri X100	100			1	20
89-4	1	4	Tri X100	400			1	12
89-5	1	4	Tri X100	10			2	23
89-6	1	4	Tri X100	40			2	19
89-7	1	4	Tri X100	100			2	19
89-8	1	4	Tri X100	400			2	17
89-9	1	4	DDA	10	EtOH	400	0	25
89-10	1	4	DDA	50	EtOH	2000	0	34
89-11	1	4	DDA	100	EtOH	4000	0	5
89-12	1	4	DDA	500	EtOH	20000	0	10
89-13	1	4	DDA	1000	EtOH	40000	0	-3
89-14	1	4	DDA	10	EtOH	400	4	-9
89-15	1	4	DDA	50	EtOH	2000	4	-34
89-16	1	4	DDA	100	EtOH	4000	4	-53
89-17	1	4	DDA	500	EtOH	20000	4	-62
89-18	1	4	DDA	1000	EtOH	40000	4	-33

Sample	Feed	Mixer	Reagent 1	Dose	Reagent 2	Dose	Note**	-C%
93-1	3	4					0	4
93-2	3	4	Tide	1942			0	48
93-3	3	4	Tide	3883			0	63
93-4	3	4	Tide	5825			0	75
93-5	3	4	Tide	7767			0	75
93-6	3	4	Tide	9709			0	82
93-7	3	4					13	25
93-8	3	4	Tide	1942			13	46
93-9	3	4	Tide	3883			13	64
93-10	3	4	Tide	5825			13	75
93-11	3	4	Tide	7767			13	79
93-12	3	4	Tide	9709			13	85
93-13	3	4					13	N.A.
93-14	3	4	Tide	1942			14	-24
93-15	3	4	Tide	3883			14	-55
93-16	3	4	Tide	5825			14	-60
93-17	3	4	Tide	7767			14	-64
93-18	3	4	Tide	9709			14	-154
93-19	3	4					4	-85
93-20	3	4	Tide	1942			4	-28
93-21	3	4	Tide	3883			4	-27
93-22	3	4	Tide	5825			4	49
93-23	3	4	Tide	7767			4	97
93-24	3	4	Tide	9709			4	79
95-1	3	4					15	-62
95-2	3	4	Tide	1942			15	16
95-3	3	4	Tide	3883			15	30
95-4	3	4	Tide	5825			15	45
95-5	3	4	Tide	7767			15	45
95-6	3	4	Tide	9709			15	38
103-7	3	4	DDS	40	HCl	11650	16	-24
103-8	3	4	DDS	40	HCl	11650	17	-36
103-9	3	4	DDS	40	HCl	11650	6	17
103-10	3	4	DDS	40	HCl	11650	18	-46
103-11	3	4	DDS	40	HCl	11650	19	-52
103-1	3	4	Tide	5825			6	74
103-2	3	4	Tide	5825			8	83
103-3	3	4	Tide	5825			20	-27
103-5	3	4	Tide	5825			21	12
103-4	3	4	DDS	40			20	-79
103-6	3	4	DDS	40			21	-38
103-15	3	4	Tide	5825			8	77
103-12	3	4	Tide	5825			13	74

Sample	Feed	Mixer	Reagent 1	Dose	Reagent 2	Dose	Note**	-C%
105-1	3	4	Tide	5825			22	-67
105-2	3	4	Tide	5825			22	-67
105-3	3	4	Tide	5825			23	72
105-4	3	4	Tide	5825			23	70
105-5	3	4	Tide	5825			23	76
105-6	3	4	Tide	5825			23	77
15-16	3	4	Alconox	1942			4	-51
15-17	3	4	Alconox	3883			4	-30
15-18	3	4	Alconox	5825			4	-37
15-19	3	4	Alconox	971			4	-1
15-6	3	4	Alconox	1942			6	28
15-7	3	4	Alconox	3883			6	41
15-8	3	4	Alconox	5825			6	53
15-9	3	4	Alconox	971			6	20

*Column definitions for Table 4:

Feed:
1. Soil Sample preparation – pulverized, screened to -100 mesh and saturated with Shannon crude oil
2. Soil as described above but without crude oil containment
3. Oily soil from Kaycee, Wyoming

Mixer:
1. Denver D-12, attrition scrubber paddles, mixed in beaker
2. Denver D-12, attrition scrubber paddles, mixed in cell supplied with scrubber kit
3. High-speed lab mixer
4. High-speed lab mixer with added impact bar

Reagent:
Tri X-100 = Triton X-100
DF 250 = Dowfroth 250
DDA = Dodecylamine
DDS = Dodecylsulfate sodium salt

Dose:
Reagent weight/pulp weight x 1000000

Note:** See Footnotes

-C%:
Percentage decrease in carbon content after scrubbing
[1-(Carbon in sample/Carbon in feed)] x 100

Notes**
0 Coarse Solids, settled in about 20 minutes
1 Coarse solids, first rinse
2 Coarse solids, second rinse

3 Coarse solids, third rinse
4 Fine solids settled from decanted liquids
5 Fine solids settled from decanted liquids after 60 hours
6 Course liquids, less than 10 minutes' settling time
7 Decanted liquids foamed in column at 0.1 cm/sec for 18 minutes, settled solids from column bottom sampled
8 Decanted liquids settled in sep-funnel, settled solids from bottom of funnel sampled
9 Decanted liquids foamed in column, liquid fed to column through foam (stripping mode), collapsed foam flocculated with CaC12, dried floc sampled
10 Column liquid (note 9) flocculated with CaC12, dried floc sampled
11 Coarse liquids, fourth rinse
12 Wash liquid and first rinse flocculated with CaC12, dried floc sampled
13 Dried bulk sample, coarse solids
14 Decanted liquids and -325 mesh solids foamed in column at 0.042 cm/sec for 25 minutes, collapsed foam sampled
21 Solids from column bottom (note 20)
22 -325 mesh solids still suspended after 24 hours
23 -325 mesh solids settled in about 24 hours
24 Coarse solids, 50% pulp density
25 Coarse solids, 1.5% pulp density

Results

The most promising chemicals used in this initial study showed about a 75% reduction in petroleum carbon content in the coarse fraction. This reduction was attributed to attrition scrubbing and demonstrates that this treatment can effectively remove such contaminants from the coarse fraction. Following the attrition scrubbing treatment, the fine fraction of the contaminated materials was used to conduct column flotation tests. The preliminary results showed that the flotation process separated hydrocarbons from the very fine soil fraction under conditions that are far from optimum. The best results showed that the carbon content of the fine size fraction was about 26% lower than that of the contaminated soil. The froth collected from the column contained 54% more carbon than the column feed. Optimization of the equipment and the chemistry of the collection and frothing system should enhance these results significantly.

It is important to assess the mass balance and the carbon balance of each experiment to provide an indication of whether or not the test is successful. In the Tide washing tests, 8.2 g of cleaned soil was typically recovered from 15 g of contaminated feed. The 15 g of contaminated soil feed contained about 2.1 g of hydrocarbon and 12.9 g of soil. In the most successful tests, the carbon content of the cleaned fraction was about 80% lower than that of the feed material (i.e., 24 mg/g to 125 mg/g). The cleaned fraction was composed of the coarser solids that settled out of the wash liquid within about 20 minutes. About half of this fraction was +325 mesh and about half was -325 mesh. Both portions were cleaned nearly equally well. Cleaning of this fraction was accomplished in the scrubber and in the settling basin. About 4.7 g of very fine soil was suspended in the wash water by the Tide. Then $CaCl_2$ was added to the wash liquid and the resulting floc was dried. About 6.2 g of flocculated material was recovered. Considering that 3.0 g of Tide and 2.0 g of $CaCl_2$ were added to the 12.9 g of soil in the feed, recovery was expected

to be about 17.9 g of solids, including 8.2 g of coarse fraction, 6.2 g of dried floc, and 2.15 g of dissolved solids, or 16.55 g of material. The data show very good mass and carbon balances, providing an indication that the technique is acceptable.

Mass balance: 16.55/17.4 = 95.1%

In:	Soil	12.9g
	Tide	2.5g
	$CaCl_2$	2.0g
	Total	**17.4g**
Out:	Course solids	8.2g
	Dried Floc	6.2g
	Dissolved Solids	2.15g
	Total	**16.55g**

Carbon Balance: 2255.0/2295.0 = 98.3%

In:	15 grams soil (124.1 mg/g)	1861.5mg
	3.0 grams of Tide	433.5mg
	Total	**2295.0mg**
Out:	Coarse Solids	226.0mg
	Fine Solids	1318.5mg
	Dissolved Solids	115.5mg
	Floated Oil	595.0mg
	Total	**2255.0mg**

Conclusions for the Scrubbing and Flotation Tests

1. Turbulence in the liquid pool is very difficult to avoid, even with very low flow rates (superficial velocities). Finch and Dobby (1990) related turbulence to the ratio of sparger area to column cross section area, noting that the sparger area should be at least two times the column cross section area of the column. Ratios of about 0.5 were used in the tests to date. The results of tests using two Mott spargers to improve this ratio were compromised by a leak in one of the spargers.

2. The use of Tide or similar surfactant as a collector/frother works better in the scrubber than the numbers in the tables indicate. The uncontaminated, untreated blanks are equivalent to an 83% reduction in carbon. An 83% reduction in the carbon in the contaminated soil may represent nearly 100% removal of the hydrocarbons. At the least,

correction for inorganic carbon would show an improvement in scrubber efficiency. The organic carbon in the soil prior to contamination may or may not be affected by the Tide. At any rate, an 83% reduction in carbon for the sample would return it to the baseline level. Several scrubber tests show carbon reductions near this level, indicating that the Tide is effective for the larger particles. Since Tide contains about 15% carbon, a 3 g dose adds about 0.45 g carbon to the system. Therefore, 1 gram of Tide removes about 4 g of carbon in the form of the organic contaminant. On a carbon/carbon basis, about 25% of the contaminant mass must be supplied as carbon in Tide to clean the soil.

3. Only one of the tests showed a significant decrease of carbon in the -325 mesh suspended soils. In this test, the column was run in the stripping mode, resulting in a 58% reduction of carbon. This result seems to indicate that hydrocarbon removal by the flotation column will work. All tests show a higher carbon content for the collapsed foam, indicating that the carbon is concentrated by flotation.

4. Mass and carbon balances close well enough to indicate that experimental methods and results were acceptable. More information regarding the distribution of hydrocarbon contaminant and organic material from Tide with regard to particle size will be useful.

Activity V. Characterization of Mercury Contaminated Materials

The use of Haz-Flote to remove mercury from contaminated materials was evaluated. Mercury contaminated soils were sampled from sites associated with manometer locations along oil and gas pipelines in northeastern Canada. The samples have been characterized for total RCRA metals (Table 5). The analysis shows that the samples contain high levels of mercury and elevated levels of lead.

Table 5. Total Concentrations of RCRA Metals Found in the Mercury Contaminated Soil

Element	Total Concentration (mg/kg)
arsenic	2.26
barium	61.5
cadmium	1.89
chromium	50
lead	132
mercury	52.4
selenium	<0.1
silver	0.68

The levels of mercury associated with the various size fractions of materials have been determined (Table 6). As expected, the -200 mesh material contains about 86% of the mercury contaminant on a wet-sieve basis and about 76% on a dry-sieve basis. This difference is expected, as a wet-sieve analysis would separate fine particles that are attached to the coarse fraction, while the coarse fraction associated with the dry-sieve analysis would contain a portion of the fine size fraction attached.

Table 6. Total Concentrations of Mercury in the Contaminated Soil by Particle Size Fraction Using Dry-Sieve and Wet-Sieve Separation Techniques

Sieve Size	Dry Sieve Hg (mg/kg)	Wet Sieve Hg (mg/kg)	Dry Sieve Wt - g (g)	Wet Sieve Wt of Soil (g)	Tot-Hg dry (mg)	Tot-Hg wet (mg)
10 Mesh	14	10	49.7	35.4	0.6958	0.354
20 Mesh	14	8.2	139.2	128.5	1.9488	1.0537
70 Mesh	23	9.8	546.7	450	12.5741	4.41
200 Mesh	47	8.8	335.5	273.9	15.7685	2.41032
325 Mesh	200	80	60.4	29.3	12.08	2.344
400 Mesh	220	110	15.6	6.3	3.432	0.693
-400 Mesh	220	250	73.3	128.9	16.126	32.225

Activity VI. Health and Safety Plan

Prior to the initiation of the work plan for the Haz-Flote evaluations, a complete health and safety plan was developed. Implementation of this plan was initiated.

Activity VII. Haz-Flote Tests for Soils Contaminated with Mercury

Scrubber Tests

The objective of these tests was to find a reagent or reagent combination capable of separating mercury contamination from a fine soil and dissolving the contaminant in the liquid phase where it is amenable to flotation. After suitable reagents were identified, further testing was conducted to reduce reagent consumption in the scrubber while maintaining or increasing mercury removal efficiency.

Procedures

For a typical test, a sample of contaminated soil was mixed with water and the test reagents. After mixing, the pulp was centrifuged and the liquid was decanted from the surface of the settled solids. The solids were then rinsed by mixing with clean water and centrifuged again. Solids and liquids from the test were analyzed to determine mercury concentrations. Quadruplicate analyses were conducted on the solids samples and the results were averaged to provide a single value for each sample. All solids analyses were converted to a dry basis for comparison with the feed values. A mercury balance was calculated for each test to verify the analytical results.

Test variables included the mixer, pulp density (weight of the feed/weight of the pulp), pH, reagents and reagent dosages, temperature, residence time, multiple stage washing, and rinse water volume. A soil sample collected from manometer sites along a gas pipeline was used for the testing. The only preparation for this material was sieving to -70 mesh. The characteristics of this soil sample are shown in Tables 5 and 6. Total organic carbon for the sample was 1.86 wt%, corresponding to 3.5 to 4.2% soil organic matter.

Samples were analyzed using the flameless atomic adsorption technique developed by Hatch and Ott (1968). A BUCK model 400 Mercury Analyzer System which measures adsorption at 253.7 nm was used for the mercury analyses. Solids samples were digested following the method detailed in Methods of Soil Analysis (Page, 1982). Liquid samples were digested in accordance with a WRI standard operating procedure. Solid samples were divided into eight subsamples. Of these, four were used for mercury determination and four were dried to determine the moisture content of the sample.

Results

The results of the tests in terms of mercury removal are summarized in Table 7. The reduction in mercury content was calculated by subtracting the mercury content of the cleaned soil from that of the feed material and dividing by the mercury content of the feed. This result was multiplied by 100 to give percentage mercury reduction. The results of four samples were averaged. Entries of OR indicate samples that were out of range for the analyzer. Entries of NA indicate the first stage of a two-stage test in which the sample was scrubbed with partially spent reagent from a previous test.

Table 7. Summary of Scrubber Tests

TESTS WITH NaOCl SOLUTION

Test #	Reagent ml	Reagent ml/g	Treatment	Efficiency %	Amt/Reag. gal/ton	Cost $/ton
1-C	120	4.69	shake 10 min, amb temp, closed bottle	93.2	1123.6	337
1-1	120	5.04	shake 90 min, amb temp, closed bottle	85.6	1208.6	363
1-2	60	2.32	shake 90 min, amb temp, closed bottle	90.5	555.3	167
1-3	120	5.11	shake 10 min, amb temp, open bottle	85.5	1224.0	367
1-4	120	4.98	shake 90 min, amb temp, open bottle	84.4	1193.5	358
1-5	60	2.62	shake 90 min, amb temp, open bottle	93.6	628.0	188
2-C	120	4.49	shake 10 min, amb temp, closed bottle	93.9	1077.3	323
2-1	60	2.20	shake 10 min, amb temp, closed bottle	90.5	526.8	158
2-2	120	5.31	shake 10 min, 35 C, closed bottle	96.8	1272.7	382
2-3	60	2.06	shake 10 min, 35 C, closed bottle	93.0	494.2	148
2-4	120	4.41	shake 10 min, 50 C, closed bottle	OR	1057.5	317
2-5	60	2.45	shake 10 min, 50 C, closed bottle	97.1	587.0	176
3-1	60	1.65	shake 10 min, amb temp, water rinse	84.0	395.1	119
3-2	110	3.67	second wash of sample # 3-1, water rinse	94.6	878.9	264
3-3	150	6.25	third wash of sample # 3-1, CaCl2 rinse	95.9	1498.1	449
3-4	40	0.89	shake 10 min, amb temp, water rinse	83.4	212.6	64
3-5	73.3	1.88	second wash of sample # 3-4, water rinse	94.7	450.5	135
3-6	100	3.03	third wash of sample # 3-4, CaCl2 rinse	96.9	726.4	218
4-1	60	2.30	2.87% NaOCl, 10 min, 50C, CaCl2 rinse	92.1	551.0	165
4-2	30	1.36	1.44% NaOCl, 10 min, 50C, CaCl2 rinse	90.0	326.9	98
4-3	15	0.57	0.72% NaOCl, 10 min, 50C, CaCl2 rinse	84.1	137.2	41
4-4	60	2.40	5.75% NaOCl, 10 min, 50C, CaCl2 rinse	97.7	575.3	173
4-5	30	1.34	5.75% NaOCl, 10 min, 50C, CaCl2 rinse	97.0	321.0	96
4-6	15	0.54	5.75% NaOCl, 10 min, 50C, CaCl2 rinse	89.0	128.4	39
7-C	120	4.38	shake 10 min, amb temp, closed bottle	94.7	1049.8	315
7-1	15	0.72	5.75% NaOCl, 10 min, 50C, CaCl2 rinse	OR	173.7	52
7-2	15	0.66	as above with cap off bottle (aeration)	OR	158.4	48
7-3	30	1.31	two washes with 15 ml, no rinse between	93.9	314.0	94
7-4	30	1.12	two washes with 15 ml, rinse between	93.1	267.3	80
7-5	30	1.18	one wash with 30 ml	93.3	282.0	85

TESTS WITH Ca(OCl)2

Test #	Reagent grams	Reagent g/g	Treatment	Efficiency %	Amt/ Reag. lb/ton	Cost $/ton
5-C			5.75% NaOCl, 10 min, amb, CaCl2 rinse	94.5		
5-1	6	0.26	oxid added dry, H2O act., CaCl2 rinse	87.8	518.4	492.4
5-2	6	0.26	oxid added dry, 5%HCl act., CaCl2 rinse	97.7	519.0	493.1
5-3	6	0.22	oxid added dry, 10% HCl act., CaCl2 rinse	92.8	444.0	421.8
5-4	6	0.23	oxid added dry, 25% HCl act., CaCl2 rinse	95.9	457.1	434.3
5-5	6	0.22	oxid added dry, 50% HCl act., CaCl2 rinse	95.7	432.0	410.4

6-C			5.75% NaOCl, 10 min, amb, CaCl2 rinse	94		
6-1	5.88	0.25	oxid added dry, 5%HCl act., CaCl2 rinse	97.1	492.3	467.6
6-2	6.04	0.23	oxid added dry, H2O act. 50C, CaCl2 rinse	96.3	455.7	432.9
6-3	2.97	0.12	oxid added dry, H2O act. 50C, CaCl2 rinse	91.9	233.5	221.8
6-4	3.05	0.14	oxid added dry, 5%HCl act., CaCl2 rinse	97.9	274.7	260.9
8-C	3.1	0.12	oxid added dry, 5%HCl act., 30 min, H2O	95.2	237.8	225.9
8-1	2.12	0.07	oxid added dry, 5%HCl act., 30 min, H2O	95.2	148.9	141.5
8-2	0.99	0.04	oxid added dry, 5%HCl act., 30 min, H2O	95.3	77.9	74.0
8-3	0.55	0.02	oxid added dry, H2O, 50C act., 30 min	OR	39.2	37.2
8-4	0.89	0.03	oxid added dry, 10%HCl act., 30 min, H2O	95.8	66.7	63.4
8-5	0.96	0.03	oxid added dry, 5% HCl 50C act., 30 min	92.8	68.8	65.4
9-C	1.13	0.04	oxid added dry, 5%HCl act., 30 min, H2O	94.6	83.6	79.5
9-1	1.01	0.04	oxid added dry, 5%HNO3 act., 30 min, H2O	95.4	77.3	73.4
9-2	1.14	0.04	oxid added dry, 5%HCl act., 10 min, H2O	91.8	83.5	79.4
9-3	0.51	0.02	oxid added dry, 5%HCl act., 30 min, H2O	OR	37.0	35.2
9-4	0.54	0.02	oxid added dry, H2O, 50C act, 30 min, H2O	OR	40.1	38.1
9-5	0.5	0.02	oxid added dry, 5%HNO3 act., 30 min, H2O	92.1	41.6	39.5
10-1	0.77	0.034	oxid added dry, 5%HCl act., 30 min, H2O	93.0	67.5	64.1
10-2	0.74	0.032	oxid added dry, 5%HNO3 act., 30 min, H2O	89.7	63.4	60.2
10-3	0.74	0.030	oxid added dry, 10%HCl act., 30 min, H2O	92.0	59.4	56.5
10-4	0.49	0.019	oxid added dry, 5%HCl act., 30 min, H2O	93.9	38.1	36.2
10-5	0.49	0.019	oxid added dry, 5%HNO3 act., 30 min, H2O	96.1	38.0	36.1
10-6	0.56	0.023	oxid added dry, 10%HCl act., 30 min, H2O	94.6	45.4	43.1
11-1	0.75	0.031	5% HCl, 30 min pretreat, + oxid, 30 min	93.9	61.0	58.0
11-2	0.75	0.030	5% HNO3, 30 min pretreat, + oxid, 30 min	93.0	59.8	56.8
11-3	0.75	0.029	10% HCl, 30 min pretreat, + oxid, 30 min	96.1	57.1	54.3
11-4	0.5	0.020	5% HCl, 30 min pretreat, + oxid, 30 min	90.2	39.1	37.2
11-5	0.5	0.018	5% HNO3, 30 min pretreat, + oxid, 30 min	90.7	36.7	34.9
11-6	0.5	0.020	10% HCl, 30 min pretreat, + oxid, 30 min	93.9	39.9	37.9
12-1	0.81	0.023	oxid added dry, 5%HCl act., 30 min, H2O	92.1	46.7	44.4
12-2	0.82	0.032	oxid added dry, 5%HNO3 act., 30 min, H2O	95.0	64.8	61.5
12-3	0.81	0.032	oxid added dry, 10%HCl act., 30 min, H2O	96.1	64.3	61.1
12-4	0.55	0.022	oxid added dry, 5%HCl act., 30 min, H2O	93.4	44.3	42.1
12-5	0.52	0.022	oxid added dry, 5%HNO3 act., 30 min, H2O	93.1	44.2	42.0
12-6	0.59	0.026	oxid added dry, 10%HCl act., 30 min, H2O	94.1	51.3	48.8
13-C	0.68	0.027	oxid added dry, 120ml 5%HCl	94.6	53.0	50.4
13-1	0.61	0.022	oxid added dry, 60ml 5%HCl	86.8	44.7	42.5
13-2	0.61	0.023	oxid added dry, 30ml 5%HCl	83.3	46.8	44.5
13-3	0.4	0.016	oxid added dry, 60ml 5%HCl	92.1	31.7	30.2
13-4	0.44	0.020	oxid added dry, 30ml 5%HCl	82.0	39.4	37.5
13-5	0.43	0.019	oxid added dry, 30ml 10%HCl	83.7	37.3	35.5

14-1	1.44	0.030	oxid added dry, 5%HCl	94.3	60.4	57.4
14-2	0.71	0.056	test 1 solids, second wash, oxid +HCl	>98.2	112.0	106.4
14-3	1.05	0.021	oxid added dry, 5%HCl	90.0	42.5	40.4
14-4	0.54	0.037	test 3 solids, second wash, oxid +HCl	97.9	74.0	70.3
14-5	0.77	0.030	oxid added dry, 5%HCl	94.3	60.9	57.8
14-6	0.24	0.009	washed with liquid from test 5 + fresh oxid	72.0	18.3	17.4
15-1	1.51	0.031	oxid added dry, 5%HCl	92.7	62.9	59.8
15-2	0.74	0.057	test 1 solids, second wash, oxid +HCl	98.6	114.0	108.3
15-3	1.01	0.021	oxid added dry, 5%HCl	93.5	42.1	40.0
15-4	0.47	0.036	test 3 solids, second wash, oxid +HCl	98.1	72.0	68.4
15-5	0.7	0.033	oxid added dry, 5%HCl	97.4	66.4	63.1
15-6	0.18	0.007	washed with liquid from test 5 + fresh oxid	73.3	15.0	14.2
16-1	2.8	0.058	two washes and rinses, fresh reagent	98.6	116.7	110.9
16-2	NA		washed with reagent from test 1 wash 2	77.6	NA	NA
16-3	0.69	0.023	second wash of test 2 solids+ fresh reagent	98.1	46.9	44.6
16-4	0.67	0.028	reagent from test 3 + fresh added	97.1	56.5	53.7
17-1	2	0.041	two washes and rinses, fresh reagent	98.8	82.5	78.3
17-2	NA		washed with reagent from test 1 wash 2	81.4	NA	NA
17-3	0.49	0.018	second wash of test 2 solids+ fresh reagent	97.0	35.5	33.7
17-4	0.49	0.020	reagent from test 3 + fresh added	96.0	40.1	38.1
18-1	1.46	0.061	two washes w/ fresh reagent, multiple rinse	99.2	121.3	115.2
18-2	0.75	0.030	three wash and rinse, small doses, fresh re	98.5	59.9	56.9
18-3	1.01	0.040	two wash and rinse, fresh reagent, 10 min.	98.6	79.7	75.8
18-4	1.00	0.042	two wash and rinse, fresh reagent, 30 min.	99.0	84.1	79.9
18-5	0.76	0.030	single wash and rinse, 60 min.	96.7	60.9	57.8

Flotation Tests

The objective of these tests was to verify that flotation can be used to rapidly separate the dissolved mercury from the scrubber solution. Further testing will be conducted to optimize the flotation step.

Procedures

The flotation tests were conducted using an adsorbing colloid flotation method described by Huang and Wilson (1976). Cupric sulfide was used as the adsorbing colloid with hexadecyltrimethylammonium bromide (HTA) as the collector. The method was reported to remove mercury from aqueous solution leaving residual mercury levels as low as 5 ppb. Also, the method was reported to be insensitive to pH variation through a range of 0.8 to 8.0.

For a typical test, $CuBr_2$ was added to the solution to bring Cu (II) concentration to 100 ppm. Na_2S was added to provide sulfide ion to coprecipitate the copper and mercury. The collector (HTA) was added to a strength of 40 ppm. The mixture was allowed to stand for 10 minutes, then the solution and floc were poured into the column and foamed for 30 minutes.

Samples were collected, and 10 ppm HTA was added, at 6-min. intervals. The samples were subsequently analyzed to determine mercury content.

Flotation tests were conducted in a glass column of 2.54 cm i.d. and 39 cm in height. A medium-porosity stainless steel frit was used as a gas sparger. A valve was provided at the bottom of the column through which samples were removed and additional collector was injected as the tests proceded. Nitrogen gas was used to generate the foam in the column. The gas flow was measured and controlled with a mass flow controller before it passed through a saturator and into the column. The HTA was from Eastman Kodak Company, and other reagents were from J.T. Baker. All of the reagents were used as they came from the bottle with no special purification. The HTA was dissolved in ethanol then diluted with water to provide a 0.2% working solution.

Initial flotation tests were conducted on a stock solution of mercuric chloride in water. In these tests the flotation removed the mercury efficiently. However, when the method was applied to a solution containing the scrubber reagents and mercuric chloride, separation was very poor. It was determined that the scrubber solution was oxidizing the sulfide ion to sulfate ion. The soluble sulfates did not precipitate, and recovery was limited by the availability of sulfide ion. This problem was overcome either by allowing the scrubber solution to age, providing time for the oxidant to disproportionate, or by adding an excess of sulfide. Once the problem of oxidizing the sulfide ion was resolved, flotation tests were conducted using the actual scrubber solution. Tests were also conducted in which the precipitate was allowed to settle for several days. Ten minutes of flotation proved to be as effective as settling for 48 hours. Both methods removed about 99.5% of the mercury from the scrubber solution.

Results

The results of the flotation/precipitation tests in terms of mercury removal are summarized in Table 8. The reduction in mercury content was calculated by subtracting the mercury content of the liquid after foaming from that of the column feed and dividing by the mercury content of the feed. This result was multiplied by 100 to give percentage mercury reduction.

Table 8. Effect of Precipitation/Flotation on Mercury Concentration in the Scrubber Solution

		Hg Concentration		Efficiency
Sample	Treatment	Initial	Final	%
Simulated scrubber solution	10 min flotation	16.69	0.025	99.8
Scrubber solution test 72-1	10 min flotation	11.88	0.059	99.5
Scrubber solution test 72-2	precipitation	8.64	0.042	99.5
Scrubber solution test 72-3	precipitation	9.4	0.043	99.5

REFERENCES

Finch, J.A., and G.S. Dobby, 1990, *Column Flotation.* Pergamon Press, Toronto, Canada.

Hatch, W. R., and W. L. Ott, 1968, Determination of submicrogram quantities of mercury by atomic adsorption spectrophotometry. Anal Chem. 40: 2085-2087.

Huang, S., and D. J. Wilson, 1976, Foam separation of mercury(II) and cadmium(II) from aqueous systems. *Sep. Sci.* 11(3):215-222.

Kim, Y. S., and H. Zeitlin, 1971, A rapid adsorbing colloid flotation method for the separation of molybdenum from seawater. *Sep. Sci.* 6(4):505-513.

Miller, M. W., and G. L. Sullivan, 1971, Foam fractionation of mercury(II) nitro complexes. *Sep. Sci.* 6(4):553-558.

Okamoto, Y., and E.J. Chou, 1975, Foam separation of mercury ion with chelating surfactant: The selectivity of the removal of cadmium and mercury ions with 4-Dodecyldiethylenetriamine. *Sep. Sci.* 10(6):741-753.

Page, A. L., R.H. Miller, and D.R. Keeney, 1982, Methods of soil analysis Part 2. American Society of Agronomy, Inc. 367-384.

Voyce, D., and H. Zeitlin, 1974, The separation of mercury from sea water by adsorption colloid flotation and analysis by flameless atomic absorption. *Anal. Chimica Acta.* 69:27-34.

WRI-98-R014

WESTERN RESEARCH INSTITUTE
"Providing solutions to energy and environmental problems"

FINAL REPORT

IN-SITU AMELIORATION OF ACID MINE DRAINAGE PROBLEMS

Prepared for
U.S. Department of Energy
Morgantown, West Virginia

May 1998

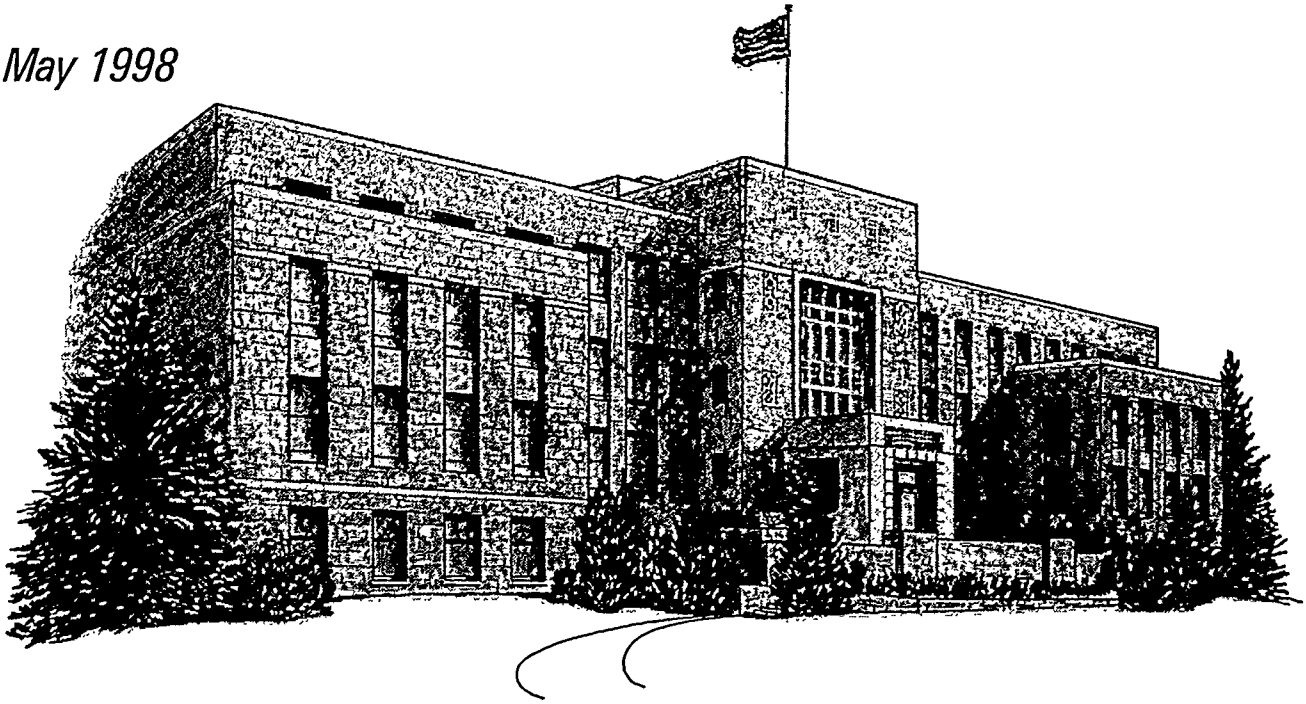

WRI-98-R014

IN-SITU AMELIORATION OF ACID MINE DRAINAGE PROBLEMS

Final Report

May 1998

By Terry H. Brown

Work Performed Under Cooperative Agreement
DE-FC21-93MC30126 Subtask 3.4

For
U.S. Department of Energy
Office of Fossil Energy
Federal Energy Technology Center
Morgantown, West Virginia

By
Western Research Institute
Laramie, Wyoming

DISCLAIMER

TABLE OF CONTENTS

LIST OF TABLES AND FIGURES

EXECUTIVE SUMMARY

The development of technologies to ameliorate acid mine drainage has had few successes. Most often, once acid mine drainage exists, the company responsible develops treatment programs to make sure that land and water resources are not contaminated. These treatments usually result in significant costs and do not cure the problem.

Much effort and money have been spent on the problems associated with acid mine drainage. However, it appears that most approaches (e.g. water treatment) have addressed the consequences of acid formation, not its prevention. Most of the work associated with the prevention of acid formation has dealt with the prevention of oxidation. Such work has included using water flooding and/or grouting to seal mines, removing oxygen from the system or preventing water flow into the mines, using bactericides to eliminate the catalytic effect of *Thiobacillus ferrooxidans*, and modifying the mining methods.

This research was initiated to closely evaluate the impact of oxidizing solutions on pyrite oxidation. The study includes: (1) characterization of overburden materials collected in east Texas that contain large quantities of potential acidity, (2) preliminary evaluations of the acid-generating capabilities of materials containing high levels of potential acidity (pyritic materials) using humidity cells, and (3) determining the effect of hydrogen peroxide, nitric acid, oxygenated water, and sodium hypochlorite on spoil materials that contain high levels of potential acidity.

The overburden material collected from an east Texas mine was thoroughly characterized for potential acidity (including S forms), neutralization potential, acidity, electrical conductivity (EC), and pH. Testing to determine the long-term acid-generating capability of the Texas overburden material was conducted for 336 days using simulated weathering containers (3 days of water-saturated air followed by 3 days of dry air).

The data indicate a reduction in pH to 2.46 after about 70 days. From 70 days to 336 days the pH fluctuated between 2.6 and 3.14. A similar relationship was found for the EC values. The EC values increased from 3.88 to about 9.16 as a result of the acceleration of the acid-forming reactions. From day 7 to day 154, the EC values of the system decreased substantially. The reduction in EC values was caused by the use of leaching as part of the weekly operation of the humidity cell, removing the reaction products from the system. Also, the kinetics of the acid-forming reactions may be slowing as a result of the chemistry of the system or the reduction of potential acidity.

Spoil materials containing high levels of potential acidity were subjected to hydrogen peroxide and sodium hypochlorite in a circulating flow-through system that simulated flow in an underground mine. This treatment was followed by phosphate and silicic acid treatments to determine whether precipitates could be formed on the surfaces of actively oxidizing pyrite.

Both hydrogen peroxide and sodium hypochlorite were very effective in promoting the oxidation of the pyritic material. Visual evidence indicated that sodium hypochlorite was initially more effective than hydrogen peroxide; however, with time the effectiveness of the two compounds seemed comparable. The pyritic material continued to form acid throughout the testing period, which indicates that the removal of the potential acidity may require considerable treatment time.

The phosphate treatment resulted in the precipitation of aluminum compounds and an increase in pH to about 3.0 for the sodium hypochlorite treated materials and to about 3.5 for the hydrogen peroxide treated materials. The silicic acid treatment did not influence the pH values of either treatment.

Spoil materials containing high levels of pyrite were subjected to hydrogen peroxide, nitric acid, oxygenated water, and sodium hypochlorite in a flow-through column system to evaluate the removal of potential acidity. The data indicate good removal rates for hydrogen peroxide and relatively concentrated nitric acid.

Continuation of this research project will be dependent on future funding from the DOE Cooperative Agreement (Base and JSR) Programs.

INTRODUCTION

Problem and Significance

Millions of acres of land are affected by acid mine drainage problems, and estimates for the costs of treating acid mine drainage from active mine sites are in the hundreds of millions of dollars annually. Dr. Paul Ziemkiewicz, the director of the National Mine Land Reclamation Center, has indicated that the coal industry in West Virginia alone spends roughly $1 million per day treating acid mine drainage. The total cost is substantially higher since it is often necessary to treat acid mine drainage from mines and refuse piles for decades following coal extraction and cleanup. A major part of the cleanup of abandoned mine sites is also associated with acid mine drainage problems. It is estimated that the cleanup of the half-million abandoned mine sites thought to exist could cost up to $71 billion. It is obvious that the problem is becoming more significant each day. Over the past five decades volumes of information on the environmental and socioeconomic impacts of acid mine drainage have been gathered. Much research has been done. However, the fact is that most of the technologies developed have not greatly reduced the acid mine drainage problem. New ideas and approaches to ameliorate the problem are needed.

Background

A considerable amount of research has been done on acid mine drainage issues over the past fifty years. Much of the work has focused on the mechanisms responsible for the formation of the acid waters and the treatment of acid waters discharging from reaction sites. These are still the topics of major research programs. Considerable effort is also being expended to find ways to prevent acid mine drainage from developing. Such procedures as mixing fly ash from power plants and kilns with spoil that contains significant amounts of potential acidity have been used successfully to prevent the generation of acid.

Most of work associated with the amelioration of acid mine drainage problems has dealt with the prevention of oxidation by sealing mines and using bactericides to eliminate the catalytic effect of *Thiobacillus ferrooxidans*. In addition, lime products and other materials, such as apatite, that react with the reaction products of the acid generation have also been used with some success to neutralize acidity. However, the fact is that most of the technologies developed have not greatly reduced the acid mine drainage problem.

The Formation of Acid Mine Drainage

Acid mine drainages typically have pH values below 2.3, acidities near 5000 mg/L, and anionic concentrations (mostly sulfate) exceeding 10,000 mg/L (Caruccio et al., 1981). Iron disulfides in the form of pyrite and marcasite are the predominate contributors to the production of acid mine drainage. The following reactions occur during the oxidation of the disulfides as described by Stumm and Morgan (1970):

$$FeS_2(s) + 7/2\,O_2 + H_2O \Rightarrow Fe^{2+} + 2SO_4^{2-} + 2H^+ \quad (1)$$

$$Fe^{2+} + 1/4O_2 + H^+ \Rightarrow Fe^{3+} + 1/2\,H_2O \quad (2)$$

$$Fe^{3+} + 3H_2O \Rightarrow Fe(OH)_3(s) + 3H^+ \quad (3)$$

$$FeS_2(s) + 14Fe^{3+} + 8H_2O \Rightarrow 15Fe^{2+} + 2SO_4^{2-} + 16H^+ \quad (4)$$

The stoichiometry of equation 1 shows that for every mole of pyrite oxidized to Fe^{2+}, there are two moles of acidity generated as H^+. Subsequently, the Fe^{2+} is oxidized to Fe^{3+} via reaction 2. This reaction proceeds quite slowly. In fact, Stumm and Morgan (1970) observed half-times for Fe^{2+} oxidation on the order of 1000 days. Once the Fe^{3+} is formed, it combines with H_2O to form insoluble $Fe(OH)_3$ as shown in equation 3. Therefore, the dissolution of each mole of pyrite results in the release of four equivalents of acidity. As the Fe^{3+} concentrations increase with increased acidity, the Fe^{3+} becomes important as an oxidizing agent.

Several research efforts have shown that pyrite is rapidly oxidized by Fe^{3+} in the absence of oxygen and at low pH values (Garrels and Thompson, 1960; Smith et al., 1968). This reaction is shown above as equation 4. Fe^{3+} becomes the only important oxidizing agent when pH values are 3 or below (Singer and Stumm, 1969). These researchers also found that the presence of O_2 did not influence the kinetics of the reaction. Since pyrite can reduce Fe^{3+} to Fe^{2+} faster than Fe^{2+} can be regenerated into Fe^{3+} by O_2, the pyrite will reduce all the Fe^{3+} and the reaction will stop. Thus the Fe^{2+} to Fe^{3+} oxidation is considered to be the rate-limiting step in the production of acid. A major catalyst of this reaction is the bacteria *Thiobacillus ferrooxidans,* which is known to increase the Fe^{2+} oxidation rate by six orders of magnitude (Singer and Stumm, 1970; Nordstrom, 1976). This reaction makes Fe^{3+} readily available for pyrite oxidation.

The amount of acid generated from pyritic materials can be reduced or eliminated by inhibition of the iron-oxidizing bacteria and the reduction in the solubility of Fe^{2+} and Fe^{3+}, with increased pH resulting from the production of alkalinity. In fact, Caruccio (1968) showed that the amount of acidity of mine drainages in western Pennsylvania was a function of (1) the pH of the ground water, (2) the presence of calcareous materials such as $CaCO_3$ within the strata, (3) the mode of occurrence of the iron disulfides, and (4) the neutralizing capacity of the ground water. Similar results were obtained in studies for eastern Kentucky (Caruccio et al., 1976; Caruccio and Geidel, 1978; and Caruccio et al., 1977).

From this brief discussion, it is apparent that materials such as $CaCO_3$ and CaO that possess neutralization potential can be used to reduce acid mine drainage problems. In fact, many studies have shown that limestone materials were effective in neutralizing acid in acid mine drainage applications (Mihok and Chamberlain, 1968; Pearson and McDonnel, 1975; Barton and Vataatham, 1976; Geidel and Caruccio, 1982). In addition, fly ash materials that possess

neutralization potential have been used with some success as amendments to surface "soils" to ameliorate acid conditions. Thus, it is apparent that clean coal technology waste grouts with significant neutralization potential would influence the development of acid mine drainage from grouted underground mines.

Treatment of Acid Mine Drainage

Many attempts to treat the acid mine drainage problem have been made. Surface materials have been removed, and lime has been applied to the surface areas to increase the alkalinity of groundwater recharge waters, which would neutralize the acidity of the discharge water. Materials such as kiln dust and fly ash have been mixed with acid-forming materials, resulting in waters that meet discharge requirements. Cropping techniques, such as growing alfalfa in the recharge areas, have also been used to reduce the amount of recharge available to the affected aquifer. Wetland sites have been constructed to provide passive treatment systems for the cleanup of acid waters. Many of these techniques if properly implemented during a mining or reclamation operation, may result in a postmining condition that does not produce acid mine drainage, at least in the short run. However, research into the containment or elimination of acid mine drainage from sites currently producing acid has shown limited success. Attempts to eliminate the continued formation of acid have included the use of bactericides, grouting, and other techniques, such as modification of mining plans to prevent oxygen and/or water from reaching the reaction zone.

OBJECTIVE

The objective of this project is to develop an understanding of pyrite oxidation resulting from the use of chemical oxidation using compounds such as hydrogen peroxide and sodium hypochlorite.

TECHNICAL APPROACH

Task 1. Evaluation of Various Oxidation Processes in the Laboratory Using Simulated Weathering Columns and Model Leaching Pads

Activity 1.1. Laboratory Simulation and Method Development

The overburden material containing the acid-forming material was placed in flexible walled permeameters and/or rigid-walled columns and leaching pads for testing. The materials were subjected to different environmental conditions that could influence acidity and alkalinity production. The environmental conditions were created using amendments such as chemical oxidants and acids; the injection of gaseous mixtures, including oxygen; wet/dry cycles; and saturated versus unsaturated water.

Activity 1.2. Elimination of the Oxidation Process

Following periods of enhanced oxidation, amendments such as lime slurries, and phosphate solutions, were added to reduce or eliminate the production of acid. Leachates were sampled and analyzed for pH and elements such as Fe, Al, and Mn.

Task 2. Adaptation of the Process to a Simulated Field Situation

A set of columns was set up that contained acid-forming materials that were actively generating acid through the oxidation of pyritic materials. Treatments that enhanced the generation of acid and reduced the development of acid were used in various combinations. The treatments were incorporated into the system with a peristaltic pump. Appropriate analyses were made of the water exiting the columns.

RESULTS AND DISCUSSION

The work accomplished includes: (1) characterization of overburden materials collected in east Texas containing large quantities of potential acidity; (2) evaluation of the acid-generating capabilities of materials containing high levels of potential acidity (pyritic materials) using humidity cells; (3) column testing to evaluate the effect of hydrogen peroxide and sodium hypochlorite on soil materials containing high levels of potential acidity; and (4) the use of various concentrations of HNO_3 in columns to deplete levels of potential acidity.

Characterization of the Overburden Materials Used in the Study

The materials used for work under Task 1 were collected from the lignite mining area of southeastern Texas. This overburden was selected as a typical material containing high amounts of potential acidity. The origin of the material is the reduced overburden collected from the Wilcox Group. These materials usually contain pyritic materials in various morphological forms, such as framboids, polyframboids, and larger sand and silt size particles with 0.1 to 1.5 % pyritic sulfur content prior to oxidation. The materials consisted of an overburden material that had been influenced by air oxidation for a considerable period and a reduced material that had recently been extracted from the overburden formation. Chemical evaluations of acid/base potential are shown in Table 1. The oxidizing overburden had a pH of 2.8 and an acid/base potential of -30.4 tons $CaCO_3$/1000 tons of overburden material, and the reduced material had a pH of 4.1 and an acid/base potential of -58.3 tons $CaCO_3$/1000 tons of overburden material. The oxidized material contained significant salt levels (EC = 9.5) compared to the unoxidized material, which has an electrical conductivity (EC) of 2.6. This difference would be expected as a result of pyrite oxidation and the subsequent release of elements.

Table 1. Potential Acidity Evaluations of the Reduced Overburden Materials

Characteristic	Reduced Overburden (No Oxidation)	Reduced Overburden (Oxidizing)
pH	4.1	2.8
EC (mS/cm)		
Total Sulfur(%)	1.86	0.78
Total S Potential Acidity (t/1000t)	58.1	24.4
Neutralization Potential (t/1000t)	-0.19	-6.06
Total S Acid/Base Potential (t/1000t)	-58.3	-30.4
Sulfate S (%)	0.27	0.35
Pyritic S (%)	1.47	0.37
Organic S (%)	0.12	0.06
Pyritic S Potential Acidity (t/1000t)	45.9	11.6
Pyritic S Acid-Base Potential (t/1000t)	-46.1	-17.6
Acidity (meq/100g)	6.06	7.03

Long-Term Acid-Generating Capacity of Acid-Forming Overburden

The acid-generating capacity of the acid-forming materials was evaluated using a humidity cell technique. The humidity cell oxidation process was allowed to proceed for 336 days. The pH and EC data collected during this period are presented in Figures 1 and 2, respectively. The acid-forming materials used in this study had an initial pH of 3.44 and an EC of 3.88 mS/cm. As the humidity cell oxidation progressed, the pH decreased to about 2.75 after 7 days and slowly decreased to about 2.46 after 70 days. From 70 days to 336 days, the pH fluctuated between 2.6 and 3.14 (Figure 1). These data indicate that the acid-forming process is initially accelerated to a level that is dictated by the mineralogy of the system.

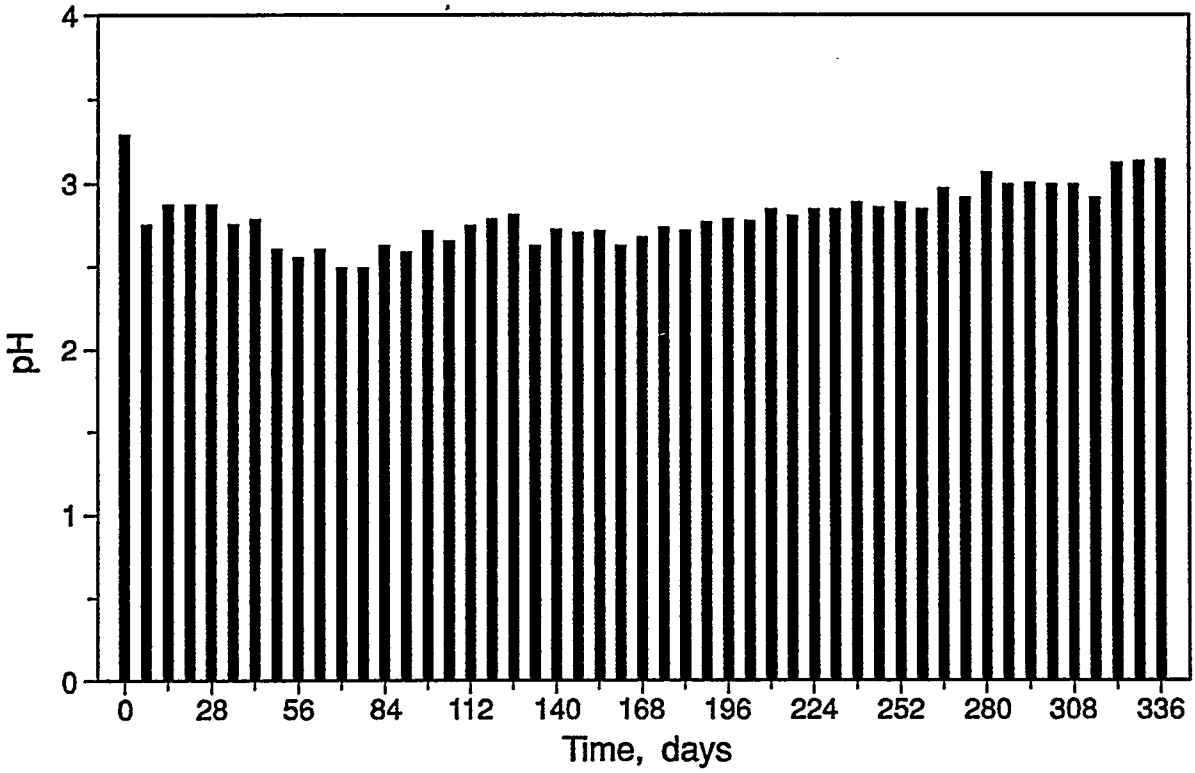

Figure 1. The Influence of Humidity Cell Treatment on the pH of the Acid-Forming Overburden with Time

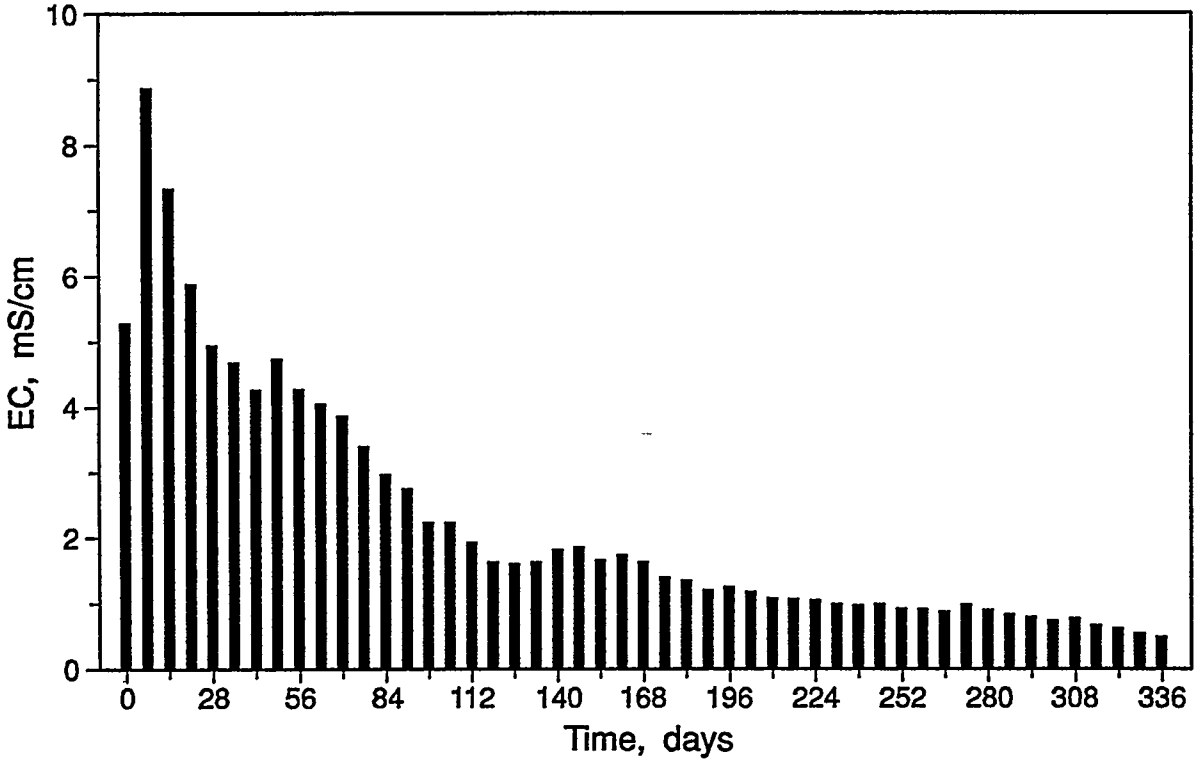

Figure 2. The Influence of Humidity Cell Treatment on the EC of the Acid-Forming Overburden with Time

The EC data shown in Figure 2 provide similar indications. The initial increase in EC from 3.88 to about 9.16 is due to the large amount of reaction products generated by the accelerated acid-forming reactions. The EC values decreased from day 7 to day 154 as the oxidation processes continued. This substantial reduction in EC values is caused by the use of leaching as part of the weekly operation of the humidity cell, resulting in the removal of reaction products from the system. In addition, the kinetics of the reactions causing the reduction of pyritic materials may be slowing.

Observations of the Pyritic Overburden Undergoing Oxidation Reactions

Initial testing was done using hydrogen peroxide and sodium hypochlorite as oxidizers and an overburden material containing large amounts of potential acidity (pyritic materials). The overburden materials were placed in rigid-walled columns and the reagents enhancing the oxidation process were poured in the top. The purpose of these tests was to qualitatively assess the nature of dispersion and encapsulation occurring in the columns. Dispersion and oxidation of the materials at the same time may remove a portion of the fine pyritic material by opening up the system, allowing the oxidizing agent easy access to the acid-forming material. In addition, after a period of time, dispersion of the fine materials may reduce the hydraulic conductivity toward the unoxidized pyritic material, preventing further generation of acid. This could result in an encapsulation due to dispersion. Also evaluated was the possibility that oxidation with the addition of appropriate elements could result in the encapsulation of overburden particles, such as indurated clays, with various mineral formations on the surface of the particles preventing oxidation of pyritic materials inside.

The hydrogen peroxide (3.15%) treatment resulted in a violent reaction and nearly immediate dispersion of the spoil material. In fact, the dispersed particles tended to fill the existing pore space reducing hydraulic conductivity significantly. As the hydrogen peroxide slowly moved through the column, the large coagulated particles (large particles made by the cohesion and adhesion of finer materials) were dispersed. Much of the pyritic material was oxidized, and the pH of the system was reduced significantly. Encapsulation of the larger particles by surface oxidation was not apparent. The larger particles dispersed prior to the formation of oxidation products that could form at the surface.

Treatments using sodium hypochlorite (5.25%) produced results similar to those of the hydrogen peroxide treatment. However, the oxidation reaction was much less violent than the hydrogen peroxide reaction. In addition, the level of dispersion was much less. In fact, many of the large coagulated particles remained intact. These particles had a formation of iron minerals at the surface, probably ferrihydrite or more likely amorphous iron precipitates. The oxidation penetrated the larger particles about 0.1 cm. It is not known if the formation of the oxidized layer would prevent penetration of the sodium hypochlorite and the further oxidation of the pyritic

materials. The oxidation of the pyritic material by sodium hypochlorite resulted in the formation of ferric oxides, which was very apparent as the system quickly became orange in color. The oxidation of the overburden using hydrogen peroxide initially turned gray, then after about 36 hours it turned orange. It seems that the initial reaction products are different.

Simulated Treatment System Using Circulating Flow

Spoil materials containing high levels of potential acidity were subjected to hydrogen peroxide and sodium hypochlorite in a circulating flow-through system that simulated the flow in an underground mine. This treatment was followed by phosphate and silicic acid treatments to determine whether precipitates could be formed on the surfaces of actively oxidizing pyrite.

Both hydrogen peroxide and sodium hypochlorite were very effective in promoting the oxidation of the pyritic material. Visual evidence indicated that sodium hypochlorite was initially more effective in oxidation than hydrogen peroxide. However, with time, both compounds seemed to be comparable. The pyritic material continued to form acid throughout the testing period. This indicates that the removal of the potential acidity may require considerable treatment time.

The phosphate treatment resulted in the precipitation of aluminum compounds and an increase in pH to about 3.0 for the sodium hypochlorite treated materials and about 3.5 for the hydrogen peroxide treated materials. The silicic acid treatment did not influence the pH values of either treatment.

Removal of Potential Acidity from Spoil Material Using Flow-Through Columns

Spoil materials containing high levels of pyrite were subjected to hydrogen peroxide, nitric acid, oxygenated water, and sodium hypochlorite in a flow-through column system to evaluate the removal of potential acidity. The data in Figure 3 show that pyrite oxidation rates for hydrogen peroxide (10%) and nitric acid (1:7 concentrated nitric acid/distilled water) were high. Rates for the oxygenated water and 0.1 N nitric acid/water were low. The combination of 0.1 N nitric acid followed by hydrogen peroxide (10%) and water resulted in low oxidation rates. The reason for this lower than expected oxidation rate is not known.

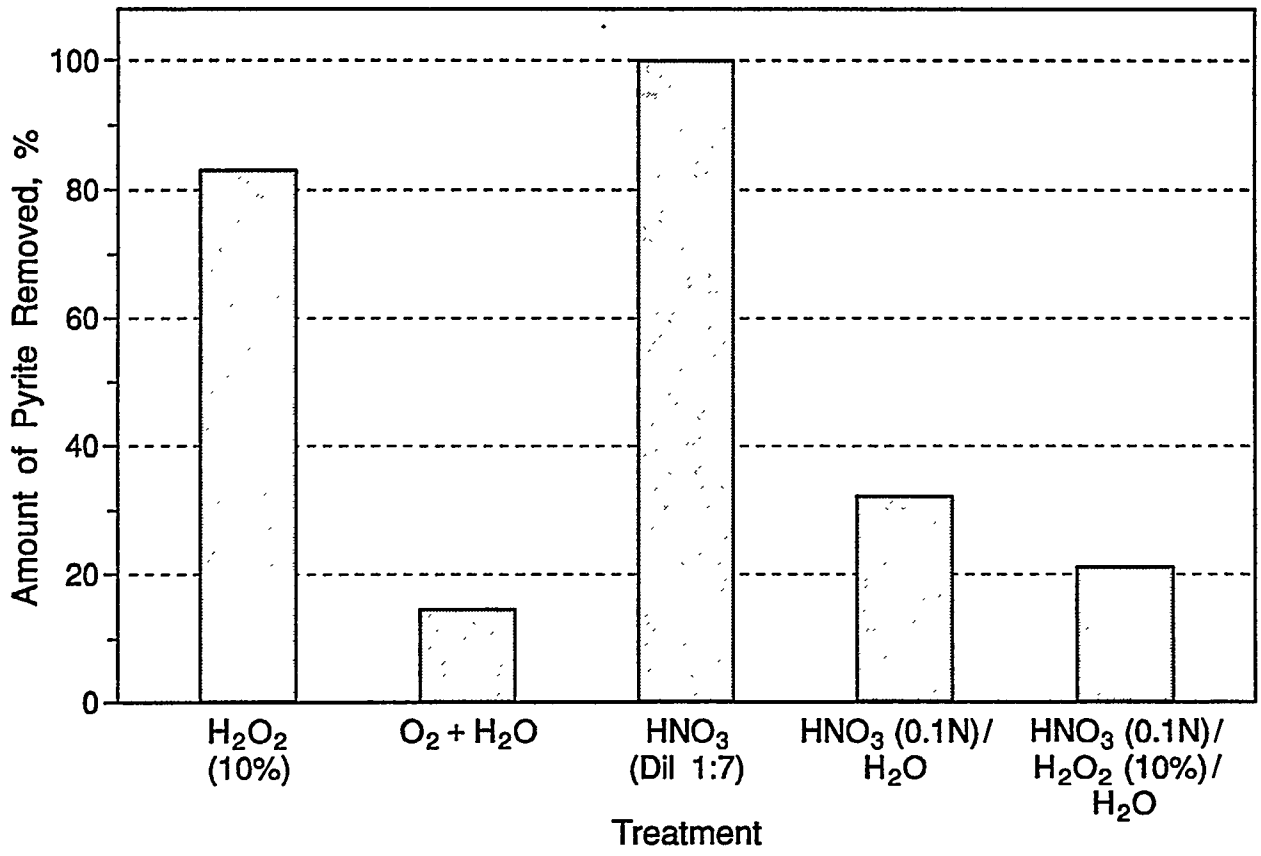

Figure 3. The Impact of Treatment on the Removal of Pyrite

CONCLUSIONS

The development of technologies to ameliorate acid mine drainage has had few successes. Most often, once acid mine drainage exists, the company responsible develops treatment programs to make sure that land and water resources are not contaminated. These treatments usually result in significant costs but do not cure the problem.

Much effort and money have been spent on the problems associated with acid mine drainage. However, most approaches (e.g. water treatment) have addressed the consequences of acid formation, not its prevention. Most of the work associated with the prevention of acid formation has dealt with the prevention of oxidation. Such work has included using water flooding and/or grouting to seal mines, removing oxygen from the system, or preventing water flow into the mines, using bactericides to eliminate the catalytic effect of *Thiobacillus ferrooxidans*, and modifying the mining methods.

This research provides some basic information relative to pyrite oxidation under differing conditions. The study includes: (1) characterization of overburden materials collected in east Texas that contain large quantities of potential acidity; (2) preliminary evaluations of the acid-

generating capabilities of materials containing high levels of potential acidity (pyritic materials) using humidity cells; and (3) determining column testing to evaluate the effect of hydrogen peroxide, nitric acid, oxygenated water, and sodium hypochlorite on spoil materials that contain high levels of potential acidity.

The overburden material collected from an east Texas mine was thoroughly characterized for potential acidity (including S forms), neutralization potential, acidity, electrical conductivity (EC), and pH. Testing to determine the long-term acid-generating capability of the Texas overburden material was conducted for 336 days using the simulated weathering containers (3 days of water-saturated air followed by 3 days of dry air).

The data indicate a reduction in pH to 2.46 after about 70 days. From 70 days to 336 days the pH fluctuated between 2.6 and 3.14. A similar pattern was found for the EC values. The EC values increased from 3.88 to about 9.16 as a result of the acceleration of the acid-forming reactions. From day 7 to day 154, the EC values of the system decreased substantially. The reduction in EC values was caused by the use of leaching as part of the weekly operation of the humidity cell, removing the reaction products from the system. Also, the kinetics of the acid-forming reactions may be slowing as a result of the chemistry of the system or the reduction of potential acidity.

Spoil materials that contain high levels of potential acidity were subjected to hydrogen peroxide and sodium hypochlorite in a circulating flow-through system that simulated flow in an underground mine. This treatment was followed by phosphate and silicic acid treatments to determine whether precipitates could be formed on the surfaces of actively oxidizing pyrite.

Both hydrogen peroxide and sodium hypochlorite were very effective in promoting the oxidation of the pyritic material. Visual evidence indicated that sodium hypochlorite was initially more effective than hydrogen peroxide; however, with time the effectiveness of the two compounds seemed comparable. The pyritic material continued to form acid throughout the testing period.

The phosphate treatment resulted in the precipitation of aluminum compounds and an increase in pH to about 3.0 for the sodium hypochlorite treated materials and to about 3.5 for the hydrogen peroxide treated materials. The silicic acid treatment did not influence the pH values of either treatment.

Spoil materials containing high levels of pyrite were subjected to hydrogen peroxide, nitric acid, oxygenated water, and sodium hypochlorite in a flow-through column system to evaluate the oxidation of pyrite. The data indicate good oxidation rates for hydrogen peroxide and relatively concentrated nitric acid.

REFERENCES

Barton, P., and T. Vatanatham. 1976. "Kinetics of Limestone Neutralization of Acid Waters." *J Env. Sci. & Tech.* 10(3):262-266.

Caruccio, F. T., G. Geidel and M. Pelletier. 1981. "Occurrence and Prediction of Acid Drainages." *Journal of the Energy Division, ASCE*, (107)167-178.

Caruccio, F. T., G. Geidel. 1978. "Geochemical Factors Affecting Coal Mine Drainage Quality." In *Reclamation of Drastically Disturbed Lands*. American Society of Agronomy, Chapter 8. pp. 129-148.

Caruccio, F. T., J. C. Horne, G. Geidel, and B. Gaganz. 1977. "Paleo Environment of Coal and its Relation to Drainage Quality." EPA Report N0. EPA-600/7-77-067. pp. 108.

Caruccio, F. T., G. Geidell, and J. M. Sewell. 1976. "The Character of Drainage as a Function of the Occurrence of Framboidal Pyrite and Ground Water Quality in Eastern Kentucky." In *Proc.* 6th Symp. Coal Mine Drainage Res., Louisville, Ky.

Caruccio, F. T. 1968. "An Evaluation of Factors Affecting Acid Mine Drainage Production and Ground Water Interactions in Selected Areas of Western Pennsylvania." In *Proc.* 2nd Symp. on Coal Mine Drainage Research. Bituminous coal Research, Monroeville, PA. pp. 107-151.

Garrels, R. M., and M. E. Thompson. 1960. "Oxidation of Pyrite in Ferric Sulfate Solution." *Am. J. Sci.* 258:57-67.

Geidel, G., and F. T. Caruccio. 1982. "Acid Drainage Response to Surface Limestone Layers." *Proc.* Symp. on Surface Mining Hydrology, Sedimentology and Reclamation. Univ. of Kentucky, Lexington, KY. pp. 403-406.

Mihok, E. A., and C. E. Chamberlain. 1968. "Factors in Neutralizing Acid Mine Waters With Limestone." *Proc.* 2nd Symp. on Coal Mine Drainage Res. Pittsburgh, PA. pp. 265-391.

Nordstrom, D. K. 1976. "Kinetic and Equilibrium Aspects of Ferrous Iron Oxidation in Acid Mine Waters." Abstract. Geol. Soc. Am. Ann. Mtg., Denver, CO.

Pearson, F. H., and A. J. McDonnell. 1975. "Limestone Barriers to Neutralize Acidic Streams." *J. of Env. Eng Div.*, ASCE. 101(EE1). pp. 139-158.

Singer, P. C., and W. Stumm. 1970. "Acid Mine Drainage: The Rate Determining Step." *Science* 167:1121-1123.

Singer, P. C., and W. Stumm. 1969. "Oxygenation of Ferrous Iron." FWQA Rep. 14010-06/69.

Smith, E. E., K. Svanks, and K. S. Shumate. 1968. "Sulfide to Sulfate Reaction Studies." 2nd Symp. Coal Mine Drainage Res., Pittsburgh, PA. p.1-11.

Stumm, W., and J. J. Morgan. 1970. *Aquatic Chemistry.* Wiley-Interscience, New York, New York.

WRI-98-R018

30126

#133

WESTERN RESEARCH INSTITUTE

"Providing solutions to energy and environmental problems"

KUZNIAR

FINAL REPORT

THE SYNAG™ PROCESS: COAL COMBUSTION ASH MANAGEMENT OPTION

Prepared for
U.S. Department of Energy
Morgantown, West Virginia

June 1998

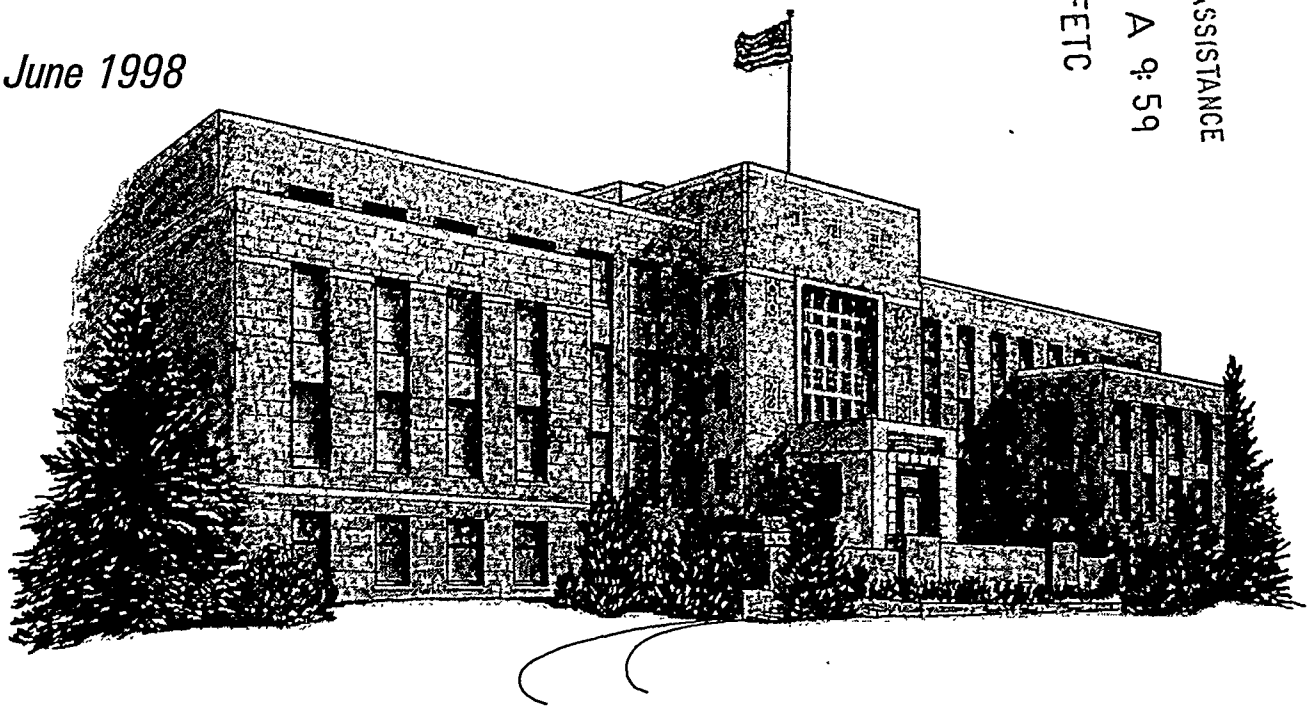

WRI-98-R018

THE SYNAG™ PROCESS: COAL COMBUSTION ASH MANAGEMENT OPTION

Final Report

February 1994 – February 1998

By
Alan E. Bland

June 1998

Work Performed Under Cooperative Agreement
DE-FC21-93MC30126
Subtask 3.3

For
U.S. Department of Energy
Office of Fossil Energy
Federal Energy Technology Center
Morgantown, West Virginia

By
Western Research Institute
Laramie, Wyoming

DISCLAIMER

LIST OF TABLES

EXECUTIVE SUMMARY

The power industry in the United States has traditionally been one of the largest generators of solid waste. Most of the ash from conventional power systems does not meet the requirements of the American Society for Testing and Materials (ASTM) for use in various construction applications. These ashes are often termed "off-spec." Although there has been a concerted effort to find uses for the solid waste materials from power plants, the United States is marketing less than 20% of the ashes generated. The clear majority of these wastes are still placed in controlled disposal facilities or transported back to the mine for backfilling. New uses for the solid wastes based on performance criteria instead of chemical constituents need to be developed if substantially larger quantities of these solid wastes are to be placed in usable applications. Alternative uses and markets for these ashes are needed since continued disposal has become a major cost of power generation, and siting of new landfills has been met with public resistance.

Western Research Institute (WRI), in conjunction with the U.S. Department of Energy (DOE), is developing a process for the production of synthetic aggregate for the construction industry from coal combustion ashes. This process, called the SYNAG™ process, represents a method for the production of normal-weight or lightweight aggregate from coal utilization ashes. Disclosures have been written and patent applications are being considered. **Therefore, information about the SYNAG process remains confidential to WRI and protected therein.**

The SYNAG process is based on the cold bonding of the fly ash to produce a hardened form and the subsequent sizing (and crushing, if needed) to produce the desired size distribution for various construction aggregate applications. The key process steps include: the hydration of the ash; the addition of chemical additives (if required); compaction or agglomeration to form a densified mass; curing of the densified ash under heat and/or steam; and finally, crushing and screening as required for shipment.

The SYNAG process is cost competitive with other processes for synthetic aggregate production and with competing natural materials. The SYNAG process does not require ashes that meet the ASTM specifications for pozzolans for cement replacement. Therefore, SYNAG represents a new market for the off-spec ashes produced at power plants. The SYNAG process also represents a market for those ashes produced during the construction off-season by allowing the open stockpiling of the SYNAG product during the winter for use during the next construction season.

A research and development effort has been initiated to evaluate the processing of coal combustion ash into a synthetic aggregate for construction applications. This program has an

overall objective of process refinement pursuant to the commercialization of the SYNAG technology. The program has the following objectives:

(1) to develop and document the use of additives for a range of conventional coal combustion ashes;

(2) to determine the optimum curing conditions for the SYNAG process; and

(3) to verify the SYNAG process and products through pilot-scale testing of the SYNAG process.

The results of the research and development program for the production of synthetic aggregate from fluidized bed combustion ashes, spray dryer ashes, and off-spec, as well as ASTM C-618 Class C and F conventional power plant ashes, have substantiated that the SYNAG process can successfully produce synthetic aggregate from these fly ashes that meets applicable ASTM and American Association of State Highway Transportation Officials (AASHTO) standards for normal-weight aggregate.

- Pelletizing trials were conducted using ashes from Plants A and B, which represent Class C and Class F ashes, respectively. The aggregate produced appears to meet the basic ASTM and AASHTO requirements for normal-weight construction aggregate.

- Properties of the SYNAG product are dependent upon the curing conditions.

- Specialized chemical additives required to control aggregate properties have been tested.

- Additives are available to make the SYNAG product lightweight and thereby meet applicable ASTM requirements.

- Process verification tests were conducted using the pelletized process option. The resulting product meets the ASTM and AASHTO specifications for construction aggregate.

1.0 INTRODUCTION

The power industry in the United States has traditionally been one of the largest generators of solid waste. Most of the ash from conventional power systems does not meet the requirements of the American Society for Testing and Materials (ASTM) for use in various construction applications. These ashes are often termed "off-spec." Although there has been a concerted effort to find uses for the solid waste materials from power plants, the United States is marketing less than 20% of the ashes generated. The clear majority of these wastes are still placed in controlled disposal facilities or transported back to the mine for backfilling. New uses for the solid wastes based on performance criteria instead of chemical constituents need to be developed if substantially larger quantities of these solid wastes are to be placed in usable applications. Alternative uses and markets for these ashes are needed since continued disposal has become a major cost of power generation, and siting of new landfills has been met with public resistance.

Western Research Institute (WRI) has developed a process for the production of synthetic aggregate from coal combustion ashes. This process, termed the SYNAG™ process, is capable of producing both normal-weight and lightweight construction aggregate. The SYNAG process is believed to be cost competitive with other processes for synthetic aggregate production and with competing natural materials. The SYNAG process does not require ashes that meet the ASTM C-618 specifications for pozzolans for cement replacement. Therefore, the SYNAG process represents a new market for the off-spec ashes produced at power plants. The SYNAG process also represents a market for those ashes produced during the construction off-season, by allowing the open stockpiling of the SYNAG product during the winter for use during the next construction season.

2.0 PURPOSE

Western Research Institute, in conjunction with the U.S. Department of Energy (DOE), is developing a process for the production of synthetic aggregate for the construction industry from coal combustion ashes. This process, termed the SYNAG process, represents a method for the production of normal-weight or lightweight aggregate from coal combustion ashes.

Several technical issues need to be resolved and the economics of the process better defined before the SYNAG process is ready to be commercialized. A research and development program to address these technical and economic issues has been initiated.

3.0 BACKGROUND

Aggregates are defined as "any of several hard, inert materials including sand, gravel, slag, or crushed stone used for mixing with cementing or bituminous materials to form concrete and concrete products, mortar or plaster or used alone as ballast or graded fill." (Bates 1984).

3.1 Aggregate Market

The aggregate market in the United States represents a major market for coal ashes, significantly larger than the existing cement market for Class C and F fly ashes. In 1996, over 1.33 billion tons of crushed stone worth $7.18 billion were produced in the United States at an average price of approximately $5.40/ton (Tepordel 1996 and Bolen 1996). In 1996, the United States also produced over 961 million tons of construction sand and gravel worth over $4 billion. Many states, however, including the southeast coastal and Rocky Mountain states, have a shortage of quality aggregate. The outlook for the crushed stone market is expected to be excellent for the short term.

Lightweight aggregate represents an attractive market for coal combustion by-products. There has traditionally been a strong market for lightweight aggregate in concrete products. Lightweight aggregate sales from shales and clay are in the range of 5 million tons annually. Expanded clay and shale sold for $25 to $45/ton in 1987. Texas alone uses over a million tons of lightweight aggregate annually. Cement block production accounted for 61% of the total production, followed by highway surfacing (19%), structural concrete (18%), and recreational and horticultural applications (2%). However, the processing of expanded clay into lightweight aggregate is an energy-intensive process that has been slowed by rising energy costs.

The market for fly ash-derived synthetic aggregate is enormous. There are a number of construction applications for these aggregates, including: (1) portland cement concrete and concrete products, (2) unpaved road stabilization, (3) road base construction, (4) asphalt paving applications, and (5) lightweight structural applications. The range of applications is sufficient to offset the adverse economics of long transportation distances for aggregate.

3.2 Competing Aggregate Processes

The production of synthetic aggregate from fly ash is not a new concept. Several processes for the production of synthetic aggregate from coal ashes have been developed and commercially applied over the last several decades (Hay and Rademaker 1987, Bland et al. 1989, 1992, 1993, 1995, Styron 1987). In general, the processes for synthetic aggregate production in the United States can be categorized as based either on sintering of the ash or on cold bonding with lime or cement.

The sintering process was actively pursued during the 1960's and 1970's when six plants operated in the United States. The process involves the mixing of 5 to 15% carbon fly ash with water and a binder and feeding the mixture into a pelletizer to form pellets up to 1.88 cm (3/4 in.) in diameter. The pellets are then placed in a sintering machine, where they are dried and fired at temperatures of 900 to 1200°C (1650 to 2190°F) to form a porous material (Burnet and Gokhale 1987). After firing, the clinkered material is crushed to the desired particle size. The LYTAG and the Neopore Systems are examples of these processes. Sintering is not common today due to the high energy costs for the process. Also, the sintering processes do not appear promising for certain ashes that contain components from the advanced sulfur emissions control technologies because of potential SO_X emissions.

The cold bond processes rely on the cementitious reactions of the fly ash with a binder material. Two processes for conventional ash have been developed to a commercial state: (1) the Resource Technology Inc. (RTI) Agglite process is commercially practiced in Chesapeake, Virginia, (Styron 1987) and (2) the Aardalite process is practiced at the Progress Material facility at Crystal River, Florida, (Hay and Rademaker 1987). These processes use either lime (3 to 6%) with Class F fly ash (Aardalite process) or portland cement (5 to 10%) with Class F fly ash (Agglite process). The cold bond processes have not been successfully applied to Class C ashes because of problems encountered during curing.

Both the patented Aardalite and Agglite processes involve the thorough mixing of the lime or cement with the coal ash and the agglomeration of the mixture into spherical-shaped aggregate (Hay and Rademaker 1987, Styron 1987). The aggregate is allowed to cure under heat and steam in the case of Aardalite or at atmospheric conditions in the case of Agglite. The production costs for these processes are lower than for sintered aggregate. Both of these cold bond processes have been operated at a commercial scale of approximately 136,200 tonnes (150,000 tons) per year. The Progress Materials facility in Crystal River, Florida, is designed to produce 136,200 tonnes (150,000 tons) per year of lightweight aggregate from Class F fly ash and is presently supplying aggregate to a local block manufacturer. The Agglite facility in Chesapeake, Virginia, was designed to supply 90,800 tonnes (100,000 tons) per year of lightweight aggregate to two block plants.

4.0 SYNAG PRODUCTION CONCEPTS

The SYNAG process is designed to produce synthetic aggregate from coal combustion ashes. The process is based on the use of specialized chemicals to cold bond the fly ash to produce a hardened form and its subsequent crushing and sizing to produce the desired size distribution for various construction aggregate applications. The SYNAG process involves the production of a hardened and compacted ash product with the properties of construction

aggregate according to ASTM and American Association of State Highway Transportation Officers (AASHTO) specifications. The process of forming the compacted ash product can be selected from a number of basic process concepts and a number of variations on each concept.

5.0 SYNAG PRODUCT MARKET

The SYNAG product is expected to meet applicable ASTM and AASHTO standards as both normal-weight and lightweight aggregate. The SYNAG process is also expected to be cost competitive with other processes for synthetic aggregate production and competing natural materials. The SYNAG process does not require ashes that meet the ASTM C-618 specifications for pozzolans for cement replacement. Therefore, SYNAG represents a new market for the off-spec ashes produced by power plants. The SYNAG process also represents a market for those ashes produced during the construction off-season by allowing the open stockpiling of the SYNAG product during the winter for use during the next construction period.

The market for SYNAG aggregate is enormous. SYNAG synthetic aggregate is expected to penetrate both the normal-weight and lightweight aggregate markets. Normal-weight SYNAG aggregate appears viable for applications such as masonry units and structural or insulating concrete, as aggregate for normal-weight concrete products, as aggregate for asphaltic concretes, as base aggregate for road and other construction subbases, and as fill material for subgrade and embankments.

Lightweight SYNAG aggregate markets include building blocks, structural and precast concrete members, and pavements. Lightweight aggregates are necessary for those applications in which weight of construction materials is a primary concern, such as for skyscrapers, parking garages, bridge decks and flooring, and similar construction projects.

The SYNAG process is expected to offer a strong cost advantage over other processes for the production of synthetic aggregate from coal combustion ashes. Although process economics are driven by market availability and transportation costs, the estimated costs for SYNAG aggregate are 30 to 50% lower than for Agglite and sintering process aggregate.

6.0 METHODOLOGY

The research and development effort to evaluate the processing of coal combustion ash into a synthetic aggregate for construction applications has the overall objective of process refinement pursuant to the commercialization of the SYNAG technology. This effort has the following objectives:

(1) to develop and document the use of additives for a range of conventional coal combustion ashes;

(2) to determine the optimum curing conditions for the SYNAG process; and

(3) to verify the SYNAG process and products through pilot-scale testing of the SYNAG process.

7.0 RESULTS AND DISCUSSION

WRI, in conjunction with the U.S. DOE, has initiated a research and development program of the proprietary SYNAG process. The SYNAG process is designed to produce synthetic aggregate from off-spec, as well as ASTM C-618 Class C and F conventional power plant ashes. Disclosures have been written and patent applications are being prepared.

Efforts to develop the appropriate operating conditions and chemical additives for the SYNAG process focused on the following:

- design of chemical additives for the activation of a range of coal combustion ashes;
- design of appropriate curing conditions for the pelletized ash;
- verification of process using the WRI pilot-scale pelletizing equipment and facilities; and
- testing of the aggregate produced according to standard ASTM and AASHTO aggregate tests;

7.1 Ash Sources and Characteristics

Coal combustion ashes vary considerably according to coal origin and combustion characteristics, as well as flue gas cleanup and fly ash processing conditions. The ash industry has developed through ASTM a set of classifications (Class C or Class F) of conventional coal combustion fly ashes for use as pozzolans in portland cement. However, the sulfur emissions control technologies now being implemented at these coal combustion facilities are changing the character of coal combustion ashes, resulting in an ash that is different from either Class C or Class F ashes.

Four plants and their associated ashes were selected for the study from the WRI data base on coal combustion ashes. The ashes selected for the testing represent a range of ash types and include Class C and Class F fly ashes, as well as ashes from the spray dryer processes. The plants and ashes represented the following:

- Plant A – western U.S. pulverized coal-fired plant burning low-sulfur subbituminous Powder River Basin coal producing Class C fly ash and an ash from a lime-based SO_2 control spray dryer system.

- Plant B – western U.S. plant burning low- to medium-sulfur bituminous coal producing Class F fly ash and an ash from the lime-based SO_2 control spray dryer.

- Plant C – eastern U.S. circulating fluidized bed combustion (CFBC) plant burning a medium-sulfur bituminous coal producing a bed ash and a fly ash.

- Plant D – western U.S. CFBC plant burning low-sulfur coal and producing a bed ash and a fly ash.

Ashes from Plants A and B represent facilities employing pulverized coal-fired units without sulfur emissions control, coupled with an additional pulverized coal-fired unit with a spray dryer scrubber for sulfur emissions control. The ashes from Plant A and the ashes from Silo A of Unit 1 of Plant B are being marketed. Neither of the spray dryer ashes (Silo C or Unit 3) are marketed in any significant quantity, nor are the Silo B ashes from Plant B, because of fluctuating loss on ignition (LOI) content.

The ashes produced by Plants C and D from CFBC systems represent a unique ash in the power industry. Plant C is combusting a medium-sulfur bituminous coal, while Plant D is combusting a low-sulfur subbituminous coal. The FBC technology produces an ash that does not meet the ASTM or AASHTO specifications for use in cement and concrete as a result of the relatively high SO_3 content.

Plants C and D were selected to ascertain whether it is possible to produce, in addition to the normal-weight aggregate, a lightweight aggregate by using chemical additives being developed under the SYNAG program. Each of the ashes were subjected to a series of chemical, physical, and geotechnical tests that served as the basis for the design of the chemical additives and the processing requirements.

Chemical/Physical Properties

The chemical and physical properties of each of the ashes according to ASTM C-311 are presented in Tables 1 and 2.

Table 1. ASTM C-311 Test Data for the Ashes from Plant A

	Plant A Units 1&2	Plant A Unit 3	ASTM C-618 Specifications	
Chemical Properties			**Class F**	**Class C**
$SiO_2+Al_2O_3+Fe_2O_3$, wt.%	56.49	41.67	70 min	50 min
Sulfur Trioxide, wt.%	2.25	14.62	5 max	5 max
Calcium Oxide, wt. %	29.46	32.05	–	–
Moisture Content, wt. %	0.05	1.55	3 max	3 max
Loss on Ignition, wt. %	0.51	3.65	6 max	6 max
Physical Properties				
Fineness, % retained 325 mesh	19.96	11.53	34 max	34 max
Pozzolanic Activity Index				
With PC, % of control @ 28 days	98.6	85.4	75 min	75 min
With Lime, Mpa @ 7 days	9.2	7.1	5.5 min	No Limit
Water Requirement, % of control	94.2	100	105 max	105 max
Soundness-Autoclave Expansion, %	0.034	-0.032	0.8 max	0.8 max

PC – portland cement
6.89 MPa = 1000 ps

Table 2. ASTM C-311 Test Data for the Ashes from Plant B

	Plant B Silo A	Plant B Silo B	Plant B Silo C	ASTM C-618 Specifications	
Chemical Properties				**Class F**	**Class C**
$SiO_2+Al_2O_3+Fe_2O_3$, wt. %	79.31	78.81	57.75	70 min	50 min
Sulfur Trioxide, wt. %	0.31	0.46	9.09	5 max	5 max
Calcium Oxide, wt. %	11.4	10.89	22.89	–	–
Moisture Content, wt. %	0.08	0.08	0.62	3 max	3 max
Loss on Ignition, wt. %	0.76	2.29	4.15	6 max	6 max
Physical Properties					
Fineness, % retained 325 mesh	13.89	27.32	10.92	34 max	34 max
Pozzolanic Activity Index					
With PC, % of control @ 28 days	91.8	83.6	81.0	75 min	75 min
With Lime, MPa @ 7 days	11.4	9.6	11.0	5.5 min	No Limit
Water Requirement, % of control	94.2	85	84.2	105 max	105 max
Soundness-Autoclave Expansion, %	-0.047	-0.034	-0.065	0.8 max	0.8 max

PC – portland cement
6.89 MPa = 1000 psi

The ashes from Plant A are classified as Class C fly ash. The fly ash from Units 1 and 2 meets the requirements of ASTM for a pozzolanic material. High calcium contents are noted. The fineness of the ash is well within the ASTM specifications. Pozzolanic activity with both cement and lime is also high, with low expansion properties. The Unit 3 fly ash, on the other hand, does not meet the chemical requirements as a pozzolan because of its high SO_3 content. However, the physical properties, pozzolanic activity, and autoclave expansions do meet the ASTM specifications.

The ashes from Plant B are classified as Class F fly ash. Although the ashes from Silo A and B have approximately 10 to 12% calcium, reported as CaO, the concentrations of SiO_2 + Al_2O_3 + Fe_2O_3 exceed the minimum requirements for a Class F fly ash. The fly ash from Silo C (spray dryer) does not meet the chemical requirements because of the high SO_3 content. The fineness of all three fly ashes meets the ASTM specifications. The pozzolanic activity with cement and lime for all three Plant B ashes also meets the ASTM specifications, and the autoclave expansions are well within the limits.

The ashes from Plants C and D cannot be classified according to the ASTM C-618 specifications. The results of the ASTM C-311 testing are presented in Table 3.

Table 3. ASTM C-311 Test Data for the CFBC Ashes from Plant C and D

	Plant C Fly Ash	Plant C Bed Ash	Plant D Fly Ash	Plant D Bed Ash	ASTM C-618 Specifications	
Chemical Properties					**Class F**	**Class C**
SiO_2+Al_2O_3+Fe_2O_3, wt. %	63.83	17.93	72.17	70.16	70 min	50 min
Sulfur Trioxide, wt. %	4.82	34.48	4.70	2.99	5 max	5 max
Calcium Oxide, wt. %	17.83	42.53	17.09	19.00	–	–
Moisture Content, wt. %	0.29	0.06	0.10	0.10	3 max	3 max
Loss on Ignition, wt. %	8.87	1.24	2.62	5.10	6 max	6 max
Available Alkalis, wt. %	0.84	0.03	0.26	nd	1.5 max	1.5 max
Physical Properties						
Fineness, % retained 325 mesh	22.63	97.98	31.64	95.99	34 max	34 max
Pozzolanic Activity Index						
With PC, % of control @ 28 days	97.5	nd	84.5	nd	75 min	75 min
Water Requirement, % of control)	109.1	nd	103.3	nd	105 max	105 max
Soundness-Autoclave Expansion, %	-0.040	nd	-0.043	nd	0.8 max	0.8 max

nd – not determined

Neither the fly ash nor the bed ash from Plants C and D meet the ASTM requirements due to the high SO_3 content. The fineness of the fly ash meets the ASTM specifications, while the bed ash is much too coarse. The pozzolanic activity with cement and lime for the fly ash meets the ASTM specifications, and the autoclave expansions are well within the limits.

Geotechnical Properties

Geotechnical tests on ashes from these facilities have been conducted and indicate that the general physical properties, strength development, and dimensional stability characteristics are sensitive to ash characteristics and sources, moisture content, and curing conditions.

The general physical properties of the ashes, including minimum and maximum densities, specific gravities, optimum moistures and maximum dry densities (ASTM D-698), and particle size (PS) are presented in Table 4.

Table 4. Physical Properties of the Ashes from Plants A, B, C, and D

	Plant A		Plant B			Plant C		Plant D	
	Units 1&2	Unit 3	Silo A	Silo B	Silo C	Fly Ash	Bed Ash	Fly Ash	Bed Ash
Minimum Density, kg/m^3	1221	713	1275	1200	764	974 (1)		706	1336
Maximum Density, kg/m^3	1701	1075	1469	1391	950	1070 (1)		822	1432
D-698 Moisture, %	12.9	28.5	16.5	15.0	28.6	30.7 (1)		35.6 (2)	
Max. Dry Density, kg/m^3 (3)	1919	1411	1514	1585	1302	1354 (1)		1259 (2)	
PS, %>325 mesh (4)	19.96	11.53	13.89	27.32	10.92	22.63	97.98	31.64	95.99
Specific Gravity, g/cc	2.64	2.50	2.31	2.36	2.38	2.55	2.87	2.69	2.49

(1) Blend of 70% fly ash and 30% bed ash
(2) Blend of 83.4% fly ash and 16.7% conditioned (6% water addition) bed ash
(3) maximum dry density determined according to ASTM D-698
(4) PS – particle size based on % retained on 325 mesh screen

The moisture-ash relationship, densities, strength development, and dimensional stability of each of the ashes were determined at (1) Proctor water content; (2) 2% less than Proctor water; and (3) 5% above Proctor water. The results for ashes from Plants A and B are presented in Table 5.

The water demand for the Class C (Unit 1 and 2) ashes is significantly less (13%) than for the spray dryer ashes of Unit 3 (28%). This also translates into differences in the moisture-density relationship. As expected, the strength development of the ashes varies with the water:solids ratio, with the strengths at or near Proctor exhibiting the highest strengths. Unit 1 and 2 ashes harden quickly, and in fact, additives are needed to prevent flash setting. The Unit 3 ash, on the other hand, shows very slow set times and early strengths.

Table 5. Summary of the Geotechnical Properties of Plant A Ashes

Plant A	Units 1 and 2	Units 1 and 2	Units 1 and 2	Unit 3	Unit 3	Unit 3
Water Added, %	11.0	13.0	18.0	26.0	28.0	33.0
Density, kg/m^3 (1)	nd	1919	nd	nd	1585	nd
UC Strength, MPa						
1 day	21.5	36.1	15.0	2.4	4.0	2.4
3 days	26.4	48.7	19.6	4.3	6.9	4.2
7 days	29.8	51.1	20.2	5.8	9.6	5.7
14 days	30.6	nd	24.5	6.9	12.1	7.1
28 days	35.6	52.5	31.0	7.5	14.9	9.6
56 days	34.3	66.5	44.3	8.7	17.2	9.0
90 days	34.0	59.0	41.8	12.8	25.4	15.2

(1) Density determined for optimum moisture by ASTM D-698
nd – not determined
UC Strength – unconfined compressive strength

Although fly ash from Units 1 and 2 of Plant A exhibits earlier and higher strength development than the Unit 3 (spray dryer) ash, it is interesting to note that the long-term strength development for the Unit 3 ash indicates that strength development will continue for an extended period (greater than 90 days). Both the Class C and the spray dryer ashes from Plant A are dimensionally stable. In fact, the ashes showed a slight shrinkage that varied with curing conditions and mixing water content.

The results of the geotechnical testing for the Plant B fly ashes are presented in Table 6. Silo A and B ashes exhibit lower water demands (15 to 16.5%), than Silo C spray dryer ash (28.5%). As described earlier, this higher water demand also translates into lower densities.

The low strength development of the Class F ashes was expected. There is insufficient calcium for the pozzolanic reactions to occur. The spray dryer ashes, on the other hand, showed low early strength development but high long-term strengths. With the spray dryer ashes, there is ample calcium for long-term strength development. It is interesting to note that a combination of approximately 50% Silo B and 50% Silo C ashes results in a chemical composition that meets ASTM C-618 specifications. Such a mixture should show excellent pozzolanic and self-hardening characteristics. The dimensional stability testing of the Class F ashes was not completed because of the low strengths of the ashes and their disintegration upon exposure to saturated and submerged conditions.

Table 6. Summary of the Geotechnical Properties of Plant B Ashes

Plant B	Silo A Ash	Silo A Ash	Silo B Ash	Silo B Ash	Silo B Ash	Silo C Ash	Silo C Ash	Silo C Ash
Water Added, %	14.5	16.5	13.0	15.0	20.0	26.5	28.5	33.5
Density, kg/m^3 (1)	1666	1746	1698	1794	1842	1490	1682	1666
UC Strength, MPa								
1 day	0.7	0.9	0.3	0.5	0.3	0.8	0.8	0.4
3 days	1.6	2.1	0.4	0.6	0.4	1.4	1.2	0.7
7 days	1.9	2.6	0.6	0.7	0.5	2.6	3.2	1.7
14 days	2.2	nd	0.7	0.8	0.6	5.0	8.3	4.3
28 days	2.1	3.0	1.2	1.5	0.7	12.9	19.1	10.9
56 days	3.1	3.5	1.8	2.0	0.9	16.5	31.4	31.8
90 days	3.1	3.5	2.4	2.3	1.3	16.3	37.3	37.1

(1) Density determined for optimum moisture by ASTM D-698
UC Strength – unconfined compressive strength
nd – not determined

The results of the geotechnical testing for the ash from Plants C and D are presented in Table 7. The results show unconfined compressive strengths in excess of 27.6 MPa, values acceptable for strength development associated with aggregate production. The dimensional stability characteristics are of minimal concern for aggregate production, since any expansion will only result in a lighter weight product.

Table 7. Geotechnical Properties of Plant C and D CFBC Ashes

	Plant C Ash Blend	Plant D Ash Blend
Water Added , %	30.7	35.6
Density, kg/m^3 (1)	1354	1259
UC Strength, MPa		
1 day	0.8	1.4
3 days	5.9	5.8
7 days	12.2	11.2
14 days	16.4	20.6
28 days	21.5	30.6
56 days	24.1	34.0
90 days	29.5	35.2

(1) Density determined for optimum moisture by ASTM D-698
UC Strength – unconfined compressive strength

7.2 Chemical Additive Testing

The development of chemical additives was initiated to affect the activation and reaction kinetics control of the hardening process for a range of coal combustion ashes.

Many of the Class C ashes have a tendency to flash set when exposed to water. This flash setting was noted for the Plant A Unit 1 and 2 Class C fly ash. Flash setting occurred within five minutes. As a result, retarders were needed to enhance the workability of the water and ash mixture. Several such retarders have been identified. The test results using one of these retarders with the ashes from Plant A Units 1 and 2 are presented in Table 8. The data show the benefit of retarder on the strength development of this Class C fly ash.

Table 8. Summary of the Effect of Chemical Additives on Strength Properties of Cured Ashes*

	Plant A – Units 1 and 2			Plant B – Silo A		Plant B – Silo C	
Retarder, % of water	0%	1%	2 %	–	–	–	–
Activator, % of solids	–	–	–	0%	5%	0%	5%
Water, % of solids	13.0%	13.0%	13.0%	16.5%	16.5%	28.6%	28.6%
UCS**, MPa @ 1 day	nd	30.6	36.1	0.9	1.8	0.8	0.7

* Cured at 23°C and 95% relative humidity

** UCS – Unconfined compressive strength

On the other hand, some ashes are very slow to develop strength and as such, require extended curing times. Previous testing with coal combustion ashes has indicated that certain activators can be used to accelerate the strength development of these ashes. Not all activators, or accelerators, are suitable for all ashes. The test results using one of these activators with the Plant B fly ash and spray dryer ash are presented in Table 8. The data show that the activator is beneficial to strength development for the Silo A Class F ash but not necessarily for the Silo C spray dryer ash.

7.3 Evaluation of Curing Conditions

The effects of different curing conditions on the pelletized ash properties were also addressed. Unique curing conditions may be required for each ash and chemical additive combination. A set of tests was conducted under 95% relative humidity at temperatures of 23° C (73°F) to 82°C (180°F). The results are presented in Table 9. The data indicate the value of elevated curing temperatures for the Plant B Class F fly ashes but not necessarily for the Plant A Class C fly ash.

Table 9. Summary of the Effect of Curing Temperature on Strength Properties of Cured Ashes*

	Plant A Units 1 and 2		Plant B Silo A		Plant B Silo A		Plant B Silo A	
Retarder, % of water	2%		–		–		–	
Activator, % of solids	–		–		5%		–	
Water, % of solids	13.0%		16.5%		16.5%		28.6%	
Curing Temperature	23°C	82°C	23°C	82°C	23°C	82°C	23°C	82°C
UCS**, MPa @ 1 day	36.1	26.3	0.9	2.1	1.8	8.6	0.8	8.4

* Cured at 23°C and 82°C and 95% relative humidity

**UCS – unconfined compressive strength

7.4 Lightweight Aggregate Additive Testing

The ability to produce a lightweight aggregate from the SYNAG process has some definite economic advantages, because typically lightweight aggregate commands a higher market price than normal-weight aggregate. As a result, one can justify the use of specialty chemicals to produce lightweight aggregate.

Testing examined the possible use of two different chemicals to transform the Plant C FBC ash into a lightweight aggregate. The results are presented in Table 10.

Table 10. Summary of Strength and Density Data Resulting from Addition of Lightweight Additives to CFBC Ashes from Plant C

Mix Proportions	Test Ctl	Test C	Test B	Test A	Test F	Test D-1	Test D-2
Fly Ash, % of ash	60	60	60	60	60	60	60
Bed Ash, % of ash	40	40	40	40	40	40	40
LW Additives, % of solids	–	0.5	1	2	4	–	–
LW Additive, ml/tonne	–	–	–	–	–	33	163
Water, % of ash	37.5	37.5	37.5	37.5	37.5	37.5	37.5
Geotechnical Properties							
UCS @ 28d, MPa (1)	16.0	6.8	5.5	6.1	4.0	7.3	1.0
UCS @ 28d, MPa (2)	15.3	7.5	7.5	6.6	4.3	6.7	1.0
Density, kg/m^3	1721	1378	1322	1299	913	1432	1075

LW – lightweight

UCS – unconfined compressive strength

(1) Sealed 23°C curing conditions

(2) Humid 23°C curing conditions

Both additives appear to be effective in reducing the specific gravity of the ash mixtures. There is a definite decrease in the density of the cured ash mixture with increased dosages of additives.

Testing was also conducted to determine the potential of producing lightweight aggregate from the Plant A ashes. The results of this testing are presented in Table 11.

Table 11. Summary of Strength and Density Data Resulting from Addition of Lightweight Additives to Ashes from the Plant A

Mix Proportions, % of mix	Test A	Test D	Test F	Test B	Test C
Unit 1&2 Ash	61.0%	81.0%	61.5%	–	–
Unit 3 Ash	20.3%	–	20.5%	72.1%	67.1%
Strength Additives	–	–	–	–	3.4%
Set Retarders,	–	0.4%	–	–	–
LW Additives	0.8%	0.8%	–	0.7%	0.7%
Water	17.9%	17.8%	18.0%	27.2%	28.8%
Geotechnical Properties					
UCS @ 28d, Mpa (1)	15.0	13.9	22.4	5.0	6.2
UCS @ 28d, Mpa (2)	14.1	11.7	22.7	4.7	2.7
Density, kg/m^3 (3)	1685	1564	2036	1462	1465

(1) Sealed 23°C curing conditions
(2) Humid 23°C curing conditions
(3) 71°C curing conditions
UCS – unconfined compressive strength

Once again, a decrease in the specific gravity of the ashes was noted. It was calculated that a reduction of approximately 20% in the specific gravity of the aggregate was required for a bulk density of the aggregate of approximately 1121 kg/m^3, the typical ASTM and AASHTO requirement for lightweight aggregate. A 1% addition of additives resulted in a 17% reduction in the specific gravity of the individual aggregate particles. Unfortunately, there was also a reduction in the strength of the ashes. A combination of strength enhancers and lightweight additives may be required for these ashes.

7.5 Verification of the SYNAG Process

A series of preliminary verification tests was conducted to confirm the chemical additives and other process options, as well as to provide information needed to assess the relative economics of the process. Both pilot-scale pelletizing trials and aggregate quality testing were conducted.

Pilot-Scale Pelletizing Trials

A series of pelletizing trials was conducted to ascertain the process behavior and water requirements and to generate sufficient aggregate for testing. These preliminary pelletizing trials were conducted at the WRI pelletizing pilot facilities. Chemicals for control of the flash setting of the Class C ashes were also employed. Since $CaSO_4$, known to be a retarder, is present in the Unit 3 fly ash, testing of a combination of Unit 1 and 2 ashes with the Unit 3 ash was conducted. Pelletizing trials were also conducted using additives to enhance strength development, particularly with the Class F fly ashes from Plant B. The results of the pelletizing trials using ash from Plants A and B are presented in Tables 12 and 13, respectively. The results indicate that heat/steam curing may be beneficial to the strength development of the pelletized Plant B ashes but not necessarily to the Plant A ashes.

In addition to the Class F and Class C ash pelletizing trials, pelletizing trials were also conducted using the CFBC ashes from Plants C and D. The bed ash was preconditioned to facilitate the exothermic and expansive nature of the lime in the ashes. The test conditions and run characteristics are presented in Tables 14 and 15 for the Plant C and D ashes, respectively.

Aggregate Testing

Aggregate produced from the pelletizing trials was subjected to a series of ASTM and AASHTO tests used by the construction industry to qualify aggregate for construction-related applications. The results of the aggregate tests for Plants A and B are presented in Tables 12 and 13.

Table 12. Summary of the SYNAG Pelletizing Trials Using Plant A Fly Ash

Plant A	Trial A-1	Trial A-1	Trial A-2	Trial A-2
Mix Components, wt. %*				
Unit 1 and 2 Fly Ash	28.85	28.85	–	–
Unit 3 Spray Dryer Ash	57.70	57.70	78.06	78.06
Additive	–	–	3.90	3.90
Water-Pin Mixer	13.45	13.45	18.03	18.03
Curing Conditions				
Temperature, °C	23°C	82°C	23°C	82°C
Sealed or Covered	Covered	Sealed-10 hrs	Covered	Sealed-10 hrs
Crush Strength, kg				
24 hrs	117	120	45	93
48 hrs	157	114	76	78
7 days	132	93	173	106
28 days	147	102	162	112
90 days	nd	141	176	168
LA Abrasion Resistance				
Grade	B	B	B	B
Loss at 28 days, %	31.68	41.00	25.34	27.16

nd – not determined

* Water added to pan not determined

Table 13. Summary of SYNAG Pelletizing Trials Using Plant B Fly Ash

Plant B	Trial B-1		Trial B-2		Trial B-3		Trial B-4	
Mix Components, wt.%*								
A Silo Class F Fly Ash	21.56		–		20.14		83.16	
B Silo Fly Ash	–		41.61		–		–	
C Silo Spray Dryer Ash	64.68		41.61		60.41		–	
Additive	–		4.16		4.03		4.16	
Water-Pin Mixer	13.76		12.61		15.42		12.68	
Curing Conditions								
Temperature, °C Sealed or Covered	23°C Covered	82°C Sealed 10 hrs	23°C Covered	82°C Sealed 10 hrs	23°C Covered	82°C Sealed 10 hrs	23°C Covered	82°C Sealed 10 hrs
Crush Strength, kg								
24 hrs	13	14	6	52	7	45	17	90
48 hrs	nd	nd	11	43	10	33	14	65
7 days	18	29	9	46	9	34	16	70
28 days	58	56	50	54	38	42	26	51
90 days	99	85	78	52	47	119	45	60
LA Abrasion Resistance								
Grade	B	B	B	B	B	B	B	B
Loss at 28 days, %	44.70	42.24	33.46	28.80	44.90	38.38	81.04	41.94

nd – not determined
* Water added to pan not determined

The results indicate that the pelletized material made from Plant A ashes exhibits sufficient strength and resistance to LA abrasion to meet the ASTM and AASHTO requirement of a maximum of 40% loss. Certain of the pelletized materials made from Plant B ashes, in particular those cured at elevated temperature, also met the ASTM and AASHTO specifications. Although the room-temperature aggregate showed very low early strengths, the strength increased with time to become comparable to the 82°C (180°F) cured pellets after 90 days.

The results of testing the CFBC fly ash and bed ash blends from Plant C, burning a medium-sulfur coal, (Table 14) and Plant D, burning a low-sulfur coal, (Table 15) indicate that the LA abrasion resistance specifications can be met. In addition, the aggregate treated with soluble carbonate as used in the SYNAG process can also meet the soundness requirements for construction aggregate.

Table 14 also shows the effect of heat curing of the aggregate on product quality. Although the aggregate that is heat-cured for 20 hours shows superior crush strength, the room-temperature cured aggregate approaches the crush strength at 28 days. The heat-cured aggregate actually showed a decrease in crush strength after 28 days, probably due to lack of water for further hydration reactions that provide strength.

Table 14. Summary of the SYNAG Pelletizing Trials Using Plant C Fly Ash and Bed Ash

Plant C	Trial 6		Trial 7		Trial 8	
Mix Proportions, wt. %						
CFBC Fly Ash	39.28		49.18		50.88	
CFBC Hydrated Bed Ash*	26.18		24.59		12.72	
Raw Bed Ash	13.09				12.72	
Mixer Water	9.85		8.51		9.87	
Pan Water	11.60		17.73		13.81	
Curing Temperature	71°C	23°C	71°C	23°C	71°C	23°C
Crush Strength, kg						
24 hrs	105.5	5.0	76.4	3.6	87.3	3.2
48 hrs	117.7	7.3	84.5	4.5	88.2	6.8
7 day	115.9	23.6	62.3	13.2	96.8	22.7
28 days	79.1	72.7	61.4	33.6	76.8	44.5
LA Abrasion Resistance						
Grade	B		B		B	
Loss at 28 days, %	28.52		34.3		28.95	
Soundness						
No Treatment						
Loss-Water Only Cycles	99.64%		nd		nd	
Treated						
Loss Magnesium Sulfate Sol. Cycles	8.22%		nd		nd	

nd – not determined *Bed ash prehydrated at 9% moisture

Table 15. Summary of the SYNAG Pelletizing Trials Using Plant D Fly Ash and Bed Ash

Plant D	Trial D-1		Trial D-2		Trial D-3		Trial D-4	
Mix Proportions, wt.%								
CFBC Fly Ash		57.02%		54.05%		55.35%		51.93%
CFBC Bed Ash*		14.26%		13.51%		13.84%		12.98%
Additive A				3.38%		3.46%		3.25%
Accelerator						0.87%		
Additive B								1.34%
Pan Water		23.52%		19.80%		21.23%		24.47%
Mixer Water		5.20%		9.26%		5.26%		6.04%
Total Water		28.72%		29.05%		26.48%		30.51%
TOTAL		100.00%		100.00%		100.00%		100.00%
Curing Temperature	23°C	71°C	23°C	71°C	23°C	71°C	23°C	71°C
Pellet Strength, kg								
Green	5.0	5.0	9.1	9.1	14.5	14.5	14.5	14.5
24 hrs	11.8	101.4	9.1	68.2	15.5	118.6	10.5	88.2
48 hr	18.6	99.1	13.6	68.2	31.8	133.6	28.2	96.8
7 days	143.2	110.9	118.2	86.4	162.3	155.5	126.4	100.0
28 days	150.0	118.2	136.4	86.4	176.4	147.7	171.8	100.9
90 days	169.5	108.2	136.4	77.3	185.9	140.0	155.0	100.0
wetted		133.6		121.8		172.7		161.8
LA Abrasion								
Grade	B	B	B	B	B	B	B	B
Loss, wt. %	19.4	27.5	20.1	28	12.7	17.2	16.8	24.2
Soundness								
Loss – Mg sulfate	-9.17%	-6.75%	-5.47%	-11.13%	0.12%	0.28%	-7.11%	-5.89%

*Bed ash prehydrated at 8% moisture

In summary, pelletizing trials were conducted using ashes from two plants representing Class C and Class F ashes. The aggregate produced appears to meet the basic ASTM and AASHTO requirements for normal-weight construction aggregate. The pelletized CFBC ash appears to meet ASTM and AASHTO specifications. Freeze-thaw durability is low and soundness durability is not within limits. With the addition of the SYNAG additive, the soundness properties have been shown to be within acceptable limits. Freeze-thaw properties are also expected to improve with SYNAG additive treatment. The properties of the SYNAG product are dependent upon the curing conditions. The addition of heat allows for the rapid hardening of the product within a 24-hour curing period.

8.0 SUMMARY

The results of the research and development program for the production of synthetic aggregate from fluidized bed combustion ashes, spray dryer ashes, and off-spec, as well as ASTM C-618 Class C and F conventional power plant ashes, have substantiated that the SYNAG process can successfully produce synthetic aggregate from Class C and Class F fly ashes that meets applicable ASTM and AASHTO standards as a normal-weight aggregate. Specific accomplishments and results include:

- Disclosures have been written and patent applications are being prepared. Copies of the disclosures have been supplied to the US DOE patent office. **Therefore, all information about the SYNAG process remains confidential to WRI and protected therein.**

- Pelletizing trials were conducted using ashes from a range of ashes representing FBC ashes and Class C and Class F ashes. The aggregate produced appears to meet the basic ASTM and AASHTO requirements for normal-weight construction aggregate.

- Properties of the SYNAG product are dependent upon the curing conditions.

- Specialized chemical additives required to control hydration reactions and aggregate properties have been tested. In addition, additives to make the SYNAG product lightweight are also available and appear to be effective.

- Process verification tests were conducted using the pelletized process option. The resulting product meets the ASTM and AASHTO specifications for construction aggregate.

9.0 REFERENCES

ASTM, 1990, *Annual Book of Standards*, Vol. 04-05, American Society of Testing Materials, Philadelphia, PA.

Bates, R.H. and J.A. Jackson, 1984, *Dictionary of Geological Terms*, 3rd ed. Anchor Press/Doubleday, Garden City, New York.

Bland, A.E., C.E. Jones, J.G. Rose and J.L. Harness, 1989, "Ash Management Options for AFBC," *Proc.,* 10th International Conference on Fluidized bed Combustion, San Francisco, CA, April 30-May 3, 1989, pp. 323-334.

Bland, A.E., R.K. Kissel and G.G. Ross, 1991, "Enhanced FBC Ash Management Using Pelletization." *Proc.,* 11th International Conference on Fluidized Bed Combustion, Montreal, April, pp. 871-876.

Bland, A.E., R. Cox, E.R. Lichty, A. Rowen, and R.A. Schumann, 1992, "Pelletizing Ash," U.S. Patent Number 5,137,753, August 11, 1992.

Bland, A.E., R. Cox, A. Rowen, E.R. Lichty, and R.A. Schumann, 1993, "Pelletization as an Ash Management Option for CFBC Ash Handling and Utilization," *Proc.,* 12th International Conference on Fluidized Bed Combustion, La Jolla, CA, May 8-13, 1993, pp. 1342-1350.

Bland, A.E., and A. Rowen, 1995, "Pelletization as a Mine Back-Haul or Aggregate production Ash Management Option" *Proc.,* 1995 International Ash Utilization Symposium, Lexington, KY, October 23-25, 1995.

Bolen, W.P., 1996, "Construction Sand and Gravel," U.S. Geological Survey–Minerals Yearbook 1996, http://minerals.er.usgs.gov/minerals/pubs/commodity/aggregates/.

Burnet, G. and A.J. Gokhale, 1987, "Experimental Studies of the Production of Lightweight Aggregate from Fly Ash/Coal Cleaning Refuse Mixtures," *Proc.,* 8th International Ash Utilization Symposium, EPRI-CS-5362, October 28-31, 1987, pp. 61-1 to 61-15.

Hay, P. and Rademaker, P.D., 1987, "AARDALITE An Economical Lightweight Aggregate from Fly Ash," *Proc.,* 8th International Ash Utilization Symposium, EPRI-CS-5362, October 28-31, 1987, pp. 57-1 to 58-7.

Styron, R.W., 1987, "Fly Ash Lightweight Aggregate: The AGGLITE Process," *Proc.,* 8th International Ash Utilization Symposium, EPRI-CS-5362, October 28-31, 1987, pp. 58-1 to 58-12.

Tepordel, V.V., 1996, "Crushed Stone," U.S. Geological Survey–Minerals Yearbook 1996, http://minerals.er.usgs.gov/minerals/pubs/commodity/aggregates/.

U.S. Department of the Interior, 1987, *Minerals Yearbook*, U.S. Bureau of Mines.

WRI-98-R017

WESTERN RESEARCH INSTITUTE

"Providing solutions to energy and environmental problems"

FINAL REPORT

CONDITIONING AND HYDRATION REACTIONS ASSOCIATED WITH CLEAN COAL TECHNOLOGY ASH DISPOSAL/HYDRATION

Prepared for
U.S. Department of Energy
Morgantown, West Virginia

June 1998

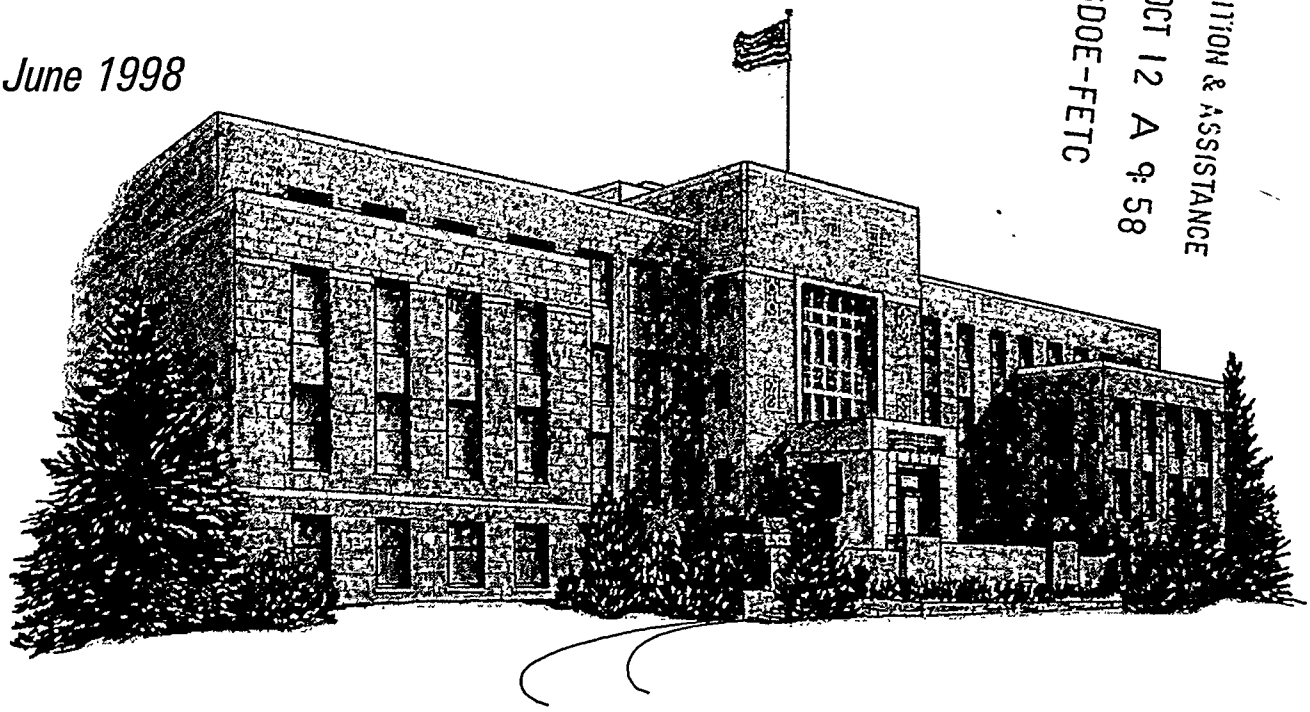

WRI-98-R017

CONDITIONING AND HYDRATION REACTIONS ASSOCIATED WITH CLEAN COAL TECHNOLOGY ASH DISPOSAL/UTILIZATION

Final Report

February 1994 – February 1998

By
Alan E. Bland

June 1998

Work Performed Under Cooperative Agreement
DE-FC21-93MC30126
Subtask 3.1

For
U.S. Department of Energy
Office of Fossil Energy
Federal Energy Technology Center
Morgantown, West Virginia

By
Western Research Institute
Laramie, Wyoming

DISCLAIMER

TABLE OF CONTENTS

LIST OF TABLES

LIST OF FIGURES

EXECUTIVE SUMMARY

The emergence of Clean Coal Technologies (CCT), such as fluidized bed combustion (FBC), sorbent injection, and sorbent spray dryers, has been rapid, and more than 100 CCT units are now in commercial operation, resulting in over 35 million tons of ash being generated annually in the United States. These CCT ash materials don't conform to the disposal and ash use practices currently employed for ashes produced from conventional power generating plants. These CCT ashes are distinctly different from conventional ashes due to the presence of partially sulfated sorbents and the operating conditions of the combustor, as in the case of FBC.

These chemical properties translate into differences in the geotechnical properties of the ashes. Certain CCT ashes have been shown to experience expansion during disposal and ash utilization. This expansion, or swelling, adversely affects disposal site stability, as well as the dimensional stability of the ashes during their use in construction applications. Although there is no agreement as to the exact nature of the chemical reactions that cause this expansion, it is generally agreed that the expansion and instability are a major obstacle to the use of the ashes and, ultimately, to the widespread commercial acceptance of clean coal technologies.

Western Research Institute (WRI), in cooperation with the U.S. Department of Energy (DOE), Federal Energy Technology Center (FETC), initiated a multi-year program to examine the relationship between CCT ash chemistry and geotechnical properties as they relate to ash disposal and utilization. The overall goal of the program was to develop the basis for processes whereby the hydration reaction chemistry, and thus the geotechnical properties, of the ash could be controlled under ash management situations. The investigation addressed the following:

- detailed characterization of the chemical, mineralogical, and physical properties of the as-produced ashes from several circulating fluidized bed combustion (CFBC) facilities operating on a range of coal and petroleum coke fuels;

- detailed conditioning investigation of the ashes to define the effect of preconditioning on the hydration of lime and other phases in the ash and the effect of the amount of conditioning on the geotechnical properties of strength and expansion;

- curing study of the conditioned and compacted ashes to determine the effect of curing conditions on the geotechnical and hydration phase chemistry of the ash; and

- an investigation of methods or processes to control these reactions and thereby stabilize these ashes.

The following results and milestones of the program have been determined:

Ash Characterization Investigation

A number of CFBC facilities agreed to supply ash from their units for the study. These include ashes from the combustion of the following fuels:

–Bituminous coal (4% sulfur) with limestone sorbent

–Bituminous coal (3% sulfur) with limestone sorbent

–Blend of bituminous coal (3% sulfur) and 25% petroleum coke (4.5% sulfur) with limestone sorbent

–Bituminous coal (1.8% sulfur) with limestone sorbent

–Subbituminous coal (0.9% sulfur) with limestone sorbent

–Petroleum coke (5-6% sulfur) with limestone sorbent.

Chemical characterization was conducted, including elemental, phase analysis, and leaching characteristics, as well as physical characterization, including bulk densities, specific gravities, and proctor moisture-density relationships of the ashes. The characterization effort employed a number of analytical techniques. X-ray fluorescence (XRF) and inductively coupled argon plasma analysis (ICAP) were used to determine the elemental composition of the ashes. High-resolution thermogravimetric analysis (TGA); X-ray diffraction (XRD) analysis and scanning electron microscopy (SEM) were used to determine the mineral phases present. Standard ASTM methods were employed to determine the physical properties and moisture-density relationships.

- The ashes were composed principally of compounds containing calcium and sulfur, which result from the addition of limestone sorbent and the subsequent capture of sulfur emissions during the combustion process and to a lesser extent, components inherent in the fuel (coal or petroleum coke) which remain after combustion.

- The composition of the ashes varied with the sulfur and ash content of the fuel used in the combustion process. The ashes resulting from the combustion of high-sulfur coals contained high percentages of sorbent-derived components, while those from the combustion of low-sulfur coals contained lower percentages. The composition of the petroleum coke-derived ash was predominantly sorbent-derived, since the petroleum coke has a very low ash content.

- The forms of calcium observed in the ashes confirmed the presence of large quantities of anhydrite [$CaSO_4$] and lime [CaO] and minor amounts of calcite [$CaCO_3$]. The presence of calcium ferrite phases was not confirmed in this study, although it is confirmed in the literature from previous studies.

Ash Conditioning Study

Conditioning tests were conducted on the ashes from each of the plants to determine the water addition required to hydrate most of the lime in the ash to dissipate the heat and swelling associated with this exothermic reaction prior to placement of the ashes into a landfill. Conditioning tests were conducted on the bed ash and fly ashes from each of the plants separately. Each ash was conditioned with a range of water additions. Fresh water was used for the tests to simulate the conditions at an operating plant. Water accounting practices were employed to account for the water as steam, residual moisture, and chemically bound water. The lime conversion was determined by XRD and TGA. The lime [CaO] and portlandite [$Ca(OH)_2$] XRD peak area intensities and the portlandite TGA data were used to determine lime conversion. Approximately 80% conversion was determined for the ashes. Testing concluded the following:

- The preconditioning level varied with the individual ash compositions. Water losses were a major part of the water added. The percentages of conditioning water added also increased with the lime content of the ash.

- ASTM D-698 and ASTM D-1557 moisture-density relationships were determined for the optimum conditioned and compacted ashes. ASTM D-698 optimum moistures ranged from 18% to 35%, and maximum dry densities ranged from 88 pcf to 116 pcf. ASTM D-1557 compactive effort resulted in a 15% relative reduction in moisture and a 7% increase in maximum dry density.

- Two ashes were preconditioned at different levels to ascertain the importance of preconditioning to the geotechnical properties of the ashes. Preconditioning of the ashes prior to secondary water addition and compaction had a significant effect on the strength development and expansion characteristics of the ash. Preconditioning enhanced strength development and reduced expansion for the ashes.

Ash Curing Conditions Study

Conditioned ash blends (blends of fly ash and bed ash from each of the plants in the proportions produced) were compacted to ASTM D-698 and D-1557 compactive effort and cured under different moisture levels and temperatures. The cured specimens were tested for strength development, expansion characteristics, and the development of hydration reaction products with time. Geotechnical properties such as strength development and expansion were determined for the conditioned ashes compacted under ASTM D-698 and D-1557 compactive effort and the conditioned and compacted ashes under sealed and saturated conditions at 23°C. The effect of temperature (23°C and 5°C) on the saturated curing of the ashes was also examined.

- The results of testing using high-sulfur coal-derived ashes showed enhanced strength development with time for the ASTM D-1557 conditioned and compacted ashes compared to

the ASTM D-698 ashes. The effect of compaction on expansion is not as clear, with only minor increases in expansion.

- The results showed increases in strength development with time for each of the ashes. The strength development varied with the type and characteristics of the ashes. The 23°C saturated curing resulted in increased strength for one of the ashes but resulted in long-term loss of strength for the high-sulfur coal-derived ashes. The application of cold (~5°C) saturated curing resulted in even further reduction of strength for these ashes.

- The results showed that expansion also increased with time for the medium- and high-sulfur coal-derived ashes. The low-sulfur coal-derived ashes and the petroleum coke-derived ashes did not show significant expansion with time. The expansion appears to be inversely related to strength development. As the strength decreased under saturated curing, the expansion increased significantly. The application of 5°C saturated curing resulted in further strength loss and increased expansion.

- Hydration reaction chemistry of the ashes after predetermined curing intervals under sealed and saturated curing was determined by X-ray diffraction and high resolution thermogravimetric analysis. The hydration reaction products appear to be principally the hydration of lime [CaO] to portlandite [$Ca(OH)_2$], the hydration of anhydrite [$CaSO_4$] to gypsum [$CaSO_4 \cdot 2H_2O$], and the precipitation of ettringite [$Ca_6Al_2(SO_4)_3(OH)_{12} \cdot 26H_2O$] from the soluble calcium, sulfates, and alumina. No thaumasite was noted in the specimens.

- The ashes appear to follow one of several hydration reaction trends: (1) ettringite-only development, (2) ettringite and/or gypsum early followed by later gypsum formation, or (3) gypsum-only formation.

- Testing has confirmed that the hydration reaction chemistry is related to the geotechnical properties of the ashes. The strength development appears to be related to ettringite and/or gypsum formation through pore filling and pore bridging. Expansion appears to be related to the formation of these same two minerals. The expansion increased with saturated curing and appears to be predominantly gypsum based.

- The formation and stability of the hydration reaction products, in particular the ettringite, appear to be controlled by the availability of reactants, as well as by the pH of the curing environment.

- Expansion was found to be related to strength development. Initially, strength increases with expansion. Thereafter, with continued expansion, strength losses were observed for the high-sulfur coal-derived ashes. This is consistent with a pore filling model.

- A pore filling model was found to be consistent with the observed relationships between hydration phases (ettringite and gypsum) and strength development and expansion, as well as SEM observations and void reduction observations. In the pore filling model, ettringite and/or gypsum are precipitated in the pores of the compacted ash, thereby providing strength until the pores become filled or bridged, after which excessive expansion and loss of strength occur. The expansion creates micro-cracks, causing strength loss and potential sites for further precipitation of hydration phases without further expansion. Micro-crack filling counteracts further strength loss, until filling and bridging result in further expansion and micro-crack formation. Under submerged conditions, certain of these hydration phases are believed to dissolve and re-precipitate, resulting in the initial strength loss upon saturation, followed by slow recovery of strength.

Development of Methods for Controlling Hydration Reaction Chemistry and Geotechnical Properties of the Ashes

Based on the results of the testing described above, conditions were defined for controlling the formation of the hydration reaction products that result in the geotechnical properties of the CFBC ashes. Two processes were reported that controlled the expansion associated with CFBC ashes.

- Invention disclosures have been written on these processes and methods of controlling the geotechnical properties of CFBC ashes

- The treatment methods effectively reduced or eliminated the expansive forces and unconfined expansion in the conditioned and cured ashes. There is a slight decrease in strength associated with certain of these treatments. However, strength remains sufficient for most disposal or ash reuse options.

1.0 INTRODUCTION

The power industry in the United States has traditionally been one of the largest generators of solid waste. The implementation of the required gaseous emissions control options for meeting the reduction goals of the Clean Air Act (CAA) and its Amendments has resulted in the rapid emergence and commercialization of Clean Coal Technologies (CCT), such as fluidized bed combustion (FBC), sorbent injection, and sorbent spray dryers. The emergence of these clean coal technologies has resulted, in turn, in an even higher generation of solid waste. In the United States over 100 CCT units are in commercial operation, generating more than 35 million tons of ash annually.

CCT ash materials don't conform to the disposal and ash use practices currently employed for ashes produced from conventional power generating plants. The disposal practices and ash re-use applications that have previously been applied to Class C and F fly ashes are not applicable to these CCT ashes. These CCT ashes are distinctly different from conventional ashes due to the presence of partially sulfated sorbents and the operating conditions of the combustor, as in the case of FBC.

These chemical properties translate into differences in geotechnical properties of the ashes. Certain CCT ashes have been shown to experience expansion during disposal and ash utilization. This expansion, or swelling, adversely affects disposal site stability, as well as the dimensional stability of the ashes during their use in construction applications. There is considerable and sometimes conflicting data on the hydration reactions that occur with CCT ashes. However, it is generally accepted that the hydration reactions that form portlandite, gypsum, ettringite, and thaumasite are the key reactions that control the geotechnical properties of CCT ashes. The formation of ettringite (and gypsum) has been attributed to the strength development, as well as the expansion, that occurs in FBC ashes. Although there is no agreement as to the exact nature of the chemical reactions that cause this expansion, it is generally agreed that the expansion and instability of the ashes are a major obstacle to their use, and ultimately to the widespread commercial acceptance of the clean coal technologies.

Methods to control these reactions must be found and processes developed for producing a stable ash product for either disposal or utilization. The development of such methods and processes requires an understanding of (1) the conditioning characteristics of CCT ashes and associated hydration reactions, (2) the stability of the reaction products, and (3) the response of these hydration reactions to chemical and physical modifications.

2.0 PURPOSE

Some preliminary assessments of the utilization potential of the CCT ashes have been made, but little effort has been directed toward determining the details of conditioning/hydration reactions. With this understanding, methods for controlling the reactions, and thereby controlling

the geotechnical properties of the conditioned ashes, can be developed. The research described herein has been focused on the definition of the chemical, physical, and geotechnical properties of the ashes as related to the development of methods to control these hydration reactions.

Western Research Institute (WRI), in cooperation with the U.S. Department of Energy (DOE), Federal Energy Technology Center (FETC), initiated a multi-year program to examine the relationship between CCT ash chemistry and geotechnical properties as they relate to ash disposal and utilization. The overall goal of the program was to develop the basis for processes whereby the hydration reaction chemistry, and thus the geotechnical properties of the ash, could be controlled under ash management situations. The investigation addressed the following:

- detailed characterization of the chemical, mineralogical, and physical properties of the as-produced ashes from several circulating fluidized bed combustion (CFBC) facilities operating on a range of coal and petroleum coke fuels;

- detailed conditioning investigation of the ashes to define the effect of preconditioning on the hydration of lime and other phases in the ash and the effect of the amount of conditioning on the geotechnical properties of strength and expansion;

- curing study of the conditioned and compacted ashes to determine the effect of curing conditions on the geotechnical and hydration phase chemistry of the ash; and

- an investigation of methods or processes to control these reactions and thereby stabilize these ashes.

3.0 BACKGROUND

The recent development of advanced combustion and emissions control technologies, such as clean coal technologies, for fossil fuel combustion has resulted in a new form of ash. These ashes are substantially different from the pulverized coal (PC) ashes typically marketed as ASTM Class C and F fly ashes. The properties of CCT ashes vary considerably according to fuel characteristics and the nature and process details of the sulfur emissions control technology employed. This is especially true for fluidized bed combustion technologies. One of the advantages of the FBC technology is the ability to use a variety of fuels (high- and low-sulfur coals, petroleum coke, mine and coal refuse, and even waste agricultural by-products). This results in the generation of ashes from FBC systems with a wide range of chemical, physical, and geotechnical properties. In addition, there are a number of FBC designs, including atmospheric fluidized bed combustion (bubbling bed and circulating bed) and pressurized fluidized bed combustion (bubbling and circulating systems). The operating conditions for these units, in addition to the design type and the fuel and sorbent characteristics, directly control the chemical characteristics and resultant physical and geotechnical properties of the ashes.

These fuel/sorbent and process operating characteristics result in differences in the composition of the CCT ash. For example, FBC ash is composed principally of components that are derived from (1) ash originating in the fuel and (2) sorbent-derived material and captured gaseous emissions. The fuel-derived ash is composed principally of quartz, iron oxides and calcined clays, while the sorbent-derived ash is composed of calcined sorbent (calcium oxide, calcium, and magnesium oxide if dolomite is used), uncalcined sorbent (calcite or dolomite), and sulfated sorbent (calcium sulfate). The ratios of these components are clearly dependent upon the fuel characteristics and the sorbent requirements. For example, the ashes from the high-sulfur fuels will contain a high proportion of sorbent-derived components. Petroleum coke-fired ashes are composed almost entirely of sorbent-derived ash since the petroleum coke contains very little ash itself. Each of these ashes contains significant amounts of calcined (CaO) and sulfated sorbent ($CaSO_4$).

The presence of these materials provides some unique properties to the ashes, including the exothermic character of the ash upon contact with water and the tendency to hydrate and harden into a solid mass. The coal-derived ash components are typical of ashes from pulverized coal units and from sorbent injection technologies but are not typical of ash from fluidized bed combustion technologies. The FBC coal ashes are different because of the lower temperatures of combustion (843°C/1550°F for FBC and 1371°C/2500°F for PC). The result is that the FBC ash is not glassy (which is typical of PC ashes). Instead, it is composed of dehydroxylated (calcined) clays and other minerals in their oxide forms. A summary of the effect of fuel characteristics on ash composition is presented in Table 1.

Table 1. Summary of Effect of Fuel Composition on FBC Ash Composition*

Fuel Type	Bituminous Coal	Bituminous Coal	Subbituminous Coal	Petroleum Coke
Fuel Ash (%)	12	6	8	<0.25
Fuel Sulfur (%)	3.5	1.5	0.5	3.0
Ash Composition (%)				
Free Lime (CaO)	23.81	25.19	10.55	35.65
Sulfated Sorbent ($CaSO_4$)	38.38	34.47	16.56	57.77
Uncalcined Sorbent ($CaCO_3$)	1.38	2.89	4.16	2.42
Fuel Derived Ash	34.40	36.04	69.27	1.26

* Assumes the SO_2 reduction of 90% and Ca/S ratio of 2.3 for high-sulfur fuels, 2.6 for medium-sulfur fuels and 2.6 for low-sulfur fuels (not including inherent calcium).

It is clear that the composition of ashes from clean coal technologies such as FBC is highly dependent upon the fuel, combustion system/gaseous emissions control configuration, and sorbent requirements. The ash management practices and ash use options are therefore highly dependent upon the source and resultant composition of the ash.

Certain CCT ashes have been shown to expand during disposal or utilization (Bigham et al. 1993, Wolfe, et al. 1992, Beeghly, et al. 1993, Bland et al. 1989b, 1991, Burwell, et al. 1993, Georgiou, et al. 1991 and 1993). This expansion, or swelling, adversely affects disposal site stability, as well as the dimensional stability of the ashes during their use in construction applications.

There are considerable and sometimes conflicting data on the hydration reactions that occur with CCT ashes. It is, however, generally accepted that the hydration reactions that form portlandite, gypsum, ettringite, and thaumasite are also the key reactions that control geotechnical properties. These hydration reactions have been studied for a number of years (Berry, et al. 1991, Bland, et al. 1989b,c, 1991, 1993, Iribarne, et al. 1993, Blondin, et al. 1993, and Anthony et al. 1995, 1997).

A number of studies of the geotechnical properties of CCT ashes have also been conducted (Georgiou, et al. 1991, 1993, Hopkins, et al. 1993). The degree of expansion reported appears to be dependent on a number of variables, including the nature of the fuel being combusted. Over the last decade, Bland and others have reported on the value of an ash pre-conditioning step in preventing lime hydration from occurring in the compacted ash product. In fact, with TVA FBC ash, Bland (1989b) has shown that expansion can be reduced from more than 10% to less than 0.5% with proper conditioning. Bland et al. (1991b) also reported that ettringite was responsible for strength development, but it was not the amount of ettringite formed that was important; it was the timing of the ettringite formation.

The research described herein has focused on the definition of the chemical, physical, and geotechnical properties of the ashes. There have been some preliminary assessments of the conditioning/hydration reactions as related to developing methods for controlling the reactions, and thereby the geotechnical properties, of the conditioned ashes.

4.0 METHODOLOGY

WRI, in cooperation with the DOE Federal Energy Technology Center, initiated a multi-year program to examine the impact of CCT ash chemistry and geotechnical properties as they relate to ash disposal and utilization. The overall goal of the program was to develop the basis for processes whereby the hydration reaction chemistry, and thus the geotechnical properties of the ash, could be controlled under ash management situations. The investigation addressed the following:

- detailed characterization of the chemical, mineralogical, and physical properties of the as-produced ashes from several circulating fluidized bed combustion (CFBC) facilities operating on a range of coal and petroleum coke fuels;

- detailed conditioning investigation of the ashes to define the effect of preconditioning on the hydration of lime and other phases in the ash and the effect of the amount of conditioning on the geotechnical properties of strength and expansion;

- curing study of the conditioned and compacted ashes to determine the effect of curing conditions on the geotechnical and hydration phase chemistry of the ash; and

- an investigation of methods or processes to control these reactions and thereby stabilize these ashes.

5.0 RESULTS AND DISCUSSION

The research and development program was composed of the following components, or tasks:

- Chemical and Physical Properties of As-Received Ashes;
- Ash Conditioning Study;
- Effect of Compactive Effort on Geotechnical Performance;
- Changes in Geotechnical and Hydration Reaction Properties of Ashes During Sealed and Saturated Curing;
- Changes in Geotechnical and Hydration Reaction Properties of Ashes During Curing at 23°C and 5°C;
- Correlation Between Hydration Reaction Product Development and Geotechnical Properties of Ash with Curing;
- Correlation Between Strength and Expansion and the Development of the Pore Filling Model; and
- Methods for Controlling CFBC Ash Geotechnical Properties.

5.1 Methods Used for the Study

American Society for Testing and Materials (ASTM) standard geotechnical testing methods modified for the CFBC ashes were used for the study. The methods used for the geotechnical, geochemistry, and hydration reaction phase analyses are described below.

5.1.1 General Physical Properties of the Raw Ash

Physical properties such as particle size, bulk densities, and specific gravities were determined according to ASTM C-311.

5.1.2 Moisture-Density Relationships

Moisture-density relationships were determined according to ASTM D 698 and D 1557. The two methods represent a difference in compactive effort of approximately 2.5 times.

5.1.3 Curing Conditions

A blend of the fly ash and bed ash from each of the plants was conditioned and compacted at the ASTM D-698 optimum moisture content. Unconfined compressive strength specimens and expansion bars were fabricated. The specimens were cured under sealed conditions and saturated conditions at 23°C. Under sealed conditions, the specimens were placed in plastic bags and containers to prevent the ingress or egress of moisture to or from the specimens. Under saturated conditions, the specimens were submerged in a saturated bath of the ash solution. A 10:1 water to ash solution was made for the submergence of the specimens. The specimens were saturated after 14 days of sealed curing. These conditions were considered to represent the extremes that the ash would encounter during either disposal or ash re-use. The curing period extended 90 to 104 days (strength) and 180 to 365 days (expansion). Specimens were removed from the curing chambers at predetermined ages and tested for geotechnical properties (strength and expansion) and hydration phase composition.

5.1.4 Unconfined Compressive Strength

Cubes 50.8 mm (2 in.) were fabricated from the conditioned ash blends using the optimum moisture and compaction density as determined by the ASTM D-698 moisture-density relationship testing. Strength was determined for the sealed specimens at 1, 3, 7, 14, 28, 56, and 90 days; and at 15, 17, 21, 28, 42, 70, and 104 days for the two saturated or submerged specimens. Modified ASTM C-109 method was used for unconfined compressive strength determinations.

5.1.5 Expansion Characteristics

Bars 2.54 cm (1 in.) square by 29.85 cm (11 ¾ inch) long were fabricated from the conditioned ash blends using the optimum moisture and compaction density as determined by the ASTM D-698 moisture-density relationship testing. Expansion bars were tested on a daily basis for the first 28 days and then at 56, 90, 180, and 365 days for the sealed cured specimens and at 42, 79, 104, 180, and 365 days for the two saturated specimens. Modified ASTM C-157 method was used for expansion determinations.

5.1.6. Chemical Characterization of Raw Ashes

Characterization methods have been developed for evaluating CFBC ashes and include those methods developed by Iribarne (1991, 1993 and Anthony et al. 1995). The chemical characterization focused on the elemental composition, including the major elements, presented as oxides. X-ray fluorescence (XRF), inductively coupled plasma spectrometry (ICPS), atomic absorption spectrometry (AAS), and a range of wet chemical methods were employed in the determination of the major elemental composition of the ashes. In addition to the elemental analysis, the mineral phases in the fly ash and bed ash were also determined by X-ray diffraction and thermogravimetric analysis (TGA).

5.1.7 Hydration Reaction Products

Determination of the hydration reaction chemistry of CCT ashes has been one of the analytical problems. WRI evaluated available methods as part of this study. A range of analytical techniques have been employed, including X-ray diffraction (XRD), thermogravimetric analysis, differential thermal analysis (DTA), differential scanning calorimetry (DSC), scanning electron microscopy (SEM), scanning electron microscopy with energy dispersive X-ray analysis (SEM/EDAX), and magic-angle spinning-nuclear magnetic resonance (MAS-NMR).

X-ray diffraction is an analytical technique that has been used for decades in the identification of the mineral phases in rocks and other materials. A Scintag powder diffractometer with Cu target tube was used for the analysis of the ettringite and ettringite/gypsum mixtures synthesized. XRD is a valuable analytical tool for defining the individual phases. However, attempts to use XRD to quantify the hydration phases have been hampered by mass absorption and preferred orientation problems.

Thermogravimetric analysis is often employed for the quantification of mineral phases. TGA involves the ramped heating of the material under a controlled nitrogen atmosphere. The weight loss is proportional to the amount of volatile decomposition of the individual mineral phases. The integrated area under the curve is proportional to the quantity of the mineral phase. However, with conventional TGA analysis, the gypsum peak shows as a small peak on the ettringite peak. Curve fitting and deconvolution routines are necessary to quantify the individual minerals.

A relatively new technique has been developed, termed high-resolution TGA. This technique is similar to the conventional TGA except that the ramping rate for the heating of the sample is variable. The result is a sharp, highly resolved weight loss curve. This technique provides for the high resolution of the gypsum and ettringite phases, allowing quantification without employing elaborate curve fitting and deconvolution routines.

Scanning electron microscopy with energy dispersive X-ray analyzer has also been used to assist in the definition of the mineral phases present in CCT ashes. With SEM/EDAX, one can

identify the individual mineral phases, as well as their morphological form and association. For example, the Al/Si ratio using EDAX of the ettringite crystals could be useful in identifying the ettringite/thaumasite solid solution series.

The present study employed XRD, high resolution TGA, and SEM techniques for the determination of the hydration reaction phases in the CCT ashes.

5.2 Ash Sources

Several high- and low-sulfur fuel-derived ash pairs were selected for evaluation from CCT facilities representing a variety of different clean coal technologies and fuel types. Ashes from coal and petroleum coke-fired facilities were selected, representing atmospheric fluidized bed combustors (AFBC).

A number of circulating fluidized bed combustion facilities supplied ash from their units for the study. The identity of the units is to be kept confidential, but the sources can be described by the type and composition of the fuel they are burning. The plants are identified as follows:

C-1 – Bituminous coal (4% sulfur), limestone sorbent

C-2 – Bituminous coal (3% sulfur), limestone sorbent

C-3 – Blend of bituminous coal (3% sulfur) and 25% petroleum coke (4.5% sulfur), limestone sorbent

C-4 – Bituminous coal (1.8% sulfur), limestone sorbent

C-5 – Subbituminous coal (0.9% sulfur), limestone sorbent

C-6 – Petroleum coke (5-6% sulfur), limestone sorbent

5.3 Chemical and Physical Properties of As-Received Ashes

The chemical, physical, and geotechnical properties of the CFBC ashes have been shown to be quite variable. As a result, the disposal practices, as well as the ash use potential, are very site- (coal) and technology-specific. Objectives of this testing were to determine relationships between the chemical and physical properties of the ashes and the geotechnical properties of the conditioned and compacted ashes. The disposal and utilization of CFBC ash requires a detailed understanding of the chemical speciation and distribution of phases, specifically the forms of calcium. This portion of the study addressed the chemical composition of the individual residue streams and characterized the physical properties and determined the respective mineral phases within the combustion residue. The chemical, mineral phase, leachate, and physical characterization study was performed on composites of each of the fly ashes and bed ashes from each of the plants.

5.3.1 Chemical Characterization.

Chemical characterization was conducted on the fly ash and bed ash from each plant. The chemical characterization testing included major element composition, as well as phase analysis.

The chemical analyses presented in Table 2 show the bed ash to be generally composed of more calcium and SO_3 than the fly ash. In addition, there is a general decrease in these components with decreasing sulfur content of the fuel burned. Fuel ash contributes silica, alumina, and certain amounts of alkalis. The ash from the petroleum coke-fired unit (Plant C-6) shows very low amounts of fuel-derived components, such as iron, silica, and alumina. This reflects the low ash content of the petroleum coke burned in this unit.

Table 2. Summary of the Chemical Composition of CFBC Ashes

Plant	Plant C-1		Plant C-2		Plant C-3		Plant C-4		Plant C-5		Plant C-6	
Ash Type	FA	BA	FA	BA	FA	BA	FA	BA	FA	BA	FA	BA
Chemical Properties												
Moisture	0.08	0.03	0.35	0.16	<0.01	0.02	0.29	0.06	0.10	0.10	0.21	0.04
LOI	4.14	0.46	6.86	1.83	2.99	1.04	8.87	1.24	2.62	5.10	5.00	2.59
SiO_2	14.61	7.85	11.44	8.84	14.53	6.81	37.27	11.12	45.95	53.15	2.29	3.12
TiO_2	0.27	0.17	0.31	0.17	0.33	0.10	0.98	0.40	1.33	0.51	0.06	0.08
Al_2O_3	6.89	4.14	14.37	3.22	5.85	2.65	21.08	5.49	23.61	15.30	1.67	1.53
Fe_2O_3	10.93	4.08	5.34	4.87	6.18	2.62	5.48	1.32	2.61	1.71	0.12	0.21
CaO	40.39	51.38	40.49	47.10	42.86	49.74	17.83	42.53	17.09	19.00	54.79	47.04
MgO	1.49	1.77	0.65	0.73	2.41	2.82	0.82	0.91	0.77	0.77	2.13	2.31
K_2O	0.76	0.18	0.38	0.21	0.76	0.19	1.64	0.40	0.66	0.56	0.02	0.01
Na_2O	0.64	0.85	0.25	0.15	0.55	0.41	0.43	0.90	0.31	0.62	0.73	0.08
P_2O_5	0.47	0.54	0.01	0.03	0.84	0.95	0.25	0.48	0.14	0.16	0.61	0.55
SO_3	19.06	28.36	20.48	32.74	19.55	32.57	4.82	34.48	4.71	2.99	32.50	42.43
Total	99.7	99.8	100.6	99.34	96.9	99.9	99.5	99.3	99.8	99.9	99.9	100.0

FA – Fly Ash, BA – Bed Ash

Phase Analysis

The fly ash and bed ashes from each of the plants were analyzed by XRD for phase analysis, and the peak area intensities are presented in Table 3. X-ray diffraction is a common method of determining crystalline phases in a solid sample. The peak area intensities are proportional to the relative concentration of the phases present in the ashes. The method generally has a detection limit of approximately 1%. It is considered to be semiquantitative since problems with quantification resulted from preferred orientation and peak overlap and mass absorption issues.

Table 3. XRD Peak Area Intensity of Phases Present in Raw Ash Blends

Intensities of Strongest Peak, angstroms (1)	Plant C-1		Plant C-2		Plant C-3		Plant C-4		Plant C-5		Plant C-6	
Ash Type (2)	FA	BA	FA	BA	FA	BA	FA	BA	FA	BA	FA	BA
Ettringite (9.73)	nd (3)	nd	nd	nd	nd	nd	nd	nd	nd	nd	nd	nd
Gypsum (7.63)	nd	nd	nd	nd	nd	nd	nd	nd	nd	nd	nd	nd
Anhydrite (3.50)	4089	4695	3704	6492	4788	7475	1245	7121	1497	632	7000	9664
Approx. wt.% (4)	35	40	32	55	41	64	11	61	13	5	60	82
Quartz (3.34)	641	263	803	605	1127	497	3431	1261	6278	10142	nd	263
Hematite (2.70)	nd	nd	939	nd	nd	nd	nd	nd	nd	nd	nd	nd
Calcite (3.04)	529	nd	1037	nd	nd	nd	nd	nd	nd	nd	nd	nd
Portlandite (2.63)	nd	nd	nd	nd	nd	761	nd	nd	nd	nd	nd	nd
Lime (2.41)	3122	4188	2279	2740	2459	2339	732	2855	1821	2742	5095	3249
Approx. wt.% (4)	18	24	13	16	14	14	4	17	11	16	29	19

(1) Peak Area Intensities Reported

(2) FA – Fly Ash, BA – Bed Ash

(3) nd – not detected

(4) semiquantitative analysis of XRD data

The data confirm the observation that the ashes are composed principally of anhydrite[$CaSO_4$], lime [CaO], quartz [SiO_2], and associated oxides of iron, magnesium, and dehydroxylated clays originating from the fuel ash components.

As expected, the bed ash generally shows a higher intensity for the anhydrite than the fly ash, indicating a higher concentration. In addition, the XRD data for the bed ash show no evidence of the minerals calcite and hematite, these minerals being found only in the fly ash. No hydration phases of the minerals, such as gypsum and ettringite, were noted from the diffractograms. Only minor amounts of portlandite were found in one of the ashes.

TCLP Tests

Leachate characteristic as per the Resource Conservation and Recovery Act (RCRA) Toxic Characteristics Leaching Procedure (TCLP) were also determined. The results of the TCLP testing are presented in Table 4. The data show the ashes to be benign with respect to these RCRA metal concentrations.

Table 4. RCRA Metals Concentrations* in TCLP Leachate Extracts

	RCRA Limits, ppm	Plant C-1		Plant C-2		Plant C-3		Plant C-4		Plant C-5		Plant C-6	
		Fly Ash	Bed Ash	Fly Ash	Bed Ash	Fly Ash	Bed Ash	Fly Ash	Bed Ash	Fly Ash	Bed Ash	Fly Ash	Bed Ash
Initial pH	na	12.7	12.5	12.7	12.6	12.3	12.1	10.4	12.5	12.5	12.5	11.5	11.8
Final pH	na	12.7	12.5	12.7	12.5	12.3	12.1	10.4	12.5	12.4	12.5	11.6	11.9
Arsenic	5.0	0.004	0.013	0.039	0.007	0.006	0.007	0.063	0.009	0.003	0.001	<0.005	<0.005
Barium	100.0	0.41	0.36	0.57	0.70	0.33	0.40	0.50	0.59	0.18	0.19	0.10	0.02
Cadmium	1.0	<0.001	<0.001	<0.001	0.002	<0.010	<0.010	<0.001	<0.001	0.007	<0.001	<0.010	<0.010
Chromium	5.0	<0.001	<0.001	<0.001	0.005	0.066	<0.008	0.007	<0.001	0.016	<0.001	0.011	0.011
Lead	5.0	<0.500	<0.500	<0.500	<0.500	<0.500	<0.500	<0.500	<0.500	<0.500	<0.500	<0.500	<0.500
Mercury	0.2	<0.002	<0.002	<0.002	<0.002	<0.002	<0.002	<0.002	<0.002	0.005	<0.002	<0.002	<0.002
Selenium	1.0	<0.200	<0.200	<0.200	<0.200	<0.200	<0.200	<0.200	<0.200	<0.200	<0.200	<0.200	<0.200
Silver	5.0	<0.01	<0.01	<0.01	<0.01	<0.01	<0.01	<0.01	<0.01	<0.01	<0.01	<0.01	<0.01

na – not applicable

* Modified to reflect the different detection limits reported by the various laboratories

5.3.2 Physical Properties Testing

The physical properties of the CFBC ashes, including specific gravity, minimum and maximum bulk density (poured and packed), as well as strength development and dimensional stability (expansion/swelling), were also determined according to appropriate ASTM procedures.

Bulk densities of the various CFBC ashes have been determined, and the data are presented in Table 5. Bulk densities are quite variable, and minimum or poured bulk densities ranged from 656.8 kg/m^3 (41.0 pcf) to 1163.1 kg/m^3 (77.6 pcf) for the fly ashes and from 1137.4 kg/m^3 (71.0 pcf) to 1557.1 kg/m^3 (97.2 pcf) for the bed ashes. Maximum or packed bulk densities ranged from 821.8 kg/m^3 (51.3 pcf) to 1376.1 kg/m^3 (85.9 pcf) for the fly ashes and from 1432.2 kg/m^3 (89.4 pcf) to 1715.7 kg/m^3 (107.1 pcf) for the bed ashes.

Table 5. Summary of Specific Gravity and Bulk Density Data

	Specific Gravity g/cc		Minimum Density kg/m^3 (pcf)		Maximum Density kg/m^3 (pcf)	
	Fly Ash	Bed Ash	Fly Ash	Bed Ash	Fly Ash	Bed Ash
Plant C-1	2.91	2.99	994.8 (62.1)	1523.5 (95.1)	1235.1 (77.1)	1616.4 (100.9)
Plant C-2	2.93	2.99	1020.5 (63.7)	1557.1 (97.2)	1376.1 (85.9)	1715.7 (107.1)
Plant C-3	2.63	2.55	712.9 (44.5)	1137.4 (71.0)	972.4 (60.7)	1480.2 (92.4)
Plant C-4	2.55	2.87	656.8 (41.0)	1449.8 (90.5)	764.2 (47.7)	1528.3 (95.4)
Plant C-5	2.69	2.49	706.5 (44.1)	1336.1 (83.4)	821.8 (51.3)	1432.2 (89.4)
Plant C-6	2.86	2.82	1163.1 (72.6)	1459.4 (91.1)	1324.9 (82.7)	1517.1 (94.7)

In addition to the bulk densities, the CFBC ashes were subjected to ASTM C-311 testing for pozzolanic properties. The results for the fly ashes from each of the plants are presented in Table 6.

Table 6. ASTM C-311 Test Data for CCT Fly Ashes

Plant Designation	Plant C-1	Plant C-2	Plant C-3	Plant C-4	Plant C-5	Plant C-6	ASTM Class F*	ASTM Class C*
Physical Properties**								
Fineness, % retained 325 mesh	30.07	na	31.0	22.63	31.64	58.07	34 max	34 max
Pozzolanic Activity Index, 28 days, %	71.8	na	69.0	97.5	84.5	50.1	75 min	75 min
Water Requirement, % of control	100.0	na	103.3	109.1	103.3	104.1	105 max	105 max
Soundness-Autoclave Expansion, %	0.016	na	0.031	0.040	0.043	0.051	0.8 max	0.8 max
Drying Shrinkage, %	0.057	na	na	0.005	0.000	0.046		

* Conducted according to ASTM C-311

** Specifications according to ASTM C-618.

na – not available

5.4 Ash Conditioning Tests

The addition of water to improve the handling and disposal characteristics of CFBC residue has been well established in the literature and in practice (Bland, 1989, 1990; Minnick, 1982). The main purpose of the conditioning is to ameliorate the initial exothermic reactions associated with the hydration of free lime in the residue. Conditioning is also designed to convert a large portion (i.e., >80%) of the free lime to calcium hydroxide, in order to reduce the potential swelling associated with the lime hydration. In addition, conditioning has been applied at many of the plant sites for dust control. Water is also provided as needed to facilitate adequate compaction of the ash and to promote the longer term hydration reactions in the landfill. This latter water addition is explained in the following section and is not considered part of this ash conditioning. WRI has established the use of an ash preconditioning step. Basically, the ash is conditioned with enough water to effect a partial conversion of the free lime in the ash. This level is typically 75-80%. The preconditioned ash is allowed to hydrate, heat up, steam, and cool down before further processing is attempted.

The conditioning of CFBC ash is influenced by a number of variables, including the nature and characteristics of the CFBC ash, the temperature of the ash, the type and size of the conditioning equipment, and to a lesser extent the chemical characteristics of the conditioning water. Conditioning tests are usually conducted at room temperature, even though the ash from the silo is at elevated temperatures. The percentage of water addition and the amount of steaming and free lime hydration at a given water addition have been shown to differ between the room-temperature and elevated conditioning scenarios. As a result, the water requirements and temperature profiles associated with laboratory-scale conditioning tests do not always correlate

with commercial-scale equipment performance. WRI has developed a protocol for the conditioning of the CFBC ashes, which was used in this testing.

Conditioning tests addressed the fly ash and the bed ash separately. Each of these ashes were conditioned with a range of water amounts. Ash temperature and weight loss during curing due to steaming were recorded for a period of 30 minutes. The conditioned ash samples were acetone dried to determine the amount of unreacted (residual) moisture. Fresh water was used as the conditioning medium. Since the performance basis of the proposed conditioning tests is compositional (i.e., water required to achieve 80% lime conversion), room-temperature conditioning was employed in the conditioning tests. The fly ash and the bed ash were conditioned at five different water addition levels. Temperature profiles were recorded. A representative split of the conditioned ashes were acetone dried at 45°C to terminate hydration reactions after 30 minutes. Water accounting practices were used to balance the amount of steam generation, residual moisture, and chemically bound water. The acetone-dried samples were analyzed by XRD and TGA to determine the amount of lime [CaO] and portlandite [$Ca(OH)_2$] they contained. Based on the target of 80% conversion of the lime to portlandite, the amount of conditioning water was determined for each of the ashes.

The optimum conditioning percentages for each of the fly ashes and bed ashes tested in this study are presented in Table 7. For those fly ashes with relatively low concentrations of lime, no preconditioning of the ash was used.

Table 7. Optimum Conditioning Levels for the Ashes from Each of the Plants

	Plant C-1 % Water	Plant C-2 % Water	Plant C-3 % Water	Plant C-4 % Water	Plant C-5 % Water	Plant C-6 % Water
Fly Ash	16	8	0	0	0	11
Bed Ash	14	8	18	10	6	21
Ash Blend	nd	8	nd	nd	nd	nd

nd – not determined

An example of the method of analysis of the degree or percentage conversion of lime to portlandite is presented in Figure 1. The results of lime and portlandite XRD analysis of the conditioned ash are plotted as a function of the water addition.

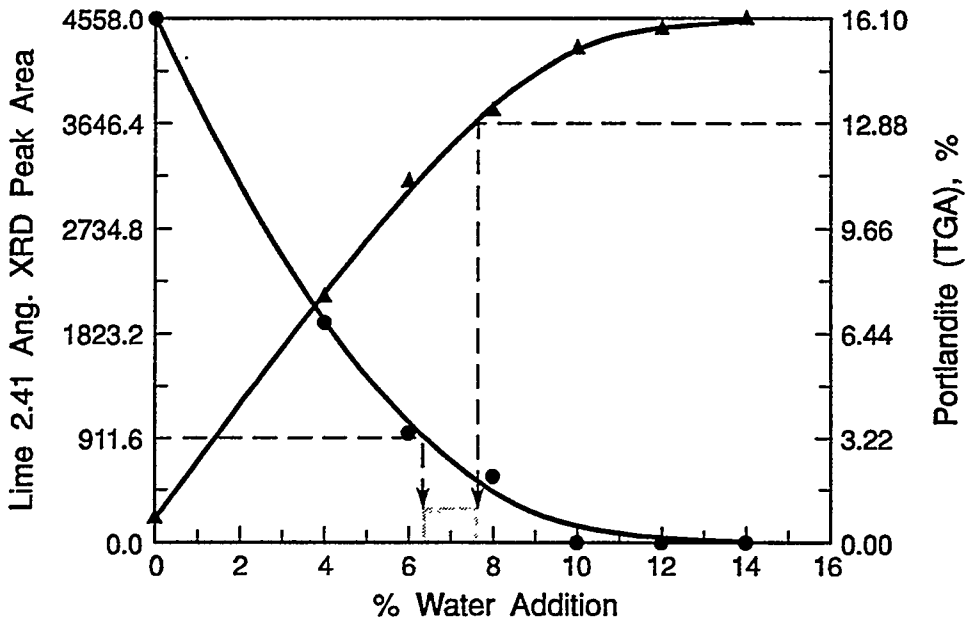

Figure 1. Relationship Between Lime and Portlandite XRD Peak Area Intensity with Preconditioning Level for a High-Sulfur Coal-Derived Fly Ash and Bed Ash

XRD analysis of the conditioned ashes indicated that the primary hydration reaction that occurred was the hydration of CaO to $Ca(OH)_2$. There was evidence in some conditioned ashes of the carbonation of a small portion of the lime to calcite during the conditioning and sample drying process. XRD data indicated that no ettringite or gypsum was present in the conditioned ash blend, although very minor weight losses that might be attributable to ettringite and/or gypsum were noted on the TGA scans.

ASTM D-698 moisture-density relationships were conducted to determine the optimum moisture and maximum dry density of the conditioned and compacted ashes. The results are presented in Table 8. ASTM D-698 optimum moistures for the fly ashes were in the range of 15 to 35%, with associated maximum dry densities in the range of 1409.7 kg/m^3 (88.0 pcf) to 1869.5 kg/m^3 (116 pcf). It was also obvious that the fly ash and the ash blend (blend of fly ash and bed ash in proportions generated) had quite distinct properties.

ASTM D-1557 moisture-density relationships were determined for the two high-sulfur coal-derived ashes (Plant C-1 and C-2) and are presented in Table 8. The data show typical results, with a decrease in the optimum moisture and an increase in the maximum dry density. ASTM D-1557 compactive effort resulted in a 15% relative reduction in moisture and a 7% increase in maximum dry density.

Table 8. Summary of the Results of the ASTM Moisture-Density Relationship Testing

	ASTM D-698		ASTM D-1557	
	Optimum Moisture, %	Max. Dry Density, kg/m^3 (pcf)	Optimum Moisture, %	Max. Dry Density, kg/m^3 (pcf)
Plant C-1	18.1	1624.4 (101.4)	15.6	1741.4 (108.7)
Plant C-2	17.7	1738.2 (108.5)	14.4	1850.3 (115.5)
Plant C-3	26.4	1409.8 (88.0)	nd	nd
Plant C-4	30.7	1783.0 (111.3)	nd	nd
Plant C-5	35.6	1706.1 (106.5)	nd	nd
Plant C-6	19.0	1869.5 (116.7)	nd	nd

nd – not determined

The hydration of the free lime can be detrimental to the dimensional stability of the conditioned and compacted ash in either landfill disposal or re-use applications. There has been an ongoing controversy concerning the need for essentially complete hydration of the lime to attain stable ashes for disposal or use. A set of tests were conducted to illustrate the effect of conditioning on the strength and expansion of two CFBC ashes. Table 9 presents the results of this testing.

Table 9. Effect of Preconditioning on the Geotechnical Properties of Conditioned and Compacted Low and High-Sulfur Coal-Derived CFBC Ashes

	Low-S Ash	Low-S Ash	Low-S Ash	High-S Ash	High-S Ash
Bed Ash Preconditioning	0 %	3 %	6 %	6%	18%
Density, kg/m^3	1382.7	1396.3	1358.2	1384.0	1365.1
Unconfined Compressive Strength, MPa					
7 days	4.2	4.0	4.2	8.8	8.5
28 days	4.0	3.3	4.5	7.0	8.9
90 days	4.7	4.7	4.7	9.1	9.2
Saturated Expansion (%)					
7 days	0.162	0.0423	0.111	0.323	0.231
28 days	0.164	0.0423	0.110	0.325	0.231
90 days	0.165	0.0433	0.111	0.329	0.234

Linear expansion measured after curing in a saturated bath of the ash
1000 psi = 6.9 MPa

A low-sulfur coal-derived CFBC ash blend and a high-sulfur coal-derived CFBC ash blend were preconditioned at different levels. Ash blends are the physical combination of the fly ash and bed ash in the relative proportions as produced at the plant. The strength and saturated expansion of the conditioned and compacted ash at various curing times is presented.

The data show a decrease in strength for the ashes with low preconditioning levels. In addition, the expansion associated with those ashes with low levels of preconditioning also increases.

Researchers (Blondin et al. 1993) have argued that complete hydration of the lime is required for a stable ash product. Others (Bland et al. 1989a,b,c, 1993) have argued that most of the lime needs to be prehydrated but not necessarily 100% of it. This controversy has led to the development of conditioning processes with distinctly different chemical approaches (Blondin et al. 1993, and Bland et al. 1991, 1993). Based on the data generated in this study, it appears that a preconditioning level of approximately 75 to 80% is warranted to provide higher strength development and lower expansion.

5.5 Effect of Compactive Effort on Geotechnical Properties of Ash

To assess if the compactive effort has a significant effect on the unconfined compressive strength for the CFBC ashes, a series of tests were conducted on the two high-sulfur coal-derived ashes from Plants C-1 and C-2. The results of testing of high-sulfur coal-derived ashes conditioned and compacted to ASTM D-698 and ASTM D-1557 compactive efforts are presented in Table 10 and Figure 2.

Table 10. Strength Development Data for High-Sulfur Coal-Derived CFBC Ashes Conditioned and Compacted at ASTM D-698 and ASTM D-1557 Compactive Efforts

Curing Age	Plant C-1 Unconfined Compressive Strength, MPa				Plant C-2 Unconfined Compressive Strength, MPa			
	D-698 Sealed	D-698 Saturated	D-1557 Sealed	D-1557 Saturated	D-698 Sealed	D-698 Saturated	D-1557 Sealed	D1557 Saturated
1 day	1.0		1.5		0.8		2.0	
3 days	1.8	Saturated	3.8	Saturated	2.4	Saturated	4.2	Saturated
7 days	6.9	After	11.2	After	5.8	After	9.9	After
14 days	13.4	14 days	20.6	14 days	12.0	14 days	18.0	14 days
15 days		11.5		25.6		10.7		14.5
17 days		13.6		18.2		12.1		10.4
21 days		16.4		27.2		14.7		18.1
28 days	20.6	18.5	31.0	22.2	19.2	17.5	25.2	23.2
42 days		19.4		24.8		20.1		24.7
56 days	24.0		35.2		26.8		30.6	
70 days		21.7		24.5		21.0		29.2
90 days	26.0		41.2		32.7		32.4	
104 days		17.3		26.4		24.0		29.0

1000 psi = 6.9 MPa

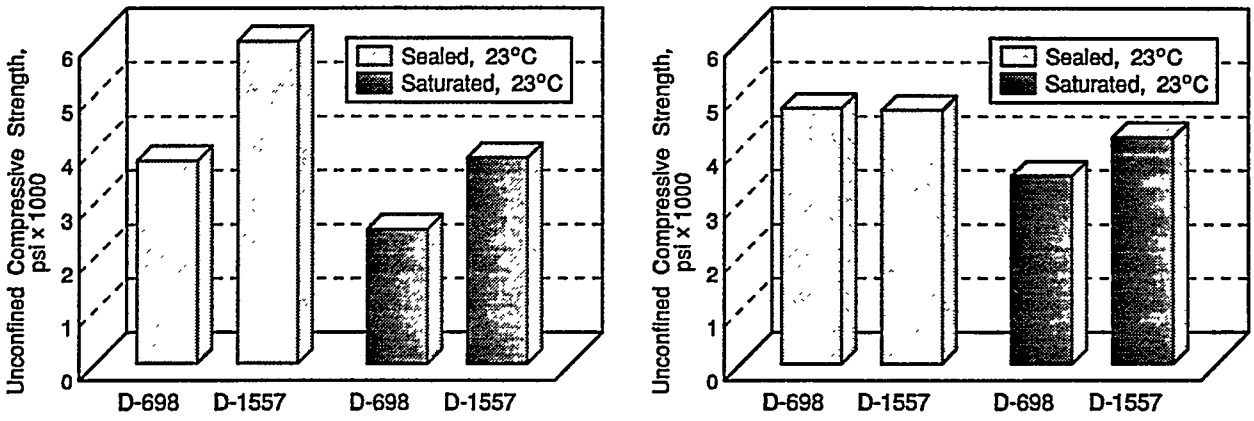

Figure 2. Strength Development Data for High-Sulfur Coal-Derived CFBC Ashes Conditioned and Compacted at ASTM D-698 and ASTM D-1557 Compactive Efforts (1000 psi=6.9 MPa)

The unconfined linear expansion of the CFBC ashes was also tested, and the results for high-sulfur coal-derived ashes conditioned and compacted to ASTM D-698 and ASTM D-1557 compactive efforts are presented in Table 11 and Figure 3.

Table 11. Unconfined Linear Expansion Data for High-Sulfur Coal-Derived CFBC Ashes Conditioned and Compacted at ASTM D-698 and ASTM D-1557 Compactive Efforts

	Plant C-1 Unconfined Linear Expansion, %				Plant C-2 Unconfined Linear Expansion, %			
Curing Age	D-698 Sealed	D-698 Saturated	D-1557 Sealed	D-1557 Saturated	D-698 Sealed	D-698 Saturated	D-1557 Sealed	D-1557 Saturated
7 days	0.302		0.387		0.387		0.484	
14 days	0.391		0.613		0.502		0.582	
15 days	0.400	0.702	0.622	0.733	0.511	0.609	0.591	0.667
17 days	0.409	0.978	na	na	0.524	0.707	0.596	0.782
21 days	0.418	1.364	0.644	1.769	0.538	0.893	0.604	1.049
28 days	0.400	1.653	0.658	2.120	0.542	1.098	0.604	1.325
56 days	0.364	1.996	0.693	2.787	0.564	1.538	0.627	1.813
90 days	0.489	2.289	0.720	3.351	0.591	2.200	0.636	2.089
180 days	0.524	3.431	0.756	4.680	0.613	5.609	0.667	4.320
365 days	0.547	TL	0.809	TL	na	na	na	na

TL – too long to measure

na – not available

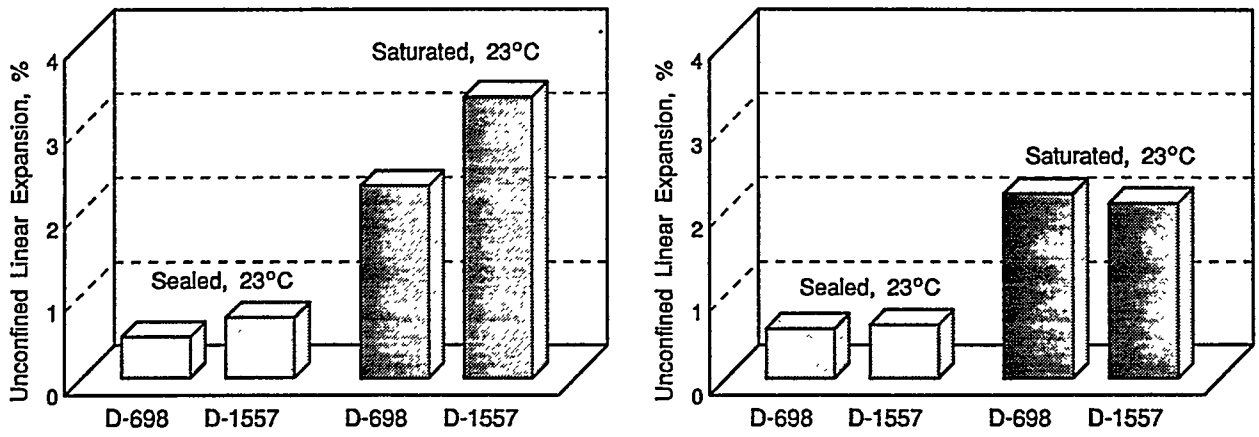

Figure 3. Unconfined Linear Expansion Data for High-Sulfur Coal-Derived CFBC Ashes Conditioned and Compacted at ASTM D-698 and ASTM D-1557 Compactive Efforts

In summary, the data clearly establishes a relationship between strength development and compactive effort. The higher the compactive effort the higher the strength. However, the data also show that the expansion increases with compactive effort. From a disposal or ash re-use perspective it appears that the ash manager must balance the need for enhanced strength with increased dimensional instability through the employment of compactive effort.

5.6. Changes in Geotechnical and Hydration Reaction Properties of Ashes During Sealed and Saturated Curing

Blends of the fly ash and bed ash from each of the plants were conditioned and compacted at the ASTM D-698 optimum moisture content. Unconfined compressive strength specimens and expansion bars were fabricated. The specimens were cured under sealed conditions and saturated conditions at 23°C. Under sealed conditions, the specimens were placed in plastic bags and containers to prevent the ingress or egress of moisture to or from the specimens. Under saturated conditions, the specimens were submerged in a saturated bath of the ash solution. A 10:1 water to ash solution was made for the submergence of the specimens. The specimens were saturated after 14 days of sealed curing. These conditions were considered to represent the extremes that the ash would encounter during either disposal or ash re-use. The curing period extended 90 to 104 days (strength) and 365 days (expansion). Specimens were removed from the curing chambers at predetermined ages and tested for geotechnical properties (strength and expansion) and hydration phase composition.

Strength Development

The data indicate that there is a decrease in strength immediately upon submergence in the saturated ash solution. The strengths tend to recover with time after submergence. There is a strength loss with the later aged saturated specimens that is particular to the high-sulfur coal. The low-sulfur coal-derived ash and the 100% petroleum coke-derived ash do not exhibit this strength loss at later ages.

The specimens that were saturated after 14 days showed a general decrease in strength, followed by a recovery and a paralleling of the strength development of the sealed specimens. The exception is the 100% petroleum coke-derived ash, which showed an enhanced strength development upon saturation.

Table 12 presents the data for the strength development of each of the ash blends under sealed and saturated conditions. Figure 4 presents the sealed and cured sample results as a function of time. The data indicate an increase in strength with time for the sealed ash blend samples. The high-sulfur coals show good strength development. The 100% petroleum coke-derived ash showed lower strength development than the coal fuel-derived ashes.

Table 12. Strength Development Data for the Ash Blends from Each of the Plants

UCS	Plant C-1		Plant C-2		Plant C-3		Plant C-4		Plant C-5		Plant C-6	
MPa	Sealed	Sat.	Sealed	Sat.	Sealed	Sat.	Sealed	Sat.	Sealed	Sat.	Sealed	Sat.
1 day	1.0		0.8		1.6		0.8		1.4		1.5	
3 days	1.8	Sat. @	2.4	Sat. @	4.2	Sat. @	5.9	Sat. @	5.8	Sat. @	2.4	Sat. @
7 days	6.9	14 d	5.8	14 d	7.5	14 d	8.1	14 d	11.2	14 d	6.2	14 d
14 days	13.4		12.0		11.2		16.4		20.6		9.1	
15 days		11.5		10.7		7.3		16.0		20.2		8.2
17 days		13.6		12.1		5.3		16.2		22.6		10.2
21 days		16.4		14.7		10.9		16.2		24.4		13.1
28 days	20.6	18.5	19.2	17.5	15.5	11.7	21.5	19.9	30.6	na	10.3	na
42 days		19.4		20.1		12.9		20.7		31.3		19.7
56 days	24.0		26.8		14.2		24.1		34.0		12.1	
70 days		21.7		21.0		15.1		25.7		33.7		20.4
90 days	26.0		32.7		17.0		29.5		35.2		14.9	
104 days		17.3		24.0		16.5		26.3		34.9		20.8

UCS – Unconfined Compressive Strength

1000 psi = 6.9 MPa

na – not available

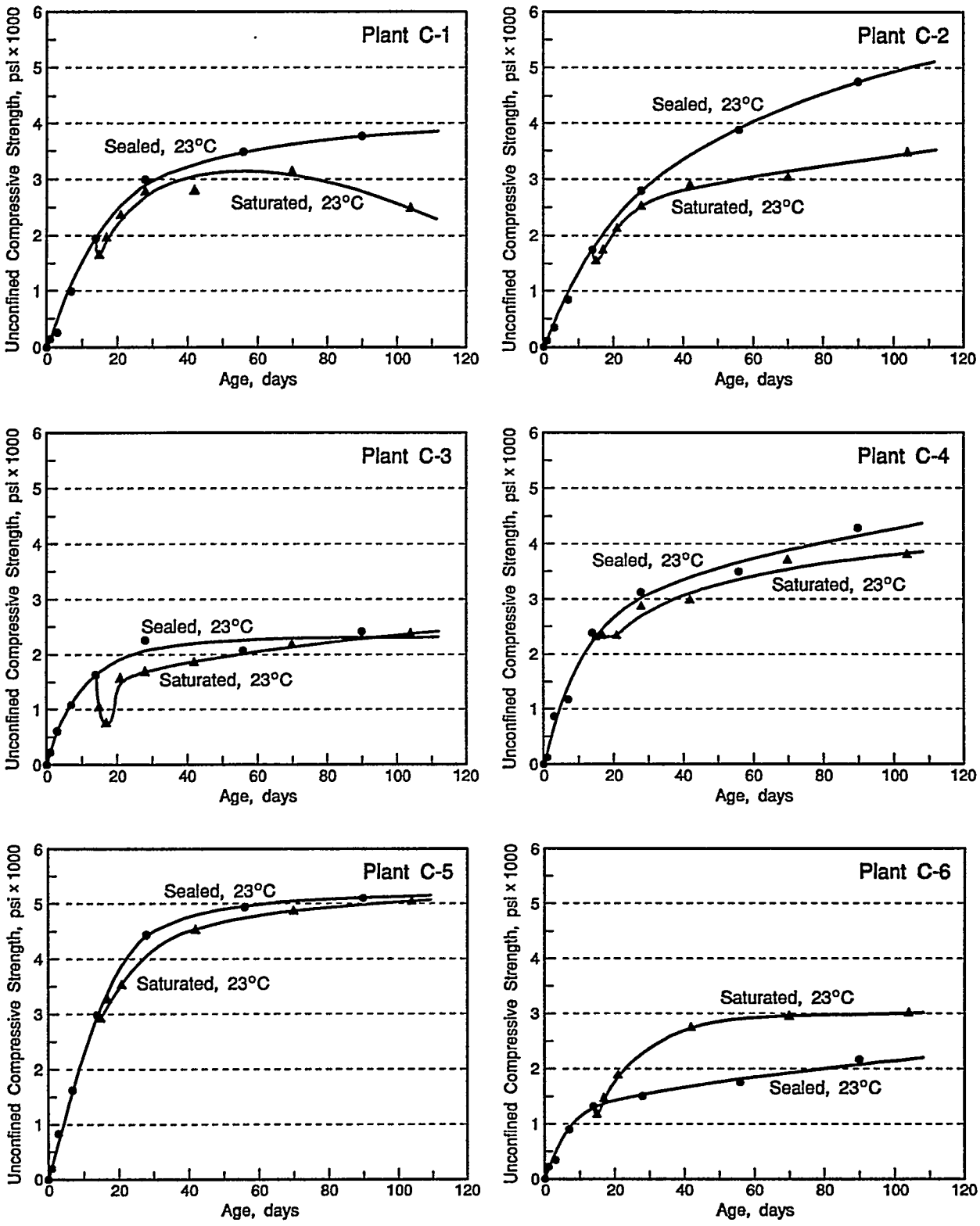

Figure 4. Strength Development of Ash Blends from Each of the Plants Under 23 °C Sealed and Saturated Curing Conditions (1000 psi = 6.9 MPa)

Expansion Characteristics

The expansion of the ashes appears to vary with the source of the ashes. The data for the ashes from the high-sulfur coal-fired units (Plants C-1, C-2 and C-3) show a steady increase in expansion with time for those specimens cured under sealed conditions. The specimens fabricated using ashes derived from the 100% petroleum coke-fired unit (Plant C-6) show little or no expansion. The low-sulfur coal-derived ash also did not show appreciable expansion.

Upon submergence of the coal-derived ash blends there is a rapid increase in expansion. This coincides with the loss in strength noted earlier. Once again, the 100% petroleum coke-derived ash shows no significant expansion.

The results at key ages are presented in Table 13, and all of the data for each of the ash blend samples are schematically presented in Figure 5.

Table 13. Summary of the Unconfined Linear Expansion Data for the Ash Blends From Each of the Plants Cured Under Sealed and Saturated Conditions

Exp.	Plant C-1		Plant C-2		Plant C-3		Plant C-4		Plant C-5		Plant C-6	
%	Sealed	Sat.	Sealed	Sat.	Sealed	Sat.	Sealed	Sat.	Sealed	Sat.	Sealed	Sat.
7 d	0.302	Sat. @	0.387	Sat. @	0.218	Sat. @	0.613	Sat. @	0.147	Sat. @	0.013	Sat. @
14 d	0.391	14 d	0.502	14 d	0.267	14 d	0.747	14 d	0.169	14 d	0.013	14 d
15 d	0.400	0.702	0.511	0.609	0.258	0.307	0.751	0.747	0.169	0.173	0.013	0.009
17 d	0.409	0.978	0.524	0.707	0.253	0.387	0.747	0.760	0.160	0.178	0.009	0.013
21 d	0.418	1.364	0.538	0.893	0.271	0.507	0.769	0.787	0.142	0.182	0.009	0.018
28 d	0.400	1.653	0.542	1.098	0.262	0.653	0.747	0.849	0.129	0.187	0.009	0.027
56 d	0.364	1.996	0.564	1.538	0.280	1.236	0.760	0.942	0.124	0.178	0.013	0.040
90 d	0.489	2.289	0.591	2.200	0.307	1.640	0.764	1.044	0.129	0.178	0.013	0.036
180 d	0.524	3.431	0.613	5.609	0.341	2.747	0.747	1.187	0.133	0.147	nd	nd
365 d	0.547	TL	na	na	0.573	8.078	0.849	1.324	0.213	0.253	0.089	0.116

d – days
TL – too long to measure
na – not available

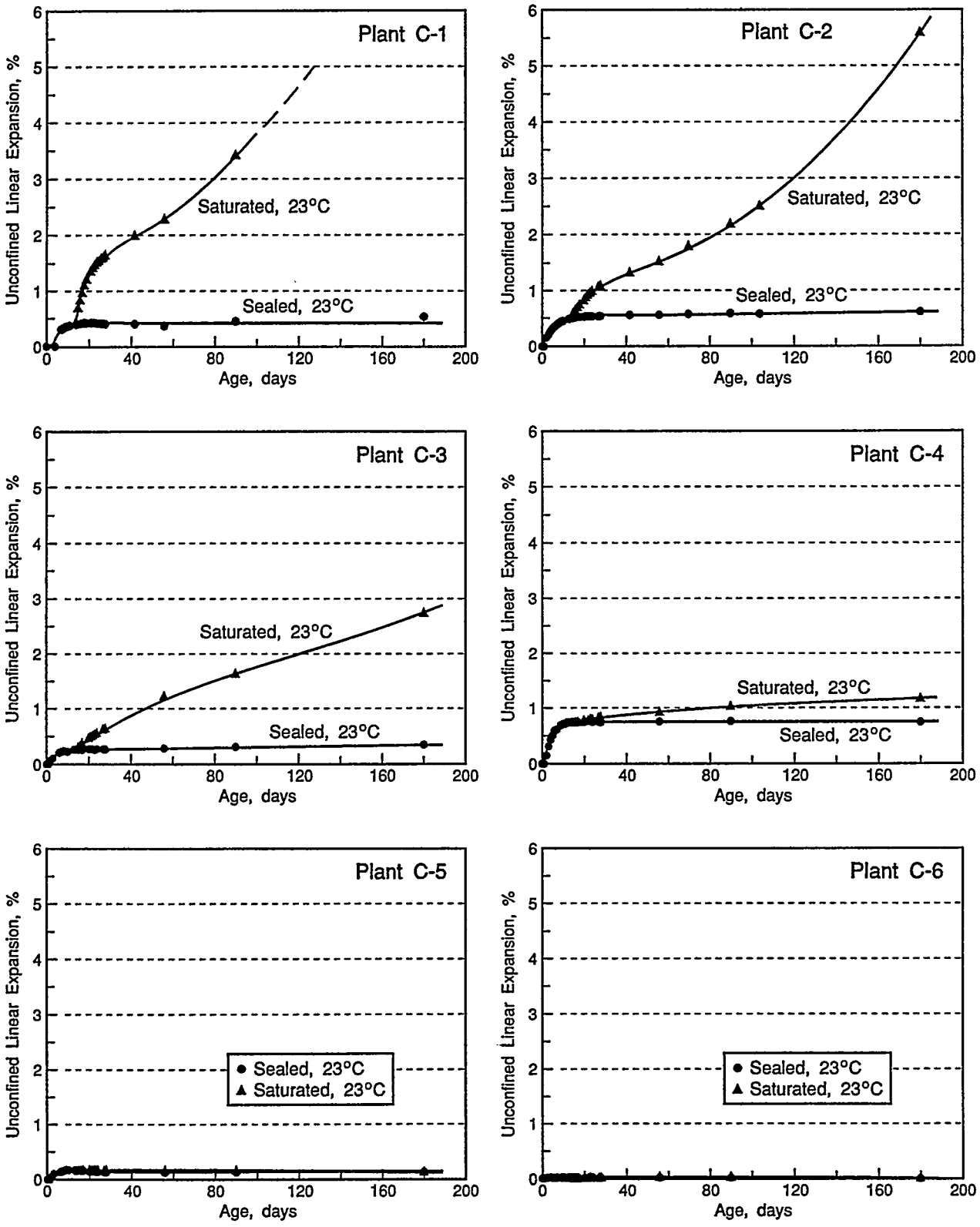

Figure 5. Unconfined Linear Expansion of the Ash Blends from Each of the CFBC Plants Cured Under Sealed and Saturated Conditions

Hydration Reaction Products

Each of the specimens used in the unconfined compressive strength testing was sampled and acetone dried at 45 °C. Acetone drying was used to stop the continuing hydration of the ashes so that the analytical determination of the phases present in the cured ash could be determined. The residual moisture (moisture loss with acetone drying) was recorded. The acetone-dried samples were then subjected to X-ray diffraction analysis, thermogravimetric analysis, and scanning electron microscopy. The phases present in the ash were analyzed by XRD techniques. These techniques have been discussed previously. The XRD peak area intensities that are measured are semiquantitatively proportional to the concentration of the phase present in the ash.

The XRD peak area intensity is proportional to the concentration of the phase present in the ash. The data also show a decrease in the amount of anhydrite, although for the sealed conditions, the hydration of anhydrite is often not complete. It is believed that the anhydrite is hydrated to form gypsum ($CaSO_4 \cdot 2H_2O$) and the soluble gypsum is consumed in the formation and precipitation of the mineral ettringite ($Ca_6Al_2(SO_4)_3(OH)_{12} \cdot 26H_2O$). The hydration reaction chemistry of the specimens cured under the sealed conditions differs considerably from that of the specimens cured under saturated conditions. The rate of anhydrite hydration to form gypsum is much higher for the saturated cured ash blend specimens. It is speculated that for the specimens cured under the sealed conditions this reaction is limited by the lack of water. The visual presence of these mineral phases has been confirmed by the TGA data and by SEM photomicrographs.

The hydration reaction chemistry is dominated by three hydration reactions resulting in (1) formation of hydrated lime or portlandite [Ca(OH)2] from lime [CaO], (2) carbonation of lime to form calcite, (3) formation of gypsum [$CaSO_4 \cdot 2H_2O$] from the hydration of anhydrite [$CaSO_4$], and (4) formation of ettringite [$Ca_6Al_2(SO_4)_3(OH)_{12} \cdot 26H_2O$] from soluble lime, gypsum, and alumina from dehydroxylated clays. These hydration reactions are generalized below.

$$CaO\ (lime) + H_2O \rightarrow Ca(OH)_2\ (portlandite) \quad (1)$$

$$CaO\ (lime) + CO_2 \rightarrow CaCO3\ (calcite) \quad (2)$$

$$CaSO_4\ (anhydrite) + 2H_2O \rightarrow CaSO_4 \cdot 2H_2O\ (gypsum) \quad (3)$$

$$2(AlO_4)^{-} + 3(SO_4)^{2-} + 6(Ca)^{2+} + 26H_2O \rightarrow Ca_6Al_2(SO_4)_3(OH)_{12} \cdot 26H_2O\ (ettringite) \quad (4)$$

The peak area intensities of the hydration phases present in the ash blend samples cured under sealed and saturated conditions are presented in Table 14 and Figure 6.

Table 14. Summary of the XRD Peak Area Intensities for the Ash Blend Specimens Cured Under Sealed and Saturated Conditions

Curing Age	Mineral Phases	Plant C-1 XRD PAI*		Plant C-2 XRD PAI*		Plant C-3 XRD PAI*		Plant C-4 XRD PAI*		Plant C-5 XRD PAI*		Plant C-6 XRD PAI*	
		Sealed	Sat.	Sealed	Sat.	Sealed	Sat.	Sealed	Sat.	Sealed	Sat.	Sealed	Sat.
0 days	Anhydrite	4331		4299		5863		3595		1350		7533	
	Ettringite	0		0		0		0		0		0	
	Gypsum	0		0		0		0		0		0	
1 day	Anhydrite	3920		4179		5358		3308		939		6271	
	Ettringite	310		455		0		1029		979		0	
	Gypsum	296		226		0		0		0		1301	
3 days	Anhydrite	3264		4411		5024		3640		471		6265	
	Ettringite	496		732		370		2068		1386		0	
	Gypsum	312		0		0		0		0		944	
7 days	Anhydrite	2388		4163		5036		2866		297		5188	
	Ettringite	370		409		498		2159		2139		0	
	Gypsum	704		0		0		202		0		1638	
14 days	Anhydrite	2170		4132		4069		2994		0		4114	
	Ettringite	923		1046		542		2305		2019		0	
	Gypsum	855		0		0		236		0		1924	
15 days	Anhydrite		1548		4110		4341		2659		61		4270
	Ettringite		951		1112		935		2368		2215		0
	Gypsum		1624		305		0		458		0		2110
17 days	Anhydrite		1080		3238		3970		2914		88		3334
	Ettringite		1103		1056		1076		2417		2660		0
	Gypsum		1819		700		1170		472		0		2061
21 days	Anhydrite		442		3333		4152		2166		0		3648
	Ettringite		1008		1174		932		2459		2350		0
	Gypsum		2042		1035		578		644		0		2349
28 days	Anhydrite	2034	256	4300	2784	4181	4681	3622	1720	0	0	4405	3196
	Ettringite	1175	1261	1066	1264	1307	1330	2383	2634	1887	2429	0	0
	Gypsum	757	2165	0	753	0	282	271	721	0	221	1709	2113
42 days	Anhydrite		0		2639		3650		953		96		2358
	Ettringite		1372		1441		944		2826		2411		0
	Gypsum		2232		805		885		1518		0		3142
56 days	Anhydrite	1979		4109		4734		2628		63		4673	
	Ettringite	1267		1184		1286		2413		2258		0	
	Gypsum	1000		0		0		213		0		2526	
70 days	Anhydrite		0		2215		1267		701		0		1830
	Ettringite		1495		1503		1363		2863		2563		0
	Gypsum		1763		784		1914		1408		0		3200
90 days	Anhydrite	2029		3979		4632		2613		89		3143	
	Ettringite	1164		1221		1241		2848		2182		0	
	Gypsum	763		0		259		268		0		2411	
104 days	Anhydrite		0		2381		435		447		0		2742
	Ettringite		1826		1278		1486		2743		2581		0
	Gypsum		2339		1139		2589		1491		0		2873

* XRD PAI – X-ray diffraction peak area intensities

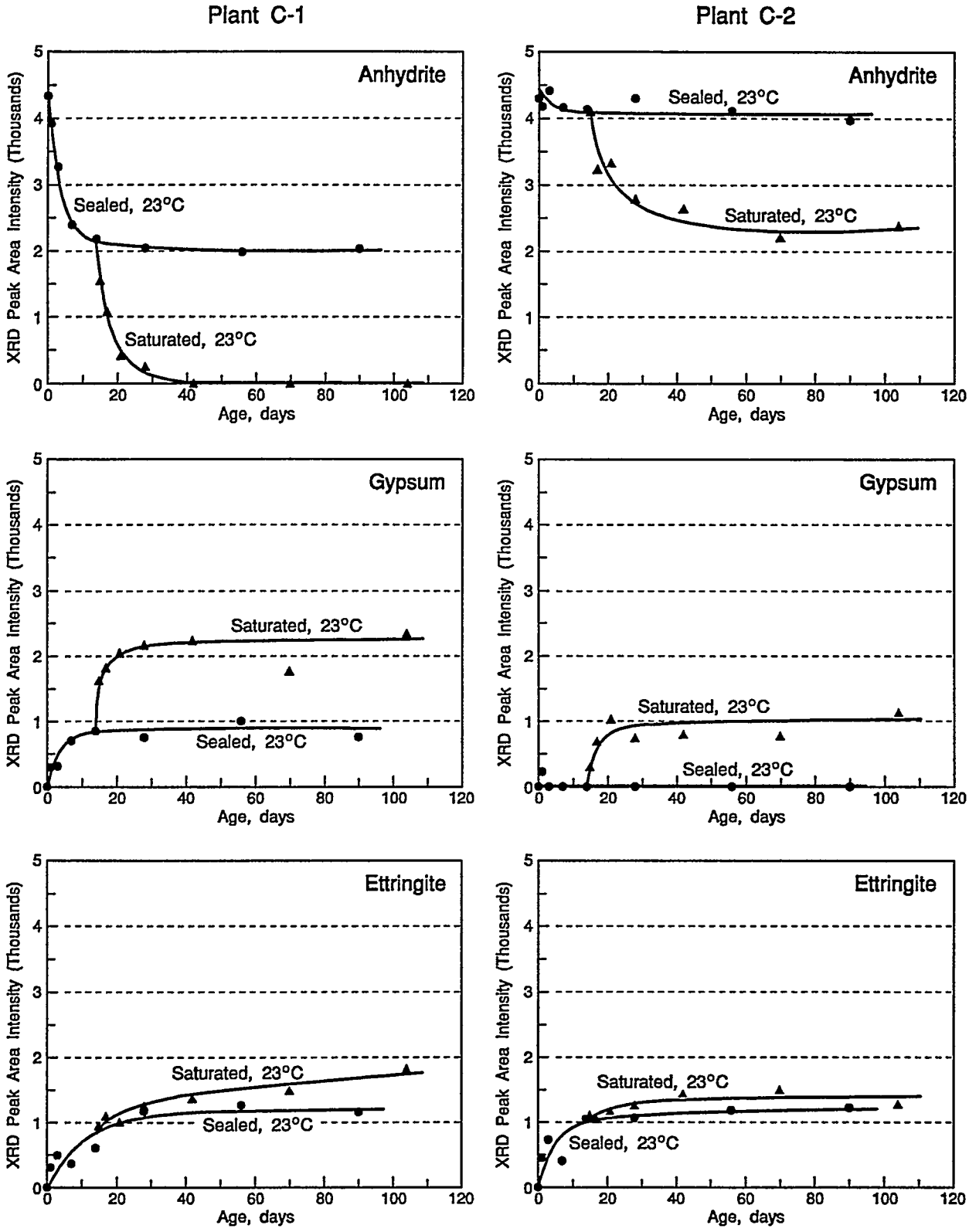

Figure 6. Hydration Phase Formation in the Ash Blend Samples from Plants C-1 and C-2 Under 23°C Sealed and Saturated Curing Conditions

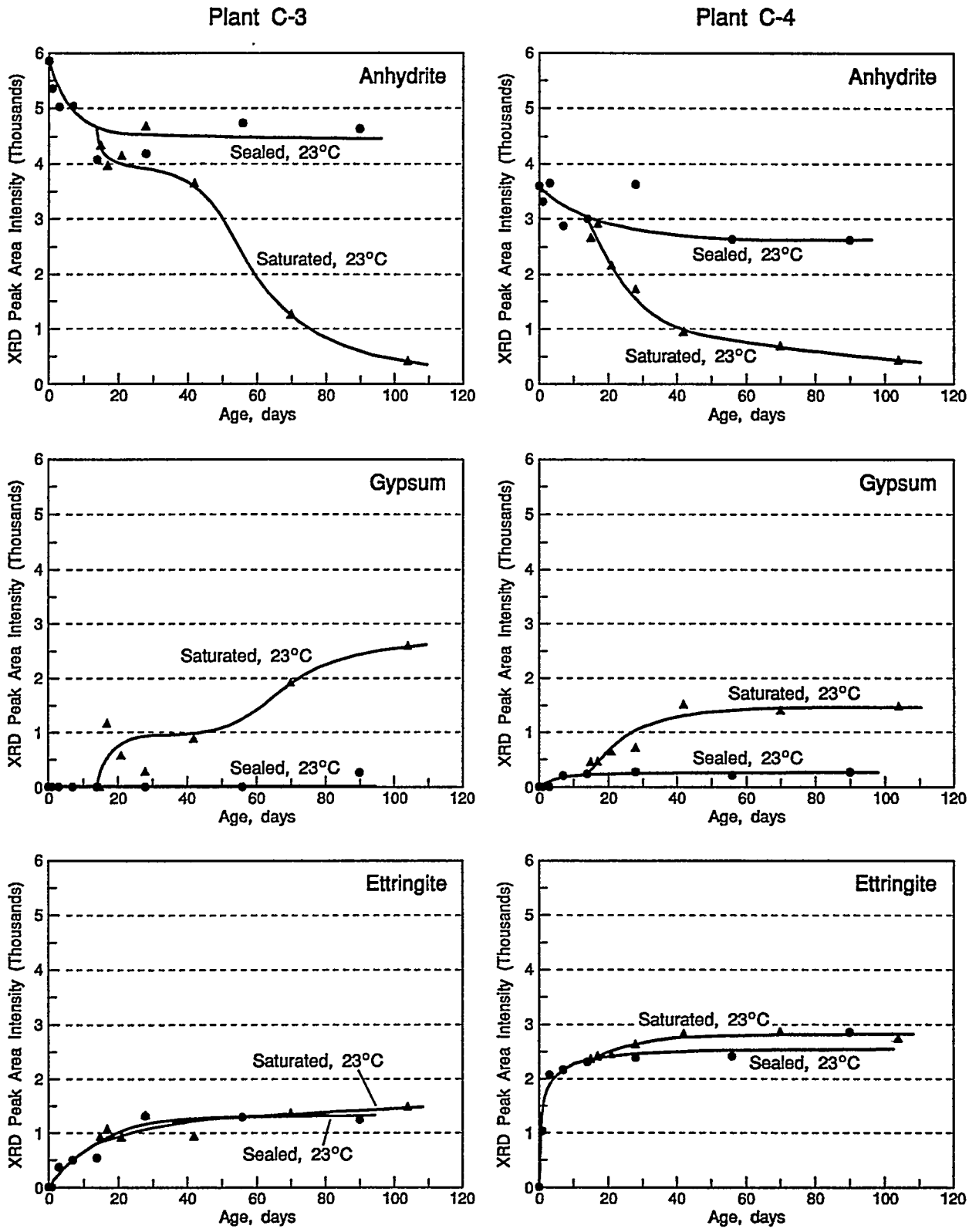

Figure 6. (Cont.) Hydration Phase Formation in the Ash Blend Samples from Plants C-3 and C-4 Under 23°C Sealed and Saturated Curing Conditions

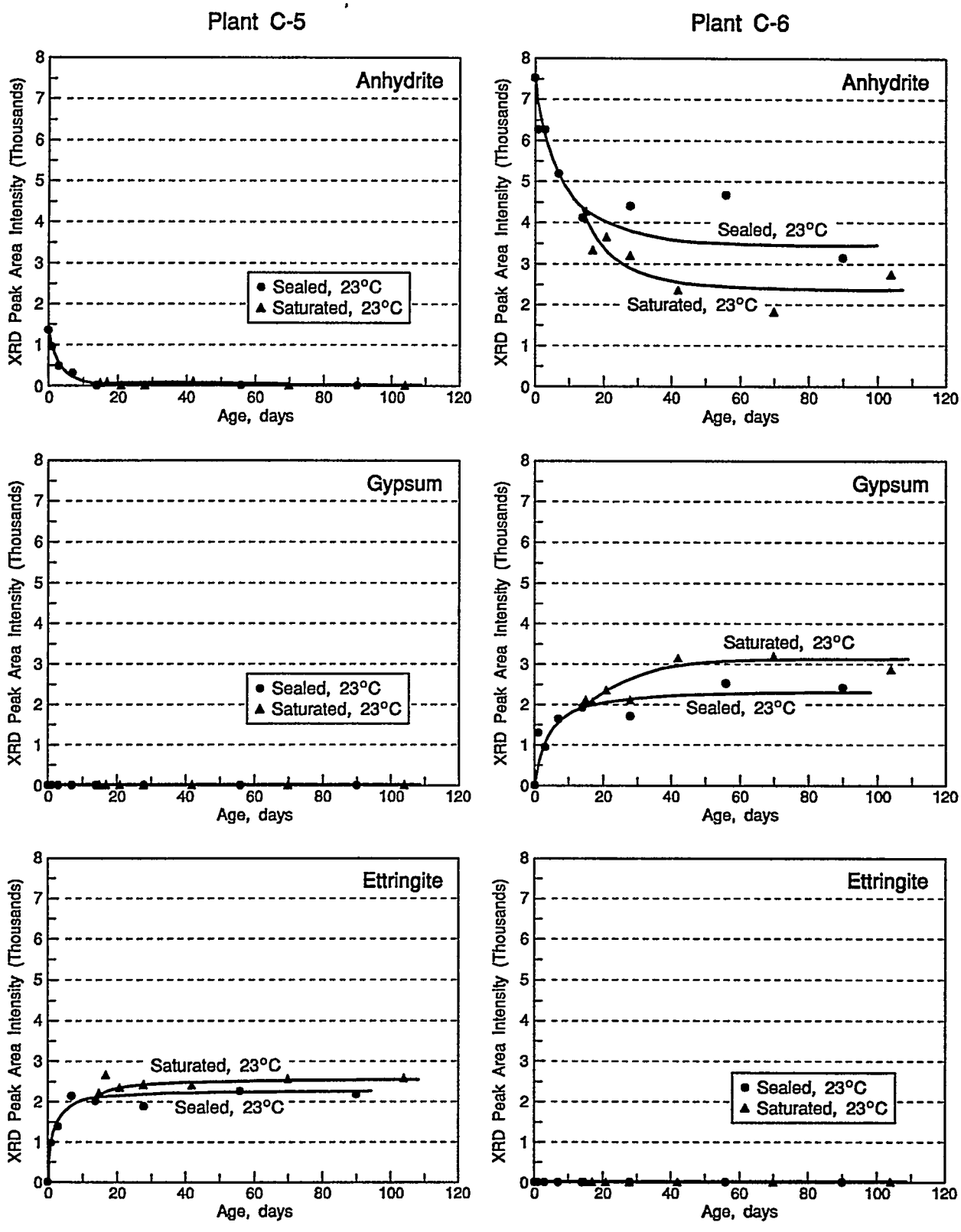

Figure 6. (Cont.) Hydration Phase Formation in the Ash Blend Samples from Plants C-5 and C-6 Under 23°C Sealed and Saturated Curing Conditions

A number of members of the ettringite and thaumasite family of minerals are collectively referred to as Af_t, The three found in hydrated CCT ashes are:

Ettringite	$[Ca_6Al_2(SO_4)_3(OH)_{12} \cdot 26H_2O]$
Thaumasite	$[Ca_6(Al,Si)_2(SO_4)_3(CO_3)_2(OH)_{12} \cdot 26H_2O]$
Sturmanite	$[Ca_6(Al,Fe)_2(SO_4)_3(OH)_{12} \cdot 26H_2O]$

Thermodynamic equilibrium calculations have been used to develop phase equilibrium diagrams for the ettringite phase. Figure 7 presents the phase equilibrium diagram for the sulfate system under saturated lime conditions. The stability range of ettringite in this pure system is quite narrow. However, in a real field situation with a multitude of other chemical species and different temperature regimes, the stability range can be quite different. The formation and stability of the ettringite phase appears to indicate the following:

- ettringite formation is very rapid and is controlled by the pH range, as well as by sulfate, calcium and alumina concentrations;
- ettringite congruently dissolves above pH 10.5; and
- ettringite incongruently dissolves below pH 10.5 to form gypsum and Al-hydroxides.

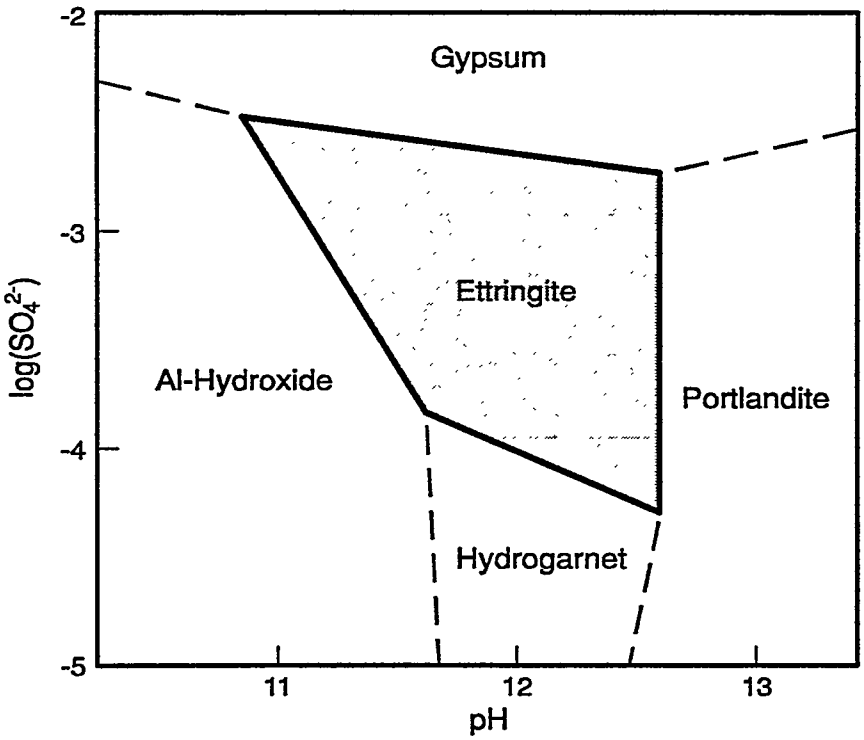

Figure 7. Phase Stability Diagram for Ettringite in Alkaline pH Environment

The conditions required for the chemical transformation of ettringite to thaumasite are debatable. A number of factors are known to influence the stability of these reaction products, including pH, temperature, and CO_2 partial pressure. No thaumasite has been noted in the 23°C temperature cured ashes in this study.

No lime (CaO) was found in any of the cured ash blend samples. The lime present in the conditioned ash appears to be completely hydrated to portlandite ($Ca(OH)_2$) by seven days (the first sample analyzed). It is suspected that this hydration of lime to portlandite takes place within minutes to hours after the addition of the secondary water.

SEM observations of the 23°C ash blend were made to substantiate the presence of the hydration phases reported by XRD and identified by TGA. Hydration products appear to form in the pores and cracks present in the cured ash. Hydration phases of gypsum and ettringite tend to form rings or liners within the pores. At later ages the pores are bridged, the number of pores decreases, and only the larger pores still have open space. Fissures or elongated pores are noted in the submerged samples, with filling by gypsum and ettringite occurring within these cracks or fissures. Ettringite has very fine crystals that appeared to coat the gypsum and other minerals in the pores. Calcium ferrite was not noted in the cured samples.

The data show a rapid hydration of the anhydrite to form gypsum upon submergence of the specimens. The specimens that were sealed generally did not reach complete hydration of the anhydrite. Those that were saturated did reach complete hydration of anhydrite, with the exception of those from C-6. The availability of moisture may be a major controlling parameter for the degree of hydration of anhydrite and the resultant formation of gypsum and ettringite. There is also an increase in the formation of ettringite upon submergence in water.

The ashes can be categorized into three groups based on the type of hydration reaction products that form. The three groups are: (1) those that form only ettringite (Plant C-5), those that form only gypsum (Plant C-6), and those that form both ettringite and gypsum (Plants C-1, C-2, C-3 and C-4). No thaumasite has been positively identified in the samples cured at 23°C. The category and type of hydration reactions that form appear to be ash specific and related to the composition (and source) of the ash and the availability of the reactants to form these hydration reaction products.

In summary, it appears that the hydration reaction products involved in influencing the geotechnical properties of the ash (strength and expansion) are limited, involving gypsum formation, ettringite formation, and possibly carbonation of lime to form calcite.

- Complete conversion of the lime [CaO] to portlandite [$Ca(OH)_2$]. This occurs principally during conditioning and is completed early after water addition for the Proctor compaction.

- Partial carbonation of lime [CaO] to calcite [$CaCO_3$] as a result of contact with CO_2 in the air and waters associated with conditioning and curing.

- Partial to complete conversion of the anhydrite to gypsum. The rate of conversion is dependent upon the curing conditions and availability of moisture. The rate of anhydrite hydration and ettringite and/or gypsum formation is considerably higher under the saturated curing conditions.

- Formation of ettringite appears to be a function of the solubility of gypsum, portlandite, and alumina in the coal ash. Ettringite appears to be dependent upon the moisture availability, as well as the other chemicals required for formation (lime, sulfates and alumina). Ettringite forms as a result of precipitation from a high pH (>10) solution containing soluble alumina and sulfate.

- Although not noted in this study, calcium ferrite phases, such as larnite and gehlenite, have been reported to be present in the raw and conditioned ashes (Iribarne 1993 and Anthony et al. 1995, 1997). The calcium ferrite phases appear to be hydrated to form a gel-like material. The lack of identification by XRD indicates a lack of crystalline structure.

- The results do not indicate the presence of monosulfate (AF_m) or thaumasite. The role of monosulfate in the expansion of CFBC ashes is unknown. The high sulfate/alumina ratio found in CFBC ash systems would tend to favor ettringite rather than AF_m as the stable phase. The lack of evidence of the formation of thaumasite is surprising in light of the availability of soluble carbonates and silicates. The presence of calcium silicate gels has also not been established.

5.7 Changes in Geotechnical and Hydration Reaction Properties of Ashes During Curing at 23°C and 5°C

Blends of the fly ash and bed ash from the C-1 plant were conditioned and compacted at the ASTM D-698 optimum moisture content and compactive effort (100% proctor). Unconfined compressive strength specimens and expansion bars were fabricated. The specimens were cured under sealed conditions (23°C) and saturated conditions at temperatures of 23°C and 5°C. The conditions for the sealed and saturated curing were the same as for the 23°C curing described earlier with the exception of the temperature. The curing period extended 90 and 104 days (strength) and 365 days (expansion). Specimens were removed from the curing chambers at predetermined ages and tested for geotechnical properties (strength and expansion) and hydration phase composition.

Strength Development

In addition to sealed and saturated curing at 23°C, the conditioned and compacted ash blends were cured under saturated conditions at 5°C. This condition was tested to ascertain the effect of temperature on geotechnical properties and hydration reaction product development of the cured ashes at various ages.

The data show that the sealed cured samples exhibited continued strength development with time, while the 23°C saturated cured samples showed a slight decrease in strength in the later ages. The strength development under the cold conditions showed continued deterioration at the later ages. It should be noted that this trend is for the high-sulfur coal-derived ash and may not be present with the medium- and low-sulfur coal-derived ashes or the petroleum coke-derived ashes. The results for the high-sulfur coal-derived ash are presented in Table 15 and Figure 8.

Table 15. Unconfined Compressive Strength Development of High-Sulfur Coal-Derived Ash Blend Cured Under 23°C Sealed, 23°C Saturated and 5°C Saturated Conditions

	Plant C-1 Unconfined Compressive Strength, MPa		
Curing Age	Sealed 23 °C	Sat. 23°C	Sat. 5°C
1 day	1.0		
3 days	1.8	Saturated	Saturated
7 days	6.9	After 14 days	After 14 days
14 days	13.4		
15 days		11.5	12.0
17 days		13.6	14.0
21 days		16.4	17.0
28 days	20.6	18.5	24.7
42 days		19.4	17.5
56 days	24.0		
70 days		21.7	14.1
90 days	26.0		
104 days		17.3	5.8

1000 psi = 6.9 MPa

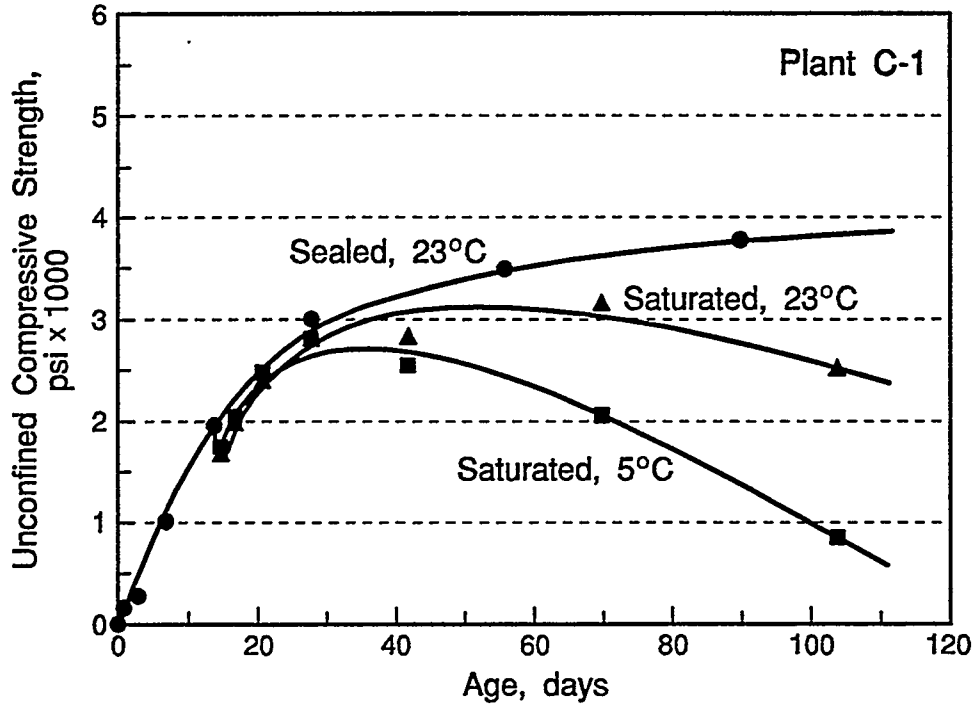

Figure 8. Effect of 23°C Sealed, 23°C Saturated and 5°C Saturated Curing Conditions on the Strength Development of the Conditioned and Compacted Ash Blend from the Combustion of High-Sulfur Coal (1000 psi = 6.9 MPa)

Expansion Testing

The results of the expansion testing involving the 5°C as well as the 23°C sealed and saturated curing are presented in Table 16 and Figure 9.

Table 16. Unconfined Linear Expansion of High-Sulfur Coal Derived Ash Blend Cured Under 23°C Sealed, 23°C Saturated, and 5°C Saturated Conditions

Unconfined Linear Expansion, %	Plant C-1		
	Sealed 23°C	Sat. 23°C	Sat. 5°C
7 days	0.302	Saturated	Saturated
14 days	0.391	After 14 days	After 14 days
15 days	0.400	0.702	0.698
17 days	0.409	0.978	0.969
21 days	0.418	1.364	1.369
28 days	0.400	1.653	1.800
56 days	0.364	1.996	2.298
90 days	0.489	2.289	2.867
180 days	0.524	3.431	5.662
365 days	0.547	TL	TL

TL – Too long to be measured

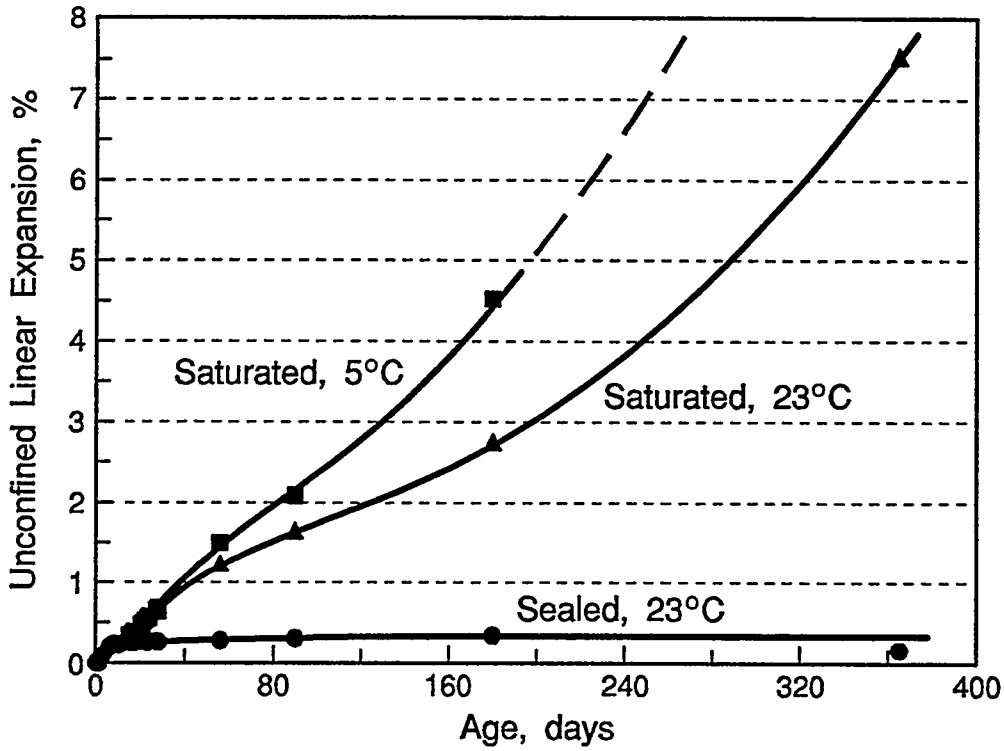

Figure 9. Effect of 23°C Sealed, 23°C Saturated, and 5°C Saturated Curing Conditions on the Unconfined Linear Expansion of the Conditioned and Compacted Ash Blend from the Combustion of High-Sulfur Coal

The data show that the sealed cured samples exhibited continued unconfined expansion with time, while the 23°C saturated cured samples showed a rapid increase in expansion upon submergence. The results show an even greater rate of expansion under cold conditions than under the 23°C conditions. The increase in expansion seems to coincide with the loss of strength noted earlier for the 5°C cured samples. Once again it should be noted that this trend is for the high-sulfur coal derived ash and may not be present for the medium- and low-sulfur coal-derived ashes or the petroleum coke-derived ashes.

Hydration Reaction Products

The effect of temperature on the hydration reaction chemistry associated with saturated curing of the CFBC ashes was also determined for the high-sulfur coal-derived ash. Selected specimens were analyzed for phase distribution. These data show the relationships between the composition and age and curing environment. The phase chemistry of the ash blend was monitored as the residue was hydrated and aged. The XRD peak area intensities for anhydrite, ettringite, and gypsum are presented in Table 17 and Figure 10.

Table 17. XRD Peak Area Intensities for Plant C-1 CFBC Ash Blend Cured Under 23°C Sealed, 23°C Saturated, and 5°C Saturated Curing Conditions

Curing Age	Mineral Phases	Plant C-1 XRD Peak Area Intensity		
		Sealed 23°C	Sat. 23°C	Sat. 5°C
0 days	Anhydrite	4331		
	Ettringite & Gypsum	0		
1 day	Anhydrite	3920		
	Ettringite	310		
	Gypsum	296		
3 days	Anhydrite	3264		
	Ettringite	496		
	Gypsum	312		
7 days	Anhydrite	2388		
	Ettringite	370		
	Gypsum	704		
14 days	Anhydrite	2170		
	Ettringite	923		
	Gypsum	855		
15 days	Anhydrite		1548	1847
	Ettringite		951	828
	Gypsum		1624	1514
17 days	Anhydrite		1080	793
	Ettringite		1103	1288
	Gypsum		1819	2003
21 days	Anhydrite		442	322
	Ettringite		1008	1266
	Gypsum		2042	2280
28 days	Anhydrite	2034	256	0
	Ettringite	1175	1261	1407
	Gypsum	757	2165	2159
42 days	Anhydrite		0	0
	Ettringite		1372	1128
	Gypsum		2232	1697
56 days	Anhydrite	1979		
	Ettringite	1267		
	Gypsum	1000		
70 days	Anhydrite		0	0
	Ettringite		1495	1550
	Gypsum		1763	2407
90 days	Anhydrite	2029		
	Ettringite	1164		
	Gypsum	763		
104 days	Anhydrite		0	0
	Ettringite		1826	1962
	Gypsum		2339	2098

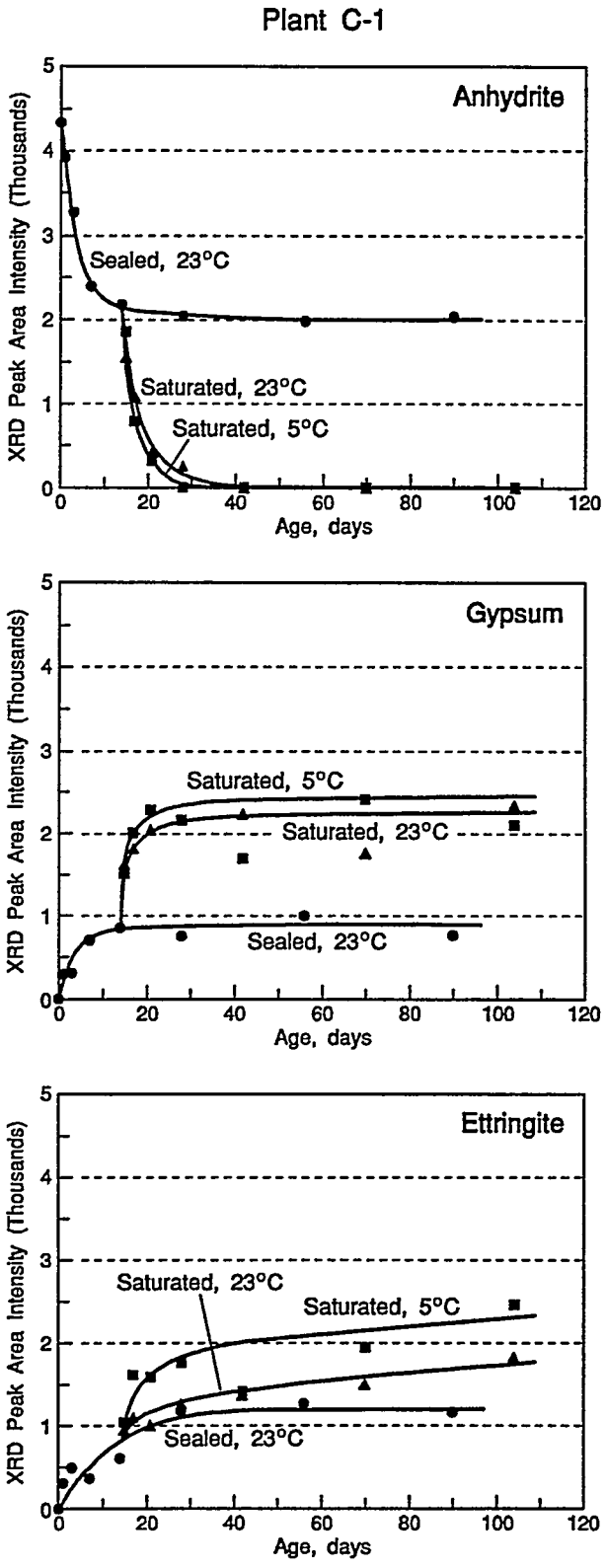

Figure 10. Anhydrite, Ettringite and Gypsum XRD Peak Area Intensities for Plant C-1 CFBC Ash Blend Cured Under 23°C Sealed, 23°C Saturated, and 5°C Saturated Curing Conditions

It is well known that the formation of hydration reaction products such as gypsum and ettringite are strongly influence by temperature of curing. Santoro et al. (1986) have demonstrated the relationship for high lime and sulfate phosphogypsum materials. This relationship can also be noted in the data for this study.

In general, the data indicate that the hydration reactions in the 5°C cured ash blends are similar to those determined for the 23°C ash blend specimens. Principally anhydrite is hydrated to form gypsum [$CaSO_4 \cdot 2H_2O$] and the reaction of the soluble gypsum with the soluble portlandite [$Ca(OH)_2$] and alumina from the ash to form ettringite [$Ca_6Al_2(SO_4)_3(OH)_{12} \cdot 26H_2O$].

As with the 23°C data, the hydration reaction chemistry of the specimens cured under the sealed conditions differs considerably from the specimens cured under the saturated conditions. The rate of anhydrite hydration to form gypsum is much higher for the 23°C saturated cured ash blend specimens than for the 23°C sealed cured specimens and even higher for the 5°C saturated cured specimens. As with the 23°C data, the 5°C data show a rapid hydration of the anhydrite and consumption of gypsum to form ettringite upon submergence of the specimens. This is related to the higher solubility of anhydrite in the 5°C temperature regime than in the 23°C temperature regime. These results are confirmed by the TGA data and by SEM.

Detrimental expansion and deterioration of the concrete or soil was attributed, at least in part, to thaumasite [$Ca_6[Si(OH)_6)2(SO_4)2(CO_3)2 \cdot 24H_2O$]. Thaumasite is considered a part of the solid solution that includes ettringite as one end-member and thaumasite as another. Ettringite and thaumasite have similar crystalline structures, and many believe that thaumasite can only form from ettringite. Thaumasite contains carbonate exchanged for sulfate and silica for the alumina in the crystal structure and has been reported to only form at cold temperatures. The other common variable that appears to be important in its formation is a high pH solution containing silica and CO_2. The influence of thaumasite in the disruption of compacted and conditioned CFBC ash, as in disposal cells, has yet to be well defined but is expected to be a contributing factor.

Unfortunately, thaumasite was not noted in the cold-cured specimens. This was possibly due to lack of access to CO_2, which may be the dominant reactant needed for thaumasite formation in CFBC ashes.

5.8 Correlation Between Hydration Reaction Product Development and Geotechnical Properties of Ash with Curing

Strength development and expansion have been attributed to the formation of ettringite and gypsum in the CFBC ashes (Berry et al. 1991). The data from the current study also indicate that strength development is strongly related to ettringite and gypsum formation.

Relationship Between Geotechnical Properties and Hydration Phases

Based on the geotechnical and hydration reaction chemistry data, it appears that both the strength development and the expansion properties of the CFBC ash blends are directly related to the formation of hydration phases during curing. The hydration reaction chemistry indicates that the hydration reaction products that are potentially involved in influencing the geotechnical properties (strength and expansion) are limited to gypsum formation, ettringite formation, and possibly carbonation of lime to form calcite. The role of calcium ferrite is unknown but is not considered a significant contributor to strength, as discussed earlier.

An examination of the relationship between the major hydration phases (ettringite, gypsum, and ettringite + gypsum) and strength and expansion of the ash blend with curing under 23°C sealed and both 23°C and 5°C saturated conditions was made. Also included in these evaluations were the data for the saturated curing conditions in addition to the sealed curing conditions. When plotted against the strength or expansion, similar trends were noted for the gypsum and ettringite alone and ettringite and gypsum combined. The combined effect of ettringite and gypsum was less scatter and is thus presented herein. Also noted were the data from Plant C-5, which showed only ettringite formation, and Plant C-6, which showed only gypsum formation. Each of these ashes showed strength development, and neither showed significant expansion. As such, a combination of reactant products seems to correlate better than either ettringite or gypsum alone.

Strength. The data from this study suggest that strength development is strongly related to both ettringite and gypsum formation. The data for each of the plants for 23°C sealed and saturated curing conditions are presented in Figure 11.

The sealed cured ashes show early formation of hydration products and very slow strength development, followed by rapid strength development with only slow hydration reaction formation. This is reflected in the relatively steep slope of the trends in Figure 11 for the sealed cured ashes.

The saturated cured ash samples exhibit a relationship similar to that found for the unconfined compressive strength, indicating the time dependence of the hydration reaction product formation. Upon saturation, there is a loss of strength associated with an increase in the formation of the hydration reaction products ettringite and gypsum. This relationship is observed even with the ash from Plant C-1, which showed increased strength development upon saturation.

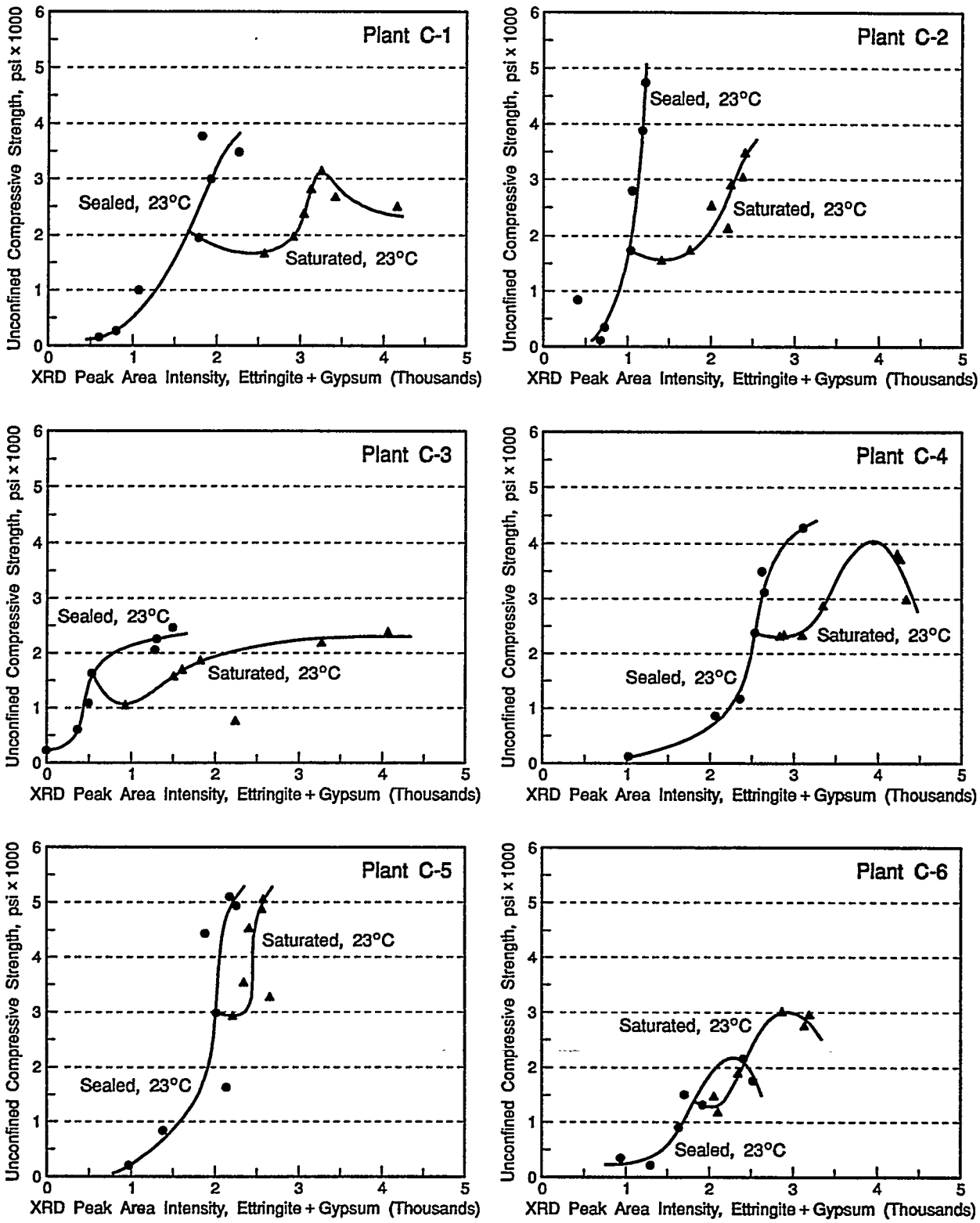

Figure 11. Relationship Between Strength Development and Ettringite and Gypsum Formation Under 23°C Sealed and Saturated Curing of Ash Blends for Plants C-1 Through C-6

The data from Plant C-1 are interesting in that they show a decrease in strength upon saturation, followed by an increase, and finally a decrease. With early growth of these phases, there is a marked increase in the strength. However, with continued formation of these phases, the strength development ceases, and under high water availability (saturated curing conditions) rapid formation of these phases occurs and strength decreases. The effect of cold (5°C) saturated curing for the Plant C-1 ash blend is shown in Figure 12.

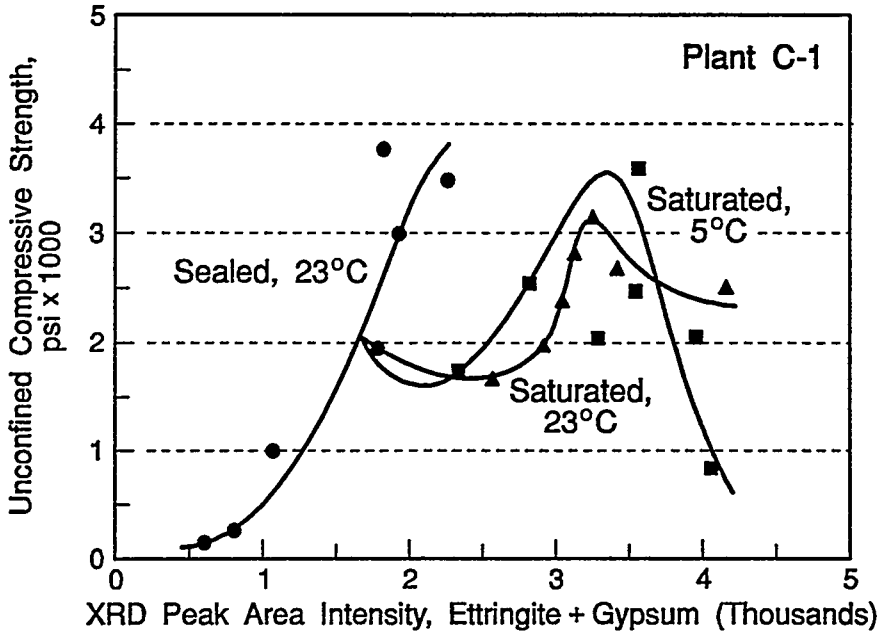

Figure 12. Relationship Between Strength Development and Ettringite and Gypsum Formation in Ash Blend from Plant C-1 Under 23°C Sealed and 23°C and 5 °C Saturated Curing

The sealed cured samples show a strength peak varying between 3000 and 4000 XRD peak area intensities. There may also be morphological differences. The hydration phases present in the sealed cured specimens tend to be less well defined. Ettringite tends to be smaller and of a fuzzy consistency, filling in among the gypsum and other particles. The saturated cured samples tend to have larger, better defined crystals of ettringite and gypsum.

The cold saturated specimens show similar hydration reaction product formation, while exhibiting a more pronounced strength loss than the 23°C cured ash blend. The 5°C curve for the saturated cured conditions reflect the continued rapid hydration of anhydrite (higher solubility at lower temperatures) and the subsequent formation of gypsum and ettringite. The cold saturated cured samples tend to have larger, better defined crystals of ettringite and gypsum.

Expansion. Expansion observed with the CFBC ashes also appears to be controlled by both ettringite and gypsum formation. Once again the data associated with Plant C-1 and C-2, as described earlier, tend to make the correlation between expansion and both ettringite and gypsum formation. Gypsum formation under submerged or saturated curing conditions appears to be more important than ettringite formation in influencing expansion. This relationship is indicated by the similarity of expansion (Figure 9) and gypsum formation (Figure 10). The role of calcium ferrite and calcium silicate hydration, as well as monosulfate formation is presently unknown.

Plotting the combined XRD peak area intensities for ettringite and gypsum against expansion indicates a series of consistent trends, as presented in Figure 13. Similar trends are noted for the ettringite and gypsum separately, but the scatter was greater. Expansion is favored under high water availability (saturated conditions) where rapid formation of these hydration phases has been noted.

Figure 13 shows two types of curves for the 23°C sealed and saturated ash blends. The trends for the ash blends from Plants C-1 through C-3 are significantly different than those for the ash blends from Plants C-4 through C-6. For the ashes from the high-sulfur coal-fired plants there is a slight expansion associated with the sealed cured ash blends. However, upon saturation, the expansion is rapid with continued hydration reaction product formation. On the other hand, the effect of saturation on the expansion of the ash blends from the medium- and low-sulfur or petroleum coke-fired plants is minor. The morphology of the ettringite and the gypsum described for the strength development may be an important key to the correlation of expansion and hydration reaction products.

The relationship of 5°C and 23°C saturated curing and the formation of ettringite and gypsum for the ash blend from Plant C-1 is presented in Figure 14. The data show a rapid expansion that occurs upon saturation, both at 23°C and at 5°C. The cold saturated cured ash blend shows a curve paralleling the 23°C curve but at a higher concentration of ettringite and gypsum XRD peak area intensities. The cold saturated ash blend also exhibits higher expansion.

5.9 Correlation Between Strength and Expansion and the Development of the Pore Filling Model

Interrelationship Between Strength and Expansion

The geotechnical properties of interest for disposal and/or ash re-use are strength development and dimensional stability (expansion). The strength of the CFBC ash blends increases with curing time to a maximum and for the high-sulfur coal-derived ash blends decreases with time, while the expansion increases with curing time. No reversal of expansion or shrinkage is observed. These properties for the CFBC ashes appear to be interrelated, and a consistent relationship exists between the strength development and the expansion during curing. Figure 15 presents this relationship between unconfined compressive strength and unconfined linear expansion for the 23°C cured ash blend samples.

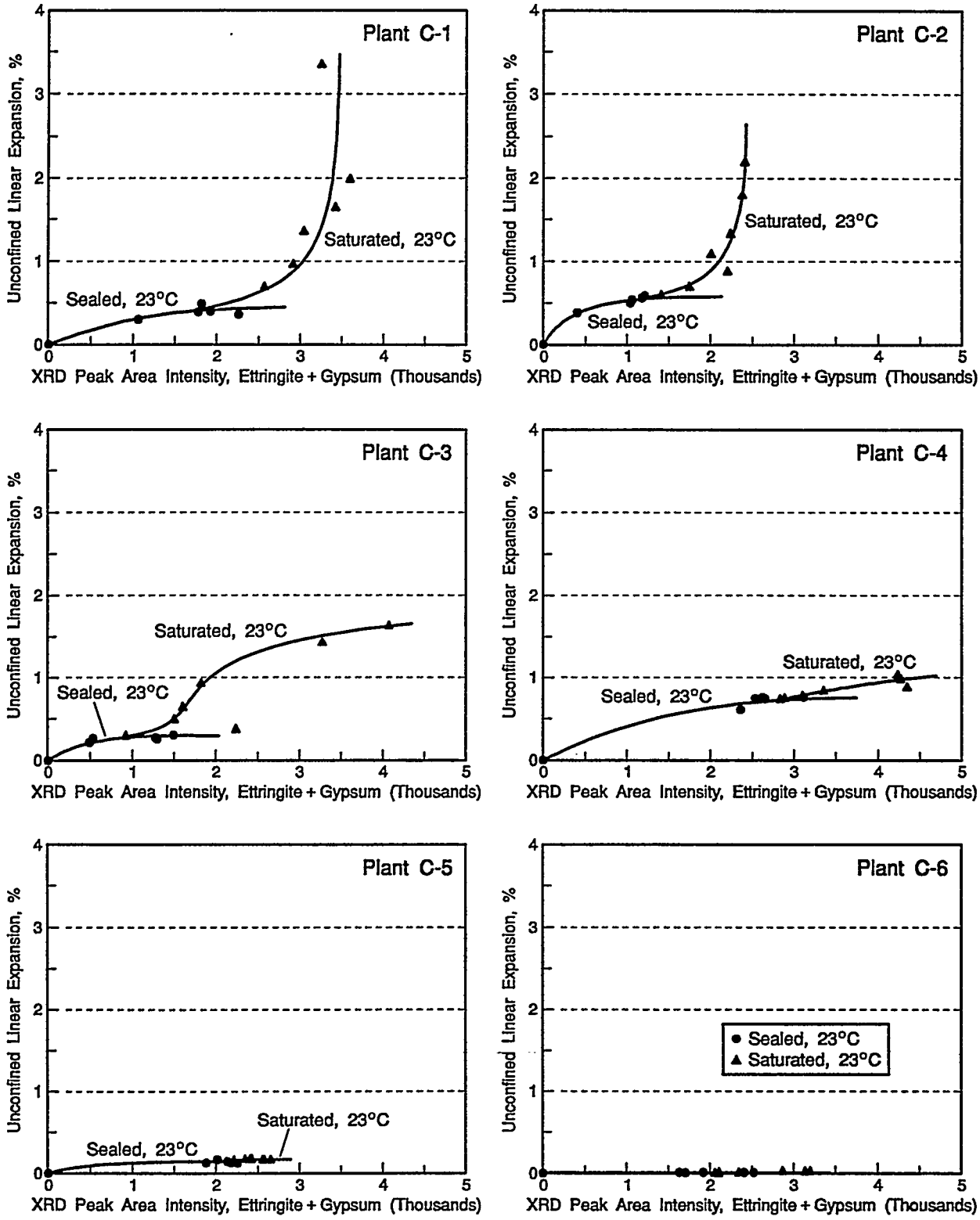

Figure 13. Relationship Between Unconfined Expansion and Ettringite and Gypsum Formation Under 23°C Sealed and Saturated Curing of Ash Blends for Plants C-1 Through C-6

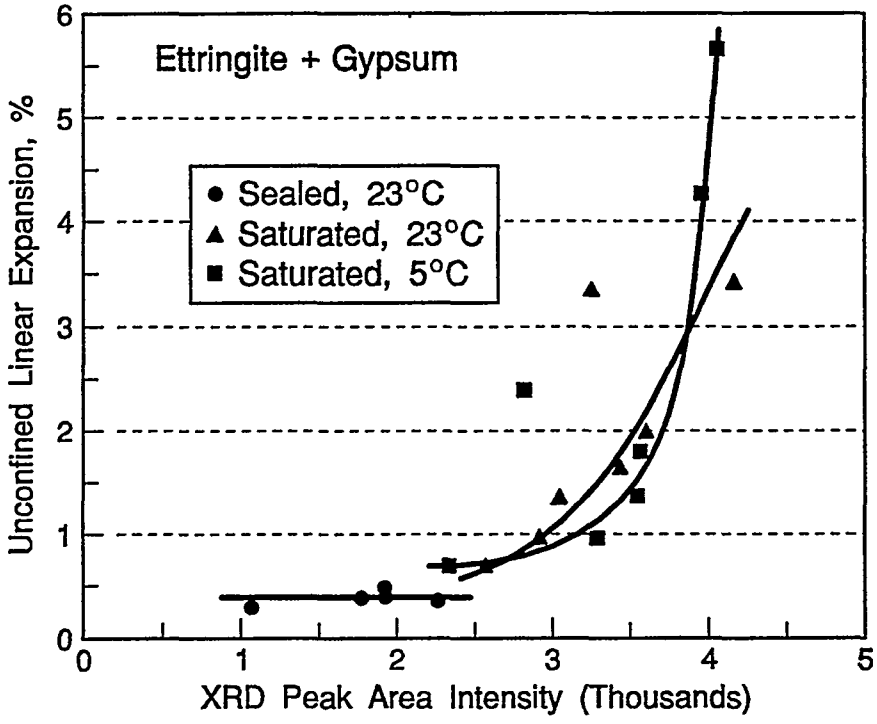

Figure 14. Relationship Between Unconfined Expansion and Ettringite and Gypsum Formation Under 23°C Sealed and 23°C and 5°C Saturated Curing of Ash Blend from Plant C-1

Figure 15 shows a series of curves for the sealed cured ash blends that are specific to the individual ash source. These curves fan to higher ettringite and gypsum XRD peak area intensities. Each curve shows an increase in strength with associated variable increases in expansion. For the sealed cured ash blends the maximum expansion is less than 1%, with strengths in excess of 5000 psi. The high-sulfur coal-derived ashes (Plants C-1 through C-3) show the highest expansion and similar strengths to the medium- and low-sulfur coal-derived ashes (Plants C-4 and C-5).

Figure 15 also presents this relationship between unconfined compressive strength and unconfined linear expansion for the 23°C saturated cured ash blend samples. The 23°C saturated cured ash blends show a series of curves specific to the individual ash source. Each curve shows an increase in strength with associated variable increases in expansion, with the exception of the high-sulfur coal-derived ashes (Plants C-1 and C-2). For these two saturated cured ash blends, at expansion there is a loss of strength. This corresponds to high hydration product formation.

The positive correlation of increasing strength with increasing expansion represents a situation in which the strength development exceeds the disruptive forces of expansion. The other portion of the curve shows an inverse relationship between strength and expansion (e.g. reduction in strength with increasing expansion) and represents a situation in which the disruptive forces of expansion exceed the strength of the material, micro-cracks develop, and strength decreases. This explanation involving micro-cracks is substantiated by the SEM photomicrographs.

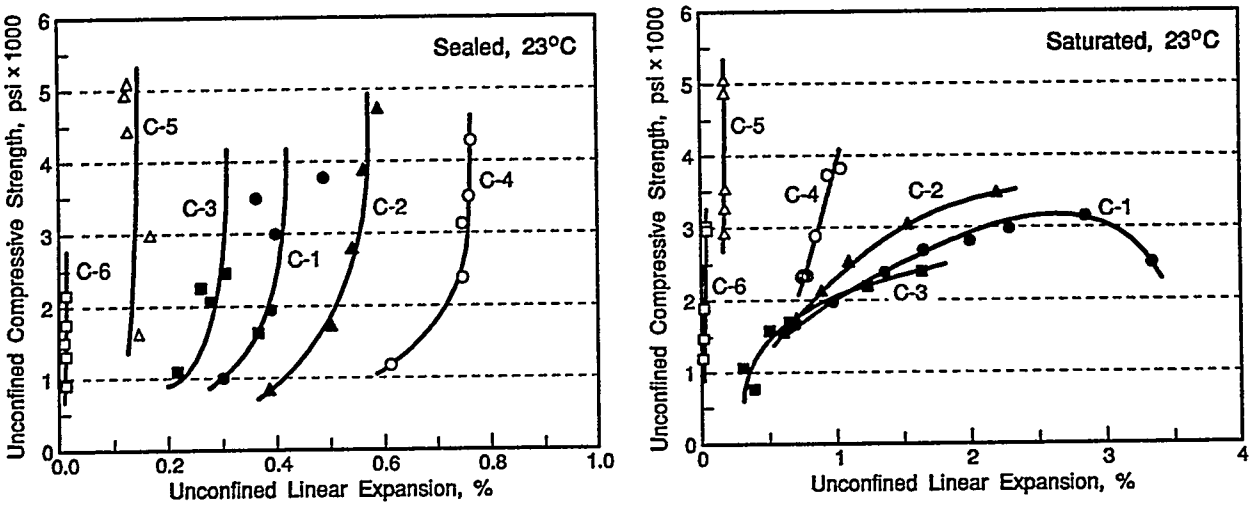

Figure 15. Relationship Between the Strength Development and Expansion for Ash Blends from Plants C-1 Through C-6

The effect of cold (5°C) saturated curing conditions on the relationship between unconfined compressive strength and unconfined linear expansion is presented in Figure 16. There is a strong positive correlation between strength and expansion during early development. The cold saturated ash blend shows a higher strength development, followed by a more rapid strength loss, than the 23°C saturated cured ash blend.

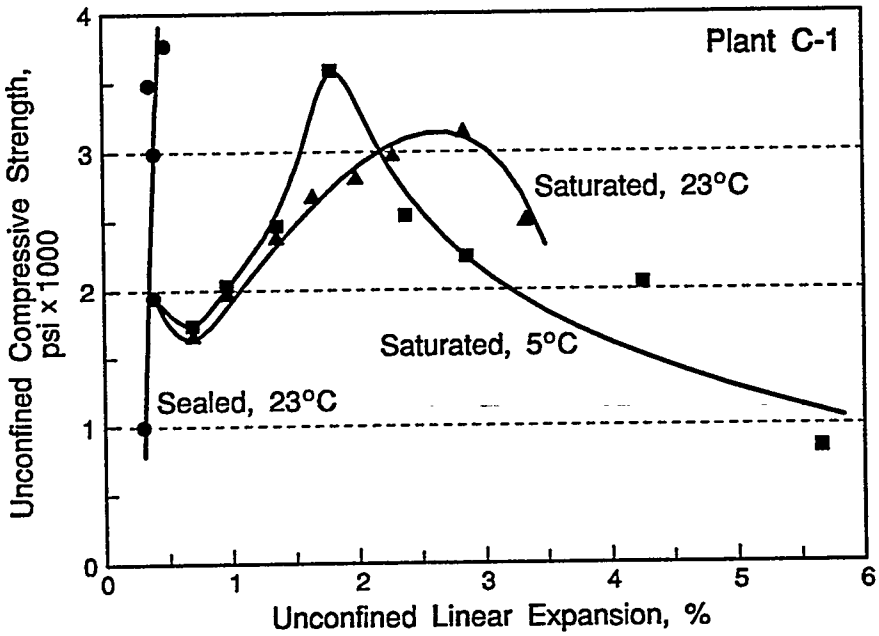

Figure 16. Relationship Between Unconfined Compressive Strength and Unconfined Linear Expansion for the 23°C Sealed and the 23°C and 5°C Saturated Curing of Ash Blends

Ettringite and gypsum growth under submerged conditions is characterized by continued expansion as a result of hydration phase formation. This corresponded to void filling and bridging. This was followed by a period of strength loss and continued expansion. The SEM photomicrographs indicate the formation of micro-cracks due to the bridging of voids.

Pore Filling Model for CFBC Ash Curing

The creation of strength and expansion in the CFBC ash blends is a complex combination of chemical and physical processes resulting in different rates and morphologies of the hydration reaction phases. The trends for strength, expansion, and hydration reaction phases are consistent with a model of pore filling as noted by SEM. The void reduction during curing, even taking into account the expansion of the specimens, also confirms the filling of pores and voids and a pore filling model.

A pore filling model for strength and expansion involves the observation that hydration phase formation occurs in the void and pores of the compacted ash. These pores are primarily filled with a solution that contains the soluble species from the adjacent ash. Precipitation of the hydration phases occurs in these pores, progressively filling from the walls of the pore inward toward the center. The filling of the pores creates strength by reinforcing the pores and reducing pore volumes and voids. However, the pores will eventually fill and the additional phase formation will exert force on the particles, pushing them apart and causing expansion. The pores do not have to be completely filled for expansion to occur, and bridging of the pores can cause expansion. Expansion can reduce strength by creating micro-cracks and fissures. These new fissures then become sites for hydration phase precipitation, and these fissure fillings will provide some strength development until the fissures fill or bridge and further precipitation creates more expansion and more micro-cracking. This dynamic process of cracking and filling, resulting in strength development and strength disruption, continues until the ingredients for phase precipitation limit further phase formation. However, the dissolution and re-precipitation of these phases can occur under submerged conditions, continuing the pore filling process during the curing of the ash.

In summary, the effect of hydration phase formation and pore filling on the design of ash fills is complex, presenting a number of obvious trade-offs affecting ash disposal or use. The presence of pores can be beneficial to the dimensional stability of the ash by allowing sites for the hydration phases to precipitate. Efforts to compact the ash into a tighter packing configuration would tend to be counterproductive. However, the lowering of the density increases the permeability of the ash, thereby allowing greater water penetration, and thereby increasing the amount and rate of the hydration phase formation and subsequent expansion. The ideal situation would involve limiting the potential for hydration phases in order to provide strength through pore filling without exceeding the void space available and thereby creating additional expansion and cracking of the compacted ash.

5.10 Methods for Controlling CFBC Ash Geotechnical Properties

It may be possible to develop methods that can either accelerate or terminate the hydration reactions that have been identified as occurring in the conditioned CCT ashes. From a disposal perspective, if methods of accelerating the expansion reactions can be found, then a stable fill can be constructed after the reactions are complete. Alternatively, if a method can be found to prevent the expansive reactions from occurring, once again a stable fill can be constructed. Dimensional stability is as important to the use of ash in construction applications as to disposal site stability.

WRI has evaluated several potential methods for controlling the hydration reactions, and thus the geotechnical properties, of the CCT ash. To date, two disclosures have been written based on these assessments. They have been filed with the U.S. DOE Patent Office and represent restricted and confidential concepts. Therefore, all information concerning these methods is restricted and confidential.

The development of methods has focused on two processes: process A and process B. Process A has been applied to a number of low-sulfur and medium-sulfur FBC ashes. The results of testing for strength development are presented in Figure 17, and the results for the expansion of conditioned and compacted CFBC ashes from low-sulfur and medium-sulfur coal-fired CFBC units are presented in Figure 18. It is clear that the process has potential, with observed doubling of strengths and nearly an order of magnitude reduction in expansion with process A treatment.

In summary, the use of process A has a positive effect on the expansion characteristics of conditioned and compacted ashes, particularly CFBC ashes, which are known to exhibit high expansion and dimensional instability.

Process B involves the addition of specialty chemicals to activate the hydration of the ash and the generation of hydration reaction phases that will contribute to strength and reduce or eliminate expansion. One of the primary concerns related to the production of construction-related materials from certain lime- and sulfate-containing ashes, such as CFBC ashes, is the subsequent formation of the mineral ettringite. Ettringite formation has been associated with the observed expansion in CFBC ashes. WRI has developed a chemical method that appears to be effective in reducing the formation of ettringite.

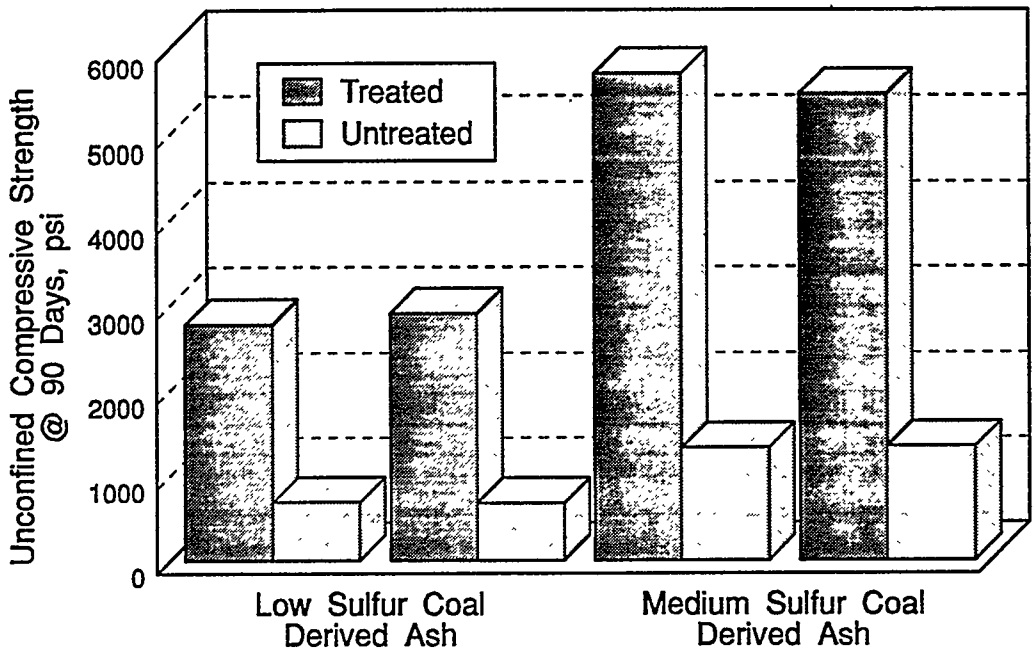

Figure 17. Effect of Process A Treatment on the Strength Development of CFBC Ashes (1000 psi = 6.9 MPa)

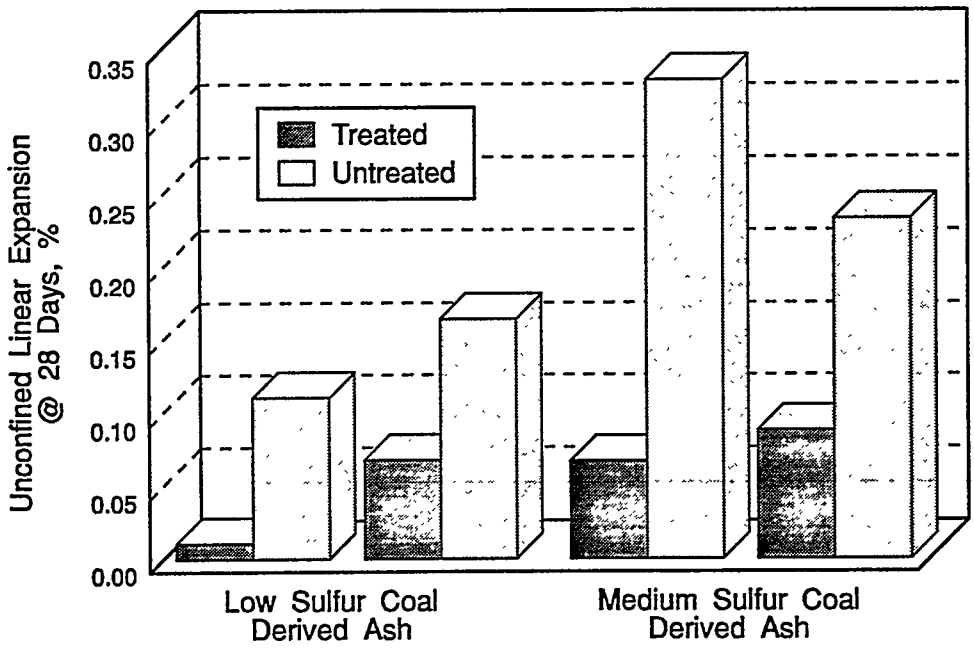

Figure 18. Effect of Process A Treatment on the Expansion Characteristics of CFBC Ashes

The proprietary chemicals can be controlled precisely, thereby controlling the amount of ettringite development that occurs. Some ettringite development is beneficial for strength development. This use of process A has little effect on strength development (Figure 19) but a significant effect on expansion (Figure 20).

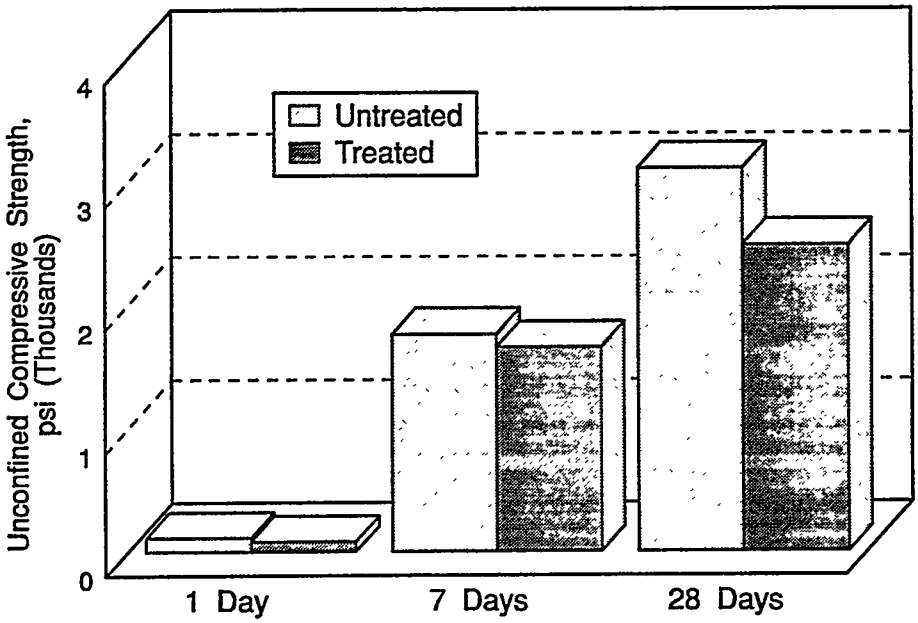

Figure 19. Effect of Process B Treatment on Strength Development of CFBC Ash (1000 psi = 6.9 MPa)

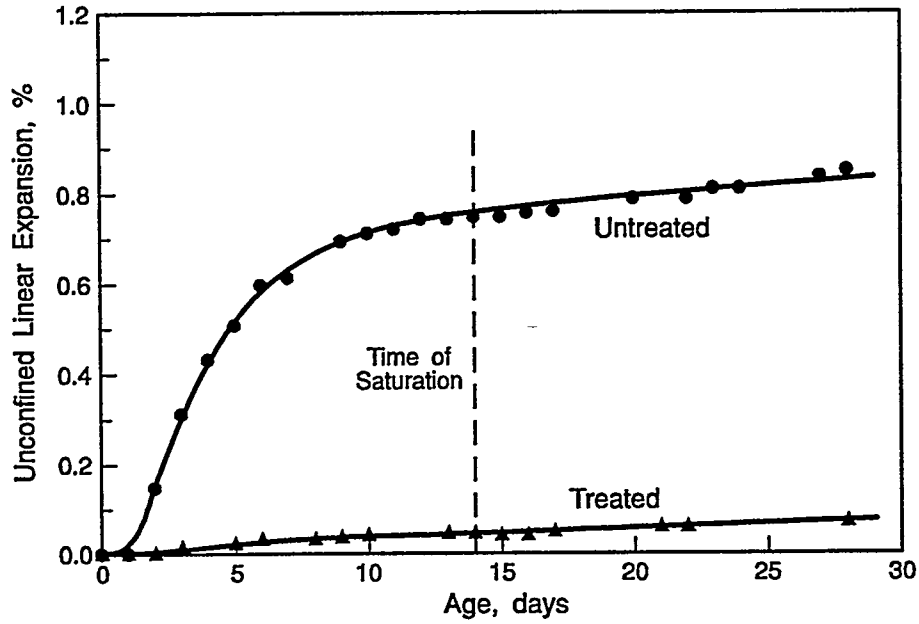

Figure 20. Effect of Process B Treatment on Expansion Characteristics of CFBC Ash

Figure 21 shows the hydration reaction products produced in a conditioned and compacted CFBC ash with and without process B treatment. The amount of ettringite and gypsum formation is reduced with the treatment, thereby reducing the expansion potential of the ash. In summary, the use of chemical additives such as employed with Process B is beneficial in that they improve the durability characteristics of the resultant mixture.

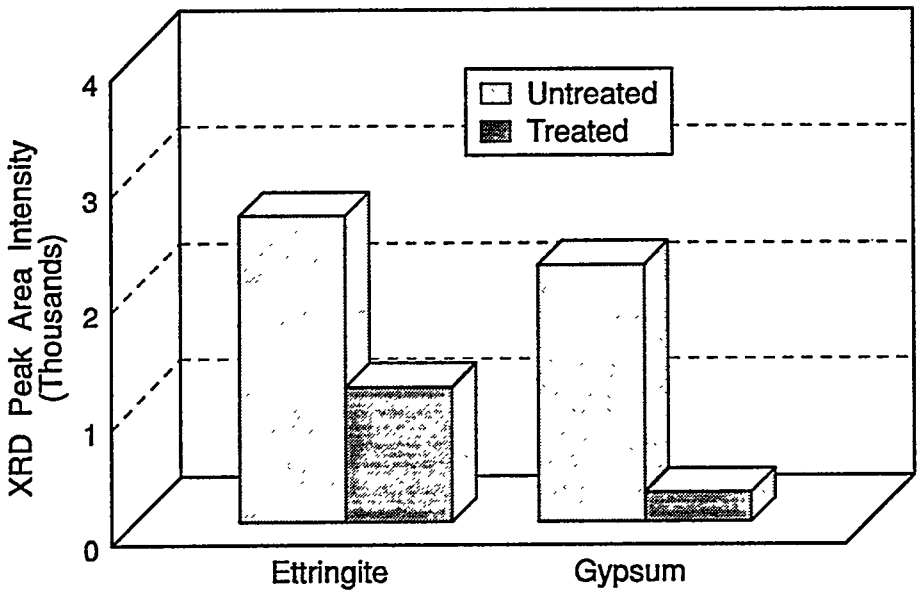

Figure 21. Effect of Process B Treatment on the Reaction Products Formed in CFBC Ash

6.0 SUMMARY AND CONCLUSIONS

Western Research Institute, in cooperation with the U.S. Department of Energy Federal Energy Technology Center, initiated a multi-year program to examine the relationship between CCT ash chemistry and geotechnical properties as they relate to ash disposal and utilization. The overall goal of the program was to develop the basis for processes whereby the hydration reaction chemistry, and thus the geotechnical properties, of the ash can be controlled under ash management situations. The investigation addressed the following:

- detailed characterization of the chemical, mineralogical, and physical properties of the as-produced ashes from several circulating fluidized bed combustion (CFBC) facilities operating on a range of coal and petroleum coke fuels;

- detailed conditioning investigation of the ashes to define the effect of preconditioning on the hydration of lime and other phases in the ash and the effect of the amount of conditioning on the geotechnical properties of strength and expansion;

- curing study of the conditioned and compacted ashes to determine the effect of curing conditions on the geotechnical and hydration phase chemistry of the ash; and

- an investigation of methods or processes to control these reactions and thereby stabilize these ashes.

The following results and milestones of the program have been determined.

6.1 Ash Characterization Investigation

A number of CFBC facilities agreed to supply ash from their units for the study. These include ashes from the combustion of the following fuels:

–Bituminous coal (4% sulfur) with limestone sorbent

–Bituminous coal (3% sulfur) with limestone sorbent

–Blend of bituminous coal (3% sulfur) and 25% petroleum coke (4.5% sulfur) with limestone sorbent

–Bituminous coal (1.8% sulfur) with limestone sorbent

–Subbituminous coal (0.9% sulfur) with limestone sorbent

–Petroleum coke (5-6% sulfur) with limestone sorbent.

Chemical characterization was conducted, including elemental, phase analysis, and leaching characteristics, as well as physical characterization, including bulk densities, specific gravities, and proctor moisture-density relationships of the ashes. The characterization effort employed a number of analytical techniques. X-ray fluorescence and inductively coupled argon plasma analysis were used to determine the elemental composition of the ashes. High-resolution thermogravimetric analysis, X-ray diffraction analysis, and scanning electron microscopy were used to determine the mineral phases present. Standard ASTM methods were employed to determine the physical properties and moisture-density relationships.

- The ashes were composed principally of compounds containing calcium and sulfur, which result from the addition of limestone sorbent and the subsequent capture of sulfur emissions during the combustion process and to a lesser extent, components inherent in the fuel (coal or petroleum coke) which remain after combustion.

- The composition of the ashes varied with the sulfur and ash content of the fuel used in the combustion process. The ashes resulting from the combustion of high-sulfur coals contained high percentages of sorbent-derived components, while those from the combustion of low-sulfur coals contained lower percentages. The composition of the petroleum coke-derived ash was predominantly sorbent derived, since the petroleum coke has a very low ash content.

- The forms of calcium observed in the ashes confirmed the presence of large quantities of anhydrite [$CaSO_4$] and lime [CaO] and minor amounts of calcite [$CaCO_3$]. The presence of calcium ferrite phases was not confirmed in this study, although it is confirmed in the literature from previous studies.

6.2 Ash Conditioning Study

Conditioning tests were conducted on the ashes from each of the plants to determine the water addition required to hydrate most of the lime in the ash to dissipate the heat and the swelling associated with this exothermic reaction prior to placement of the ashes into a landfill. Conditioning tests were conducted on the bed ash and fly ashes from each of the plants separately. Each ash was conditioned with a range of water additions. Fresh water was used for the tests to simulate the conditions at an operating plant. Water accounting practices were employed to account for the water as steam, residual moisture, and chemically bound water. The lime conversion was determined by XRD and TGA. The lime [CaO] and portlandite [$Ca(OH)_2$] XRD peak area intensities and the portlandite TGA data were used to determine lime conversion. Approximately 80% conversion was determined for the ashes. Testing concluded the following:

- The preconditioning level varied with the individual ash compositions. Water losses were a major part of the water added. The percentages of conditioning water added also increased with the lime content of the ash.

- ASTM D-698 and ASTM D-1557 moisture-density relationships were determined for the optimum conditioned and compacted ashes. ASTM D-698 optimum moistures ranged from 18% to 35%, and maximum dry densities ranged from 88 pcf to 116 pcf. ASTM D-1557 compactive effort resulted in a 15% relative reduction in moisture and a 7% increase in maximum dry density.

- Two ashes were preconditioned at different levels to ascertain the importance of preconditioning to the geotechnical properties of the ashes. Preconditioning of the ashes prior to secondary water addition and compaction had a significant impact of the strength development and expansion characteristics of the ash. Preconditioning enhanced strength development and reduced expansion for the ashes.

6.3 Ash Curing Conditions Study

Conditioned ash blends (blends of fly ash and bed ash from each of the plants in the proportions produced) were compacted to ASTM D-698 and D-1557 compactive effort and cured under different moisture levels and temperatures. The cured specimens were tested for strength development, expansion characteristics, and the development of hydration reaction products with time. Geotechnical properties such as strength development and expansion were determined for the conditioned ashes compacted under ASTM D-698 and D-1557 compactive

effort and the conditioned and compacted ashes under sealed and saturated conditions at 23°C. The effect of temperature (23°C and 5°C) on the saturated curing of the ashes was also examined.

- The results of testing using high-sulfur coal-derived ashes showed enhanced strength development with time for the ASTM D-1557 conditioned and compacted ashes compared to the ASTM D-698 ashes. The effect of compaction on expansion is not as clear, with only minor increases in expansion.

- The results showed increases in strength development with time for each of the ashes. The strength development varied with the type and characteristics of the ashes. The 23°C saturated curing resulted in increased strength for one of the ashes but resulted in long-term loss of strength for the high-sulfur coal-derived ashes. The application of cold (~5°C) saturated curing resulted in even further reduction of strength for these ashes.

- The results showed the expansion also increased with time for the medium- and high-sulfur coal-derived ashes. The low sulfur coal derived ashes and the petroleum coke-derived ashes did not show significant expansion with time. The expansion appears to be inversely related to strength development. As the strength decreased under saturated curing, the expansion increased significantly. The application of 5°C saturated curing resulted in further strength loss and increased expansion.

- Hydration reaction chemistry of the ashes after predetermined curing intervals under sealed and saturated curing was determined by X-ray diffraction and high resolution thermogravimetric analysis. The hydration reaction products appear to be principally the hydration of lime [CaO] to portlandite [$Ca(OH)_2$], the hydration of anhydrite [$CaSO_4$] to gypsum [$CaSO_4 \cdot 2H_2O$], and the precipitation of ettringite [$Ca_6Al_2(SO_4)_3(OH)_{12} \cdot 26H_2O$] from the soluble calcium, sulfates and alumina. No thaumasite was noted in the specimens.

- The ashes appear to follow one of several hydration reaction trends: (1) ettringite-only development, (2) ettringite and/or gypsum early followed by later gypsum formation, or (3) gypsum-only formation.

- Testing has confirmed that the hydration reaction chemistry is related to the geotechnical properties of the ashes. Strength development appears to be related to ettringite and/or gypsum formation through pore filling and pore bridging. Expansion appears to be related to the formation of these same two minerals. The expansion increased with saturated curing and appears to be predominantly gypsum based.

- The formation and stability of the hydration reaction products, in particular the ettringite, appear to be controlled by the availability of reactants, as well as by the pH of the curing environment.

- Expansion was found to be related to strength development. Initially, strength increases with expansion. Thereafter, with continued expansion, strength losses were observed for the high-sulfur coal-derived ashes. This is consistent with a pore filling model.

- A pore filling model was found to be consistent with the observed relationships between hydration phases (ettringite and gypsum) and strength development and expansion, as well as SEM observations and void reduction observations. In the pore filling model, ettringite and/or gypsum are precipitated in the pores of the compacted ash, thereby providing strength until the pores become filled or bridged, after which excessive expansion and loss of strength occur. The expansion creates micro-cracks, causing strength loss and potential sites for further precipitation of hydration phases without further expansion. Micro-crack filling counteracts further strength loss until filling and bridging resulted in further expansion and micro-crack formation. Under submerged conditions, certain of these hydration phases are believed to dissolve and re-precipitate, resulting in the initial strength loss upon saturation, followed by slow recovery of strength.

6.4 Development of Methods for Controlling Hydration Reaction Chemistry and Geotechnical Properties of the Ashes

Based on the results of the testing described above, conditions were defined for controlling the formation of the hydration reaction products that result in the geotechnical properties of the CFBC ashes. Two processes were reported that controlled the expansion associated with CFBC ashes. The treatment methods effectively reduced or eliminated the expansive forces and unconfined expansion in the conditioned and cured ashes. There is a slight decrease in strength associated with certain of these treatments. However, strength remains sufficient for most disposal or ash reuse options. Invention disclosures have been written on these processes and methods of controlling the geotechnical properties of CFBC ashes

7.0 REFERENCES

ASTM 1990 – 1993. *Annual Book of Standards*. Various Vol., American Society of Testing and Materials, Philadelphia, PA.

Anthony, E.J., A.P. Iribarne and J.V. Iribarne. 1995. "Study of Hydration During Curing of Residues from Coal Combustion with Limestone Addition." *Proc.* 13th International Conference on Fluidized bed Combustion, ASME, Orlando FL, May, 7-10, 1995, Vol. 2, pp. 1113-1121.

Anthony, E.J., A.P. Iribarne and J.V. Iribarne, 1997, "Study of Hydration During Curing of Residues from Coal Combustion with Limestone Addition." *Journal of Energy Resources Technology*, Vol. 19, pp. 89-95.

Beeghly, J.H., J. Bigham and W.A. Dick. 1993. "The Ohio Based Study on Land Applications of Dry FGD By-Products." *Proc.* 10th International Ash Use Symposium, Vol. 2, pp. 59-1 to 59-14.

Berry, E.E., R.T. Hemmings and B.J. Cornelius (Matex Consultants, Inc.). 1991. "Commercialization Potential of AFBC Concrete: Part 2 Mechanistic Basis for Cementing Action." EPRI Report 2708-4, January, 1991, pp. 5-23.

Bigham, J., W. Dick, L. Forster, F. Hitzhusen, E. McCoy, R. Stehouwer, S.W. Traina, W. Wolfe and R. Haefner. 1993. "Land Application Uses for Dry FGD By-Products," Phase 1 Report. USDOE (METC) Report.

Bland, A.E., C.E. Jones, J.G. Rose and J.L. Harness. 1989a. "Ash Management Options for Bubbling Bed AFBC Technologies." *Proc.* 1989 Joint Power Generation Conference, Ash Handling, Disposal and Utilization from Coal Fired Fluidized Bed Boilers, Dallas, Texas, October 22-26, pp. 9-19.

Bland, A. E., C. E. Jones, J. G. Rose and J. L. Harness, 1989b, "Ash Management Options for AFBC," *Proc.* 10th International Conference on Fluidized Bed Combustion, ASME, San Francisco, CA, April 30-May 3, 1989, pp. 323-324.

Bland, A. E., and R. K. Kissel, 1989c, "Laboratory Evaluation of CFBC Waste Disposal and Utilization Options," *Proc.* 10th International Conference on Fluidized Bed Combustion, ASME, San Francisco, CA, April 30-May 3, 1989, pp. 1141-1148.

Bland, A.E., R.K. Kissel and G.G. Ross. 1991. "Utilization of CFBC Ashes in Roller Compacted Concrete Applications." *Proc.* 11th International Conference on Fluidized Bed Combustion, April, Montreal, Canada, pp. 857-863.

Bland, A.E., D.N. Georgiou and E.J. Anthony. 1993. "Sea Water Conditioning of CFBC Ash." *Proc.* 12th International Conference on Fluidized Bed Combustion, May 9-13, La Jolla, CA, Vol. 2, pp. 835-846.

Blondin, J., E. J. Anthony, and A. P. Iribarne, 1993, "A New Approach to Hydration of FBC Residues." *Proc.* 12th International Conference on Fluidized Bed Combustion, May 9-13, 1993, La Jolla, CA, Vol. 2, pp. 827-834.

Burwell, S.M., R.K. Kissel, A.E. Bland and D.M. Golden. 1993. "Fluidized Bed Combustion Ash Concrete." *Proc.* 12th International Conference on Fluidized Bed Combustion, May 9-13, La Jolla, CA, Vol. 2, pp. 847-858.

Georgiou, D. N., R. K. Kissel and G. G. Ross, 1991, "Geotechnical Characteristics and Landfilling of CFBC Residue," *Proc.* 11th International Conference on Fluidized Bed Combustion, April, 1991, Montreal, Canada, pp. 849-855.

Georgiou, D. N., A. E. Bland and Sundstrom, D., 1993, "Laboratory Evaluation of a Low Sulphur Coal CFBC Residue for Use as a Structural Fill." *Proc.* 12th International Conference on Fluidized Bed Combustion, May 9-13, 1993, La Jolla, CA, Vol. 1, pp. 629-639.

Hopkins, T.C., M.N. Wu, R.A. Winschel and T.L. Robl. 1993. "The Ohio Coal Development Office Coolside Waste Management Demonstration Project." *Proc.* 10th International Conference Ash Utilization Symposium, Orlando, FL, January, pp. 60-1 to 60-16.

Iribarne, A.P., E.J. Anthony and J. Blondin. 1993. "The Phase Analysis of Coal Combustion Residues." *Proc.* 12th International Conference on Fluidized Bed Combustion, La Jolla, CA, May 9-13, pp. 641-647.

Minnick, L.J. 1982. "Development of Potential Uses for the Residue from Fluidized Bed Combustion Processes." Report No. DOE/ET/10415-T6, United States Department of Energy.

Ross, G.G., R.K. Kissel, E.J. Anthony, and C.C. Doiron. 1989. "Field Demonstration of Fluidized Bed Combustion Residue Management." *Proc.* 10th International Conf. on Fluidized Bed Combustion, San Francisco, CA.

Santoro, L., I. Aletta and G.L. Valenti. 1986. "Hydration of Mixtures Containing Fly Ash, Lime and Phosphogypsum." *Thermochimica Acta*, Vol. 98, pp. 71-80.